This is to certify that the
dissertation entitled

CHEMICAL APPROACHES TO THE STABILIZATION OF NON-COVALENT COMPLEXES IN MATRIX-ASSISTED LASER DESORPTION/IONIZATION MASS SPECTROMETRY

presented by

Anne M. Distler

has been accepted towards fulfillment
of the requirements for the

Ph.D. degree in Chemistry

John Allison

Major Professor's Signature

5.6.2003

Date

CHEMICAL APPROACHES TO THE STABILIZATION OF NON-COVALENT COMPLEXES IN MATRIX-ASSISTED LASER DESORPTION/IONIZATION MASS SPECTROMETRY

By

Anne M. Distler

A DISSERTATION

Submitted to
Michigan State University
in partial fulfillment of the requirements
for the degree of

DOCTOR OF PHILOSOPHY

Department of Chemistry

2003

ABSTRACT

CHEMICAL APPROACHES TO THE STABILIZATION OF NON-COVALENT COMPLEXES IN MATRIX-ASSISTED LASER DESORPTION/IONIZATION MASS SPECTROMETRY

By

Anne M. Distler

While non-covalent complexes have been detected using matrix-assisted laser desorption/ionization mass spectrometry (MALDI MS), often these weakly bound complexes dissociate in the MALDI experiment. In our studies, double-stranded oligonucleotides serve as a model for all types of non-covalent complexes. Since the non-covalent interactions that hold the complexes together are disrupted during the MALDI experiment, it is important to examine each phase of the MALDI process. The various steps of the experiment will be presented and considered as points in the experiment where the duplex is disrupted. Methods for the stabilization of non-covalent complexes in MALDI MS will also be discussed. It is widely known that duplex oligonucleotides interact with a variety of stabilizing species in solution. While these compounds are often used to visualize oligonucleotides in gels or assist in X-ray crystallographic analysis, the presence of these compounds can also stabilize duplex oligonucleotides in the MALDI process.

The methods developed from the oligonucleotide studies were then applied to other molecular complexes. The cytochrome c oxidase enzyme from the *Rhodobacter sphaeroides* bacteria exists as a complex of four peptide subunits, two hemes, and a variety of lipids and metal ions. Although our goal is the stabilization of the intact

complex, information can be determined from the detection of the components of this complex. Molecular weight information was determined for all components of the enzyme and structural information was determined for the lipids. The partial dissociation of the cytochrome c oxidase enzyme allowed for the determination of subunit-subunit and subunit-lipid interactions. The unique connectivity information from the partial dissociation of the enzyme in mass spectrometry added a new dimension to the understanding of the lipid/protein complex.

ACKNOWLEDGMENTS

My graduate studies at Michigan State University have been very challenging and rewarding. Many people have contributed to my success along the way. I would like to thank my family for all their support. My parents and my brothers, Mike and Brian, have been both a source for encouragement and a source of advice. A special thanks to Mark for always listening and understanding.

Thank you also to my advisor John Allison who provided me with many challenges along the way. I would also like to thank the people at the Mass Spectrometry Facility especially Susanne Hoffmann-Benning and Rhonda Husain and the people at the Macromolecular Structure, Sequencing, and Synthesis Facility especially Colleen Curry, Stacy Trzos, and Joe Leykam. You have been a source of knowledge during my studies here.

I would also like to thank Shelagh Ferguson-Miller and her group members especially Carrie Hiser, Ling Qin, and Yasmin Hilmi. I have enjoyed working with all of you over the past year and have benefited greatly from your expertise in biochemistry.

Thanks to the many friends I have met here including Jamie, Qian, Anne, Doug, and Eric. I appreciate all you have done for me.

TABLE OF CONTENTS

LIST OF TABLES

LIST OF FIGURES

LIST OF ABBREVIATIONS

ACN	Acetonitrile
ATT	6-Aza-2-thiothymine
CcO	Cytochrome c oxidase
CHCA	α-Cyano-4-hydroxycinnamic acid
CL	Cardiolipin
Da	Dalton, mass unit
DAHC	Diammonium hydrogen citrate
DGD	Digalatosyldiacylglycerol
DHAP	2,4-Dihydroxyacetophenone
DHB	2,5-Dihydroxybenzoic acid
D/I	Desorption/ionization
DNA	Deoxyribonucleic acid
ESI	Electrospray ionization
Et	Ethidium bromide
FTMS	Fourier transform mass spectrometry
GDP	Guanosine diphosphate
GTP	Guanosine triphosphate
His	Histidine
HPA	3-Hydroxypicolinic acid
Ht	Histidine Tag
ICR	Ion cyclotron resonance
IR	Infrared

LC ..... Liquid chromatography

$[M-H]^-$ ..... Deprotonated analyte

$[M+H]^+$ ..... Protonated analyte

M_1M_2 ..... Double-stranded oligonucleotide

MALDI ..... Matrix-assisted laser desorption/ionization

MB ..... Methylene blue

Met ..... Methionine

MGD ..... Monogalatosyldiacylglycerol

MSA ..... 5-Methoxysalicylic acid

MS ..... Mass spectrometry

MW ..... Molecular weight

m/z ..... Mass-to-charge ratio

NMR ..... Nuclear magnetic resonance

PAGE ..... Polyacrylamide gel electrophoresis

PC ..... Phosphatidyl choline

PE ..... Phosphatidyl ethanolamine

PG ..... Phosphatidyl glycerol

PNA ..... Peptide nucleic acid

ppm ..... Parts per million

PS ..... Phosphatidyl serine

PSD ..... Post-source decay

RNA ..... Ribonucleic acid

SA ..... Sinapinic acid

SDS ..... Sodium doceyl sulfate

SL ..... Sulfolipid

sp ..... Spermine

T ..... Matrix

TFA ..... Trifluoroacetic acid

THAP 2,4,6-Trihydroxyacetophenone

T_m ..... Melting temperature

TOF ..... Time-of-flight

TRIS ..... tris[hydroxymethyl]-aminomethane

UV ..... Ultraviolet

CHAPTER 1. INTRODUCTION

I. Non-covalent Complexes in Mass Spectrometry

In organic synthesis, the main focus is the making and breaking of covalent bonds. In the field of biochemistry, many processes involve non-covalently bound complexes. These types of complexes have great significance since cellular function is often triggered by weak non-covalent interactions between enzyme and substrate, protein and drug, and antibody and antigen [1]. These complexes are under intensive investigation in order to achieve a better understanding of how the human body functions or malfunctions. Often drug discovery efforts involve the development of new compounds that non-covalently bind to proteins in order to prevent a disease [2]. The detection of these complexes is a crucial part of drug development.

Analyses of non-covalent complexes have traditionally been performed using techniques such as gel permeation chromatography [3], centrifugation [4], and sodium dodecyl sulfate polyacrylamide gel electrophoresis (SDS-PAGE) [5]. While frequently used to study biomolecular complexes, these techniques provide little or no information about the molecular mass and binding stoichiometry of the complexes. The more advanced techniques of x-ray crystallography and nuclear magnetic resonance (NMR) can provide detailed information about the structure of the complex. However, these techniques can be difficult and time consuming. For example, when using x-ray crystallography, homogenous crystals are needed for the analysis. The growth process for the crystals is lengthy, tedious, and often unsuccessful. For this reason, mass spectrometry would be a useful technique for analyzing non-covalent complexes to

determine molecular weight information rapidly and without extensive sample preparation.

In order to detect non-covalent complexes using mass spectrometry, the desorption/ionization technique must meet several conditions. Most importantly the ionization method must transfer enough energy to the molecule to allow for its ionization and desorption, but not enough energy to cause the dissociation of the complex. Also, a mass spectrometry technique that allows the complex to be analyzed while in a buffered solution would also be useful. Non-covalent complexes are often sensitive to changes in temperature or pH of the solution. If the analysis could be performed in a solution buffered to biological pH, the non-covalent complex would be more stable during the course of the experiment.

Two desorption/ionization techniques potentially meet the requirements for analyzing non-covalent complexes: matrix-assisted laser desorption/ionization (MALDI) and electrospray ionization (ESI). The developments of MALDI [6] and ESI [7] pushed mass spectrometry into the realm of biomolecules. Recently, mass spectrometry has become an important technique in the analysis of proteins, DNA, carbohydrates, and lipids [1, 8-10]. With the use of MALDI or ESI, the mass range for mass spectrometric analysis increased to include proteins and other biomolecules weighing over 100 kilodaltons (kDa). The amount of sample needed for analysis also decreased to the picomole (pmol) level.

The technique of electrospray ionization has had success when analyzing a variety of non-covalent complexes [11-22]. In specific, protein-DNA complexes [23-24], DNA-drug [25], and catechin-peptide [26] complexes have also been detected using ESI-

MS. ESI-MS is advantageous because it allows the sample to be introduced in a buffered solution without requiring the formation of a solid phase target. In ESI-MS, the experiment yields a distribution of peaks arising from differing charge states of the analyte. The charge state of the analyte is dependent on the analyte size, as well as the pH of the starting solution with a lower pH providing a more highly charged analyte ion. The mass analyzer in ESI-MS is often a quadrupole or ion trap with a maximum detectable mass-to-charge ratio of 2000. Due to the limited mass range, the analyte needs to exist in a highly charged state. For example, the protein bovine serum albumin has a molecular weight of around 66,000 g/mol. In order to be detected using a quadrupole ion trap, the protein must accumulate greater than 33 charges. This can lead to complications since the acidic conditions necessary for ESI analysis can denature non-covalent complexes [1,2].

While ESI-MS has had many documented successes in the analysis of non-covalent complexes, there are complications and this type of analysis is still not routine. One protein of particular interest is the ras protein. The ras protein is involved in the formation of a wide range of human tumors [27] and plays a central role in the signaling of cell growth [28]. This protein exists in either an inactive form with a guanosine diphosphate (GDP) non-covalently bound to the protein or an active form with a guanosine triphosphate (GTP) non-covalently bound to the protein [29]. In oncogenic ras, the mutated ras protein becomes locked in the active form, resulting in unregulated cell growth and tumor formation. The Ganguly group designed and synthesized a series of drugs to bind, non-covalently, to the mutated ras protein to inhibit the conversion of the inactive form of the ras protein to the active form [1,30]. The Ganguly group was

interested in studying these complexes using ESI-MS. Before the ras-GDP-drug complexes could be studied, it was important to stabilize the ras-GDP complex in the experiment. When analyzing the ras-GDP complex, the majority of the peaks present in the spectrum represented the dissociated complex, Figure 1.1. When looking at the deconvoluted ESI spectrum shown in the inset of Figure 1.1, the peak representing the dissociated complex is more intense than the peak representing the intact complex.

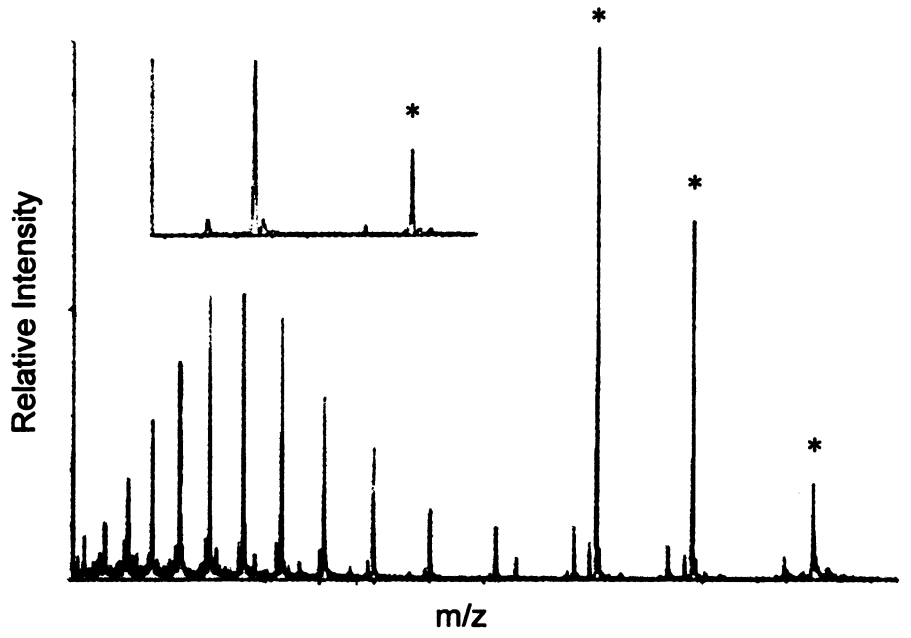

Figure 1.1. Electrospray ionization mass spectrum of the ras-GDP protein. The inset spectrum is the deconvoluted mass spectrum. The asterisks denote peaks representing the intact complex. The other peaks in the spectrum represent the components of the complex. This figure was adapted from reference 1.

While the detection of non-covalent complexes in ESI-MS has been documented, there are disadvantages for the technique. As shown in Figure 1.1, there is a distribution of peaks in the electrospray spectrum that represents each species present in solution. There are over 12 peaks representing the ras protein and 3 peaks representing the ras-GDP complex detected in the experiment. As a result of this charging, spectra for

mixtures can be very complex with multiple peaks for each component. Samples for ESI-MS analysis must also be highly purified in order to prevent clogging of the capillary tubing by non-volatile salts. While the presence of salts is not necessary for the stabilization of all analytes, cations are known to stabilize biomolecules such as duplex oligonucleotides. The removal of these salts may destabilize the complex. Also, when hydrophobic forces are involved in the formation of non-covalent complexes, the solvents used in mass spectrometric analysis are very important. Under the conditions needed for electrospray ionization, the non-covalent interactions are often destroyed [31]. Although ESI-MS has its advantages, the complicated spectra, organic solvents, and extensive sample purification necessary for ESI analysis make MALDI an attractive choice for analysis of biomolecules.

While the desorption/ionization technique of MALDI should allow for the study of non-covalent complexes, often such complexes are not detected on a routine basis. For example, a peptide nucleic acid (PNA) is structurally similar to proteins and deoxyribonucleic acid (DNA). PNA has shown promise for the development of gene therapeutic agents, diagnostic devices for genetic analysis, and as molecular tools for nucleic acid manipulations [32]. When duplex PNA is analyzed using MALDI MS, interesting results are seen [33], Figure 1.2. The actual sequence of the PNA duplex is not important. It is only important to note that it consists of PNA strand 1 non-covalently bound to PNA strand 2. The peak representing the non-covalent complex, labeled (1+2), is detected, but it is of low intensity when compared to the peaks representing the single strands, labeled (1) and (2). Also, peaks representing the homodimers, (1+1) and (2+2),

are detected as well. When ions such as (1+1) are formed, and 1 is not known to bind to itself, this may suggest that the non-covalent complex

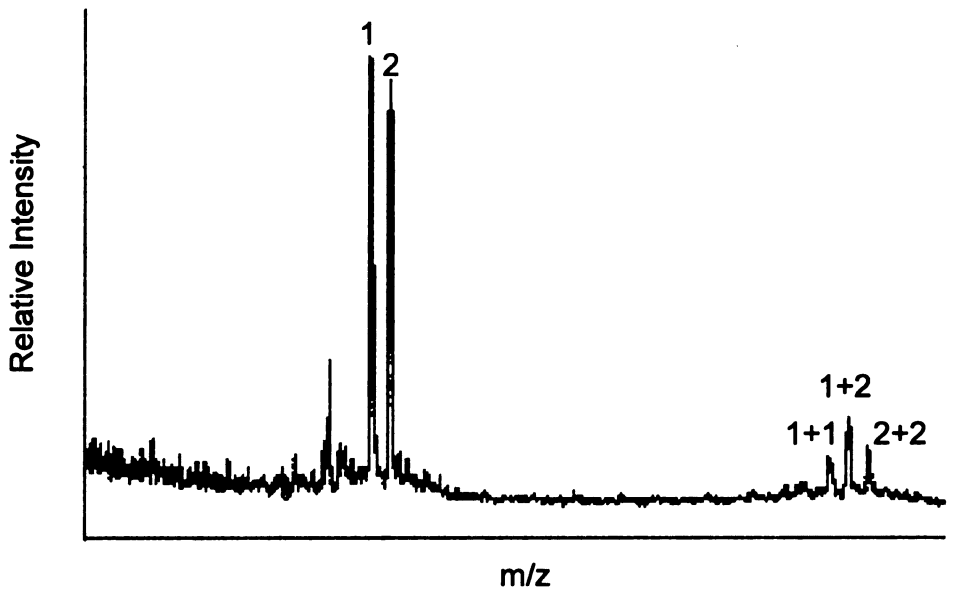

Figure 1.2. MALDI mass spectrum of a PNA duplex. This figure was adapted from reference 33.

completely dissociates early in the experiment. The single strands then randomly associate and co-precipitate during growth of the MALDI target crystals. The dissociation of the complexes in MALDI has been seen with other types of non-covalent complexes including those involving peptides bound to DNA [34]. RNA-peptide complexes have been detected using MALDI MS although the peaks representing the components of the complex are more intense than the peak representing the intact complex [35].

Since MALDI MS does not allow for the routine detection of non-covalent complexes, the MALDI process must be closely examined to find the cause of the dissociation. In order to explore MALDI analysis of non-covalent complexes, a model

analyte for all types of complexes can be employed. For these studies, DNA has been selected. Double-stranded DNA is an example of a non-covalent complex in which the single strands of DNA are held together by hydrogen bonds and are stabilized through other non-covalent interactions. Using a technique such as MALDI MS, a double-stranded oligonucleotide can be desorbed and ionized as a singly charged, gas phase ion although only a few examples have been reported [36-38]. Often, there is no direct evidence that Watson-Crick interactions remain intact throughout the MALDI experiment and in the gas phase. When a double-stranded oligonucleotide, M_1M_2, is analyzed using various desorption/ionization techniques, ions representing the two single strands are detected [39]. Since M_1M_2 is not detected as $(M_1M_2-H)^-$ or $(M_1M_2+H)^+$ in MALDI MS, the duplex must dissociate at some point before acceleration and detection of the ions.

Since molecular complexes are difficult to maintain in the MALDI experiment, it is important to more closely study the behavior of these complexes. The various steps of the MALDI process will be examined in order to define the point in the MALDI experiment where the complex dissociates. In these studies, double-stranded oligonucleotides will serve as a model for all types of non-covalent complexes. Since the non-covalent interactions that hold the complexes together are disrupted during the MALDI experiment, each phase of the MALDI process will be examined. The various steps of the experiment will be presented and considered as points in the experiment where the duplex is disrupted. Methods for the stabilization of non-covalent complexes in MALDI MS will also be discussed. It is widely known that duplex oligonucleotides interact with a variety of stabilizing species in solution. While these compounds are often used to visualize oligonucleotides in gels or assist in X-ray crystallographic

analysis, the presence of these compounds could also stabilize duplex oligonucleotides in the MALDI process.

The methods developed from the oligonucleotide studies were then applied to other molecular complexes. The cytochrome c oxidase enzyme from the *Rhodobacter sphaeroides* bacterium exists as a complex of four peptide subunits, two hemes, and a variety of lipids and metal ions. Although our goal is the stabilization of the intact complex, information can be determined from the detection of the components of this complex. Molecular weight information was determined for all components of the enzyme and structural information was determined for the lipids. The lipid content of the enzyme solution was also examined after various purification steps in order to determine which lipids were removed after the purification processes. The partial dissociation of the cytochrome c oxidase enzyme allowed for the determination of subunit-subunit and subunit-lipid interactions. The unique connectivity information from the partial dissociation of the enzyme in mass spectrometry added a new dimension to the understanding of the lipid/protein complex.

REFERENCES

1. Pramanik, B.N.; Bartner, P.L.; Mirza, U.A.; Liu, Y.H.; Ganguly, A.K. Electrospray ionization mass spectrometry for the study of non-covalent complexes: an emerging technology. *J. Mass Spectrom.* **1998**, *33*, 911-920.

2. Ganguly, A.K.; Pramanik, B.N.; Huang, E.C.; Liberles, S.; Heimark, L.; Liu, Y.H.; Tsarbopoulos, A.; Doll, R.J.; Taveras, A.G.; Remiszewski, S.; Snow, M.E.; Wang, Y.S.; Vibulbhan, B.; Cesarz, D.; Brown, J.E.; del Rosario, J.; James, L.; Kirschmeier, P.; Girijavallabhan, V. Detection and Structural Characterization of Ras Oncoprotein-Inhibitors Complexes by Electrospray Mass Spectrometry. *Bioorg. Med. Chem.* **1997**, *5*, 817-820.

3. Compagnini, A.; Fisichella, S.; Foti, S.; Maccarrone, G.; Saletti, R. Isolation by gel-permeation chromatography of a non-covalent complex of Cibacron Blue F3G-A with human serum albumin. *J. Chromatography A.* **1996**, *736*, 115-123.

4. Chen, S.Y.; Matsuoka, Y.; Compans, R.W. Assembly of G1 and G2 glycoprotein oligomers in Punta Toro virus-infected cells. *Virus Res.* **1992**, *22*, 215-225.

5. Robyt, J.F.; White, B.J. *Biochemical techniques: Theory and Practice*; Waveland Press, Inc.: Prospect Heights, Illinois, 1987.

6. Karas, M.; Bachmann, D.; Bahr, U.; Hillenkamp, F. Matrix-assisted ultraviolet-laser desorption of nonvolatile compounds. *Int. J. Mass Spectrom. Ion Processes.* **1987**, *78*, 53-68.

7. Fenn, J.B.; Mann, M.; Meng, C.K.; Wong, S.F.; Whitehouse, C.M. Electrospray ionization for the mass spectrometry of large biomolecules. *Science.* **1989**, *246*, 64-71.

8. Nordhoff, E.; Kirpekar, F.; Roepstorff, P. Mass spectrometry of nucleic acids. *Mass Spectrom. Rev.* **1996**, *15*, 67-138.

9. Guo, B. Mass spectrometry in DNA analysis. *Anal. Chem.* **1999**, *71*, 333-337.

10. Griffiths, W.J.; Jonsson, A.P.; Liu, S.; Rai, D.K.; Wang, Y. Electrospray and tandem mass spectrometry in biochemistry. *Biochem. J.* **2001**, *355*, 545-561.

11. Bayer, E.; Bauer, T.; Schmeer, K.; Bleicher, K.; Maier, M.; Gaus, H. Analysis of double-stranded oligonucleotides by electrospray mass spectrometry. *Anal. Chem.* **1994**, *66*, 3858-3863.

12. Ding, J.; Anderegg, R.J. Specific and nonspecific dimer formation in the electrospray ionization mass spectrometry of oligonucleotides. *J. Am. Soc. Mass Spectrom.* **1995**, *6*, 159-164.

13. Cheng, X.; Gao, Q.; Smith, R.D.; Jung, K.; Switzer, C. Comparison of 3',5'- and 2',5'- linked DNA duplex stabilities by electrospray ionization mass spectrometry. *Chem. Commun.* **1996**, 747-748.

14. Smith, R.D.; Light-Wahl, K.J. The observation of noncovalent interactions in solution by electrospray-ionization mass spectrometry – promise, pitfalls, and prognosis. *Biol. Mass Spectom.* **1993**, *22*, 493-501.

15. Smith, D.L.; Zhang, Z. Probing noncovalent structural features of proteins by mass-spectrometry. *Mass Spectrom. Rev.* **1994**, *13*, 411-429.

16. Przybylski, M.; Glocker, M.O. Electrospray mass spectrometry of biomacromolecular complexes with noncovalent interactions - new analytical perspectives for supramolecular chemistry and molecular recognition processes *Angew. Chem. Int. Ed. Engl.* **1996**, *35*, 806-826.

17. Smith, R.D.; Bruce, J.E.; Wu, Q.; Lei, Q.P. New mass spectrometric methods for the study of noncovalent associations of biopolymers. *Chem. Soc. Rev.* **1997**, *26*, 191-202.

18. Loo, J.A. Studying non-covalent protein complexes by electrospray ionization mass spectrometry. *Mass Spectrom. Rev.* **1997**, *16*, 1-23.

19. Winston, R.L.; Fitzgerald, M.C. Mass spectrometry as a readout of protein structure and function. *Mass Spectrom. Rev.* **1997**, *16*, 165-179.

20. Veenstra, T.D. Electrospray ionization mass spectrometry in the study of biomolecular non-covalent interactions. *Biophys. Chem.* **1999**, *79*, 63-79.

21. Schalley, C.A. Molecular recognition and supramolecular chemistry in the gas phase. *Mass Spectrom. Rev.* **2001**, *20*, 253-309.

22. Daniel, J.M.; Friess, S.D.; Rajagopalan, S.; Wendt, S.; Zenobi, R. Quantitative determination of noncovalent binding interactions using soft ionization mass spectrometry. *Int. J. Mass Spectrom.* **2002**, *216*, 1-27.

23. Gabelica, V.; Vreuls, C.; Filee, P.; Duval, V.; Joris, B.; De Pauw, E. Advantages and drawbacks of nanospray for studying noncovalent protein-DNA complexes by mass spectrometry. *Rapid Commun. Mass Spectrom.* **2002**, *16*, 1723-1728.

24. Donald, L.J.; Hosfield, D.J.; Cuvelier, S.L.; Ens, W.; Standing, K.G.; Duckworth, D.C. Mass spectrometric study of the *Escherichia coli* repressor proteins, IcIR and GcIR, and their complexes with DNA. *Protein Sci.* **2001**, *10*, 1370-1380.

25. Triolo, A.; Arcamore, F.M.; Raffaelli, A.; Salvadori, P. Non-covalent complexes between DNA-binding drugs and double-stranded deoxyoligonucleotides: a study by ionspray mass spectrometry. *J. Mass Spectrom.* **1997**, *32*, 1186-1194.

26. Sarni-Manchado, P.; Cheynier, V. Study of non-covalent complexation between catechin derivatives and peptides by electrospray ionization mass spectrometry. *J. Mass Spectrom.* **2002**, *37*, 609-616.

27. Nishimura, S.; Sekiaya, T. Human cancer and cellular oncogenes. *Biochem. J.* **1987**, *243*, 313-327.

28. Hall, A. The cellular functions of small GTP-binding proteins. *Science.* **1990**, *249*, 635-640.

29. De Vos, A.M.; Tong, L.; Milburn, M.V.; Matias, P.M.; Jancarik, J.; Noguchi, S.; Nishimura, S.; Miura, K.; Ohtsuka, E.; Kim, S.H. Three-dimensional structure of an oncogene protein: catalytic domain of human c-H-ras p21. *Science* **1988**, *239*, 888-893.

30. Taveras, A.G.; Remiszewski, S.W.; Doll, R.J.; Cesarz, D.; Huang, E.C.; Kirschmeier, P.; Pramanik, B.N.; Snow, M.E.; Wang, Y.S.; delRosario, J.D.; Vibulbhan, B.; Bauer, B.B.; Brown, J.E.; Carr, D.; Catino, J.; Evans, C.A.; Girijavallabhan, V.; Heimark, L.; James, L.; Liberles, S.; Nash, C.; Perkins, L.; Senior, M.M.; Tsarbopoulos, A.;, Ganguly, A.K.;, Aust, R.;, Brown, E.;, Delisle, D.; Fuhrman, S.; Hendrickson, T.; Kissinger, C.; Love, R.; Sisson, W.; Villafranca, E.; Webber S.E. Pas oncoprotein inhibitors: the discovery of potent, ras nucleotide exchange inhibitors and the structural determination of a drug-protein complex. *Bioorg. Med. Chem.* **1997**, *5*, 125-133.

31. Robinson, C.V.; Chung, E.W.; Kragelund, B.B.; Knudsen, J..; Aplin, R.T.; Poulsen, F.M.; Dobson, C.M. Probing the nature of noncovalent interactions by mass spectrometry: a study of protein-CoA ligand binding and assembly. *J. Am. Chem. Soc.* **1996**, *118*, 8646-8653.

32. Ray, A.; Nordén, B. Peptide nucleic acid (PNA): its medical and biotechnical applications and promise for the future. *FASEB J.* **2000**, *14*, 1041-1060.

33. Butler, J.M.; Jiang-Baucom, P.; Huang, M.; Belgrader, P.; Girard, J. Peptide nucleic acid characterization by MALDI-TOF mass spectrometry. *Anal. Chem.* **1996**, *68*, 3283-3287.

34. Lin, S.; Cotter, R.J.; Woods, A.S. Detection of non-covalent interaction of single and double stranded DNA with peptides by MALDI-TOF. *Proteins* **1998**, *33*, 12-21. Supplement 2.

35. Thiede, B.; von Janta-Lipinski, M. Noncovalent RNA-peptide complexes detected by matrix-assisted laser desorption/ionization mass spectrometry. *Rapid Commun. Mass Spectrom.* **1998**, *12*, 1889-1894.

36. Lecchi, P.; Panell, L.K. The detection of intact double-stranded DNA by MALDI. *J. Am. Soc. Mass Spectrom.* **1995**, *6*, 972-975.

37. Kirpekar, F.; Berkenkamp, S.; Hillenkamp, F. Detection of double-stranded DNA by IR- and UV-MALDI mass spectrometry. *Anal. Chem.* **1999**, *71*, 2334-2339.

38. Little, D.P.; Jacob, A.; Becker, T.; Braun, A.; Darnhofer-Demar, B.; Jurinke, C.; van den Boom, D.; Köster, H. Direct detection of synthetic and biologically generated double-stranded DNA by MALDI-TOF MS. *Int. J. Mass Spectrom. Ion Processes.* **1997**,*169/170*, 323-330.

39. Tang, K.; Taranenko, N.I.; Allman, S.L.; Chen, C.H.; Chang, L.Y.; Jacobson, K.B. Picolinic-acid as a matrix for laser mass-spectrometry of nucleic-acids and proteins. *Rapid Commun. Mass Spectrom.* **1994**, *8*, 673-677.

II. Instrumentation

Time-of-Flight Mass Spectrometry

Matrix-assisted laser desorption/ionization mass spectrometry is a pulsed technique. For this reason, MALDI is often coupled to a time-of-flight (TOF) mass analyzer. In TOF-MS, the ions formed in the MALDI process are accelerated out of the ion source to a fixed kinetic energy and the velocity of the ions is dependent on their mass-to-charge (m/z) ratio. Ions of different m/z values will then separate from each other and strike the detector at varying times. The m/z values of the ions can then be determined by measuring the flight time. In most TOF instruments, the accelerating voltage is between 10-30 kV. The path lengths are typically 0.5-3 m.

Time-of-flight mass analyzers have several advantages when compared to other types of mass analyzers. First, TOF mass analyzers allow for the analysis of ions with large m/z values. Time-of-flight instruments also have good mass accuracy with deviations of 1 Da for m/z 5000 and is the only mass analyzer to measure within 100 Da for m/z 50,000 [1]. The TOF instruments also exhibit great sensitivity and scanning speed. Many recent advancements in TOF technology have contributed to the success of the technique [2].

However, TOF instruments have several disadvantages. Time-of-flight mass analyzers have a poor dynamic range. There is also a no potential for tandem mass spectrometry (MS/MS) experiments on a linear TOF and only a limited with potential reflectron TOF instruments. While deviations of 1 Da can be seen with ions around m/z 5000, this still does not allow for exact mass determination. Time-of-flight is also limited by the resolution. In both linear and reflectron TOF instruments, the ions formed from

MALDI often have a large energy distribution. The initial energy spread of the ions leads to peak broadening at the detector leading to poor mass resolution.

Two time-of-flight mass spectrometers were used in this work. The first is the PerSeptive Biosystems (Framingham, MA) Voyager DE, delayed-extraction time-of-flight linear (TOF) mass spectrometer equipped with a nitrogen laser (337 nm, 3 ns pulse), Figure 1.3. This mass spectrometer was a linear instrument that did not have reflectron or PSD capabilities. The length of the flight tube was 1.2 meters.

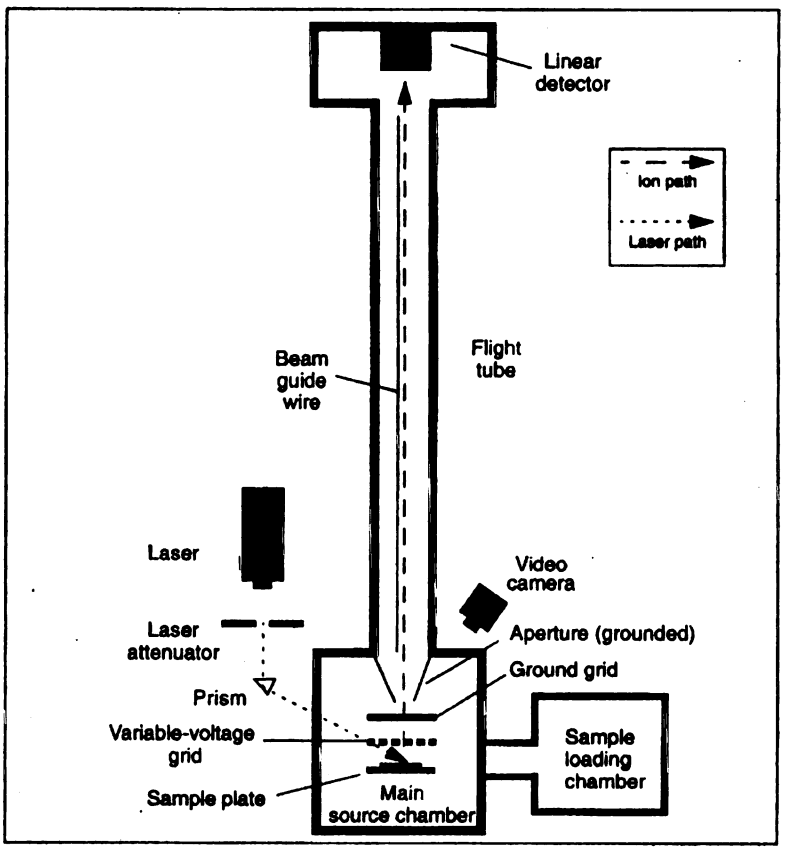

Figure 1.3. Schematic of a Voyager-DE mass spectrometer. This figure was reproduced from reference 3.

While TOF instruments have very limited capabilities for MS/MS experiments, many reflectron instruments are capable of performing post-source decay (PSD)

experiments. PSD analysis allows for the detection of fragment ions formed in the field-free region of the mass spectrometer [4]. These fragment ions are structurally significant and can often provide clues as to the structure of the precursor ion. For those PSD spectra shown in this work, an instrument in the Michigan State University Mass Spectrometry Facility (East Lansing, MI) was used. This instrument was the PerSeptive Biosystems (Framingham, MA) Voyager STR, delayed-extraction time-of-flight reflectron mass spectrometer, Figure 1.4. This instrument is also equipped with a nitrogen laser (337 nm, 3 ns pulse), but has a longer flight tube of 2.0 meters.

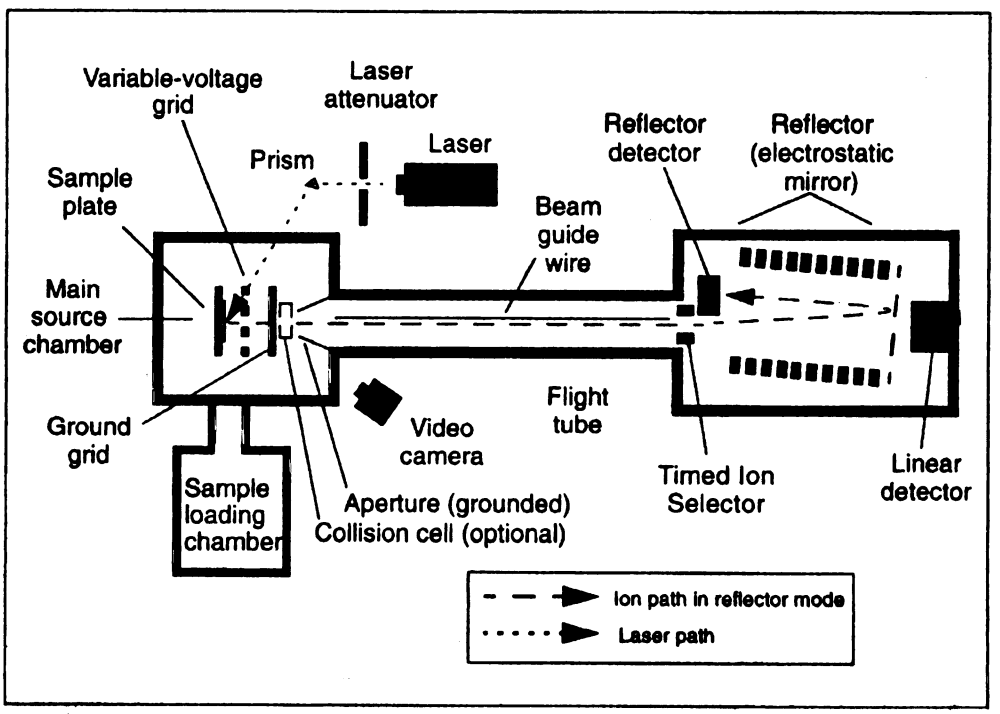

Figure 1.4. Schematic of a Voyager-DE STR mass spectrometer. This figure was reproduced from reference 3.

Fourier Transform Mass Spectrometry

The technique of Fourier transform mass spectrometry (FTMS) is based on a phenomenon called ion cyclotron resonance (ICR). In a uniform magnetic field, an ion will move in a circular orbit around the center of the magnetic field in a periodic motion. This motion is known as cyclotron motion and the frequency of this motion is known as the cyclotron frequency. In this technique, the resolution seen in the resulting spectra is much higher than in TOF experiments. In TOF, the resolution is lowered by the distribution of kinetic energies present for ions of having the same m/z value. In FTMS, there is no dependence on kinetic energy, only a dependence on the cyclotron frequency of the ions. Since all ions of a given m/z value will have the same cyclotron frequency, the resolving power of this technique is very high. A decrease in resolution during an FTMS experiment can be caused by a space-charge effect [5]. If too many ions are stored in the cell, ions of the same m/z value, traveling in a packet, will begin to repel each other. This repulsion will increase the distribution of the ions in the cell decreasing resolution and also affected the mass accuracy [6]. A number of reviews have been written on the technique [7-8].

In a typical FTMS experiment, resolution of 30000 can be attained. FTMS exhibits high mass accuracy as well with errors less than 5 parts per million (ppm). In addition to the high resolution and mass accuracy of the technique, FTMS has the ability to perform MS/MS experiments. Ions trapped within the FTMS cell collide with neutral gas molecules and induce fragmentation of the analyte ions. This allows structural information to be determined using FTMS. While the MS/MS experiments in FTMS are similar to PSD experiments, the fragmentation patterns differ in the two techniques.

There are usually more fragment ions formed in the FTMS experiment and FTMS also allows for higher order experiments ($MS/MS/MS....MS^n$).

Time-of-Flight versus Fourier Transform Mass Spectrometry

In a typical FTMS experiment, resolution of 30000 can be attained while in a TOF experiment resolution of less than 1000 is typically seen. In order to demonstrate the change in resolution that can be expected for FTMS, it is important to see spectra from both techniques. In Figure 1.5(A), this is a mass spectrum from a MALDI-TOF experiment for a protein around 5200 Da. In Figure 1.5(B), this is a deconvoluted ESI spectrum for an FTMS experiment for the same protein. A drastic increase in resolution is seen when compared to the resolution achieved in the TOF experiment. For comparison, in figure 1.5(C), there is a theoretical isotope distribution for the same protein. The FTMS technique allows comparisons to be drawn between the expected isotope pattern and that recorded in the mass spectrum.

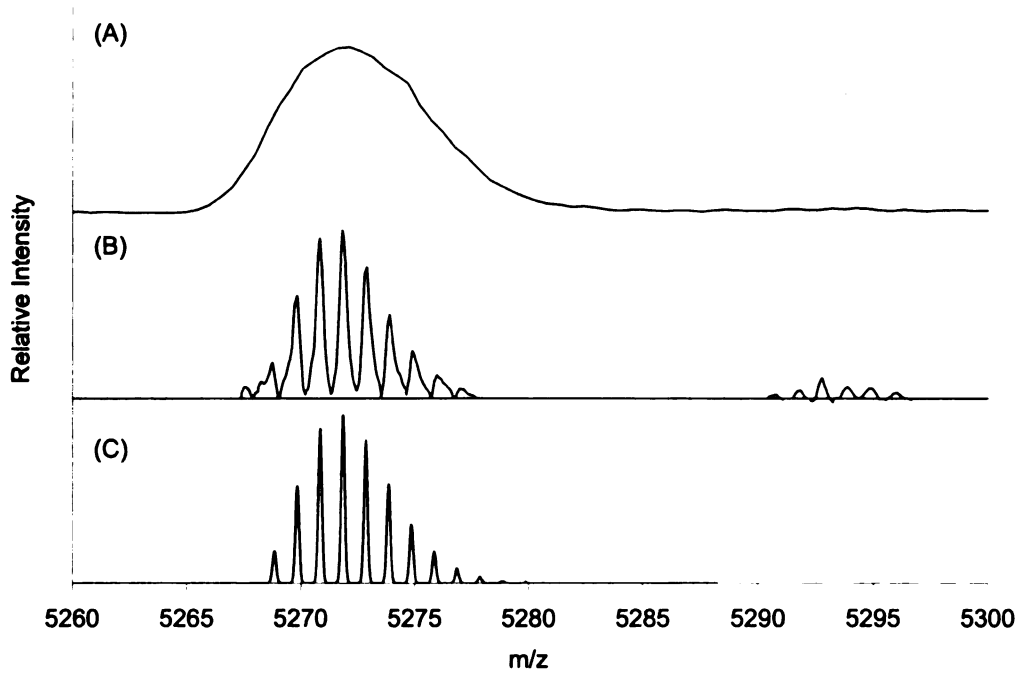

Figure 1.5. (A) UV MALDI-TOF mass spectrum of a protein with a molecular weight around 5270 Da. (B) Deconvoluted ESI-FTICR mass spectrum of the same protein. (C) Theoretical isotope distribution of the protein.

Also, it is important to note the increased mass accuracy. In the TOF experiment, the mass for the peak could be determined within ± 1 mass unit. In the FTMS experiment, the mass error of each of the peaks was less than 5 ppm different than the mass of the peaks shown in the theoretical distribution.

References

1. Jennings, K.R.; Dolnikowski, G.G. Mass analyzers. In *Methods in Enzymology,* McCloskey, J.A., Ed.; Academic Press, Inc.: San Diego, CA, 1990; p. 55.

2. Weickhardt, C.; Moritz, F.; Grotemeyer, J. Time-of-flight mass spectrometry: state-of-the-art in chemical analysis and molecular science. *Mass Spectrom. Reviews,* **1996**, *15*, 139-162.

3. PerSeptive Biosystems, Inc. *Voyager Biospectrometry Workstation with Delayed Extraction™ Technology: User's Guide.* Framingham, MA: PE Biosystems, 1999.

4. Spengler, B. Post-source decay analysis in matrix-assisted laser desorption/ionization mass spectrometry of biomolecules. *J. Mass Spectrom.* **1997**, *32*, 1019-1036.

5. Taylor, P. K.; Amster, I. J. Space charge effects on mass accuracy for multiply charged ions in ESI-FTICR. *Int. J. Mass Spectrom.* **2003**, *222*, 351-361.

6. Easterling, M. L.; Mize, T. H.; Amster, I. J. Routine ppm mass accuracy for high mass ions: space-charge effects in MALDI FT-ICR. *Anal. Chem.* **1999**, *71*, 624-632.

7. Amster, I.J. Fourier transform mass spectrometry. *J. Mass Spectrom.* **1996**, *31*, 1325-1337.

8. Dienes, T.; Pastor, S.J.; Schürch, S.; Scott, J.R.; Yao, J.; Cui, S.; Wilkins, C.L. Fourier transform mass spectrometry-advancing years (1992-Mid. 1996). *Mass Spectrom. Reviews*, **1996**, *15*, 163-211.

CHAPTER 2. STABILIZATION OF DOUBLE-STRANDED DNA IN MALDI MS

I. Structure of DNA

In order to understand the behavior of an analyte in the MALDI experiment, the structure of the analyte must be taken into account. Deoxyribonucleic acid (DNA) is a biopolymer consisting of subunits called nucleotides, Figure 2.1 (A). A nucleotide is composed of a nitrogen containing base: adenine (A), thymine (T), cytosine (C), or guanine (G), Figure 2.1 (B). These nitrogen bases are covalently bound to a deoxyribose sugar that has a phosphate group bound to the 5' carbon. Nucleotides are joined together by a phosphodiester linkage from the 5'-hydroxyl group of one nucleotide attached to the 3'-hydroxyl group of a neighboring nucleotide. This is demonstrated in the schematic of DNA structure shown in Figure 2.1 (A). Several nucleotides bound together are referred to as an oligonucleotide. The uniqueness of oligonucleotide strands resides in the sequence of the bases.

There are many interactions present in double-stranded DNA (dsDNA), but a major focus in simple discussions is the base-specific pairing via hydrogen bonding. Opposing strands are held together by two hydrogen bonds between an adenine-thymine base pair and three hydrogen bonds between a cytosine-guanine base pair. When adenine binds to thymine and cytosine binds to guanine, it is referred to as Watson-Crick base pairing. To form double-stranded DNA, or duplex DNA, two complementary oligonucleotide strands are non-covalently bound together by Watson-Crick base pairing. When the two strands are bound together to form the duplex, the strands bind antiparallel

to each other. In other words, the 5' end of one strand will bind to the 3' end of the other strand, Figure 2.1 (A).

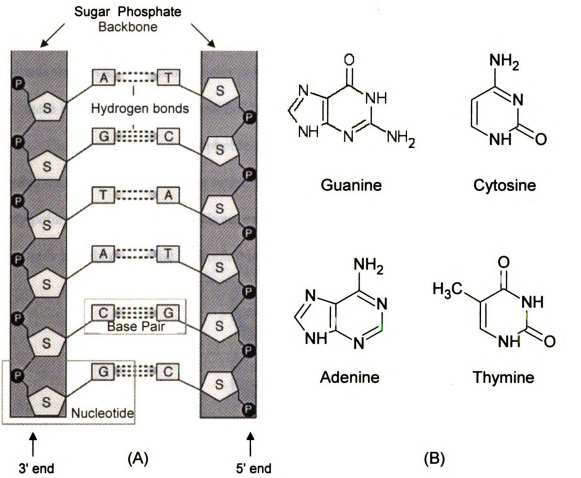

Figure 2.1. (A) Double-stranded DNA. The oligonucleotide strands are composed of nucleotide repeating units. The 3' end of one strand bind to the 5' end of its complement. (B) Structure of the nitrogen bases. There are 3 hydrogen bonds formed in G-C base pairs and two hydrogen bonds formed in A-T base pairs. S represents the sugar, deoxyribose, and P represents the phosphate group bound to the 5' end of the nucleoside. This figure was adapted from reference 1.

When two oligonucleotides are bound together, the two chains twist together to form a right-handed double-helix. In this helical structure, the hydrophobic nitrogen

bases from each chain are stacked in pairs. These base pairs are in close proximity to each other and are situated perpendicular to the long axis of the double helix. The hydrophilic backbone, consisting of alternating sugars and negatively-charged phosphate groups, runs along the outside of the helix. This backbone is exposed to that water that surrounds the DNA. The double helix is held together entirely by non-covalent forces. First, there is hydrogen bonding that holds together the complementary bases of opposing strands. Then, there are the hydrophobic interactions. These non-covalent interactions are what cause the bases to tucked inside the double helix, shielded from water with the highly polar sugar-phosphate backbone exposed, Figure 2.2. The stability of the helical structure is largely due to the hydrophobic interactions.

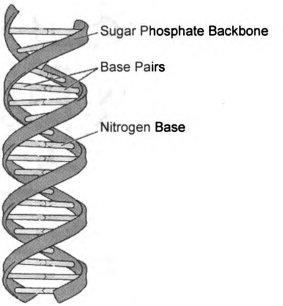

Figure 2.2. Double-helical structure of DNA. The hydrophobic bases are stacked within the double-helix while the sugar-phosphate backbone is exposed. This figure was adapted from reference 1.

In addition to the base pairing and hydrophobic interactions that occurs in DNA, there are many other interactions that take place. In cells, DNA is negatively charged due

to the ionization of hydroxyl groups in the phosphodiester backbone. The phosphate groups are affiliated with counter ions such as sodium, calcium, magnesium, and protonated amines [2,3]. These various cations are responsible for stabilizing the DNA by reducing the repulsive forces between the phosphate backbones of the complementary strands. The cations also contribute to the compact tertiarystructure of the DNA. An X-ray crystal structure of the duplex, d(CGCGAATTCGCG)$_2$, is shown in Figure 2.3. In the crystal structure, there are several examples of species known to affiliate with DNA including magnesium, spermine, and water molecules. Even during the crystal-growth process, the water remains bound the oligonucleotide.

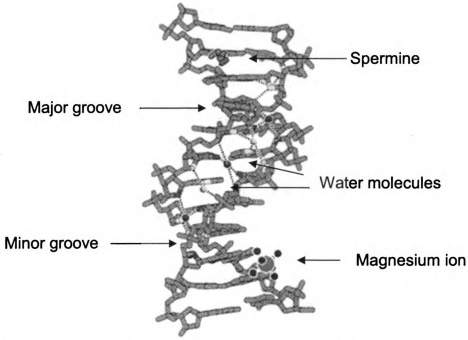

Figure 2.3. X-ray crystal structure of a d(CGCGAATTCGCG)$_2$. This figure was adapted from reference 2.

For an oligonucleotide consisting of 12 bases, the 11 phosphate groups can accumulate a charge as great as –11. The neutral oligonucleotide with fully protonated phosphate groups, (O^{-11} + 11 H^+), is referred to as the free acid form, or M. Oligonucleotide ions are detected in a protonated, $(M + H)^+$, or deprotonated, $(M - H)^-$, form. Although both the protonated and deprotonated species will be studied, here we focus in this discussion on the negative ions, since they are generated in higher abundance and exhibit greater resolution in MALDI MS than the positive ion forms [4].

Oligonucleotides and DNA have many interesting and unique properties. The UV spectroscopic properties of oligonucleotides are particularly relevant to this work. Oligonucleotides exhibit strong absorption maxima around 259 nm. This absorption is due to the electronic transitions in the purine and pyrimidine bases. The molar extinction coefficient of an oligonucleotide is dependent on the state of the base-pairing interactions. When a double-stranded oligonucleotide is formed, there is a decrease in the molar extinction coefficient, a hypochromic effect. When heated, a solution of double-stranded DNA should yield a 10% increase in absorbance due to this effect [5]. When the UV absorption of a nucleic acid sample is measured as a function of temperature, the resulting plot is known as a melting curve, Figure 2.4. At low temperatures, the oligonucleotide solution has a low absorbance. As the temperature increase, the double helix begins to denature. As the duplex denatures, the absorbance of the solution increases until duplex completely dissociates. The midpoint in the increase of absorption versus temperature is known as the melting temperature, T_m. This point is marked in Figure 2.4.

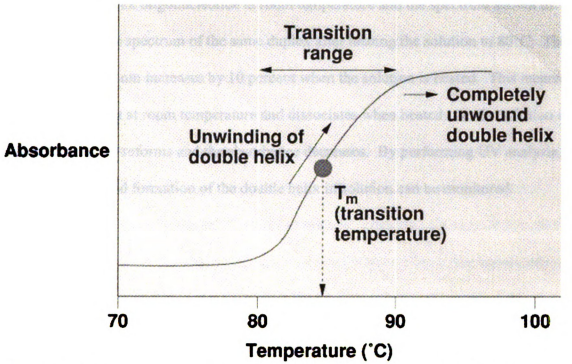

Figure 2.4. Melting temperature plot of a double-stranded oligonucleotide. Absorbance is plotted as a function of temperature. This figure was taken from reference 6.

The melting temperature is important because it is an indication of how stable a duplex will be at room temperature. Much research has been done on the melting temperature of oligonucleotides [7-10]. Generally, T_m increases with the length of the strands, increases with the salt concentration of the solution, and is dependent on the sequence of the bases and the types of counter-ions present [11]. The DNA structure is known to be sensitive to changes in ionic strength [12]. Melting point studies carry important information on duplex stability that should be considered in the analysis of the solution phase aspects of the experiment.

The melting temperature studies shown in this work will be displayed as a plot of the absorbance of the oligonucleotide solution as a function of wavelength. An example of a melting temperature study is shown in Figure 2.5. The UV spectrum in black is the

spectrum of a duplex oligonucleotide at room temperature and the spectrum shown in grey represents the spectrum of the same duplex after heating the solution to 80°C. The absorbance at 259 nm increases by 10 percent when the solution is heated. This means the duplex is intact at room temperature and dissociates when heated. As the solution is cooled, the duplex reforms and the absorbance decreases. By performing UV analysis, the dissociation and formation of the double helix in solution can be monitored.

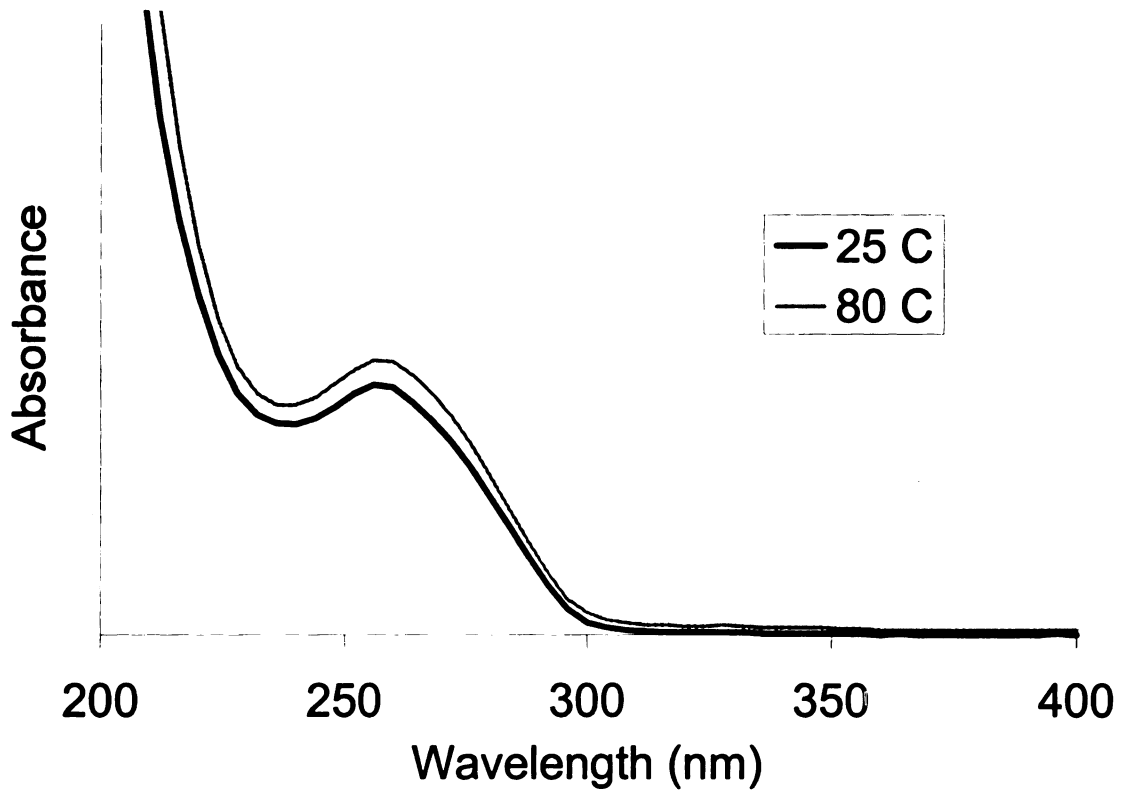

Figure 2.5. UV melting temperature study of a duplex oligonucleotide in solution.

For the majority of the work shown here, two duplex oligonucleotides were used. Several important aspects of the experiment were considered when selecting oligonucleotides to analyze using MALDI MS. First, the mass of the oligonucleotide is important. As the molecular weight increases, the obtainable resolution decreases for a

time-of-flight experiment. In order to study oligonucleotides bound to a small drug or a metal such as platinum, the resolution must be sufficiently high. For this reason, double-stranded species with molecular weights lower than 10,000 g/mol are desired. The size is also important regarding the stability of the duplex. Short sequences can have melting temperatures below room temperature, but duplexes of complementary strands, each with at least 10 bases, have melting points greater than 30° C [13]. It is also important to understand the behavior of the single-stranded species in the MALDI experiment. Are both strands detected in the experiment and how does this correlate to the appearance of the double-stranded ion? In order to study differences in ionization between the two strands, there must be a significant mass difference between them.

The duplex oligonucleotides used in these experiments are shown in Table 2.1. The table lists the three duplexes used in this work. The duplex sequences are written in the 5' to 3' direction for the top sequence and the 3' to 5' direction for the bottom sequence. This demonstrates the base pairing that takes place in the duplex. The average molecular weights for the single-stranded oligonucleotides are written in the column next to the sequence. The abbreviation M_1 will be used to denote the strand of lower molecular weight and M_2 will be used to denote the strand of higher molecular weight. The column labeled **Duplex MW** lists the molecular weight information for the duplex with specific base-pairing (Watson-Crick base pairing) listed as M_1M_2 as well as the molecular weight information for the non-specific duplexes, M_1M_1 and M_2M_2. The last column provides the melting temperature for the duplex. This provides insight into the stability of the duplexes at room temperature.

Table 2.1. Duplexes Used in This Work

Name	Sequence	Oligonucleotide MW(avg) in g/mol	Duplex MW (avg) in g/mol	T_m (°C)
Duplex 1	CCGGAATTGGCC GGCCTTAACCGGTT	3646 (M_1) 4254 (M_2)	7292 (M_1M_1) 7900 (M_1M_2) 8508 (M_2M_2)	40
Duplex 2	TTTTTGGTTTTT AAAAACCAAAAA	3638 (M_1) 3648 (M_2)	7276 (M_1M_1) 7286 (M_1M_2) 7296 (M_2M_2)	28
Duplex 3	ACCCACCCACCC TGGGTGGGTGGG	3480 (M_1) 3813 (M_2)	6960 (M_1M_1) 7293 (M_1M_2) 7626 (M_2M_2)	42

Duplex 1 will be most often used in the duplex DNA experiments. This duplex has a melting point of 40 °C. The single strands of duplex 1 differ by 608 g/mol due to the two thymine extension on the one strand. They also contain the CG and AT binding motifs on the single strand. These motifs are necessary for the binding of many drugs. Lastly, a desirable oligonucleotide would not be self-complementary in order to prove that Watson-Crick pairing has been preserved. For example, suppose two strands, M_1 and M_2, are complementary. These strands are annealed together to form a duplex. When analyzed using MALDI, there are many possible ions that may be observed including $(M_1M_1-H)^-$, $(M_1M_2-H)^-$, and $(M_2M_2-H)^-$. If all three species are detected in a 1:2:1 ratio of intensities, the complexes are produced at random and we would assume that the Watson-Crick base pairing has not been maintained. If the strand is self-complementary, the spectrum provides no information on non-specific complexation. In the case of duplex 1, the specific and non-specific complexes would have mass differences of 608 Da making the complexes easy to distinguish.

While the Dickerson dodecamer, d(CGCGAATTCGCG), does not meet all of the criteria, it will also be used in many experiments. This oligonucleotide has been the subject of many studies and much is known about its interactions with salts and polyamines [2]. This nucleic acid also contains the adjacent CG and AT rich region needed to bind drugs. There is much data on the binding of the Dickerson dodecamer to chemotherapeutic drugs such as Hoechst 33258 [14]. For this reason, it will be a useful tool for analysis.

References

1. Leja, Darryl. N.D. Jan. 6, 2003. DNA-A More Detailed Description http://www.accessexcellence.org/AB/GG/dna2.html.

2. Shui, X.; McFail-Isom, L.; Hu, G.G.; Williams, L.D. The B-DNA dodecamer at high resolution reveals a spine of water on sodium. *Biochemistry.* **1998**, *37*, 8341-8355.

3. Halle, B.; Denisov, V.P. Water and monovalent ions in the minor groove of B-DNA oligonucleotides as seen by NMR. *Biopolymers.* **1998**, *48*, 210-233.

4. Nordhoff, E.; Cramer, R.; Karas, M.; Hillenkamp, F.; Kirpekar, F.; Kristiansen, K.; Roepstorff, P. Ion stability of nucleic acids in infrared matrix-assisted laser desorption/ionization mass spectrometry. *Nucleic Acids Res.* **1993**, *21*, 3347-3357.

5. Norman, D. Techniques applied to nucleic acids. In *Nucleic Acids in Chemistry and Biology* (eds. Blackburn, G.M.; Gait, M.J.), Oxford University Press, **1996**, 445-499.

6. Campbell, M.K. *Biochemistry*, 3rd ed.; Harcourt Brace and Company: Orlando, FL, 1999, Text Figure 07.13.

7. Marky, L.A.; Breslauer, K.J. Calculating thermodynamic data for transitions of any molecularity from equilibrium melting curves. *Biopolymers*, **1987**, *26*, 1601-1620.

8. Blake, R.D. Cooperative lengths of DNA during melting. *Biopolymers*, **1987**, *26*, 1063-1074.

9. Gotoh, O.; Tagashira, Y. Stabilities of nearest-neighbor doublets in double-helical DNA determined by fitting calculated melting profiles to observed profiles. *Biopolymers*, **1981**, *20*, 1033-1042.

10. Korolev, N.I.; Vlasov, A.P.; Kuznetsov, I.A. Thermal denaturation of Na- and Li-DNA in salt-free solutions. *Biopolymers*, **1994**, *34*, 1275-1290.

11. Schildkraut, C.; Lifson, S. Dependence of the melting temperature of DNA on salt concentration. *Biopolymers.* **1965**, *3*, 195-208.

12. McConnell, K.J.; Beveridge, D.L. DNA structure: what's in charge? *J. Mol. Biol.* **2000**, *304*, 803-820.

13. Tong,B.Y.; Leung, M.L.C. Correlation between percentage guanine-cytosine content and melting temperature of deoxyribonucleic acid. *Biopolymers*. **1977**, *16*, 1223-1231.

14. Quintana, J.R.; Lipanov, A.A.; Dickerson, R.E. Low-temperature crystallographic analyses of the binding of Hoechst 33258 to the double-helical DNA dodecamer CGCGAATTCGCG. *Biochemistry*. **1991**, *30*, 10294-10306.

II. Oligonucleotides and Mass Spectrometry

Matrix-assisted laser desorption/ionization mass spectrometry (MALDI MS), developed by Karas *et al.*[1], has been extensively used to analyze biological compounds at the sub-picomole level. To date, most of the published MALDI MS work has involved the analysis of peptides and proteins, but some work has been done using oligonucleotides [2,3]. The development of MALDI matrices optimized for the analysis of oligonucleotides has lagged behind that for peptides [4], but is currently receiving considerable attention.

Oligonucleotides and DNA behave very differently than peptides and proteins in the MALDI experiment. Differences of note include the sensitivity, resolution, extent of prompt fragmentation, and the need for cleanup prior to analysis. For all classes of biomolecules studied by MALDI, as sample handling methods and TOF instruments have been developed, typical sample sizes used for analysis have decreased. Peptide analysis at the subpicomole level was rapidly achieved, while it has taken longer to realize similar MALDI detection limits for oligonucleotides. There have been significant advances from earlier reports of MALDI analyses of oligonucleotides, in which 10-100 pmol of material were required, to recent reports that show oligonucleotide detection at the femtomole level [5,6].

When a pure peptide is analyzed by MALDI-TOF MS, it usually yields a single mass spectrometric peak representing the intact molecule in either a protonated or a deprotonated form. Matrices and sample conditions have been reported to increase the extent of prompt fragmentation of peptides in MALDI [7], but generally there is little predictable control over the process. In contrast, oligonucleotides frequently fragment

promptly and extensively in linear time-of-flight mass spectrometry [8]. While fragmentation is useful for structure determination, a decrease in sensitivity can also be seen.

In terms of the spectra that result, salts have a very different impact when analyzing peptides compared to oligonucleotides. The analysis of pure samples certainly makes mass spectral interpretation easier for all biomolecules. Depending on whether compounds are isolated from biological sources, from electrophoresis experiments (gels or membranes), or are synthesized, peptides and oligonucleotides may be presented for MS analysis in the presence of compounds such as salts, buffers, and glycerol, frequently in higher relative amounts than the analytes. In all cases, high amounts of salts can sufficiently change the MALDI target material to lower analyte signals. The presence of compounds, such as glycerol, can lead to problems during the crystal growth step of the MALDI experiment is to grow crystals. Salts in the analyte or matrix solutions can also be very detrimental. If NaCl is present, two peaks may appear representing a single peptide in positive ion mode, most frequently representing the $[M+H]^+$ and $[M+Na]^+$ ions, separated by 22 Da. As the salt contribution increases, sodium adducts become more intense. The presence of salts has a much more dramatic influence on the MALDI spectra of oligonucleotides, Figure 2.6. With an ionic phosphodiester backbone, oligonucleotides can contain a large number of anionic sites that must combine with an assortment of cationic species such as H^+, Na^+ and K^+ to desorb in a singly-charged form. Combinations of cations to provide a charge balance can lead to a substantial number of peaks representing the intact molecule. Whenever ions for a single species are generated with a range of m/z values, detection limits are lowered. Also, it becomes much more

difficult to detect multiple components of similar mass. The ideal situation is to generate one mass spectral peak per component and not several peaks. In Figure 2.6, there are up to four sodium ions bound to the phosphate groups of the oligonucleotide. As a result, multiple peaks in the spectrum represent the intact oligonucleotide.

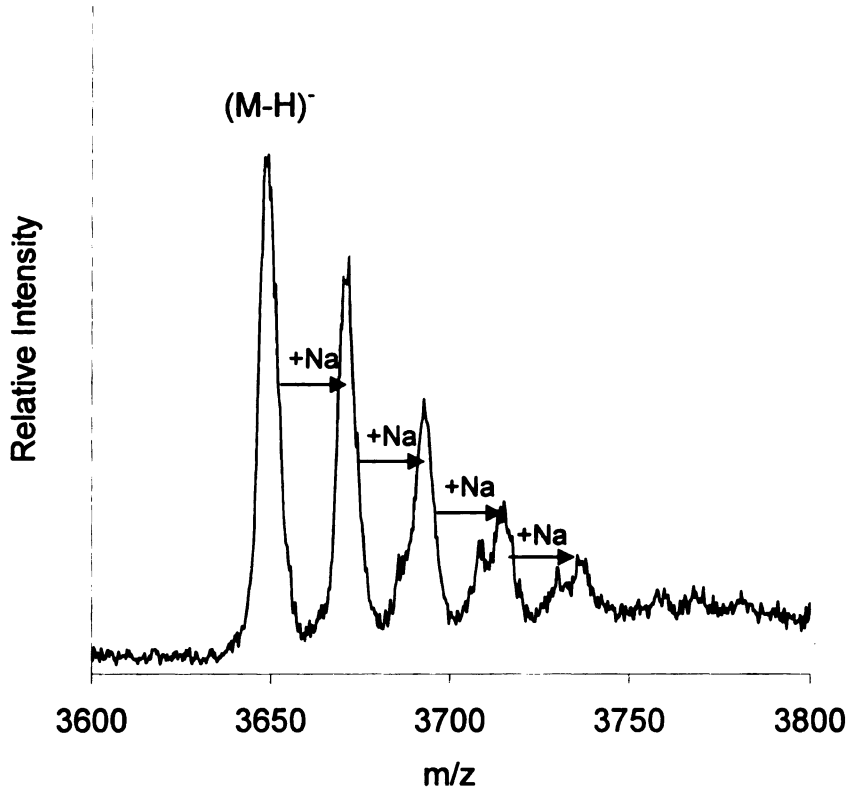

Figure 2.6. Negative-ion MALDI mass spectrum of the Dickerson dodecamer, d(CGCGAATTCGCG), using HPA as the matrix. There are four sodium ions bound to the oligonucleotide.

In the analysis of oligonucleotides by MALDI TOF MS, the resolution achieved is often less than what would be realized for peptides of similar size. Adduct formation and nucleotide base loss have frequently been cited as causes of the reduced resolution [9]. For larger oligonucleotides, this is clearly the case. However, even for smaller sequences with resolved sodium and potassium adducts, resolution for an oligonucleotide

peak is less than that obtained for a peptide peak of similar mass on the same instrument. The use of an ion reflector does not dramatically improve the resolution of oligonucleotides in MALDI-MS [10]. Often, we were unable to detect oligonucleotides using the reflectron mode of the mass spectrometer. One of the few instances in which relatively small oligonucleotides were analyzed by MALDI and spectra containing isotopic resolution were obtained was recently published, using a MALDI TOF instrument with an extended flight tube [11].

The differences in MALDI analysis of oligonucleotides and peptides are evident when examining Figure 2.7. In Figure 2.7 (A), an oligonucleotide with a molecular weight around 3600 g/mol has been analyzed in negative-ion mode using ATT as the matrix. In Figure 2.7 (B), a peptide of similar mass to the oligonucleotide has been analyzed in positive-ion mode using the same matrix. There are some notable differences. First, when looking at the peaks representing the molecular ion in each spectrum, the peptide peak has much higher resolution than that of the oligonucleotide peak. In Figure 2.7 (B), there is only one peak detected that represents the intact peptide ion. No fragmentation has occurred and no alkali ions are seen bound to the peptide. When examining figure 2.7 (A), there is extensive fragmentation. Peaks representing fragment ions from the oligonucleotide are more intense than the peak representing the intact, deprotonated oligonucleotide. Also, there are two resolved peaks that have higher m/z values than that of the oligonucleotide. The first peak represents a sodium ion binding to a phosphate and the second peak represents a potassium ion binding to a phosphate. Since there are three species detected that all represent the intact

oligonucleotide, there is a decrease in sensitivity of the analyte. The sensitivity is also decreased by the fragmentation of the analyte.

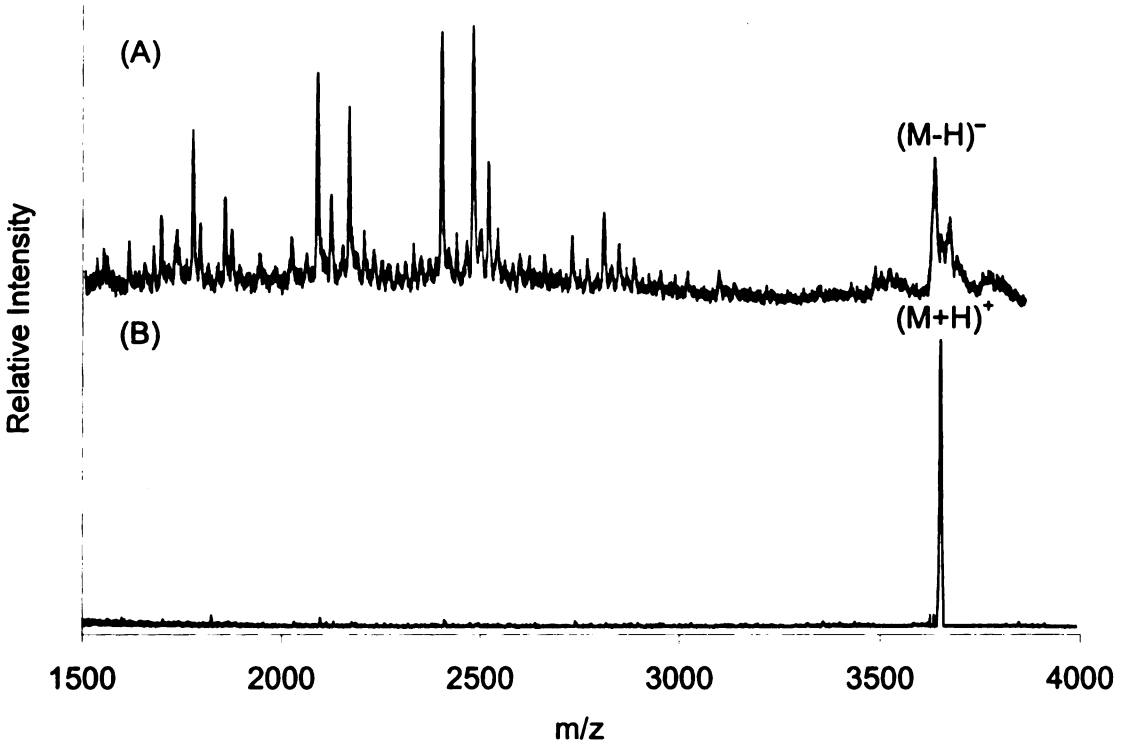

Figure 2.7. MALDI mass spectrum of (A) an oligonucleotide taken in negative-ion mode and (B) a peptide taken in positive-ion mode. ATT was the matrix for both experiments.

While peptides and oligonucleotides have many differences in terms of their MALDI MS analysis, they also have some notable similarities in terms of the development of the analytical utility of MS for their analysis. Early in the history of MALDI, demonstrations of the ability to generate signals from large, intact, ionized proteins maintained excitement for this new method, allowing it to be further developed. While positive results have been reported for proteins with molecular weights of several hundred thousand, the mass spectral peaks were very broad, and it was difficult to extract what would be considered an accurate mass. The early results showed that, in most cases, the molecular weight information determined from MALDI MS was more useful

than that derived from gel electrophoresis. Today, the real strength of MALDI in protein analysis does not lie in its ability to generate ions of intact proteins, but in the subpicomolar sensitivity obtainable for smaller peptides. The analysis of enzymatic and chemical digestion products is the application contributing greatly to protein analysis.

Scientists have certainly worked to demonstrate that large oligonucleotides can be characterized by MALDI as well. While a few reports have been published demonstrating the detection of oligonucleotides containing 50 or greater bases, the MALDI response is much more sharply a function of molecular weight than is observed for peptides, making the detection of large oligonucleotides far from routine. Since a potential application was the use of mass spectrometry to replace gel electrophoresis when sequencing DNA using the Sanger method, the requirement of a mass spectrometric method was different than when sequencing peptides. Peaks with good resolution must be detectable not only at low m/z values, but over a very wide mass range. The DNA sequencing approach is based on a ladder sequencing method. While mass spectrometry techniques may not, in the near future, replace gels for DNA sequencing, other powerful applications are still emerging, notably the analysis of single nucleotide polymorphisms (SNPs) [12,13]. In this area, mixtures of small oligonucleotides, usually with molecular weights less than 6,000 Da, are generated which are indicative of errors in genetic code. This is an application to which MALDI MS is well suited.

The need continues to develop methods for improved analysis of oligonucleotides of all sizes. The SNP application is clearly driving method development for analyses of oligonucleotides of sizes for which the challenges are not the creation of new

instruments, but improved matrix chemistry. In order to successfully analyze SNPs using mass spectrometry, several goals must be achieved. The first of these is lower detection limits. Often, when analyzing SNPs, there is a limited amount of sample available. The ability to perform analyses with less or no cleanup is also an important. If contaminants in a sample interfere with the analysis, the impurities must be removed. The purification steps needed to remove such contaminants can lead to sample loss. Experimental conditions in which fragmentation is decreased or eliminated must be defined as well. In the analysis of mixtures, if one could rely on generating only one peak per component, as is common for peptides, then the analysis of oligonucleotide mixtures would be much easier. Lastly, MALDI MS is being automated for the analysis of multiple samples. If automation is to be successful, a homogeneous MALDI target must be grown in the initial step. If the MALDI crystals are not homogeneous, the automated system may not find an ideal sample spot and the data from the experiments would be unreliable.

Many matrices have been developed for peptide analysis [14,15] by MALDI such as nicotinic acid, ferulic acid, sinapinic acid, and 2,5-dihydroxybenzoic acid. Since, generally, these are not as useful for oligonucleotide analysis, alternate matrices have been identified [16,17]. Several matrices were found to be compatible for the analysis of oligonucleotides using UV lasers, including 3-hydroxypicolinic acid (HPA) [18] and 6-aza-2-thiothymine (ATT) [19]. Since the development of these matrices, HPA has become the standard matrix for the analysis of larger nucleic acids while ATT is used for sequences containing less than 25 bases [2]. In addition to UV-MALDI, work has been done using infrared (IR) lasers [20, 21]. Successful matrices for IR-MALDI include succinic acid and urea [22].

Since matrix selection alone does not overcome some of the problems associated with the MALDI MS analysis of oligonucleotides, a number of matrix additives have been developed. The utility of ammonium salts has been demonstrated to reduce the formation of alkali ion adducts. Ammonium acetate was the first to be used in the MALDI experiment [8]. Since then, other ammonium salts have appeared in the literature with the most successful being diammonium hydrogen citrate [23, 24]. Thus, if an oligonucleotide exists in solution in polyanionic form (O^{-n}) containing an n number of charges, it forms a singly-charged anion by adding combinations of H^+, Na^+, and K^+ ions. If NH_4^+ ions are present, these compete effectively with alkali ions in complexing with negatively charged phosphates. During the desorption/ionization process, ammonia is lost, leaving protons behind. In this paper, the fully protonated form of an oligonucleotide, $[O^{-n} + n\ H^+]$, or the free acid form, will be referred to as M. If no alkali ions are involved and all of the phosphates are neutralized by protons, negative ion MALDI yields deprotonated molecules, designated as $[M-H]^-$. In our lab, the role of polyamines as matrix additives has been explored and spermine was found to improve MALDI spectra for single-stranded oligonucleotides, eliminating both the need for ammonium citrate as well as desalting [5, 25, 26].

In order to study non-covalent complexes in MALDI, DNA was selected as a model for all types of non-covalent complexes. Oligonucleotides are easy to synthesize. Specific sequences can be designed and synthesized in order to explore the effects of composition and molecular weight of the analyte. DNA is also of biological interest to further understand the role of DNA binding molecules such as chemotherapy agents.

Double-stranded DNA is also a useful model because the interaction of the analyte with other molecules can be monitored by other methods such as UV spectrophotometry.

References

1. Karas, M.; Bachmann, D.; Bahr, U.; Hillenkamp, F. Matrix-assisted ultraviolet-laser desorption of nonvolatile compounds. *Int. J. Mass Spectrom. Ion Processes.* **1987**, *78*, 53-68.

2. Nordhoff, E.; Kirpekar, F.; Roepstorff, P. Mass spectrometry of nucleic acids. *Mass Spectrom. Rev.* **1996**, *15*, 67-138.

3. Limbach, P.A. Indirect mass spectrometric methods for characterizing and sequencing oligonucleotides. *Mass Spectom. Rev.* **1996**, *15*, 297-336.

4. Zhang,L.-K.;Gross,M.L. Matrix-assisted laser desorption/ionization mass spectrometry methods for oligodeoxynucleotides: improvements in matrix, detection limits, quantification and sequencing. *J. Amer. Soc. Mass Spectrom.* **2000**, *11*, 854-865.

5. Asara, J.; Allison, J. Enhanced detection of oligonucleotides in UV MALDI MS using the tetraamine spermine as a matrix additive. *Anal. Chem.* **1999**, *71*, 2866-2870.

6. Roskey, M.T.; Juhasz, P.; Smirnov, I.P.; Takach, E.J.; Martin, S.A.; Haff, L.A. DNA sequencing by delayed extraction-matrix-assisted laser desorption/ionization time of flight mass spectrometry. *Proc. Natl. Acad. Sci.* **1996**, *93*, 4724-4729.

7. Lavine, G.; Allison, J. Evaluation of bumetanide as a matrix for prompt fragmentation matrix-assisted laser desorption/ionization and demonstration of prompt fragmentation/post-source decay matrix-assisted laser desorption/ionization mass spectrometry. *J. Mass Spectrom.* **1999**, *34*, 741-748.

8. Currie, G.; Yates, J. III. Analysis of oligodeoxynucleotides by negative-ion matrix-assisted laser desorption mass spectrometry. *J. Am. Soc. Mass Spectrom.* **1993**, *4*, 955-963.

9. Nordhoff, E.; Cramer, R.; Karas, M.; Hillenkamp, F.; Kirpekar, F.; Kristiansen, K.; Roepstorff, P. Ion stability of nucleic-acids in infrared matrix-assisted laser desorption/ionization mass spectrometry. *Nucleic Acids Res.* **1993**, *21*, 3347-3357.

10. Juhasz, P.; Roskey, M.T.; Smirnov, I.P.; Haff, L.A.; Vestal, M.L.; Martin, S.A. Applications of delayed extraction matrix-assisted laser desorption ionization time-of-flight mass spectrometry to oligonucleotide analysis. *Anal. Chem.* **1996**, *68*, 941-946.

11. Koomen, J.M.; Russell, D.H. Ultraviolet matrix/assisted laser desorption/ ionization mass spectrometric characterization of 2,5-dihydroxybenzoic acid-induced reductive hydrogenation of oligonucleotides on cytosine residues. *J. Mass Spectrom.* **2000**, *35*, 1025-1034.

12. Griffin, T.J.; Smith, L.M. Genetic identification by mass spectrometric analysis of single-nucleotide polymorphisms: ternary encoding of genotypes. *Anal. Chem.* **2000**, *72*, 3298-3302.

13. Fei, Z.; Smith, L.M. Analysis of single nucletide polymorphisms by primer extension and matrix-assisted laser desorption/ionization time-of-flight mass spectrometry. *Rapid Commun. Mass Spectrom.* **2000**, *14*, 950-959.

14. Börnsen, K.O.; Schär, M.; Widmer, H.M. Matrix-assisted laser desorption ionization mass spectrometry and its applications in chemistry. *Chimica.* **1990**, *44*, 412-416.

15. Hillenkamp, F.; Karas, M.; Ingendoh,A.; Stahl, B. Matrix assisted UV-laser desorption/ionization: a new approach to mass spectrometry of large biomolcules. In *Biological Mass Spectrometry*, Burlingame, A.; McCloskey, J.A., Eds.; Elsevier Scientific: Amsterdam, 1990; p.49

16. Parr, G.R. Fitzgerald, M.C.; Smith, L.M. Matrix-assisted laser desorption/ionization mass spectrometry of synthetic oligodeoxyribonucleotides. *Rapid Comm. Mass Spectrom.* **1992**, *6*, 369-372.

17. Spengler,B.; Pan, Y.; Cotter, R.J.; Kan, L.S. Molecular weight determination of underivatized oligodeoxyribonucleotides by positive-ion matrix-assisted ultraviolet laser-desorption mass spectrometry. *Rapid Commun. Mass Spectrom.* **1990**, *4*, 99-102.

18. Wu, K.J.; Steding, A.; Becker, C.H. Matrix-assisted laser desorption time-of-flight mass spectrometry of oligonucleotides using 3-hydroxypicolinic acid as an ultraviolet-sensitive matrix. *Rapid Comm. Mass Spectrom.* **1993**, *7*, 142-146.

19. Lecchi, P.; Le, H.M.T.; Pannell, L.K. 6-aza-2-thiothymine: a matrix for MALDI spectra of oligonucleotides. *Nucleic Acids Res.* **1995**, *23*, 1276-1277.

20. Kirpekar, F.; Berkenkamp, S.; Hillenkamp, F. Detection of double-stranded DNA by IR- and UV-MALDI mass spectrometry. *Anal. Chem.* **1999**, *71*, 2334-2339.

21. Berkenkamp, S.; Kirpekar, F.; Hillenkamp, F. Infrared MALDI mass spectrometry of large nucleic acids. *Science.* **1998**, *281*, 260-262.

22. Nordhoff, E.; Ingendoh, A.; Cramer, R.; Overberg, A.; Stahl, B.; Karas, M.; Hillenkamp, F.; Crain, P.F. Matrix-assisted laser desorption/ionization mass spectrometry of nucleic acids with wavelengths in the ultraviolet and infra-red. *Rapid Commun. Mass Spectrom.* **1992**, *6*, 771-776.

23. Li, Y. C. I.; Cheng, S.W.; Chan, T.W.D. Evaluation of ammonium salts as co-matrices for matrix-assisted laser desorption ionization mass spectrometry of oligonucleotides. *Rapid Commun. Mass Spectrom.* **1998**, *12*, 993-998.

24. Pieles, U.; Zürcher, W.; Schär, M.; Möser, H.E. Matrix-assisted laser-desorption ionization time-of-flight mass-spectrometry – A powerful tool for the mass and sequence-analysis of natural and modified oligonucleotides. *Nucleic Acid Res.* **1993**, *21*, 3191-3196.

25. Asara, J.M.; Hess, J.S.; Lozada, E.; Dunbar, K.R.; Allison, J. Evidence for binding of dirhodium bis-acetate units to adjacent GG and AA sites on single-stranded DNA. *J. Am. Chem. Soc.* **2000**, *122*, 8-13.

26. Distler, A.M.; Allison, J. 5-Methoxysalicylic acid and spermine: a new matrix for the matrix-assisted laser desorption/ionization mass spectrometry analysis of oligonucleotides. *J. Am. Soc. Mass Spectrom.* **2001**, *12*, 456-462.

III. Matrix-assisted laser desorption/ionization

Matrix-assisted laser desorption/ionization mass spectrometry (MALDI MS) has become an important technique for the analysis of biomolecules such as peptides and oligonucleotides. In a typical MALDI experiment, an excess of an organic matrix is combined with an analyte. The concentration of the matrix solution is typically three orders of magnitude greater than the concentration of the analyte solution. For example, one may mix 1 μL of a 1 μM solution of a peptide with 1 μL of a near-saturated solution of a matrix such as α-cyano-4-hydroxycinnamic acid, with a concentration of approximately 25 mM. If crystals representative of the solution are formed, the relative molar amounts of matrix:analyte present will be 25,000:1. In the UV MALDI process, the analyte is co-crystallized with a matrix. The matrix is usually a small organic molecule that absorbs light at the same wavelength as a laser. While visible and infrared lasers can be used in the MALDI experiment, most often a nitrogen laser is used. A nitrogen laser emits pulses of light at a wavelength of 337 nm. In the MALDI process, the pulses of the laser light irradiate the sample and desorb the analyte from matrix/analyte crystals to yield gas phase ions, Figure 2.8. The matrix also minimizes the sample degradation due to the laser irradiation [1].

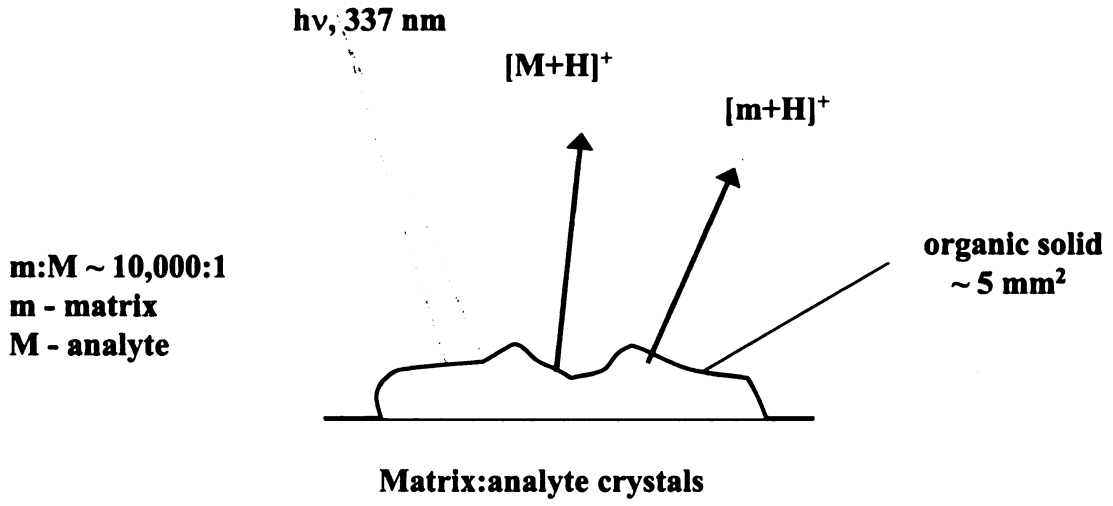

Figure 2.8. Schematic of the MALDI experiment.

While the mechanism of MALDI is not fully understood, there are several functions the matrix must serve. First, the matrix must absorb the energy from the laser light and transfer it into the excitation energy of the solid system. A small volume of the matrix/analyte crystals undergo a near instantaneous phase transition to a gaseous state [2]. During this process, the analyte molecules and matrix molecules are desorbed simultaneously with only limited internal excitation.

The matrix must also serve as a solid state "solvent" for the analyte molecules [3]. A small volume of solution containing a micromolar concentration of the analyte is deposited with an equal volume of a millimolar matrix solution. The analyte molecules are incorporated in a large excess of matrix molecules. After the solvent evaporates, analyte molecules can be isolated from each other in a solid solution of analyte molecules in the matrix. It is also believed that the formation of the crystals provides an in-situ cleaning of the sample, leading to the high tolerance against contaminants [2]. While it is believed the analyte must co-crystallize with the matrix, this is again an area of debate.

Experiments have led to the conclusion that protein incorporation into the crystals of the solid MALDI matrices is not a prerequisite for MALDI [4].

The matrix may also play a role in the ionization of the analyte. The matrix molecules may be photoexcited or photoionized. These excited matrix molecules on ions may then transfer a proton to the analyte molecules. Two UV photons provide the necessary ionization energy by the pooling of excitation energy from two excited molecules or by the absorption of a second photon from an already-excited molecule [3]. Chemical reactions can lead to the formation of the quasimolecular ion as either $[M + H]^+$ or $[M - H]^-$. The effect of the gas-phase proton affinities of the matrices has been discussed [5-6].

Lastly, it is believed that the matrix must be easy to sublime [7]. Often matrices like sinapinic acid and dihydroxybenzoic acid have enhanced volatility with the photochemical or pyrolytic cleavage of functional groups such as carboxylic acids or hydroxyl groups upon irradiation. The thermodynamic properties of the matrix compounds are also proposed to be important in the MALDI process [8]. It is proposed that there is a bottleneck of energy transfer to the analyte molecules that is caused by the high rate of the sublimation of the excited matrix molecules. With all of the requirements for a matrix, only a small set of organic molecules has been successful in the MALDI experiment.

Sample Preparation

While there is no universal sample preparation method allowing for the analysis of many analytes, there is a standard method of sample preparation. The analyte is dissolved at a concentration of around 1 pmol/uL. The matrix is dissolved at a concentration of around 25 mM. A variety of solvents and solvent systems have been used to dissolve the matrix. It is helpful if the solvents used for the matrix are miscible with the solvent used for the analyte. Most commonly, the analyte is dissolved in water and the matrix is dissolved in a mixture of acetonitrile and water. The presence of acetonitrile increases the volatility of the matrix solution and assists in the formation of the mixed crystals, or crystals containing the analyte surrounded by the matrix. The matrix is selected based on the type of analyte. Several matrices and their applications are listed in the Table 2.2.

Two types of additional components may be present in the target that is grown from solution. One class of components is impurities including compounds such as salts, buffers, detergents, and/or acids and bases. For many analytes, additional components have been identified that have a positive influence on the experiment. These are referred to as additives.

Several additives have been used with MALDI samples to enhance the quality of the mass spectra. Additives can serve several different purposes. Additives have been found to increase the homogeneity of the MALDI crystals and increase sample-to-sample reproducibility. These effects can be helpful when using automated systems or during quantitation experiments. Also, additives can decrease or increase the amount of analyte fragmentation. An increase in fragmentation would allow for more structural information

to be determined and a decrease in fragmentation would allow for an increase in the sensitivity of the analyte. Additives can also decrease the levels of cationization, increase ion abundance, and increase resolution.

Table 2.2. Matrices and their Applications

Matrix	Application
Sinapinic Acid	Peptides, Proteins (Molecular Weight > 10,000 g/mol)
α-Cyano-4-hydroxycinnamic acid	Peptides, Proteins (Molecular Weight < 10,000 g/mol)
2,5-Dihydroxybenzoic acid	Peptides, Proteins, Carbohydrates, Lipids, Polymers, Small molecules
2-(4-Hydroxy-phenylazo)-benzoic acid	Proteins, Polymers, Lipopolysaccharides
3-Hydroxypicolinic acid	Oligonucleotides, DNA
Dithranol	Nonpolar polymers
2,4,6-Trihydroxyacetophenone	Small oligonucleotides
Trans-3-indoleacrylic acid	Nonpolar polymers
Picolinic acid	Nucleic acids, Proteins
6-Aza-2-thiothymine	Small oligonucleotides, Proteins

In MALDI analysis of peptides and proteins, one of the first additives used was trifluoroacetic acid (TFA). TFA was needed to enhance the solubility of proteins in water. For analysis of polymers, compounds such as polystyrene are only ionized and detected in the MALDI experiment if copper or silver ions are present to bind to the double bonds in the compound [9]. Mixing additives such as 2-hydroxy-5-methoxybenzoic acid with DHB (10%) have improved sensitivity 2-3 fold. This mixture also known as "super DHB" is now widely used in MALDI when studying compounds such as glycoproteins.

In oligonucleotide MALDI MS, the first additives developed were ammonium salts such as ammonium hydrogen citrate [10] and ammonium fluoride [11-12]. When used in oligonucleotide analysis, the molar amount of ammonium salts introduced into the MALDI target is similar to the amount of matrix. Both the matrix and additive are typically present in the initial solution at concentrations of approximately 25 mM. The ammonium ions in the target preparation have a significant impact on the species desorbed and ionized in the MALDI experiment. It is assumed that the additive alters the state in which the analyte exists in the target crystals. In addition to the elimination of multiple alkali-ion adduction, the ammonium salt seems to play a significant role in enhancing both the desorption and the ionization of intact oligonucleotides [11]. Since the discovery of ammonium salts as additives, several other additives have been developed for the MALDI analysis of oligonucleotides, notably the tetrammine spermine [13-14], related amines [15], and fucose [16].

Additives have been used in the MALDI experiment with a variety of analytes in order to improve MALDI analysis. In Table 2.3, several matrix additives are listed along with the analyte and the effect of the additive on the resulting MALDI spectra.

Table 2.3. Matrix Additives

Additive	Sample Type	Effect
Ammonium salts	Oligonucleotides	Decrease Na^+ adducts, improves sensitivity
Ammonium salts	Phosphopeptides	Aid in detection
Cesium Iodide	Polymers	Aids in ionization
Copper salts	Polymers	Aids in ionization
Fucose	Oligonucleotides	Improves sample spot homogeneity
Nitrocellulose (substrate)	Peptides Proteins	Decrease Na adducts, improves sensitivity
Silver Trifluoroacetate	Polymers	Aids in ionization
Sodium Iodide	Polymers	Aids in ionization
Spermine	Phosphopeptides DNA	Decreases Na adducts, improves sensitivity
Sucrose	Peptides Oligonucleotides	Improves sample spot homogeneity
Trifluoroacetic acid (TFA)	Peptides Proteins	Increases protonation and solubility of analyte

MALDI Mechanism

When analyzing non-covalent complexes in MALDI, it is important to consider the different steps of the experiment. In order to determine the point in the MALDI experiment at which double-stranded oligonucleotides dissociate, a model or mechanism for the experiment must be used. Many aspects of the MALDI mechanism have been proposed, refuted, and discussed. New models continue to appear. Each of the processes proposed for investigation here may or may not be an important step in the MALDI experiment. A number of reviews and summaries have been recently published that guided the formation of this model [5, 17-20].

Since M_1M_2 is not detected as $(M_1M_2\text{-}H)^-$ or $(M_1M_2\text{+}H)^+$ in the MALDI experiment, it must dissociate at some point before the acceleration and detection of the ions. There are many steps in the MALDI experiment where the double-stranded species could denature. Shown in Table 2.4 are the proposed steps in the MALDI experiment leading to both the preservation of the double-strand as well as the steps leading to dissociation. Table 2.4 is divided into the three main processes involved in a MALDI experiment: 1) Liquid Phase:Evaporation, 2) Solid Phase: Excitation, and 3) Solid Phase: Desorption/Ionization. In order to discuss these steps, the nomenclature recently introduced by Karas [17] will be used.

Table 2.4. Proposed Steps in the MALDI Experiment

Steps Leading to Double-Stranded Ions		Steps Leading to Single Strand Ions	
Liquid Phase: Evaporation			
$M_1M_{2\ (sol'n)} + T_{(sol'n)} \rightarrow$ [∞T/(M_1M_2)] **MALDI target**	(1)	$M_1M_{2\ (sol'n)} + T_{(sol'n)} \rightarrow$ [∞T/(M_1+M_2)] **MALDI target**	(1')
Solid Phase: Excitation			
[∞T/(M_1M_2)] + n hv→ [∞T*/(M_1M_2)]	(2)	[∞T/M_1M_2] + n hv → [∞T*/(M_1+M_2)]	(2')
Solid Phase: Desorption/Ionization			
[∞T*/(M_1M_2)] → $nT_{(g)}$	(3a)		
[∞T*/(M_1M_2)] → $(T\text{-}H)^-_{(g)}$	(3b)	$(M_1M_2\text{–}H)^-(g) \rightarrow (M_1\text{–}H)^-_{(g)} + M_2$	(3'b)
[∞T*/(M_1M_2)] → $(M_1M_2\text{-}H)^-_{(g)}$	(3c)	[∞T*/(M_1M_2)] → $(M_1\text{–}H)^-_{(g)}/(M_2\text{–}H)^-_{(g)}$	(3'c)
[∞T*/(M_1M_2)] → $\{nT^*+M_1M_2\}_{(g)}$	(3d)	[∞T*/(M_1M_2)] → ∞T+M_1M_2 → M_1+M_2	(3'd)
$\{nT^*+M_1M_2\}_{(g)} \rightarrow (M_1M_2\text{–}H)^-_{(g)}$	(3e)	$\{nT^*+M_1M_2\} \rightarrow (M_1\text{–}H)^-_{(g)}/(M_2\text{–}H)^-_{(g)}$	(3'e)

In the liquid phase/evaporation process, a solution of the double-stranded oligonucleotide, M_1M_2, is combined with a saturated matrix (T) solution. If the experiment proceeds without dissociation of the strands, the MALDI target will contain intact analyte molecules surrounded by matrix molecules as shown in equation (1). However, in the solvent evaporation step, the strands may dissociate, equation (1').

If the duplex is not denatured during the liquid phase/evaporation step, matrix molecules in the crystal surround it. The next part of the MALDI experiment involves the excitation of the solid phase, equations (2) and (2'). In the excitation process, UV or IR light irradiates the solid phase and the matrix absorbs energy. The asterisks in the table denote an energetically excited species. If sufficient energy flows from matrix molecules to the lattice and into the analyte, the double-stranded species may denature, equation (2').

If the double-stranded species is maintained throughout the first two steps, the dissociation must occur during the solid phase desorption/ionization process, equations (3'b-3'e). After excitation, various species are desorbed from the MALDI target as shown in equation (3a-3e). Included in Table 2.4 is the direct generation of ions from the excited target, as well as the evolution of gas phase ions through intermediate gas phase clusters, as has recently been proposed by Karas *et al.* [17]. Brackets indicate the condensed phase, braces indicate desorbed gas phase clusters, and parentheses are used to indicate gas phase ions. The double-stranded analyte may be desorbed in this part of the experiment, only to dissociate once in the gas phase, equation (3'b). It is also possible that only ions representing the single strands are desorbed, equation (3'c) and (3'e).

Lastly, the double-stranded species may desorb from the solid phase with no charge, equation (3'd). Only charged species will be detected in the MALDI experiment.

Quantifiers

In order to measure the success of an experiment, several criteria will be used. When analyzing the annealed double-stranded species, M_1M_2, the single strands $(M_1\text{-}H)^-$ and $(M_2\text{-}H)^-$ are detected. The strand with the lower molecular weight will be denoted as M_1 while the strand with a greater molecular weight will be denoted as M_2. It is of interest to monitor the ratio of the intensity (I) of the $(M_1\text{-}H)^-$ peak to the intensity of the $(M_2\text{-}H)^-$ peak. This ratio is referred to as the single strand distribution (SSD), equation (4).

$$SSD = \frac{I(M_1)}{I(M_2)} \qquad (4)$$

To the extent that the single strand ions evolve from the duplex, it is also important to determine how the SSD value correlates with other variables in the experiment, and to determine if the SSD correlates with single strand composition. If the single strand ions are fragments of the singly charged gas phase duplex, then one may expect that the decision of which strand retains the charge would be determined by the base composition of the individual strands. To determine if, in fact, the SSD is in some way related to the presence of the duplex, it is important to perform all of the experiments proposed in this work both on annealed double strands as well as on 1:1 mixtures of the single strands. The goal of this work is to optimize the ratio of the intensity of the double strand peak when compared to the intensities of the single strand peaks. This is called the double strand retention ratio (DSRR), equation (5).

$$DSRR = \frac{I(M_1M_2)}{I(M_1)+I(M_2)} \qquad (5)$$

While larger DSRR value is desirable, the peaks detected in the duplex region must be the result of specific pairing and not random dimerization. The goal of this work is to retain the maximum extent of Watson-Crick base pairing when detecting a double-stranded species. If the M_1M_2 duplex dissociates during crystal formation, some fraction of M_1 and M_2 may recombine. However, during crystal formation, the single strands may also group together in non-Watson-Crick pairing. As mentioned previously, M_1 and M_2 can form three different duplexes: M_1M_1, M_1M_2, and M_2M_2. In order to quantify the amount of Watson-Crick pairing involved, we will calculate a Watson-Crick Selectivity Factor (WCSF), equation (6).

$$WCSF = \frac{I(M_1M_2)}{I(M_1M_1)+I(M_1M_2)+I(M_2M_2)} \qquad (6)$$

If we begin with equimolar amounts of M_1 and M_2 and the WCSF value of a given spectrum is 0.5, this suggests that the distribution of duplex peaks was dictated by probability and not by the Watson-Crick base pairing. As the value of the WCSF approaches 1, Watson-Crick pairing is preserved and the non-covalent forces were maintained throughout the MALDI experiment. As we change the variables in different experiments, the value of the WCSF will provide information about the nature of the species detected and give direction to subsequent experiments.

The resolution will also be monitored to aid in spectral analysis. If the resolution is poor, the peaks representing the duplex in the spectra may be several hundred mass units wide. If this is the case, a small molecule, such as a drug, could not be detected bound to the oligonucleotide. Thus, the resolution must be optimized in the experiments as well. Since the single-stranded oligonucleotides used in these experiments are of similar molecular weight, the resolution for the peaks representing each of the single

strands is comparable. For this reason, the resolution will be determined for the M_1 peak in all the experiments. The resolution of the peak representing the double-stranded oligonucleotide, M_1M_2, will also be determined.

Exploring Non-covalent Complexes in the MALDI Experiment

In the following sections, the MALDI process will be presented in the three parts denoted in Table 2.4, 1) the Liquid Phase: Evaporation, 2) the Solid Phase: Excitation, and 3) the Solid Phase: Desorption/Ionization. In each section, the possible problems that could lead to the dissociation of the non-covalent complex will be presented. The research performed for this work will be presented by posing a series of questions regarding the steps of the MALDI experiment. In each section, the question will be presented and experiments designed to prove or disprove the hypothesis will be introduced and the results of these experiments will be discussed.

Since the MALDI process has been artificially divided into three portions, it is still important to note each step is highly dependent on the other steps. For example, changing a condition in the liquid phase of the MALDI experiment may affect the outcome of the desorption/ionization step. Similarly, changing a variable to affect the outcome of the excitation step, may also affect the outcome of the crystal growth step.

Also, when using double-stranded DNA as model for all types of non-covalent complexes, it is important to note the nature of the oligonucleotide. With the negatively charged phosphodiester backbone, oligonucleotide MALDI spectra exhibit improved resolution, increased sensitivity, and increased signal-to-noise ratios when analyzed in negative-ion mode. For this reason, all MALDI spectra shown in the DNA experiments were performed in negative-ion mode.

References

1. Bakhtiar, R.; Tse, F.L.S. Biological mass spectrometry: a primer. *Mutagenesis.* **2000**, *15*, 415-430.

2. Bahr, U.; Karas, M.; Hillenkamp, F. Analysis of biopolymers by matrix-assisted laser desorption/ionization (MALDI) mass spectrometry. *Fres. J. Anal. Chem.* **1994**, *348*, 783-791.

3. Karas, M.; Bahr, U.; Giebmann, U. Matrix-assisted laser desorption ionization mass spectrometry. *Mass Spectrom. Rev.* **1991**, *10*, 335-357.

4. Horneffer, V.; Dreiseward, K.; Ludemann, H.-C. Hillenkamp, F.; Lage, M.; Strupat, K. Is the incorporation of analytes into matrix crystals a prerequisite for matrix-assisted laser desorption/ionization mass spectrometry? A study of five positional isomers of dihydroxybenzoic acid. *Inter. J. Mass Spectrom.* **1999**, *185/186/187*, 859-870.

5. Breuker, K.; Knochenmuss, R.; Zenobi, R. Gas-phase basicities of deprotonated matrix-assisted laser desorption/ionization matrix molecules. *Inter. J. Mass Spectrom.* **1999**, *184*, 25-38.

6. Jorgensen, T.J.D.; Bojesen, G.; Rahbek-Nielsen, H.R. The proton affinities of seven matrix-assisted laser desorption/ionization matrices correlated with the formation of multiply charged ions. *Eur. Mass Spectrom.* **1998**, *4*, 39-45.

7. Beavis, R.C.; Chait, B.T. Factors affecting the ultraviolet laser desorption of proteins. *Rapid Commun. Mass Spectrom.* **1989**, *3*, 233-237.

8. Vertes, A.; Bijbels, R.; Levine, R.D. Homogeneous bottleneck model of matrix assisted UV laser desorption of large molecules. *Rapid Commun. Mass Spectrom.* **1990**, *4*, 228-233.

9. Mowat, I.A.; Donovan, R.J.; Maier, R.R.J. Enhanced cationization of polymers using delayed ion extraction with matrix-assisted laser desorption/ionization. *Rapid Commun. Mass Spectrom.* **1997**, *11*, 89-98.

10. Pieles, U.; Zürcher, W.; Schär, M.; Möser, H.E. Matrix-assisted laser-desorption ionization time-of-flight mass-spectrometry – A powerful tool for the mass and sequence-analysis of natural and modified oligonucleotides. *Nucleic Acid Res.* **1993**, *21*, 3191-3196.

11. Li, Y. C. I.; Cheng, S.W.; Chan, T.W.D. Evaluation of ammonium salts as co-matrices for matrix-assisted laser desorption ionization mass spectrometry of oligonucleotides. *Rapid Commun. Mass Spectrom.* **1998**, *12*, 993-998.

12. Cheng, S-W.; Chan, T-WD. Use of ammonium halides as co-matrices for matrix-assisted laser desorption/ionization studies of oligonucleotides. *Rapid Commun. Mass Spectrom.* **1996**, *10*, 907-910.

13. Asara, J.; Allison, J. Enhanced detection of oligonucleotides in UV MALDI MS using the tetraamine spermine as a matrix additive. *Anal. Chem.* **1999**, *71*, 2866-2870.

14. Distler, A.M.; Allison, J. 5-Methoxysalicylic acid and spermine: a new matrix for the matrix-assisted laser desorption/ionization mass spectrometry analysis of oligonucleotides. *J. Am. Soc. Mass Spectrom.* **2001**, *12*, 456-462.

15. Chou, C-W.; Williams, P.; Limbach, P.A. Matrix influence on the formation of positively charged oligonucleotides in matrix-assisted laser desorption/ionization mass spectrometry. *Int. J. Mass Spectrom.* **1999**, *193*, 15-27.

16. Distler, A.M.; Allison, J. Improved MALDI-MS analysis of oligonucleotides through the use of fucose as a matrix additive. *Anal. Chem.* **2001**, *73*, 5000-5003.

17. Karas, M.; Glückmann, M.; Schäfer, J. Ionization in matrix-assisted laser desorption/ionization: singly charged molecular ions are the lucky survivors. *J. Mass Spectrom.* **2000**, *35*, 1-12.

18. Zenobi, R.; Knochenmuss, R. Ion formation in MALDI mass spectrometry. *Mass Spectrom. Rev.* **1998**, *17*, 337-366.

19. Knochenmuss, R.; Stortelder, A.; Breuker, K.; Zenobi, R. Secondary ion-molecule reactions in matrix-assisted laser desorption/ionization. *J. Mass Spectrom.* **2000**, *35*, 1237-1245.

20. Liao, P.C.; Allison, J. Ionization processes in matrix-assisted laser-desorption ionization mass-spectrometry – matrix-dependent formation of $[M+H]^+$ vs $[M+Na]^+$ ions of small peptides and some mechanistic comments. *J. Mass Spectrom.* **1995**, *30*, 408-423.

IV. The Liquid Phase: Evaporation

The creation of the target is an important part of a successful MALDI experiment. A micromolar solution of the analyte is combined with an equal volume of a saturated or near-saturated matrix solution. In order to facilitate the dissolution of the organic matrix, a mixture of acetonitrile and water is often used as the solvent of choice. The presence of the acetonitrile in the matrix solution also aids in the rapid formation of crystals due to its volatility. As the solvents evaporate, the volume decreases, the concentrations rise, and the solubility limits of the components are reached [1]. When the precipitate begins to form with rapid evaporation, the matrix crystals grow under kinetic control [2] and can trap the analyte molecules within, equation (1) and (1') in Table 2.4.

By the time the crystals are formed, are there any double-stranded oligonucleotide molecules remaining? During the formation of the MALDI target, there are many points at which a double-stranded oligonucleotide could dissociate. Several variables will be investigated including pH, choice of matrix, solvent, crystal growth rates, temperature, and the presence of other solution components.

Do matrix molecules in the initial solution induce the fragmentation of the duplex?

Several matrices are commonly used for the analysis of oligonucleotides using UV light at 337 nm. These include 3-hydroxypicolinic acid (HPA) [3] and 6-aza-2-thiothymine (ATT) [4]. The structures of these matrices are very similar to those of species known to stabilize DNA such as Hoechst 33258, which binds in the minor groove of the duplex [5]. However, the solution used to create the MALDI target has 1,000-100,000 times more matrix molecules than analyte molecules. With such an excess, the aromatic matrix molecules could interfere with the hydrogen bonding in the DNA by penetrating between the two strands. If matrix molecules insert between the two strands, they may competitively hydrogen bond to each strand, forcing the duplex to dissociate, reaction (1') in Table 2.4.

Typical MALDI spectra of duplex 1 are shown in Figure 2.9. In Figure 2.9(A), 6-aza-2-thiothymine (ATT) was used as the matrix. In Figure 2.9(B), 3-hydroxypicolinic acid (HPA) was used as the matrix. The peaks representing the single-stranded species $(M_1-H)^-$ and $(M_2-H)^-$ are the most intense peaks in the spectra. The duplex regions of the spectra have been magnified and clearly no peaks representing the duplex have been detected. This means, at some point during the MALDI experiment, all of the duplex has dissociated.

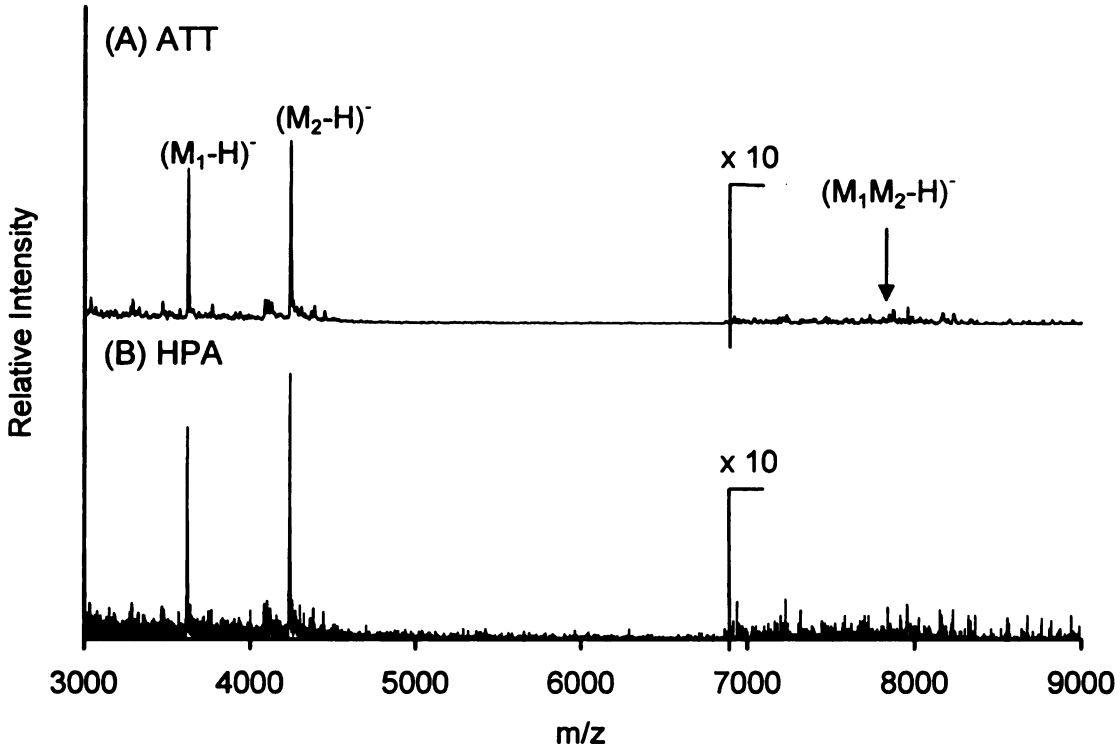

Figure 2.9. Negative-ion MALDI mass spectrum of duplex 1 using (A) ATT as the matrix and (B) HPA as the matrix.

Survey of MALDI Matrices

If no duplex ions are detected when ATT or HPA is used as the matrix, perhaps these choices of matrices do not allow for the detection of non-covalent complexes. In order to investigate the effect of the matrix on the double-stranded DNA, a series of MALDI experiments were performed. A variety of compounds were tested as matrices in the MALDI experiment including 3-aminobenzoic acid, 5-aminosalicylic acid, and 3-hydroxyanthranilic acid, with no success. These matrices are listed in Table 2.5 with the relative signal intensities recorded for the single-stranded oligonucleotide. No peaks representing the double-stranded species were detected in any of the experiments using the compounds in Table 2.5 as matrices.

While no compounds listed in Table 2.5 allowed for the detection of double-stranded DNA, we have discovered a new matrix, 5-methoxysalicylic acid, for analysis of single-stranded oligonucleotides with limited fragmentation, high resolution, and good signal-to-noise ratios [6]. A reprint of the article is included in Appendix A.

A traditional MALDI matrix has an aromatic ring and can have conjugated, acidic functional groups such as a carboxylic acid. Many of the compounds tested as matrices shown in Table 2.5 possess functional groups such as carboxylic acids and hydroxyl groups. These functional groups on the compounds may be responsible for the denaturation of the complex. Matrices with more unusual structures were tested as well including the mercaptobenzothiazoles, Figure 2.10. 2-Mercaptobenzothiazole (MBT) and 5-chloro-2-mercaptobenzothiazole (CMBT) are effective for analyzing peptides, glycolipids, oligosaccharides, and synthetic polymers [7]. However,

Table 2.5. Tested Matrices and Results

Matrix	Intensity of $(M_1-H)^-$
Aminobenzamide	X
5-Aminobenzoic acid	X
2-Amino-4-chloro benzoic acid	X
Aminoisoquinoline	X
4-Aminosalicylic acid	X
3-Aminoquinoline	X
Anthranilonitrile	X
α-Cyano-hydroxycinnamic acid	X
1,8-Diamino-4,5-Dihydroxyanthraquinone	X
1,5-Diaminonapthalene	X
Dihydroxyacetophenone	*
2,5-Dihydroxybenzoic acid	**
Diphenylbutadiene	*
2,3-Diphenyl maleic anhydride	X
Dithranol	*
3-Hydroxyanthranilic acid	X
N-Hydroxynapthalimide	X
2-(4-Hydroxyphenylazo)benzoic acid	*
5-Methoxysalicylic acid	**
Phenazine	X
Sinapinic acid	*
Thymidine	X
Trihydroxyacetophenone	

X-no signal, *-weak signal intensity, **-strong signal intensity

mercaptobenzothiazoles did not allow for the detection of intact double-stranded oligonucleotides. The spectra of the single-stranded oligonucleotides had much lower signal-to-noise ratios and poorer resolution when compared to HPA, ATT, and MSA.

The mercaptobenzothiazoles in Figure 2.10 do not possess hydroxyl group or carboxylic acid groups, but they do possess thiol groups. These thiol groups are capable of proton donation as well. Oligonucleotides are charged in solution and those charges may be retained when trapped in the MALDI crystals. When dealing with a charged analyte, the matrix would not need to participate in the ionization of such species. Also,

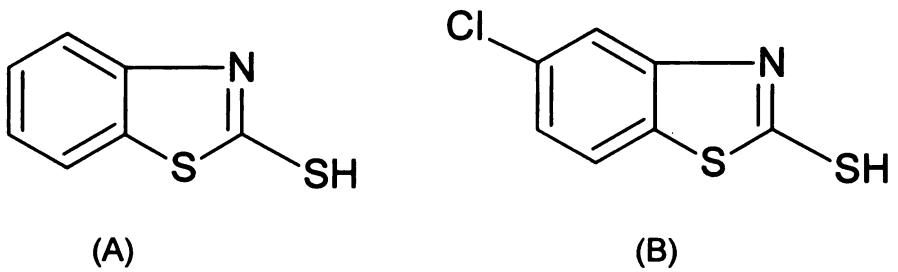

(A) (B)

Figure 2.10. The structures of (A) 2-Mercaptobenzothiazole and (B) 5-chloro-2-mercaptobenzothiazole.

when using a matrix that has acidic groups, a saturated solution of that matrix may have a pH value of less than 3. Such a pH value will denature the DNA duplex as well. For this reason, simple organic molecules with no functional groups may be ideal for the MALDI analysis of DNA. In order to test this theory, aromatic molecules such as anthracene with no acidic groups were tested as matrices for oligonucleotides.

Several problems arise when such organic compounds are used. First, organic compounds with no functional groups tend to be insoluble in water. Since oligonucleotides are soluble in water, this poses a problem when forming the MALDI target. The organic solvents used to dissolve compounds such as anthracene are immiscible with water. The matrix would have to be spotted and dried before adding the aqueous solution of the analyte. Anthracene/oligonucleotide crystals could only be formed when anthracene was dissolved in ethanol. While ethanol and water are miscible, the samples were still difficult to spot due to the volatility of the alcohol, making it difficult to pipette accurately. After formation of the MALDI target with the anthracene/alcohol solution, only ions of anthracene were detected. No analyte molecules were detected in the experiment.

Similar to anthracene, the compound di(cyclopentadienyl)iron was used. This compound is commonly referred to as ferrocene. The structure of ferrocene is shown in Figure 2.11. This compound absorbs light at 337 nm and can successfully be desorbed and ionized without the presence of a matrix. When used as a matrix, ion from the ferrocene were detected in the experiment. No peaks were detected that represented the single or double-stranded oligonucleotides. So, while the ferrocene molecule is an efficient absorber at 337 nm, the molecule must not allow for the desorption or ionization of the analyte.

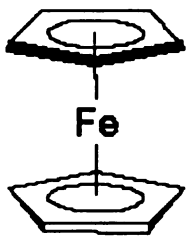

Figure 2.11. Structure of ferrocene.

Lastly, another class of organic compounds was tested for their utility in analyzing oligonucleotides. Dyes are commonly used in a variety of fields including microscopy, biochemistry, and analytical chemistry. Often, these molecules are used to visualize materials such as membranes, DNA, organelles, or proteins [8]. These dyes can be organic molecules that are neutral, cationic, or anionic [9]. Examples of each type of dye are shown in Figure 2.12. In Figure 2.12, Alizarin Red S is a negatively charged dye in solution while chlorophenol red is a neutral dye. Methyl violet is an example of a cationic dye with a fixed charge on the nitrogen group.

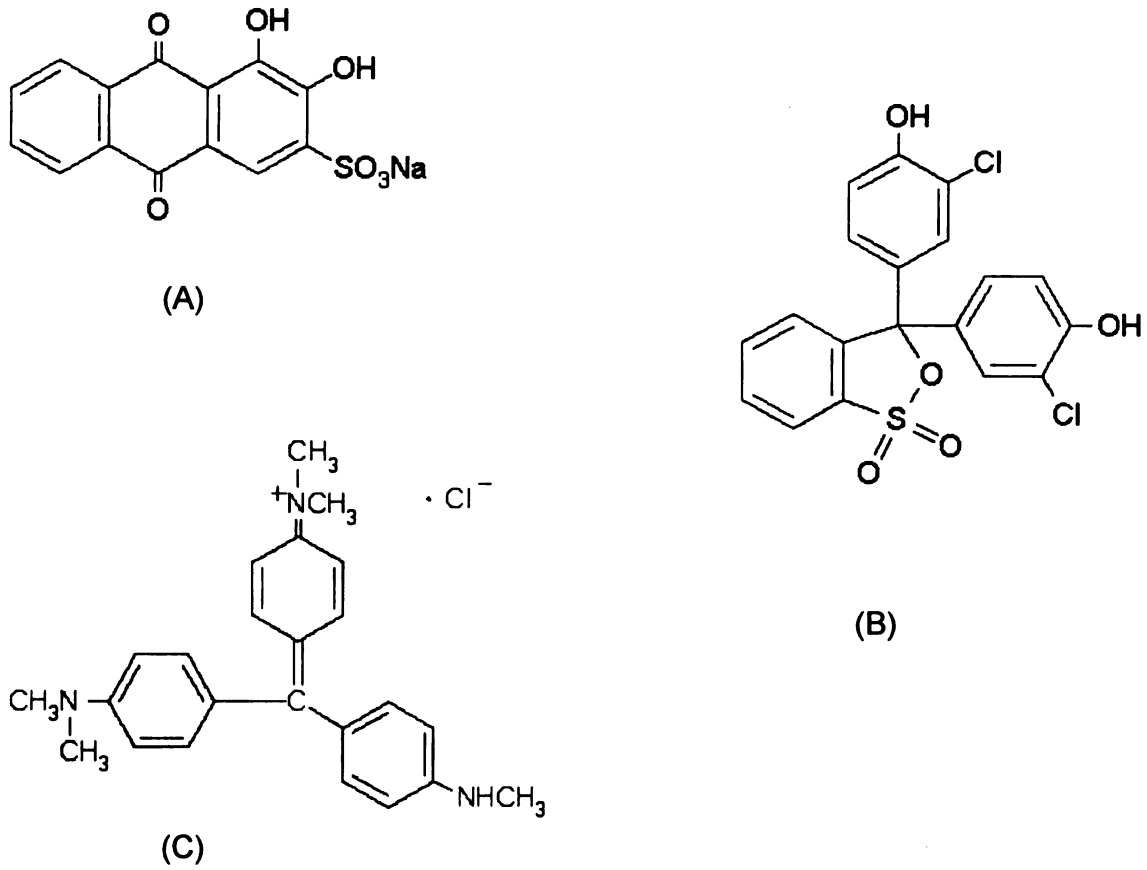

Figure 2.12. Structure of (A) Alizarin Red S, (B) Chlorophenol Red, and (C) Methyl Violet.

Dyes absorb in the ultraviolet/visible region of the spectrum and ionize/desorb after laser irradiation without the presence of a matrix. Due to their ability to harvest the light from the laser, dyes may be suitable matrices. The dyes used as matrices in the MALDI experiment are listed in Table 2.6. In each of these experiments, ions representing the intact dye molecules were seen in the resulting spectra. No ions from the oligonucleotides were detected in any of the experiments.

Table 2.6. Organic Dyes Tested as Oligonucleotide Matrices

Alizarin Red S	Clayton Yellow
Alizarin Yellow G	Cresol Purple
Bromochlorophenol Blue	Cresol Red
Bromocresol Green	Metacresol Purple
Bromophenol Blue	Methyl Orange
Bromophenol Red	Methyl Violet
Chlorophenol Blue	Phenol Red
Chlorophenol Red	Thymol Blue

I tested a variety of compounds as matrices in the MALDI experiment. These compounds were structurally diverse. None of these compounds allowed for the detection of the double-stranded oligonucleotides. While many of the compounds used in this study had structures similar to that of known matrix molecules, often these compounds did not allowed for the detection of single-stranded oligonucleotide ions or peptide ions. Only very few compounds are successful as matrices in the MALDI experiment.

Melting Temperature Studies

Of the over 100 compounds that I have tested as matrices in the MALDI experiment, only three compounds allowed for the detection of single-stranded oligonucleotides: HPA, ATT, and MSA. The structures of these three matrices are shown in Figure 2.13.

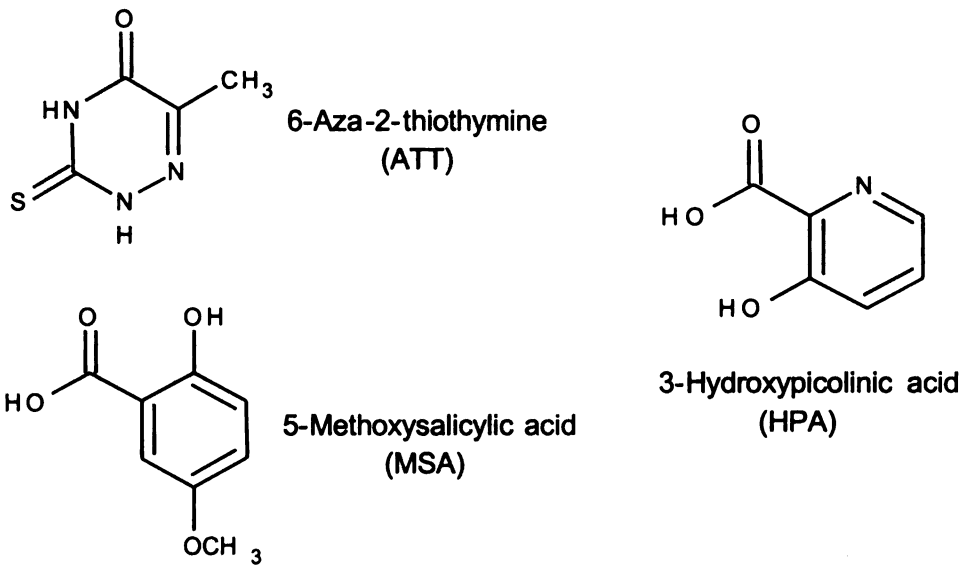

Figure 2.13. The structures of ATT, MSA, and HPA.

These matrices allowed for the detection of oligonucleotides in the MALDI experiment and were the most promising choice for analyzing duplex oligonucleotides. The matrices ATT and HPA will be of particular interest because their use as oligonucleotide matrices has been highly documented. Since these matrices did not allow for the detection of duplex DNA, could these compounds be dissociating the duplex in solution? In order to explore the effect of the matrix molecule in solution with DNA, melting temperature studies were performed.

The UV spectrophotometer used in this study did not allow for analysis of saturated matrix solutions due to the high molar absorptivity of the matrix compounds from 250-400 nm. The first matrix compound studied was ATT. Several solutions of ATT were created in order to find the optimal concentration for the UV study. For the purpose of this experiment, a concentration of 50 micromolar yielded good results. A UV spectrum of ATT was recorded at room temperature. The ATT solution was then heated to 80°C and another UV spectrum was recorded. There was no change in the absorbance spectrum. This proved the molar absorptivity of ATT does not depend on the temperature of the solution, so the presence of ATT would not interfere with the melting temperature study.

A solution of ATT was added to a solution of the Dickerson dodecamer duplex so the final concentration of the ATT was 50 micromolar and the final concentration of the duplex was one micromolar. The absorbance at 259 nm was monitored for 30 minutes and no increase in absorbance was detected. At a micromolar concentration, the addition of the ATT molecules did not denature the double stranded species even when the duplex oligonucleotide was in solution with the ATT for a time exceeding that of the typical MALDI experiment.

The oligonucleotide solution was then stored for one week at room temperature and another melting temperature study was performed, Figure 2.14. For this study, a UV spectrum of the incubated solution was acquired. This solution was heated and a 10% increase in absorbance was detected. These data show the oligonucleotide duplex had not been denatured after 1 week in a 50 micromolar solution of matrix. Another study was performed using duplex 1 as the analyte. Similar results were found. ATT does not

cause the dissociation of the duplex even after a one week incubation period. While the concentration of the ATT solution was lower than that for a typical MALDI experiment, the matrix molecules were in contact with the duplex for an extended period of time.

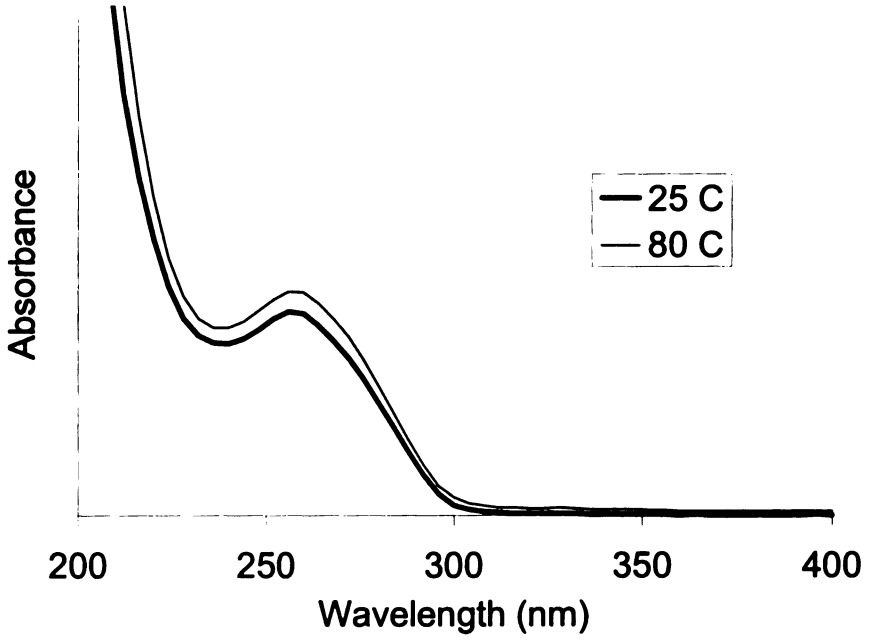

Figure 2.14. UV analysis of duplex oligonucleotide incubated with ATT for 1 week at room temperature.

Is this experiment really kinetically relevant? The following reaction (7) occurs in solution at a specific rate:

$$M_1M_2 + T \rightarrow M_1 + M_2 + T \qquad (7)$$

Suppose the reaction proceeds under simple kinetics, equation (8).

$$\frac{-d[M_1M_2]}{dt} = k[M_1M_2][T] \qquad (8)$$

Here the concentration of the matrix, [T], is less than $1/100^{th}$ of the concentration used in a typical MALDI experiment. However, the length of time, or dt, is over 1000 times

greater than a typical MALDI experiment. So, the same effect should be seen in the melting temperature study when compared to the MALDI experiment.

Melting temperature studies were also performed using HPA and MSA with similar results. So, it was concluded that the matrix molecules in solution with the duplex DNA do not appear to cause the dissociation of the non-covalent complex.

Could the use of organic solvents disrupt the non-covalent forces in double-stranded DNA?

While organic solvents are typically used in a MALDI experiment to dissolve the organic matrix, the common crystallization process must often be re-evaluated. For example, many kinds of samples have been analyzed by MALDI using the water/acetonitrile/trifluoroacetic acid (TFA) solvent system and is a recommended solvent system for variety of peptides and proteins [10]. Originally this solvent system was designed specifically for the analysis of peptides, although it has now been applied for MALDI analysis in general. Since analysis of oligonucleotides is enhanced when using negative-ion mode and the oligonucleotides are readily soluble in water, TFA is not needed in these experiments to enhance protonation or solubility of the analyte. For this reason, TFA will not be used in any of the experiments discussed here.

While TFA is not needed for oligonucleotide analysis, the use of acetonitrile is still necessary to facilitate the dissolution of the matrix. The presence of organic co-solvents, such as acetonitrile, may induce the dissociation of the double-stranded oligonucleotides. It is possible for an organic solvent to induce separation of the duplex since several common organic solvents are known to denature DNA including alcohols such as methanol, ethanol, and n-propanol, and amides such as formamide, N,N-dimethylformamide, and propionamide [11].

In order to determine if acetonitrile denatures DNA duplexes with fewer than 15 bases per strand, a series of melting temperature studies were performed. A one micromolar solution of duplex 1 was formed using a 1:1 acetonitrile:water solution. The absorbance of the solution was scanned from 200-400 nm. The solution was then heated

and another UV spectrum was acquired. There was a ten percent increase in absorbance at 259 nm when compared to that for the sample at room temperature, Figure 2.15. This indicates that the duplex remains intact when in the presence of acetonitrile. It was concluded that the acetonitrile in the starting solution does not denature the duplex. This experiment was performed at several concentrations of acetonitrile. Even with a 3:1 mixture of acetonitrile:water, the duplex remained intact. Since acetonitrile evaporates from the MALDI target at a higher rate than the water, the MALDI target will never contain greater than 50% acetonitrile.

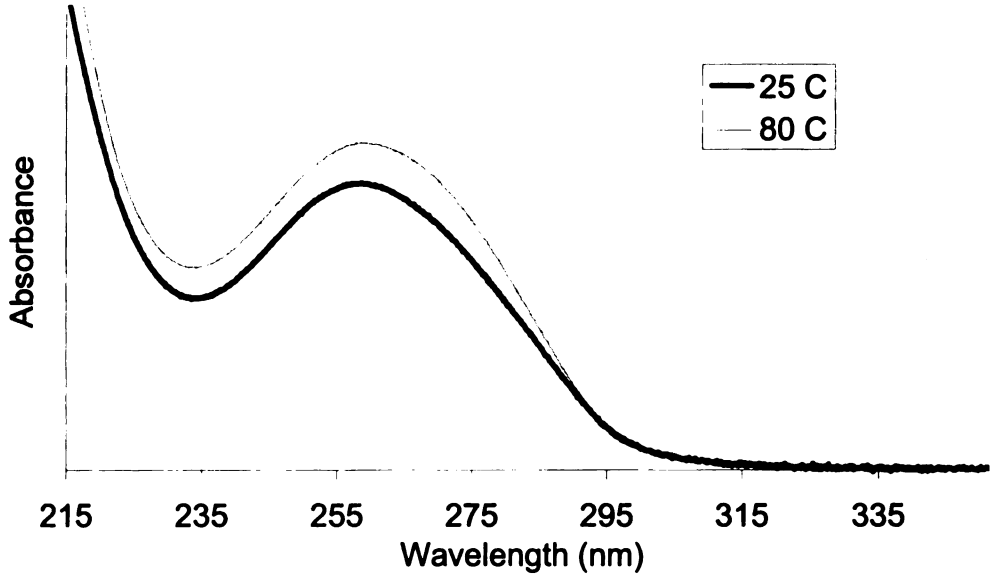

Figure 2.15. UV melting study using the acetonitrile/water solvent system.

It is also important to consider the timescale of the two experiments. In the melting temperature studies, the duplex remained in contact with the acetonitrile between 15-60 minutes. In a typical MALDI experiment, the duplex is in contact with the

acetonitrile for less than 2 minutes. Since the duplex is in contact with the acetonitrile for a relatively short period of time during the MALDI experiment, there are fewer opportunities for dissociation of the duplex in the MALDI experiment when compared to that of a melting temperature experiment.

While acetonitrile does not dissociate the duplex in the UV experiment, the organic co-solvent is still an important variable in the MALDI experiment. A solvent is used not only to dissolve the matrix, but to assist in the rapid formation of the crystals as well. If the solvent affects the crystal growth, using solvents with varying volatility could alter the result of experiments. I have tested many solvent combinations in the MALDI experiment using ATT and HPA as the matrices. Solvent combinations used include only water, water/acetonitrile combinations, water/methanol, acetone, water/alcohols, and water/fluorinated alcohols. Methanol and ethanol used alone were difficult to spot on the MALDI target due to sample spreading. Combinations of water with these alcohols proved unsuccessful as well. When alcohols were used in solution preparation, no peaks representing the duplex or any dimers were detected, giving a DSRR value of zero. Other organic solvents and solvent systems were examined for dissolution of the matrix including pyridine, pyridine/water, and acetonitrile. Again, spectra from these experiments contain no duplex or dimer peaks.

While the presence of acetonitrile does not disrupt the non-covalent forces in double-stranded DNA, we have seen interesting results when only water is used to dissolve the matrix. In this experiment, a saturated aqueous solution of HPA was used. The HPA was mixed with the double stranded analyte and spotted on the sample plate. After spotting, the solution was dried with a heat gun to facilitate crystal formation.

Heating was used in an attempt to offset the fact that, without acetonitrile present, it would take much longer for the 1 μL droplet to evaporate. A microliter of a 1:1 ACN/H_2O solution evaporates in approximately 30 seconds, while 1 μL of H_2O evaporates in roughly 5 minutes. While heating can eliminate time as a variable for the comparison, it introduces temperature as a new variable. The effect of temperature is discussed further in another section of this chapter. The results of the water only experiment are shown in Figure 2.16. Compared to Figure 2.9, the peaks representing the single-stranded species are still the most intense peaks in the spectrum, with a SSD of 1.0; the peak for the smaller strand has increased in relative intensity.

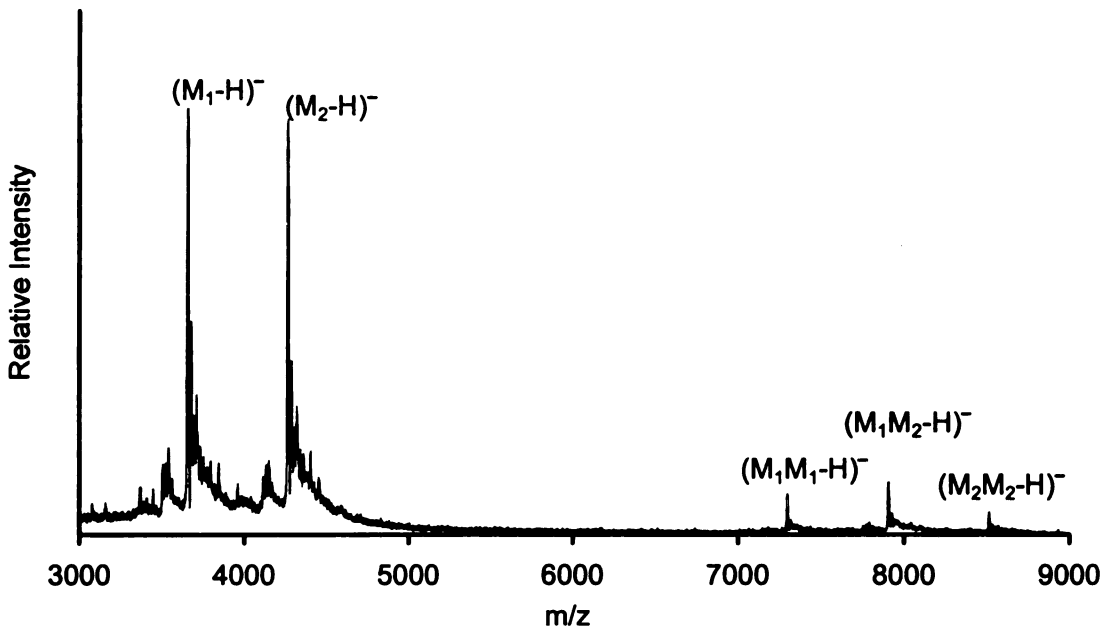

Figure 2.16. Negative-ion MALDI mass spectrum of duplex 1 using HPA as the matrix. Only water was used to dissolve the matrix.

In the spectrum, relatively intense peaks were observed in the duplex region. Using this method, the value of the DSRR increases from 0 to 0.1. From one standpoint, conditions have been found that allow for duplex molecules to be detected. However, the

WCSF is 0.5, suggesting that the initial duplex has not been retained. One interpretation is that the duplex completely dissociates during the crystal growth step, and when water alone is used as the solvent, single strands are more likely to dimerize during crystal growth.

Similar results are seen when aqueous solutions are used without any heating. That is, the appearance of the dimers is not related to heating or length of time needed for crystal growth, but rather to the use of only water in the preparation of the MALDI target. It is interesting to note that higher laser powers were needed when the crystal growth time was increased. As the length of time needed for crystal growth increases, the analyte may not be trapped as efficiently in the matrix crystals. If the analyte is not fully incorporated into the matrix, more laser power would be needed to generate ions.

In order to explore the effects of different solvents, several experiments were performed using a variety of solvents. With HPA as the matrix, water was the only solvent that led to changes in the values of the spectral quantifiers. When these experiments were repeated using ATT as the matrix, this effect was not seen. The DSRR value for ATT in water alone was zero and the intensity of the peaks representing the single-stranded species were of low intensity.

Does the pH of the matrix:analyte solution cause the dissociation of the non-covalent complex?

Often in MALDI MS of peptides and proteins, matrices such as sinapinic acid and α-cyano-4-hydroxycinnamic acid are used. When these matrices are dissolved in an acetonitrile/water solution, the pH of the matrix solution can be lower than 3. These highly acidic conditions can denature non-covalent complexes. Previously, it has been shown that using buffered solutions, near physiological pH, can lead to enhanced detection of non-covalent complexes when using acidic matrices [12-13]. Even for basic matrices with a solution pH of 6-7, the detection of non-covalent complexes is enhanced by using buffers [14-15].

Could the addition of a biological buffer maintain the pH throughout the MALDI experiment? In order to explore the effect of pH on the DSRR values, a series of MALDI experiments was performed. Previously, buffers using compounds such as ammonium citrate [14-15] and ammonium bicarbonate [12] had been used to stabilize protein-protein and duplex DNA complexes in MALDI MS. These buffers were used first in this work. Ammonium citrate and ammonium bicarbonate solutions were made at concentrations of 10 mM, 25 mM, 50 mM, and 100 mM. Matrix solutions of HPA and ATT were made by dissolving the matrix in a 1:1 acetonitrile:buffer solution. While SSD values changed slightly in the experiments, there was no increase in the DSRR. No duplex peaks were detected in any of the experiments.

Other buffer solutions were used in the MALDI experiment. These buffer solutions included N-2-hydroxyethylpiperazine-N'-2-ethanesulfonic acid (HEPES), piperazine-N,N'-bis(ethanesulfonic acid) (PIPES), tris-(hydroxymethyl)aminomethane

(TRIS), imidazole, tricine, and several phosphate buffers. These buffers, when used in the MALDI experiment, did not allow for the detection of the duplex oligonucleotides. Also, the HEPES, PIPES, TRIS, and imidazole buffers suppressed the signal for the single-stranded oligonucleotides as well. The phosphate buffers were formed by dissolving phosphate salts with sodium and potassium as the counter ions. While the phosphate buffers used did not suppress the signal for the single-stranded oligonucleotide, the presence of the sodium and potassium ions caused a decrease in resolution, sensitivity, and an increase in the alkali ion adduction seen in the spectra.

Does the length of time associated with crystal growth affect the dissociation of the duplex?

As mentioned previously, the matrix and/or solvents may play a role in the dissociation of the duplex, shown below, equation 10.

$$M_1M_2 + nX \rightarrow M_1X_m + M_2X_p \quad (X = \text{solvent or matrix}) \quad (10)$$

This reaction, if it occurs, does so at some rate. While it has been demonstrated that the matrices and solvents do not denature the duplex in solution, the duplex could still be dissociating during the crystal growth step. Since the matrix solution is saturated or nearly saturated, the matrix will be the first component in solution to precipitate. As the matrix precipitates, the duplex may interact with the growing crystal surface and dissociate. If the crystal growth process is slow, the duplex will have more opportunities to interact with the growing crystal surface. By decreasing the time needed for crystal growth, the double-stranded molecules may be trapped in the MALDI target before denaturation occurs. A variety of variables can affect the length of time needed for crystal growth including the solvents, temperature, volume of solution deposited, and atmospheric conditions as well.

Solvent selection determines the rate of crystal growth with the addition of volatile organic solvents decreasing the time necessary for formation of crystals compared to that for water alone. The use of volatile solvents may also facilitate the incorporation of the double-stranded oligonucleotides into the matrix. If the solvents quickly evaporate, the analyte molecules may become trapped among the matrix molecules more quickly than they are separated, by some mechanism, in solution. In

addition to using volatile solvents, the sample plate may be heated in order to increase the rate of crystal growth, or cooled to decrease evaporation rates.

In order to increase the rate of precipitation, volatile solvents were used including long chain alcohols. Long chain alcohols serve as an excellent model because while there is structural similarity, the evaporation rates (vapor pressures) decrease as alkyl chain length increases. For these experiments, four alcohols were selected, methanol, ethanol, propanol, and butanol. These solvents were used alone or in a 1:1 solution with water to dissolve the matrix. In each of these experiments, no change in the DSRR was seen.

In order to further explore the effect of crystal growth time, the plate was heated and cooled during sample preparation to adjust evaporation times. While the heating of the sample plate had little effect on the spectral quantifiers, cooling the sample plate seemed to have a great effect. When a cold plate was used, the time of sample spot evaporation increased from 1-2 minutes to 5-10 minutes depending on the solvent system used. When these sample spots were analyzed, it was difficult to detect even the single-stranded oligonucleotides. Most likely, given a longer period of time, the MALDI crystals containing analyte embedded in the matrix were not formed. These mixed MALDI crystals are necessary for a successful MALDI experiment. Instead, the oligonucleotides likely crystallized separately from the matrix (thermodynamic limit) and could not be desorbed and ionized.

The amount of sample deposited on the sample plate was also varied. Instead of depositing 1 μL of a solution on a MALDI plate and waiting for it to evaporate, the target was constructed in several steps. For example, a fifth of a microliter of matrix was

deposited with an equal volume of matrix. Since the evaporation time is proportional to volume, reducing the volume allows the crystals to grow more quickly without introducing any new variables. A variety of experiments were performed with differing volume deposited in differing orders. Despite the changes, the experiments yielded the same DSRR as the traditional one-microliter approach.

The atmospheric conditions were also altered. While MALDI crystals are normally grown under atmospheric pressure, the solutions could be added to the MALDI target and then placed in a vacuum. Again, this allows for all the solution variables to remain constant. Similarly, the MALDI solutions were deposited on the target and dried under a stream of nitrogen. This increased the rate of evaporation. When the crystals were grown under vacuum or a stream of nitrogen gas, no changes in the spectral quantifiers were seen, even though droplet evaporation time changed substantially. Since no duplex ions were detected in this experiment, it was concluded that the length of time associated with the crystal growth does not affect the dissociation of the duplex.

Does contact with a surface denature the double-stranded oligonucleotides?

During crystal growth formation, the duplex oligonucleotides are in contact with the matrix molecules, solvents, and also the sample plate. We have discussed the interaction of the DNA with the matrix molecules, the solvents, and the growing matrix crystals. The non-covalent complex also comes in contact with the sample plate during the course of a MALDI experiment. Often in MALDI MS, sample plates can be stainless steel, gold, or Teflon-coated. The surface may be completely flat or have depressions known as wells. These sample wells can vary in size. A mass spectrometrist would not consider the sample plate to be a variable although there are many types of sample plates available.

Biological materials such as proteins and oligonucleotides are known to interact with a variety of surfaces including membranes [16], mica [17], and gold [18]. Enzymes are often complexes that consist of multiple protein subunits held together by non-covalent forces. When an enzyme comes in contact with a metal surface, a decrease in the activity of the enzyme is often seen. A decrease in the activity is often caused by the denaturation of the complex. Similarly, when the duplex is spotted onto the sample plate, the interaction with the metal surface may cause dissociation. In order to explore this theory, another melting temperature study was performed. A solution of duplex 1 was placed in a cuvette. A scan was taken to form the baseline for the experiment. Then, a solid gold washer was placed in the cuvette to simulate the surface of gold plate. Scans were taken immediately after the addition of the gold and then every ten minutes for an hour. No increase in absorbance was seen at 259 nm, Figure 2.17. The cuvette containing the gold and duplex 1 was sealed and stored at room temperature for 24 hours.

Another spectrum was obtained. The solution was then heated to 80°C and another UV spectrum was acquired. A 10% increase in the absorbance of the solution was detected at 259 nm. When the gold is in contact with duplex 1 for 24 hours, the duplex still remains intact.

An identical experiment was performed using a stainless steel washer. Similar results were seen. It was then concluded that contact with the metal surface of the MALDI target does not cause the dissociation of double-stranded DNA in solution.

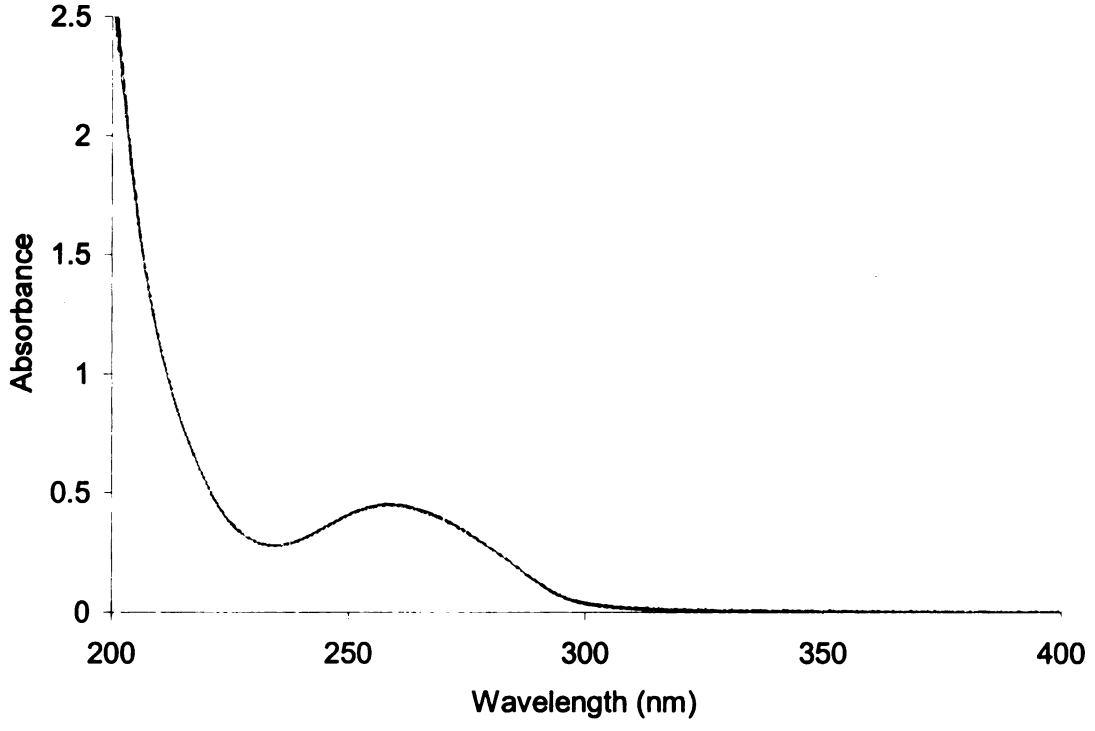

Figure 2.17. Four overlapped UV spectra of double-stranded DNA (1) before contact with the gold surface, (2) immediately after the addition of the gold surface, (3) 10 minutes after the addition of the gold surface, and (4) 30 minutes after addition of the gold surface.

To further explore the effect of the surface of the sample plate, a Nafion® coating was placed on the stainless steel plate. A small amount of Nafion® was spread on a traditional MALDI sample plate and dried with a heat gun. The structure of the Nafion® is shown below in Figure 2.18.

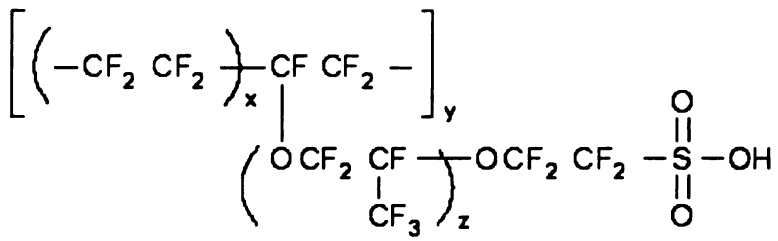

Figure 2.18. Structure of Nafion®.

The layer of Nafion® on the sample plate did not improve the DSRR and WCSF values for the experiments. However, the Nafion® surface is hydrophobic and allowed for larger sample volumes to be deposited on the gold or stainless steel MALDI target. This was helpful when dealing with a dilute solution of analyte. Teflon coated plates were also used to analyze double-stranded DNA, but again no increase in the DSRR value was seen.

In order to explore a different type of desorption/ionization experiment, a DIOS plate was purchased from Mass Consortium (San Diego, CA). DIOS is the desorption/ionization on silicon and has been recently used to desorb/ionize peptides and proteins without the use of a matrix [19-21]. The porous silicon surface of the DIOS plate has a strong ultraviolet absorption that enhances the laser desorption/ionization process [19]. In this technique, the analyte is deposited on the surface and can be

desorbed/ionized without a matrix. A sample of duplex 1 was deposited on the DIOS sample plate. When analyzing duplex 1 using DIOS, no peaks representing the single or double-stranded oligonucleotides were detected in either negative or positive ion mode. Since no oligonucleotide peaks were detected, the DIOS technique may not allow for the desorption of negatively-charged species such as an oligonucleotide. However, this surface could still be used to perform a MALDI experiment. A solution of duplex 1 was combined with either a HPA or ATT matrix solution. These solutions were then deposited on the DIOS plate. Again, no peaks representing the intact duplex were detected. In this experiment, duplex is never exposed to any metal surface.

When examining the data from the melting temperature studies, combined with the data from the MALDI experiments, it does not appear to be the surface of the MALDI target that causes the duplex dissociation.

Conclusions

For the variables in the liquid phase portion of the experiment, the solution to the problem of duplex dissociation could involve multiple changes to the experiment. For example, the most success may come from using water/methanol solution to dissolve the matrix, ATT as the matrix, and depositing the matrix/analyte solution onto a heated plate to reduce the crystal growth time. A variety of combinations of the different variables were used in the MALDI experiments. No increases in the DSRR values were seen with any of the experiments.

While the variables in the liquid phase have been examined, the complex could still dissociate during this portion of the experiment. Dissociation during the liquid phase would explain the non-specific dimerization seen in Figure 2.16. It is possible the complex could dissociate when the duplex contacts the growing matrix crystals. Since a reduction in crystal growth time has no effect on the outcome of the experiment, another approach must be taken to stabilize the duplex. The variables that will be discussed in the solid phase portions of the MALDI experiment may also affect the liquid phase portion of the experiment.

References

1. Asara, J.M. *Enhancing spectra in desorption/ioniziation mass spectrometry through the use of chemical additives*. Michigan State University: East Lansing, MI, 1999.

2. Nishioka, K., Thermodynamic vs. kinetic critical nucleus and the reversible work of nucleus formation. In *Advances in the understanding of crystal growth mechanisms*, Nishinaga, T.; Nishioka, K.; Harada, J.; Sasaki, A.; Takei, H., Eds.; Elsevier Science, St. Louis, MO, 1997; p. 3.

3. Wu, K.J.; Steding, A.; Becker, C.H. Matrix-assisted laser desorption time-of-flight mass spectrometry of oligonucleotides using 3-hydroxypicolinic acid as an ultraviolet-sensitive matrix. *Rapid Comm. Mass Spectrom.* **1993**, *7*, 142-146.

4. Lecchi, P.; Le, H.M.T.; Pannell, L.K. 6-aza-2-thiothymine: a matrix for MALDI spectra of oligonucleotides. *Nucleic Acids Res.* **1995**, *23*, 1276-1277.

5. Quintana, J.R.; Lipanov, A.A.; Dickerson, R.E. Low-temperature crystallographic analyses of the binding of Hoechst 33258 to the double-helical DNA dodecamer CGCGAATTCGCG. *Biochem.* **1991**, *30*, 10294-10306.

6. Distler, A.M.; Allison, J. 5-Methoxysalicylic acid and spermine: a new matrix for the matrix-assisted laser desorption/ionization mass spectrometry analysis of oligonucleotides. *J. Am. Soc. Mass Spectrom.* **2001**, *12*, 456-462.

7. Xu, N.X.; Huang, Z.H.; Watson, J.T.; Gage, D.A. Mercaptobenzothiazoles: a new class of matrices for laser desorption ionization mass spectrometry. *J. Am. Soc. Mass Spectrom.* **1997**, *8*, 116-124.

8. Kiernan, J.A. Classification and naming of dyes, stains, and fluorochromes. *Biotech. Histochem.* **2001**, *5/6*, 261-277.

9. Green, F.J. The Sigma-Aldrich Handbook of Stains, Dyes, and Indicators. Milwaukee, WI: Aldrich Chemical Co, 1990.

10. PerSeptive Biosystems, Inc. *Voyager Biospectrometry Workstation with Delayed Extraction™ Technology: User's Guide.* Framingham, MA: PE Biosystems, 1999.

11. Levine, L.; Gordon, J.; Jencks, W.P. The relationship of structure to the effectiveness of denaturing agents for deoxyribonucleic acid. *Biochemistry.* **1963**, *2*, 168-173.

12. Woods, A.S.; Buchsbaum, J.C.; Worrall, T.A.; Berg, J.M.; Cotter, R.J. Matrix-assisted laser desorption/ionization of noncovalently bound complexes. *Anal. Chem.* **1995**, *67*, 4462-4465.

13. Woods, A.S.; Huestis, M.A. A study of peptide-peptide interaction by matrix-assisted laser desorption/ionization. *J. Am. Soc. Mass Spectrom.* **2001**, *12*, 88-96.

14. Lecchi, P.; Panell, L.K. The detection of intact double-stranded DNA by MALDI. *J. Am. Soc. Mass Spectrom.* **1995**, *6*, 972-975.

15. Lin, S.; Cotter, R.J.; Woods, A.S. Detection of non-covalent interaction of single and double stranded DNA with peptides by MALDI-TOF. *Proteins Suppl.* **1998**, *2*, 12-21.

16. Vestling, M.M.; Fenselau, C. Poly(vinylidene difluoride) membranes as the interface between laser desorption mass spectrometry, gel electrophoresis, and in situ proteolysis. *Anal. Chem.* **1994**, *66*, 471-477.

17. Fang, Y.; Hoh, J.H. Early intermediates in spermidine-induced DNA condensation on the surface of mica. *J. Am. Chem. Soc.* **1998**, *120*, 8903-8909.

18. Gearheart, L.A.; Ploehn, H.J.; Murphy, C.J. Oligonucleotides adsorption to gold nanoparticles: a surface-enhanced Raman spectroscopy study of intrinsically bent DNA. *J. Phys. Chem. B.* **2001**, *105*, 12609-12615.

19. Wei, J.; Buriak, J.; Siuzdak, G. Desorption/ionization mass spectrometry on porous silicon. *Nature* **1999**, *399*, 243-246.

20. Shen, Z.; Thomas, J.J.; Averbuj, C.; Broo, K.M.; Engelhard, M.; Crowell, J.E.; Finn, M.G.; Siuzdak, G. Porous silicon as a versatile platform for laser desorption/ionization mass mpectrometry. *Anal. Chem.* **2001**, *33*, 179-187.

21. Thomas, J.J.; Shen, Z.; Crowell, J.E.; Finn, M.G.; Siuzdak, G. Desorptin/ionization on silicon (DIOS): a diverse mass spectrometry platform for protein characterization. *Proc. Nat. Acad. Sci. USA.* **2001**, *98*, 4932-4937.

V. Solid Phase: Excitation

The next portion of the MALDI experiment involves the excitation of the crystalline MALDI target. After the solvent evaporates, a crystal of matrix molecules is formed with analyte molecules trapped within the matrix network, Figure 2.19 (A). The solid target is then irradiated with either IR or UV light. In the case of UV MALDI, the matrix molecules absorb the light to form electronic excited states, equation (2) and (2') from Table 2.4. Intersystem crossings yield highly vibrationally excited matrix molecules. Vibrational energy is transferred into the host lattice, and the vibrational temperature of some portion of the crystal rises to the point where a phase transition occurs, leading to desorption. Vertes has proposed a bottleneck model, in which energy from the host lattice, or matrix, moves only very slowly into the analyte molecules, due to the vibrational energy frequency mismatch between weak hydrogen bonds of the lattice and strong covalent bonds in the analyte [1-3].

While models are still being developed to describe energy flow and content following excitation, it is clear that the host absorbs the energy, and it is transferred to the analyte thereafter, as time allows. In an ideal situation, the energy distributed in the lattice would be large enough to dissociate the non-covalent bonds holding the lattice together, but not large enough to dissociate the bonds holding the complex together, Figure 2.19 (B). If large amounts of energy are available, and energy flow is rapid relative to desorption rates, then energy could move into a DNA duplex that exceeds the bond dissociation energy. In this case, the analyte could dissociate into the two single strands, Figure 2.19 (C). It is important to note that the Vertes bottleneck model was developed at a point in time when scientists were trying to understand why, in a MALDI-

linear TOF MS experiment, peptides would yield a single peak with no fragmentation. This could be rationalized by considering that energy flow into the analyte in a very short time-frame could be minimal. It has more recently been found that some energy does flow since analyte ions do fragment. The situation could be very different when the analyte is an oligonucleotide duplex. Because the duplex is held together by hydrogen bonds, energy does not need to flow from the lattice into the covalent bonds of the analyte to induce fragmentation. The energy must only flow into the hydrogen bonds that hold the strands together. This may occur much more efficiently. Since a lattice of non-covalently bound matrix molecules is broken in the MALDI process, it is likely that the non-covalent bonds between the duplex oligonucleotides could be broken as well.

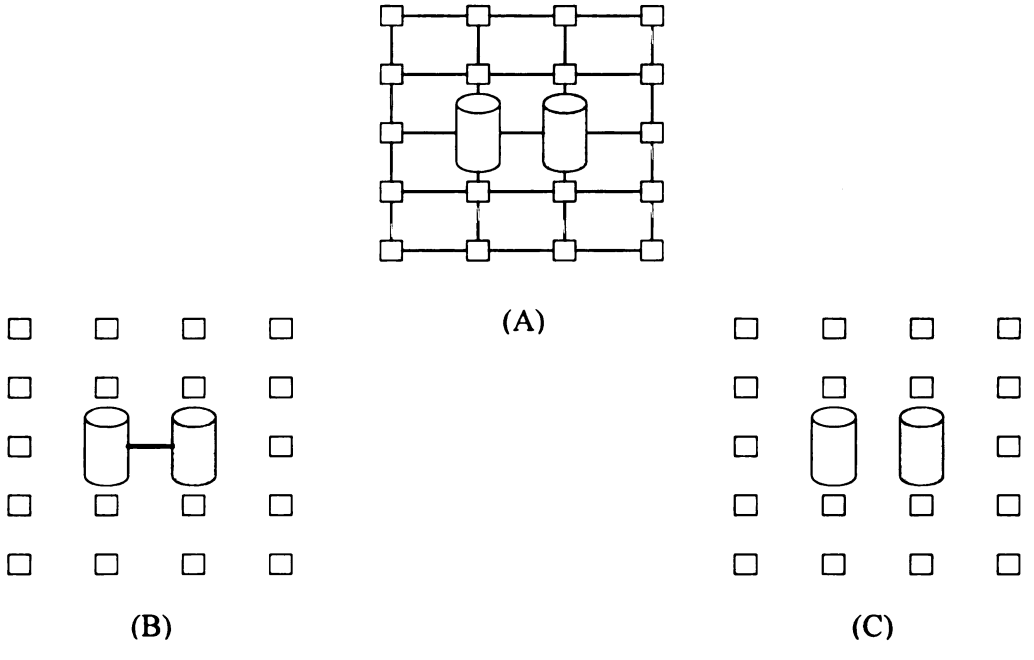

Figure 2.19. (A) The crystal lattice is composed of analyte (cylinders) trapped within the network formed between the matrix molecules (squares). Non-covalent bonds are represented by the lines connecting the boxes and cylinders. (B) The distribution of energy into the lattice can break the non-covalent interactions that hold the matrix molecules together in the lattice, (C) if the flow of energy into the lattice breaks the non-covalent bonds between the matrix molecules, it could also break the non-covalent bonds that hold the complexes together.

Also, it is important to note that, while peptides do not fragment in linear MALDI-TOF MS, oligonucleotides do. This is undoubtedly due to a combination of effects. Low energy fragmentation pathways may be available to oligonucleotides that are not options for peptides. However, clearly all fragmentation of analytes requires energy transfer into these analytes following irradiation.

If too much energy is being deposited into the analyte molecule following irradiation, how can the amount of energy deposited into the analyte be decreased?

The energy deposited during the excitation process allows the analyte and matrix to desorb from the target. When the energy is transferred into the lattice, the energy breaks the non-covalent bonds that form the lattice. If the energy left after the excitation process is sufficiently large, the strands may dissociate, Table 2.4 equation (2'). In order to maintain the duplex, the amount of energy transferred to the lattice can be decreased. This could be achieved in several ways.

First, the laser irradiation can be decreased. The influence of laser power is complex. The available energy increases, at least over some energy range, as more power is provided. As the crystals absorb the energy during irradiation, two scenarios may result. In the first example, more energy flows into the analyte, yielding fewer duplex ions. In contrast, the desorption of the analyte ions could occur more quickly, with less time for energy to flow into the analyte, yielding more abundant duplex ions.

A detailed study of how the proposed quantifiers vary with laser power was performed. The MALDI mass spectrometer used in this study was equipped with a N_2 laser, operated at constant power. The sample irradiation was controlled by an attenuator. This attenuator was assigned arbitrary values that ranged from 0, for full attenuation, to 4600 for unattenuated laser irradiation. These experiments were started at the threshold energy, or the lowest laser power that yielded ions. The laser power was increased in increments of 50 arbitrary units. After each increase, the SSD, DSRR, and WCSF values were calculated and recorded. At high laser powers, the ions representing the single-strands became saturated. No laser power allowed for an increase in the DSRR.

In addition to the laser power, the choice of matrix will affect the flow of energy into the lattice. Since the molar absorptivity of the matrix as well as the heat of sublimation and vaporization must be considered in the MALDI experiment, a variety of matrices were used in the laser power study. Matrices such as α-cyano-hydroxycinnamic acid and sinapinic acid are considered to be "hot" matrices, or matrices that tend to induce fragmentation of the analyte [4,5]. Other matrices such as HPA and ATT are considered to be "cool" matrices, or matrices that tend to reduce the amount of fragmentation of the analyte [4,5]. One proposed explanation for the hot and cold nature of matrices involves the temperature at which they sublime, and hence, desorb the analyte [6]. These four matrices were selected for the laser power study.

Another option is to decrease the energy absorption of the target crystal. A typical crystal lattice is shown in Figure 2.20 (A). The non-covalent complex is entirely surrounded by matrix molecules. Each matrix molecule has the potential to absorb the

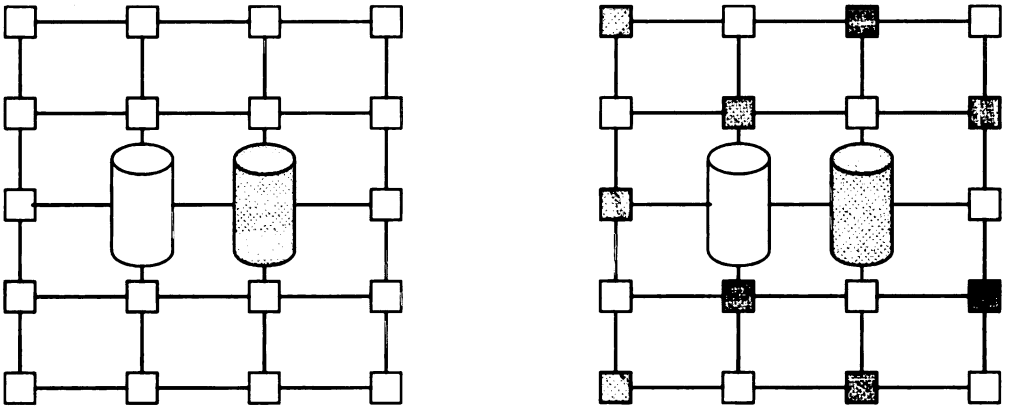

(A) (B)

Figure 2.20. (A) A crystal lattice containing the matrix molecules and analyte. The analyte is entirely surround by absorbing compounds. (B) A crystal lattice containing the analyte surrounded by both the matrix (white boxes) and a non-absorbing component (grey boxes).

energy from the laser and transfer this energy into the analyte, dissociating the complex. If the energy flowing into the crystal lattice exceeds that of the bond dissociation energy of the duplex, the duplex would dissociate. What if the lattice was composed of a non-absorbing compound as well, Figure 2.20 (B)? In Figure 2.20 (B), the matrix molecules are shown in the white boxes and the non-absorbing component is depicted by the gray boxes. The analyte is now surrounded by components that do not absorb all energy from the laser. This could decrease the amount of energy transferred to the lattice, and eventually the analyte, in the MALDI excitation process.

In order to explore the effect of matrix diluents, compounds were needed that would not absorb light from the laser. One such compound was the monosaccharide fucose. The structure of fucose, also known as deoxygalactose, is shown in Figure 2.21.

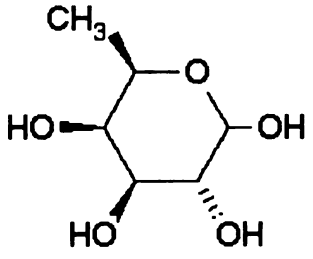

Figure 2.21. The structure of fucose.

Fucose has been used in previous experiments and has been shown to increase resolution and sample homogeneity in the analysis of peptides [7-8]. Since fucose does not absorb light at 337 nm, it decreases the amount of energy absorbed by the crystal lattice at a given spot on the target. The amount of fucose used in the experiments was varied in order to find the optimal concentration. Fucose was found to be most effective at concentration similar to that of the matrix and has been found to improve the quality of

the spectra of oligonucleotides, as it does for peptides [9]. A number of similar sugars have been investigated. Compared to fructose, sucrose, glucose, galactose, and maltose, the influence of fucose is, in fact, unique. The role of fucose in the MALDI experiment has been fully investigated and the results published [9]. A reprint can be found in Appendix B. .

In order to explore the role of fucose in the MALDI experiment, several experiments were performed. Several duplexes were used as the analyte with HPA or ATT as the matrix. The concentration of fucose was also varied. The effect of fucose is most apparent when used at a concentration of 25 mM, a concentration similar to that of the matrix. When fucose is used as an additive, the analyte is first spotted on the plate. Then, equal amounts of fucose and matrix are added to the MALDI target and allowed to dry. Figure 2.22 shows when fucose is used with duplex 1 and ATT, the DSRR value increases from 0.05 to 0.15. However, a WCSF value of 0.6 suggests that the Watson-Crick base pairing is not preserved in this MALDI experiment. This experiment suggests that the duplex may be dissociating in the liquid phase and fucose facilitates the random dimerization process.

When the matrix, analyte, and fucose are in solution together, it is not known if the resulting crystals retain this bulk composition. Due to the differing solubilities of the matrix, fucose, and the analyte, it is unknown if the crystal composition mirrors that of the solution composition. As the matrix/analyte/fucose solution used to make the MALDI target begins to evaporate, the first solubility limit encountered is that of the matrix, so matrix crystals begin to grow. At some point, the analyte and fucose must be incorporated into the matrix crystals because ions of both fucose and the analyte are

detected in the MALDI experiment. At some later point in the evaporation process, the solubility limit of fucose is encountered, and the composition of the crystals may change.

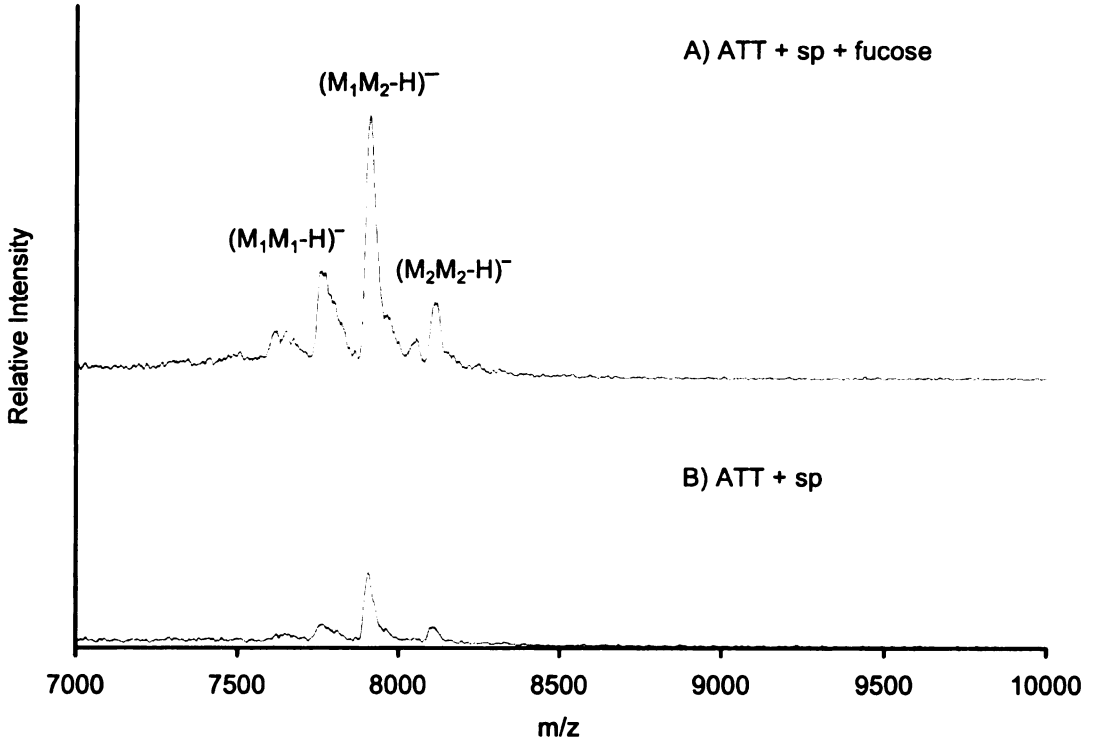

Figure 2.22. A portion of the negative ion MALDI mass spectrum of duplex 1 with A) ATT/sp/fucose and B) ATT/sp as the matrix. While the WCSF is 0.5 for both experiments, the DSRR is 0.05 without the fucose and 0.15 with the addition of fucose to the MALDI target.

While there are certainly a number of possible explanations for the mechanism through which fucose acts, the effect is real. If crystals are grown from a matrix/analyte solution containing fucose, the absorber has been diluted, and this should allow for some intervention in terms of energy deposition and redistribution.

Can additives stabilize the double-stranded DNA during the excitation process?

Many compounds exist that will bind to the nitrogen bases or to the phosphate groups in an oligonucleotide, either alone or in a duplex. Nucleic acids interact reversibly with a variety of chemical species including water, metal ions such as Na^+ and Mg^{2+}, and small organic (usually cationic) molecules. The interaction of the DNA with such species can be classified as electrostatic, groove-binding, or intercalating [10]. All species binding to DNA will bind to the DNA by one of these binding modes. A schematic of the binding modes of DNA is shown in Figure 2.23.

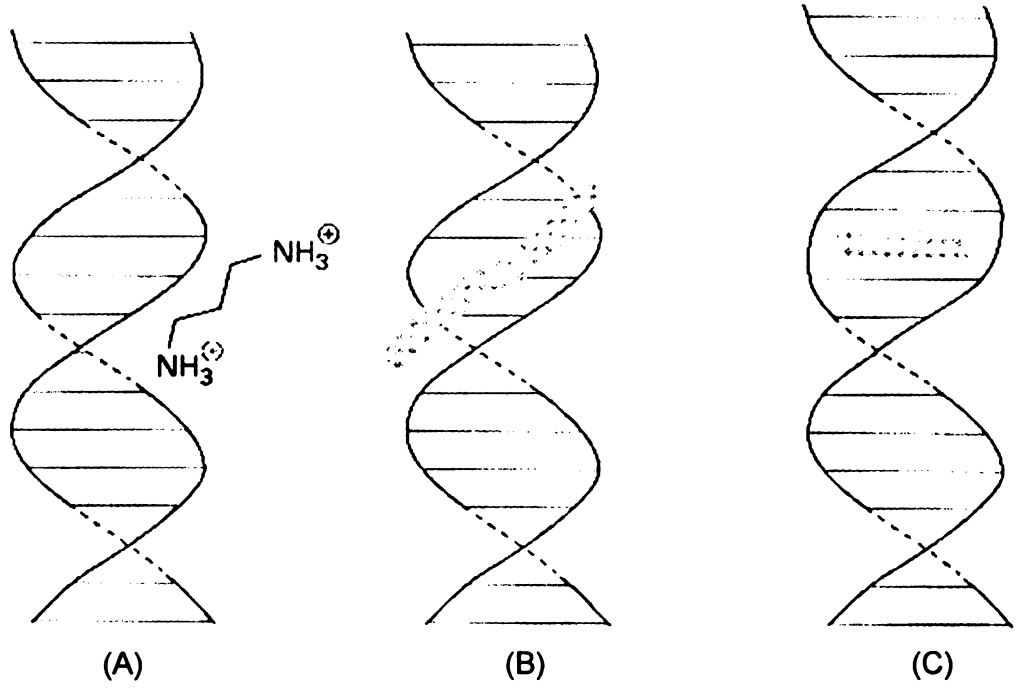

Figure 2.23. Bind modes of DNA. (A) External electrostatic, (B) Groove Binding, (C) Intercalation. The figure was adapted from reference 10.

Electrostatic interactions occur along the exterior of the helix through non-specific interactions such as those between alkali metal ions and the negatively charged phosphate groups. In Figure 2.23 (A), this has been demonstrated with a positively-charged polyamine. This positively charged amine can actually decrease the effective charge on the DNA by neutralizing two phosphate groups. There are a variety of ions that interact with DNA and a number of these species carry multiple positive charges. In contrast, groove-binding interactions, Figure 2.23 (B), involve the direct interactions of the bound molecule with the edges of the base pairs in the major or minor groove. Compounds can bind in either the major or minor groove of the DNA double-helix. Groove binding molecules, since they interact with the base pairs of DNA, can often be sequence specific binding in regions rich in A-T or G-C base pairing. Chromomycin, distamycin, and Hoechst 33258 bind in the minor groove of DNA and stabilize the double-stranded species [10]. Intercalation of a planar aromatic ring system between the base pairs can occur as well, Figure 2.23 (C). Intercalators include ethidium, daunomycin, and adriamycin [10].

Compounds binding to DNA through any of these binding modes may help maintain the duplex throughout the experiment. If these molecules were added to the initial matrix solution, the oligonucleotides may be trapped in the matrix crystals with these compounds attached. The presence of intercalators, groove-binders, and cationic species may stabilize the double-stranded species during the formation of the MALDI target. The compounds may also stabilize the duplex during the excitation phase, so the distribution of energy in the crystal lattice does not cause the dissociation of the complex. Lastly, the presence of stabilizing additives in the MALDI complex may stabilize DNA

duplex throughout the desorption/ionization process. The solid phase processes are closely linked. For this reason, it would be difficult to discern if the addition of an additive stabilizes the duplex through either step or both steps. The effect of stabilizing additives will be presented here, but discussed further in the Solid Phase: Desorption/Ionization section.

Electrostatic interactions

Amines

As mentioned previously, oligonucleotides have a negatively charged phosphate backbone when in solution. In order to form a singly charged anion, combinations of hydrogen, potassium, and sodium ions form adducts with the phosphate groups. In mass spectrometry, the desalting of samples leads to simplified spectra containing fewer alkali ion adducts and better resolution. Desalting/cleanup is commonly performed in MS laboratories prior to analysis using desorption/ionization methods. While the spectra have better resolution and peaks have fewer cation adducts, desalting the analyte solution can decrease the stability of the double stranded species due to the repulsion of the negatively charged phosphate groups [11].

The MALDI process typically yields only singly charged ions. However, oligonucleotides can be trapped in the MALDI crystals with a higher charge state. If desolvation energies increase as the number of charges increase [12-13], MALDI sensitivity for oligonucleotides should be low. Additives were developed to not only eliminate the alkali ion problem, but to provide protons to allow oligonucleotide desorption as a singly charged ion. These additives improve spectra for oligonucleotides without desalting the samples. When ammonium ions are present in solution, they compete effectively with the alkali ions in complexing with the negatively-charged phosphate groups. Adding ammonium salts such as ammonium acetate and diammonium hydrogen citrate reduces the formation of alkali ion adducts [14-16]. If multiple charges on a single strand prohibit desorption, multiple charges on a duplex create more problems due to interchain repulsions. Thus, additives such as ammonium salts and spermine

become more important when attempting to analyze double-stranded DNA. Their effective use reinforces the importance of ionic forms of oligonucleotides during crystal growth.

While diammonium hydrogen citrate (DAHC) is very useful in the analysis of oligonucleotides, its does not influence the formation/preservation of double-stranded oligonucleotide complexes. When DAHC is used as an additive in the MALDI experiment, the DSRR values for the spectra do not increase. The resolution of the peaks representing the single-stranded species increases. Also, there are fewer peaks representing the binding of alkali ions to the phosphate groups. So, DAHC is helpful when analyzing the single-stranded components of the duplex DNA, but does not help maintain the non-covalent interactions between the two strands.

Polyamines

Previously, the role of polyamines as matrix additives has been explored and spermine was found to improve MALDI spectra for single-stranded oligonucleotides, eliminating the need for ammonium citrate as well as desalting [17-19]. While the presence of spermine enhances the detection of the single-stranded oligonucleotides, could spermine stabilize the duplex in the MALDI experiment? Spermine and other polycations increase the stability of duplexes in solution. This fact is demonstrated by the increase in the melting temperatures of the double-stranded species when in the presence of polyamines. If spermine stabilized duplex DNA in solution, it is possible for spermine to stabilize DNA in the MALDI experiment.

Spermine is a polyamine that is of particular interest. Spermine is known to assist in the analysis of oligonucleotides in MALDI [17-19]. Spermine also serves a key role in the nucleus of cells. In the nucleus, spermine efficiently counteracts the repulsive electrostatic interactions that occur between negatively charged strands and allows the DNA to condense into a more compact structure [20]. The binding of spermine to an oligonucleotide is demonstrated in Figure 2.24.

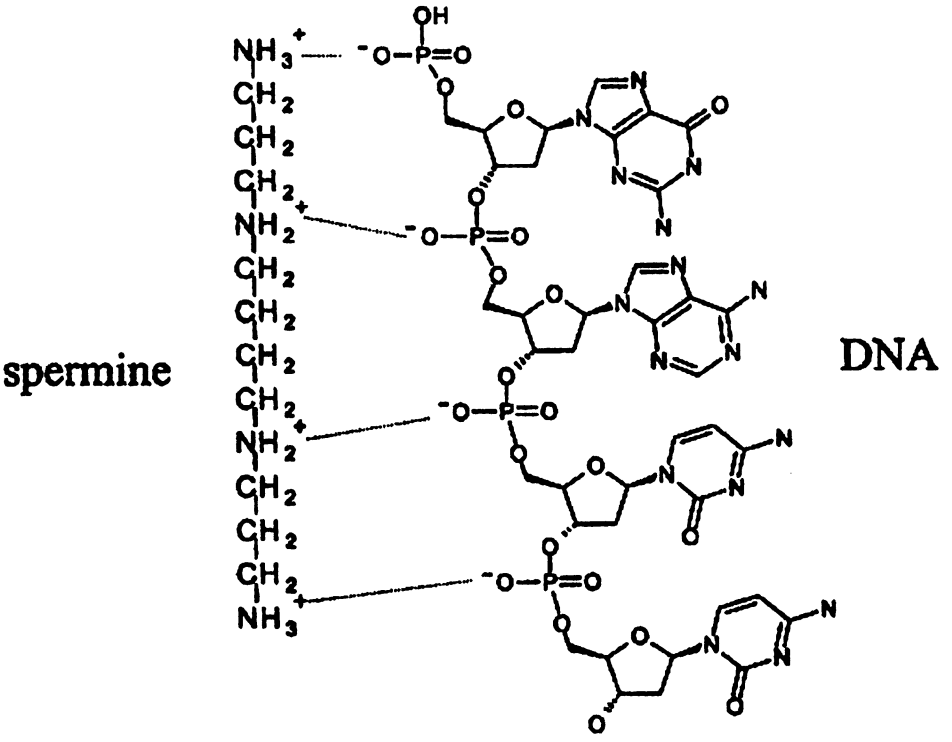

Figure 2.24. Interaction of spermine with an oligonucleotide. This figure was reproduced from reference 12.

Spermine is also used by crystallographers when growing crystals for X-ray crystallographic analysis. When spermine is present at high concentration compared to that of the oligonucleotide, homogenous crystals of the DNA will grow from the solution.

When these crystals are analyzed using X-ray crystallography, spermine is typically not resolved in the final crystal structure.

Additives such as spermine could aid in the stabilization of the double stranded species in the crystal formation process and the subsequent steps of excitation and desorption/ionization. Figure 2.25 shows results of an experiment in which a double-stranded oligonucleotide was analyzed using ATT as a matrix.

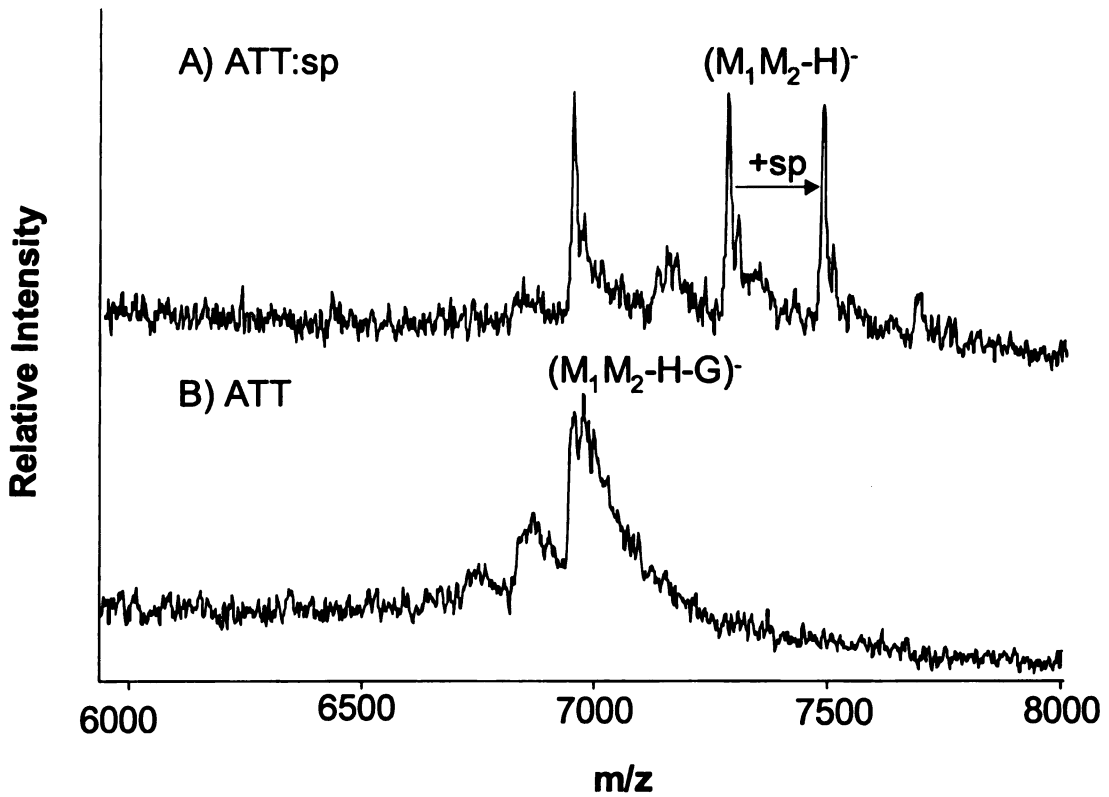

Figure 2.25. The negative-ion UV MALDI mass spectra of duplex 2 using (A) ATT/spermine as the matrix and (B) ATT alone as the matrix.

It is important to note that previously duplex 1 was analyzed using ATT as the matrix and no ions representing the duplex were detected. However, when duplex 2 is analyzed using ATT:sp or ATT as the matrix, Figure 2.25, the single strands are detected in

addition to the double-stranded oligonucleotide with the loss of the guanine (G) base, $(M_1M_2-G-H)^-$. When spermine was added, the intact duplex, $(M_1M_2-H)^-$, was detected as well as its spermine adduct. While the DSRR values of 0.05 for the duplex peaks were relatively small, the WCSF value was 1. These results are significant and suggest that additives known to complex with the duplex in solution may play an important role in stabilizing the duplex in the MALDI experiment as well. Also, the spermine stabilizes the duplex in the experiment and also remains bound to the duplex throughout the excitation and desorption/ionization steps. It is also important to note the dramatic increase in resolution when examining the $(M_1M_2-G-H)^-$ peak in both spectra.

The influence of spermine has been further investigated. In the development of spermine as an effective additive for single strand oligonucleotides, studies of the additive influence over a broad concentration range led to the identification of an optimum amount to use. Similarly, a set of experiments was performed with the duplex as the analyte. The optimal concentration of spermine as a co-matrix was 12.5 mM.

Often in MALDI analysis of oligonucleotides, the resulting spectra are dependent on the sequence of the analyte. For this reason, all experiments were performed with duplexes having different sequences. When duplex 1 is analyzed using the ATT/spermine matrix, the results of experiment are different, Figure 2.26. The DSRR value is 0.15 with the SSD and WCSF having values of 1.00. A peak representing a spermine bound to the duplex is also detected.

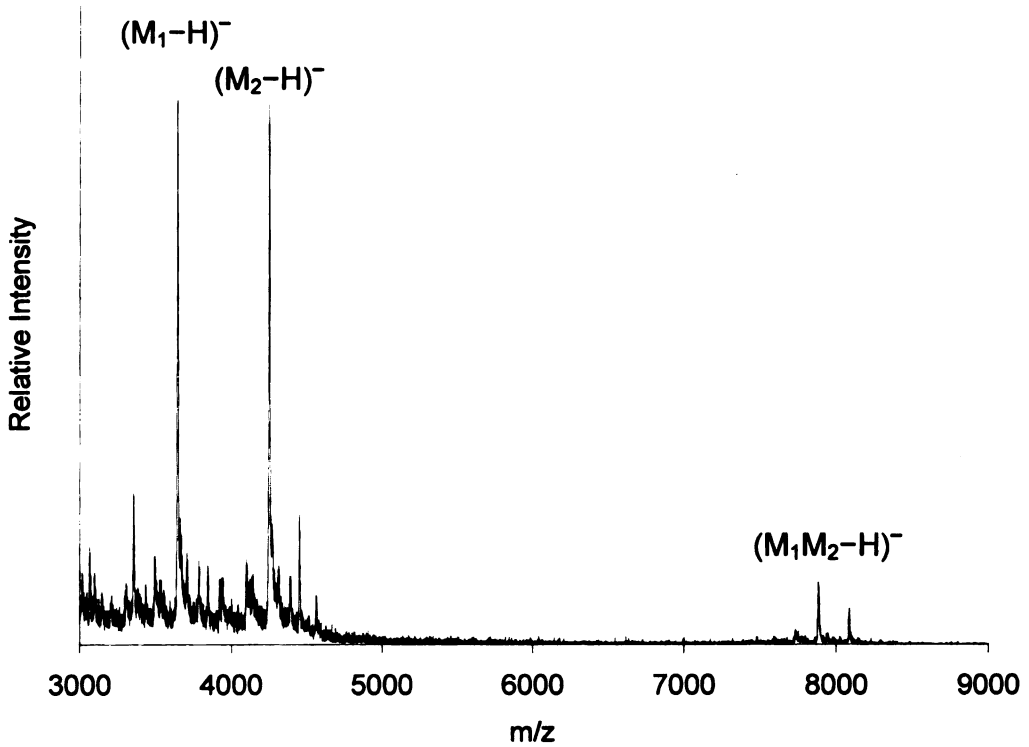

Figure 2.26. Negative-ion UV MALDI mass spectrum of duplex 1 using ATT/spermine as the matrix. The DSRR value is 0.15, the WCSF is 1.00, and the SSD is 1.00.

Crystallographic Condensing Agents

When crystals of double-stranded DNA are grown for analysis by X-ray crystallography, there are a variety of condensing agents used to neutralize the anionic strand-strand repulsions, allowing regular crystals to form [21]. These agents, often polycationic, include the polyamines, spermine and spermidine, that have already been discussed and other inorganic compounds such as ruthenium(III) hexammine chloride [22] and cobalt (III) hexammine chloride. Similar to spermine, these inorganic compounds play a key role in crystal growth and are frequently not resolved in the resulting crystal structure. These crystallographic condensing agents may be largely eliminated as part of the crystal growth process. For example, when growing crystals of d(AGGBrCATGCCT) in the presence of cobalt(III) hexammine, no cobalt hexammine ions are bound to the DNA in the resulting crystal structure [23]. Since spermine improved the MALDI analysis of duplex DNA, perhaps other condensing agents would have a similar effect. The cobalt hexammine counterion exhibits behavior similar to that of the spermine when in the presence of duplex oligonucleotides [24]. Cobalt (III) hexammine also decreases inter-strand repulsions of the duplex by decreasing the net effective charge on the phosphate groups. In a crystal structure, a hydrated cobalt(III)hexammine is found to bind to the phosphate groups of oligonucleotides [25].

When cobalt hexammine is added to the MALDI matrix, there are significant changes in the resulting spectrum, Figure 2.27. The peaks at m/z 8000 represent the

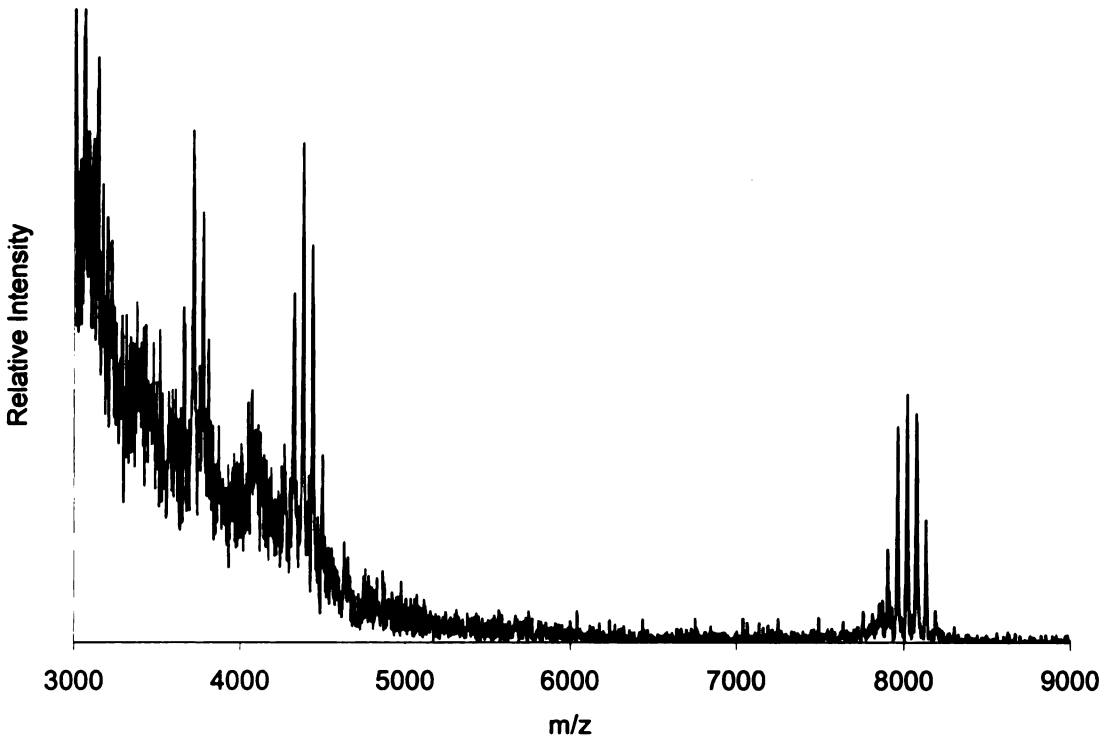

Figure 2.27. Negative-ion UV MALDI mass spectrum of duplex 1 using ATT as the matrix and cobalt(III) hexammine as an additive.

duplex, with approximately 50% of the complex remaining intact. From an analytical standpoint, it is important to realize that, using MALDI MS, if a peptide P is analyzed, a peak in the positive ion spectrum will appear corresponding to $(M+H)^+$, and frequently as $(M-H)^-$ if negative ions are being analyzed. However, if a noncovalently bound complex such as a duplex is analyzed, only the components may be detected. To detect the intact duplex present in a solution, Co(III) hexammine can be added to stabilize the complex.

Details of the mass spectral data reveal how Co(III) hexammine participates in this experiment, Figure 2.28. A peak representing the intact duplex in ionic form is observed, $(M_1M_2-H)^-$, at m/z 7899. Peaks at higher m/z values represent duplexes containing one or more cobalt ions. Cobalt addition accompanies the loss of 2 hydrogen

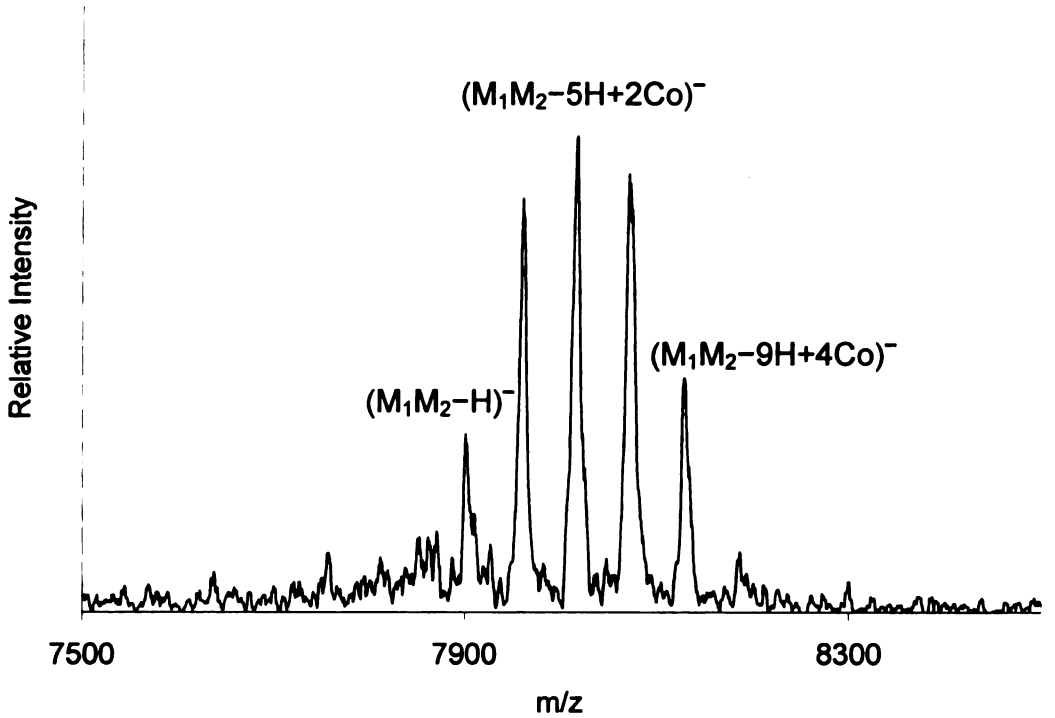

Figure 2.28. Detailed view of the duplex region of the spectrum shown in Figure 2.27. At m/z 7899, the deprotonated duplex is detected. For this experiment, with the particular amount of additive used, complexes containing up to 4 Co(II) ions can be observed. The peak at m/z 8013 corresponds to the addition of 2 Co(II) ions and the loss of 5 protons. At m/z 8127, 4 Co(II) ions are bound to the duplex and 9 protons are displaced. Complexes with more Co ions attached are observed at higher additive concentrations, but at the expense of sensitivity.

atoms. This, in addition to the fact that the overall charge on all of the ions observed is -1, indicates that the cobalt atoms are bound as Co^{+2}. Multiple cobalt adducts of both the single strand and duplex ions are formed. Experiments performed over a range of $Co(III)(NH_3)_6$ concentrations suggest that the maximum number of Co ions that can be attached to an oligonucleotide is proportional to the number of phosphates present, with one cobalt able to complex with 2 phosphate groups. When the cobalt is in a +3 state, the metal:phosphate ratio of 1:3 is observed in solution complexes, as measured using circular dichroism. This ratio of complexation appears to be a prerequisite to crystal

formation [26]. Since multiple metal complexes are observed for the single strands, it is assumed that a single cobalt ion interacts with two adjacent phosphate groups of a single chain-intrachain interactions need not be considered. It should be noted that experiments have been reported in which $FeCl_3$ was used as an additive to study small, single-strand oligonucleotides by MALDI-MS. In these experiments, iron as both Fe^{3+} and Fe^{2+} was observed to complex with these analytes in the gas phase [27].

In MALDI mass spectrometry, the ideal situation is to have one mass spectral peak represent one analyte. When multiple peaks are formed, distributing information over a number of m/z values, detection limits may be lowered. However, in this case, the reagent provides a substantial increase in sensitivity that outweighs the appearance of multiple peaks.

The effect of enhancing MALDI signals for duplexes is not observed when Co(II) compounds such as $CoCl_2$ are added to the solution from which the MALDI matrix crystals are grown, a surprising observation since the cobalt appears in the gas phase ionic species as Co(II). This suggests that a redox step is key in the formation of the observed species. In addition to the obvious utility of Co(III) hexammine as a tool in MALDI MS, the example presented here suggests that MALDI may also prove to be a useful analytical tool for investigating the processes through which reagents react with duplexes and assist in the generation of condensed phase samples.

Metal ions

Similar to amines and polyamines, metal ions are known to stabilize duplex DNA structures. In order to explore the effects of metals as additives, several experiments were performed. A variety of metal ions were selected due to their documented interactions with DNA. In a previous study, potassium, cesium, and sodium were found to increase the melting temperature or duplex DNA in solution at concentration of up to 1 M [11]. A variety of concentrations were used as well in order to record the DNA/metal ion ratio and its effect on the DSRR and WCSF values. Salts of other metals including copper, nickel, iron, lithium, calcium, silver, zinc, and lead were also used. With the addition of these metal ions, the DSRR values did not increase. The resolution of the single-stranded species did decrease significantly. As the positively charged metal ions interacted with the negatively charged oligonucleotide, metal-DNA adducts were formed complicating the spectra and decreasing the resolution of the peaks.

Compounds such as spermine and DAHC have been found to decrease the number of alkali ions that bind to the phosphate groups of DNA during the MALDI process. The experiments described above were repeated using ATT:spermine, ATT:DAHC, or HPA:spermine as the matrix. While the number of peaks representing the metal ions binding to the DNA decreased, there was still no increase in the DSRR values for any of the experiments.

Major and Minor Groove Binders

The major and minor grooves of DNA are very different. As a result, different types of compounds tend to bind in the types of grooves. Molecules that bind in the minor groove of DNA are typically polycyclic compounds that have the ability to twist their structure to fit into the helical curve of the minor groove. The major groove of DNA is more suited to the binding of proteins and peptides. Groove-binding molecules tend to be more sequence specific than other types of compounds that interact with DNA.

One of the first groove-binding compounds studied was chromomycin. Chromomycin has been found to bind readily to DNA containing a –XCGX– motif in the presence of magnesium ions [28-29]. In this motif, X is simply any nucleotide. Chromomycin and compounds similar in structure bind to DNA not as a monomer but as a dimer.

Experiments were performed using chromomycin as an additive with the duplex d(CCGGAATTGGCC)-d(TTGGCCAATTCCGG). This duplex was selected because it contained the consecutive CG base pairs. The initial experiment was performed by mixing a microliter of a 25 micromolar solution of duplex with a 25 mM solution of chromomycin. A microliter of this solution was then mixed with a microliter of either the ATT or HPA matrix solution. Both experiments yielded DSRR values of 0. Another set of experiments was performed by incubating the chromomycin solution with the duplex solution in the presence of 1) no magnesium ions, 2) 1 mM magnesium chloride, 3) 10 mM magnesium chloride, or 4) 25 mM magnesium chloride. These solutions were analyzed using ATT and HPA after 1) 0 minutes, 2) 1 hour, 3) 12 hours, and 4) 24 hours. The incubated solutions were held at 37°C for the allotted time period. After incubation,

the solutions were analyzed in MALDI with HPA or ATT as the matrix. No duplex ions were detected.

Similar studies were performed using groove-binding compounds known to bind in A-T sequences of the DNA minor groove. These compounds are mostly crescent shaped and contain an amino group capable of hydrogen bonding with the A-T base pairs. These are not capable of binding with GC pairings due to the amino group on the guanine. Distamycin, known to bind in the AATT minor groove of the oligonucleotide d(CGCAAATTTGCG), had no effect on the DSRR values for the MALDI experiments. The aromatic diamidines, berenil and 4',6-diamidino-2-phenylindole (DAPI), were also used. Again, studies performed with DAPI and berenil also gave DSRR values of 0. Lastly, Hoechst 33258 was used with similar results.

Histones and Peptides

If some small molecules that are known to interact with DNA can stabilize the duplex in the MALDI experiment, larger molecules such as proteins and peptides may also have a stabilizing effect. Interactions between DNA and proteins play important roles in various biochemical processes. Chromosomes contain DNA and an equal mass of histone and non-histone proteins [30]. Histones have molecular weights between 13,000 and 30,000 g/mol. Histones are proteins that are highly conserved across species and contain many basic (Arg, Lys) residues. It is proposed that these positively charged amino acid side chains interact with and stabilize the DNA through salt bridges. In sperm cells, DNA is tightly packed due to the presence of arginine-rich proteins called protamines. Protamines bind to DNA with their α-helices in the major groove of the DNA, where they neutralize the charge of the phosphates and enable the tight packing of the duplexes [10]. While the main driving forces for protamine-DNA binding are the ionic interactions, there is a distinct co-operativity that cannot be explained on the basis of electrostatic interactions alone [31]. Protamines perform functions similar to histones, but are generally much smaller, with molecular weights between 4,000 and 10,000 g/mol [32]. The effect of the presence of peptides on double-stranded oligonucleotides has not been examined.

In an experiment designed in our laboratory to explore the differences in resolution and sensitivity between a peptide and an oligonucleotide in UV-MALDI-MS, a solution was prepared that contained equal amounts of a peptide and oligonucleotide of similar molecular weights. In the resulting spectra, peaks were detected for the peptide, $(P+H)^+$, the oligonucleotide, $(O+H)^+$, and a peptide-oligonucleotide complex, $(P+O+H)^+$.

Similar results have been reported previously [33]. In order to examine the influence of peptides on double-stranded oligonucleotides, several peptides were combined with duplex oligonucleotides and analyzed by UV MALDI-MS. The peptides were used at a level of 1 pmol or less. An additive that is most effective at a level similar to that of the analyte, rather than that of the matrix, will be referred to as a microadditive.

The peptides, dynorphin A, cytochrome c, fibrinogen binding inhibitor peptide (FBI peptide), β-melanocyte stimulating hormone (β-MSH), katacalcin, kemptide, β-casein, ubiquitin, kassinin, and oxytocin were all purchased from Sigma (St. Louis, MO) and used without further purification. Peptides were dissolved in MilliQ water at concentrations of 1.0 pmol/μL. A microliter of a peptide stock solution was combined with a microliter of the stock double-stranded oligonucleotide solution. When incubated, the peptide/oligonucleotide solution was heated to 37° C for 15 minutes. A microliter of the resulting solution was spotted onto the MALDI target with a microliter of the matrix solution. Samples analyzed with fucose were prepared by mixing 1 μL of the peptide/oligonucleotide solution with 1 μL of the fucose solution and 1 μL of the co-matrix solution on a gold sample plate. The mixture was then allowed to air-dry.

The duplex of d(CCGGAATTGGCC) bound to d(TTGGCCAATTCCGG) was used for the experiments designed to evaluate peptides as microadditives with ATT:spermine as the matrix, Figure 2.29(A). The SSD is 0.7 and the DSRR is 0.006. While the intact duplex, $(M_1M_2-H)^-$ is detected in this experiment, the peak representing the $(M_2M_2-H)^-$ species is surprisingly intense, giving the spectrum a WCSF of 0.3.

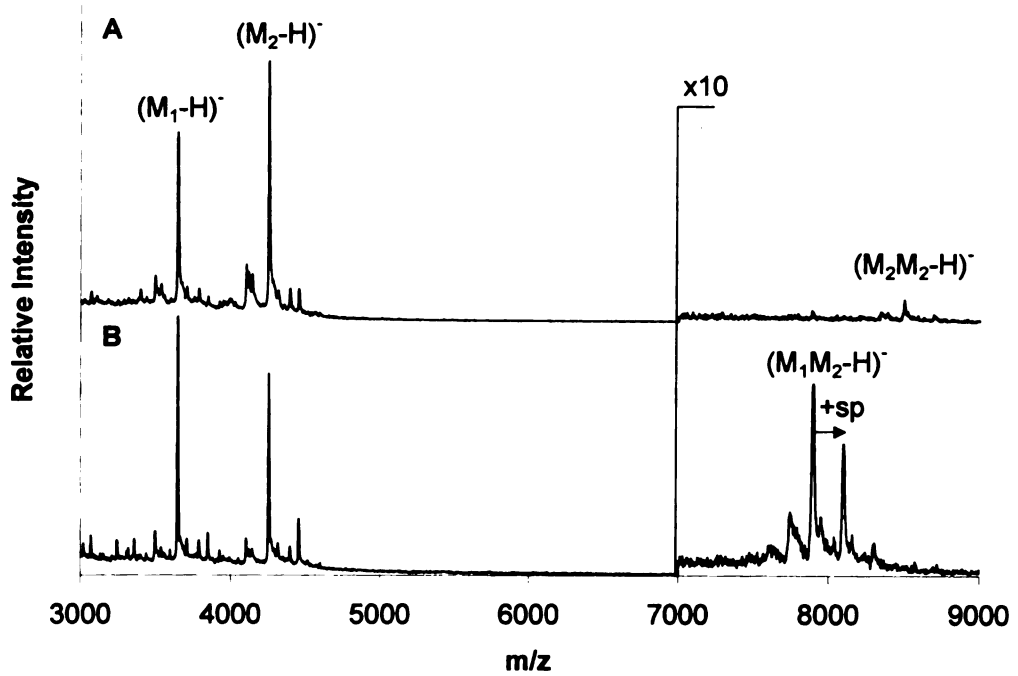

Figure 2.29. Negative-ion MALDI mass spectra of duplex 1 with A) no peptide present and B) with β-MSH present. ATT:sp was used as the matrix for both experiments. 25 pmol of duplex and 1pmol of β-MSH were deposited onto the MALDI target. For A), the SSD is 0.7, the DSRR is 0.006, and the WCSF of 0.3. For B), the SSD is 1.1, the DSRR is 0.06, and the WCSF is 1.0. The peptide:duplex ratio is 1:25.

When only 1 pmol of β-MSH was added to the target (which contained 25 pmol of duplex) used to obtain Figure 2.29(A), the spectrum shown in Figure 2.29(B) is obtained. The SSD changes dramatically to 1.1, the DSRR is 0.06, and the WCSF is 1.0. There are no peaks representing either $(M_1M_1-H)^-$ or $(M_2M_2-H)^-$. In this experiment, β-MSH stabilized, to some extent, double-stranded DNA ions in UV MALDI MS, *when present at a level of one picomole on the MALDI target.* Other peptides evaluated are listed in Table 2.7. All peptides were used as additives by adding 1 pmol of peptide to 25

pmol of duplex 1 and analyzed using ATT:sp as the matrix. The DSRR and SSD values are listed in the table. All WCSF values are 1.

The peptides evaluated as microadditives can be grouped based both on their size and amino acid content. It is possible that the most successful experiments would have involved peptides that have a size similar to that of the oligonucleotide. From spermine experiments performed previously [17-19], we have learned that additives capable of multiple interactions with the oligonucleotides are important. For this reason, the number of basic residues in the peptide may be important, with multiple basic residues increasing the number of electrostatic interactions possible. Previously it was determined that peptides containing basic residues increase the melting temperature of duplex oligonucleotides in solution [34]. Protonated backbone nitrogens may aid in stabilization as well.

When examining the data in Table 2.7, attempts were made to correlate the experimental results with the structural features of the peptides. The two peptides used with the most notable success were dynorphin A and β-MSH. Both of these larger peptides contain basic residues with three arginines and two lysines out of the 17 amino acids in dynorphin A and six basic residues out of the 22 amino acids residues in β-MSH including three lysines, two arginines, and one histidine. Dynorphin A and β-MSH presumably interact with the double-stranded oligonucleotides at multiple sites. The backbone nitrogens may be important in the stabilization of the duplex. A positively-charged backbone in a peptide may behave similarly to spermine in solution. The side chains of the peptide may also play an important role. The amino acids, tyrosine, phenylalanine, and tryptophan, contain aromatic side chains. These side chains may

Table 2.7. Peptide Additives and their Influence on UV MALDI Spectra of Duplex 1

Peptide	Peptide Sequence	SSD	WCSF	DSRR	% Arg	% Lys	MW
Dynorphin A	YGGFLRRIRPKLKWDNQ	1.1	1.0	0.1	17.65	11.76	2147.50
β-MSH	AEKKDEGPYRMEHFRWGSPPKD	1.1	1.0	0.1	9.09	13.64	2660.90
Katacalcin	DMSSDLERDHRPHVSMPQNAN	1.1	1.0	0.0	9.52	0.00	2436.60
Kemptide	LRRASVA	0.9	1.0	0.0	28.57	0.00	771.90
FBI peptide	HHLGGAKQAGDV	1.0	1.0	0.0	0.00	8.33	1189.30
Trilysine	KKK	1.0	1.0	0.0	0.00	100.00	402.50
N-ε-acetyl-Lys	K	1.0	1.0	0.0	0.00	100.00	188.23
Leucine Enkephalin	YGGFL	1.0	1.0	0.0	0.00	0.00	555.60
Boc-MNF amide	BMNF	0.8	1.0	0.0	0.00	0.00	510.60
Hexaalanine	AAAAAA	1.0	1.0	0.0	0.00	0.00	444.50
Trialanine methyl ester	AAA	0.9	1.0	0.0	0.00	0.00	305.30
Triserine	SSS	1.1	1.0	0.0	0.00	0.00	279.20

partially intercalate between the nitrogen-containing bases of the oligonucleotide, stabilizing the duplex. Increases in the melting temperature of duplex DNA have been reported when in the presence of peptides containing phenylalanine residues [34]. Basic side chains may also play an important role as discussed previously.

Since peptides containing only alanine residues were not as successful as additives, it appears that the backbone nitrogens are not effective in stabilizing the duplex. Small peptides containing basic residues such as Lys-Lys-Lys were found to increase the DSRR value although these smaller peptides were less effective than Dynorphin A and β-MSH. Similarly, peptides containing aromatic side chains were also capable of increasing the DSRR values for the experiments.

Since the best results are seen with the peptides Dynorphin A and β-MSH, which contain both aromatic and basic amino acids, it is not perhaps the size of the peptide that is of primary importance, but the spacing between basic amino acids. When basic amino acids in a larger peptide are separated by other residues, the separation between those basic residues may be similar to the spatial separation between the phosphates of the oligonucleotide. This may lead to greater stabilization of the duplex. Clearly, more work is required to find the optimal peptide, but these experiments establish structural aspects of the additives that are important and show that peptides can, at relatively low levels, stabilize to some extent duplexes in the UV MALDI experiment.

In order to maximize the interaction between the peptides and the double-stranded oligonucleotides, several conditions were varied in the experiments. At first the peptide and oligonucleotide were combined on the MALDI plate before the addition of the matrix. To insure thorough mixing, peptide and oligonucleotide solutions were also pre-

mixed before deposition on the target. There was no difference between spectra acquired using on target mixing or pre-mixed solutions. A solution of the peptide and oligonucleotide was also pre-mixed and incubated at both room temperature and at 37°C prior to MALDI analysis. When incubated at either temperature, samples again yielded spectra similar to the unincubated samples.

For the data shown in Table 2.7, one picomole of each peptide was used in the formation of the MALDI target. While 1 pmol was optimal for most peptides, improvements were seen with as little as 50 fmol of peptides present in the target. FBI peptide, katacalcin, and β-MSH all yielded duplex spectra with improved DSRR values with less than 1 pmol of peptide present in the target. While addition of these peptides to the MALDI target improved the DSRR, the β-MSH peptide gave the best results. Figure 2.30 shows the negative-ion MALDI mass spectrum of a target containing 100 fmol of β-MSH and 25 pmol of double-stranded oligonucleotide, using ATT:sp as the matrix. The SSD was 0.94, the DSRR was 0.09 and the WCSF was 1.00. The presence of the peptide still influences the resulting mass spectrum even when the relative concentration of the oligonucleotide:peptide is 250:1.

Here we show that certain peptides can stabilize, to some extent, double-stranded DNA ions in MALDI, *when present at levels of less than one picomole on the target.* Since they are most effective at levels similar to that of the analyte, rather than the matrix, we will refer to these generally as microadditives.

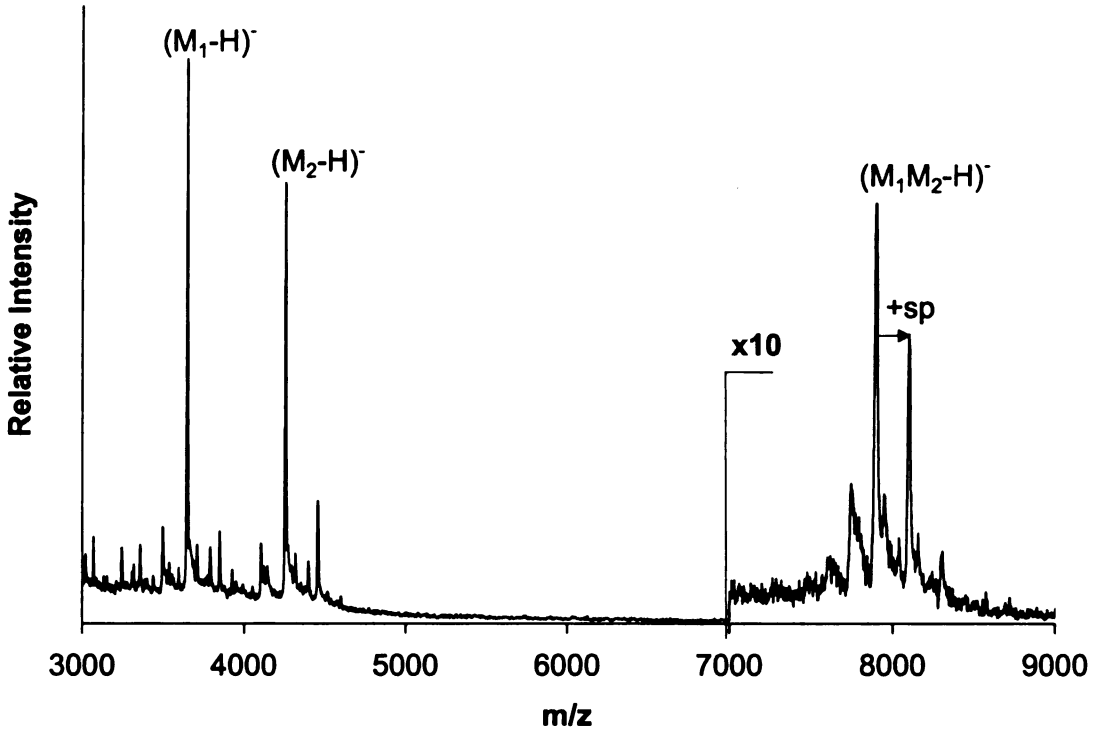

Figure 2.30. Negative-ion MALDI mass spectrum of duplex 1 with 100 fmol of β-MSH and ATT:sp as the matrix. The SSD was 0.94, the DSRR was 0.09 and the WCSF was 1.00. The peptide:duplex ratio is 1:250.

Intercalators

Intercalators are planar, aromatic cations that insert themselves into the aromatic ring system between the DNA base pairs. As a results of this insertion, often intercalators cause the DNA helix to unwind, distorting the DNA backbone. Two main intercalators were studied. These are methylene blue and ethidium bromide. While it was believed that methylene blue could act as both a groove-binder and as an intercalator, spectroscopic data clearly indicates the intercalation of methylene blue between two consecutive base pair of an oligonucleotide [35-36].

Stock solutions of methylene blue and ethidium bromide were made at a concentration of 1 mM in water. Saturated matrix solutions of ATT and HPA were made using a 1:1 acetonitrile/water solution and a saturated ATT/spermine co-matrix was made using a 1:1 solutions of acetonitrile and 25 mM aqueous spermine solution. For experiments performed with ethidium bromide and methylene blue, the oligonucleotide solution was mixed with an equal volume of the additive solution prior to spotting on the sample plate. A microliter of matrix was then added.

After formation of the target, the oligonucleotide/methylene blue/matrix crystals were analyzed. It was that methylene blue binds to the single-stranded oligonucleotide in the MALDI expeirment. The resulting spectrum is shown in Figure 2.31, with the structure of the methylene blue cation. While methylene blue (MB) is observed bound to the single-stranded species, its presence appears to stabilize the duplex as well, Figure 2.31. In this experiment, the DSRR value was 0.03, the SSD was 0.9, and the WCSF was 1.0. With a WCSF of 1.0, it appears that a portion of the duplex was maintained

throughout the entire UV-MALDI experiment, due to the presence of this additive, although the duplex represents only a small percentage of the initial complex.

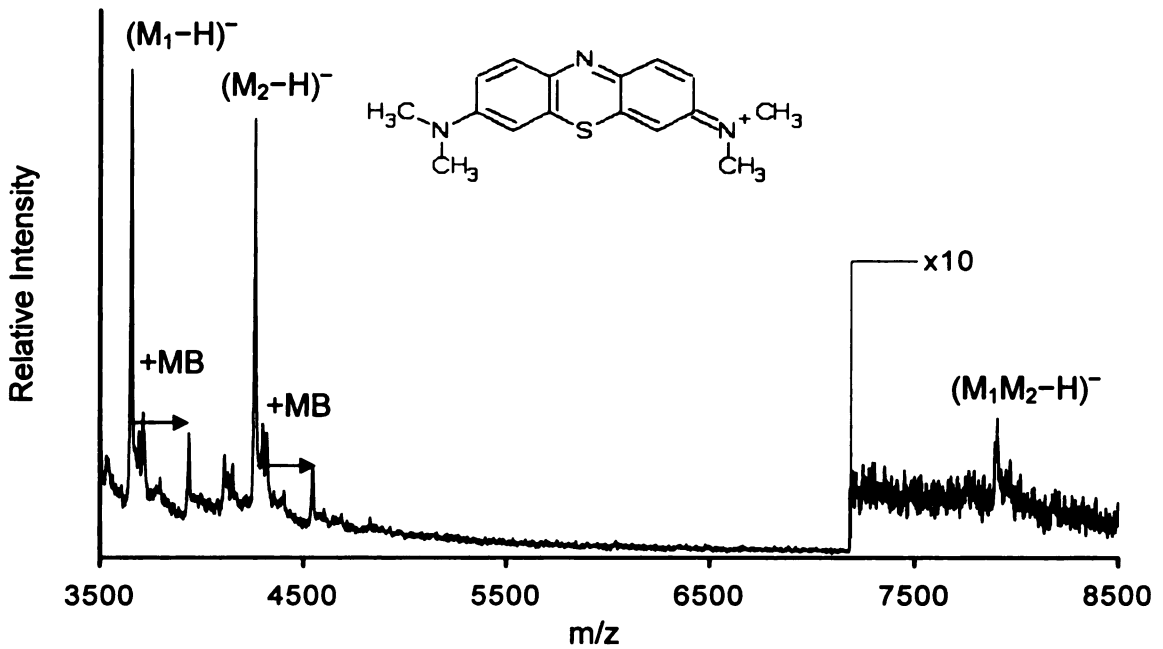

Figure 2.31. The negative-ion MALDI mass spectrum of duplex 1 with methylene blue as an additive. ATT was used as the matrix. The SSD was 0.9, the DSRR was 0.03, and the WCSF was 1.0. The additive duplex ratio is 40:1.

As discussed previously, the presence of spermine can lead to an improvement in resolution of oligonucleotide MALDI expeirments. The addition of spermine to the matrix solution may also improve the results of experiments using other additives such as methylene blue. If the methylene blue experiment from Figure 2.31 is repeated with an ATT matrix solution containing spermine, the resolution in the duplex region is improved, the DSRR value increases, and a methylene blue adduct is detected in the

duplex region, Figure 2.32. The DSRR increases significantly from 0.03 in Figure 3 to 0.07 in Figure 5. The WCSF is 1.0 and the SSD is 0.9.

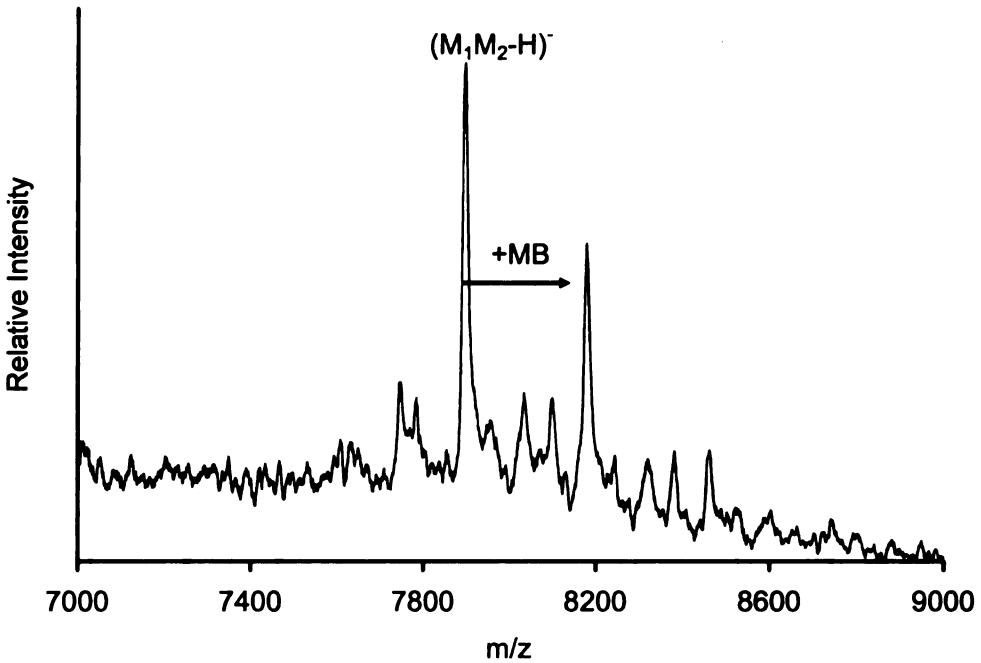

Figure 2.32. A portion of the negative-ion MALDI mass spectrum of duplex 1 with methylene blue (MB) as an additive. ATT:sp was used as the matrix. The DSRR is 0.05 and the WCSF is 1.0. The spermine:MB:duplex ratio is 500:40:1.

As mentioned previously, ethidium bromide has been found to stabilize duplexes in solution. When used in the MALDI experiment, equal volumes of duplex 1 and ethidium bromide solutions were combined. One microliter of the oligonucleotide:ethidium solution was spotted on the MALDI target with one microliter of the HPA matrix solution. The molar amounts of components of the target are matrix:additive:oligo, 2000:40:1. This is typical since effective additives for MALDI MS are usually present at molar amounts greater than the analyte. The resulting spectrum is shown in Figure 2.33, with the structure of the ethidium ion. The ethidium cation binds

to both the single and double-stranded species of duplex 1. That is, in addition to analyte ions, $(A-H)^-$, there are also $(A-2H+Et)^-$ ions observed. With the appearance of the dimer peaks, the DSRR increases from 0 (in Figure 1 B) to 0.05.

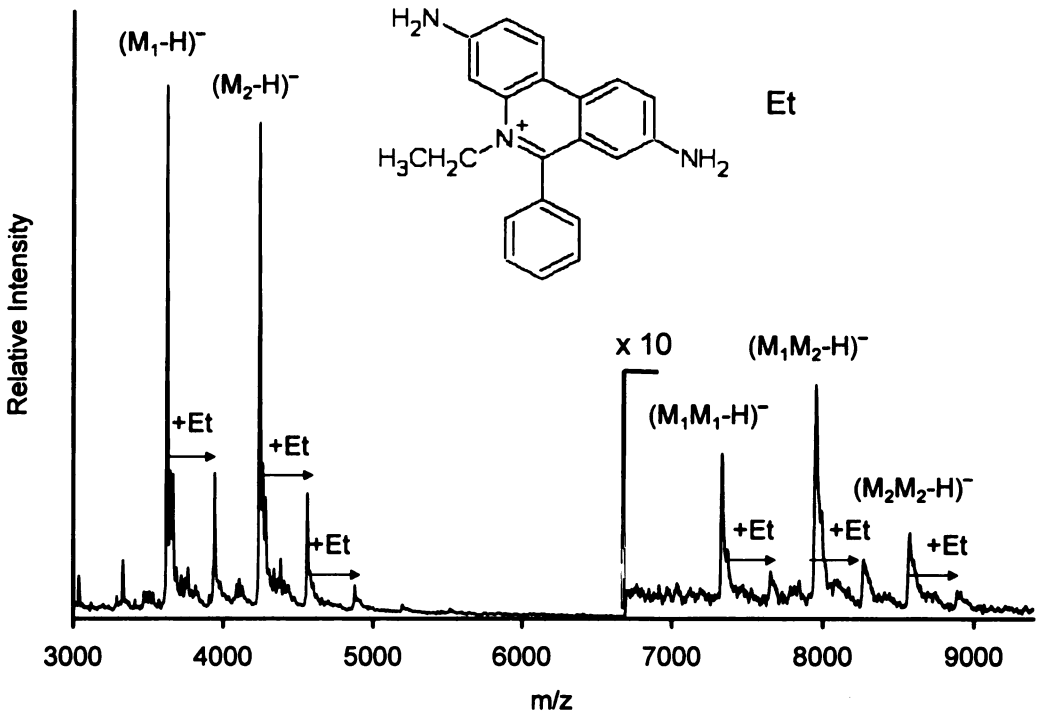

Figure 2.33. The negative-ion MALDI mass spectrum of duplex 1. HPA was used as the matrix with ethidium (Et) bromide as an additive. Ethidium adducts of both the single and double-stranded oligonucleotides are observed. The SSD is 1.0, DSRR is 0.05 and the WCSF is 0.5. The additive duplex ratio is 40:1.

In Figure 2.33, while there are peaks representing the $(M_1M_2-H)^-$ species, there are also peaks representing the $(M_1M_1-H)^-$ and $(M_2M_2-H)^-$ species. While the DSRR increased from 0 to 0.05, the WCSF is 0.5, suggesting random dimerization. If random dimerization occurs, the duplex may completely dissociate and the single strands are likely dimerizing with no sequence specificity as the crystals are growing. Thus, while

ethidium addition does result in "dimer ions", we conclude that this additive does not stabilize the initial duplex throughout the UV-MALDI experiment.

References

1. Vertes, A.; Gijbels, R.; Levine, R.D. Homogeneous bottleneck model of matrix-assisted ultraviolet-laser desorption of large molecules. *Rapid Commun. Mass Spectrom.* **1990**, *4*, 228-233.

2. Vertes, A.; Levine, R.D. Sublimation versus fragmentation in matrix-assisted laser desorption. *Chem. Phys. Lett.* **1990**, *171*, 284-290.

3. Bencsura, A.; Navale, V.; Sadeghi, M.; Vertes, A. Matrix-guest energy transfer in matrix-assisted laser desorption. *Rapid Commun. Mass Spectrom.* **1997**, *11*, 679-682.

4. Zenobi, R.; Knochenmuss, R. Ion formation in MALDI mass spectrometry. *Mass Spectrom. Rev.* **1998**, *17*, 337-366.

5. Karas, M.; Bahr, U.; Strupat, K.; Hillenkamp, F.; Tsarbopoulos, A.; Pramanik, B.N. Matrix dependence of metastable fragmentation of glycoproteins in MALDI TOF mass-spectrometry. *Anal. Chem.* **1995**, *67*, 675-679.

6. Karas, M.; Bahr, U.; Stah-Zeng, J.R. Steps toward a more refined picture of the matrix function in UV MALDI. In: Large Ion: Their Vaporization, Detection and Structural Analysis; T. Baer; C.Y. Ng; I. Powis (Eds.); Wiley: London, 1996.

7. Billeci, T.M.; Stults, J.T. Tryptic mapping of recombinant proteins by matrix-assisted laser desorption/ionization mass spectrometry. *Anal. Chem.* **1993**, *65*, 1709-1716.

8. Gusev, A.I.; Wilkinson, W.R.; Proctor, A.; Hercules, D.M. Improvement of signal reproducibility and matrix/comatrix effects in MALDI analysis. *Anal. Chem.* **1995**, *67*, 1034-1041.

9. Distler, A.M.; Allison, J. Improved MALDI-MS analysis of oligonucleotides through the use of fucose as a matrix additive. *Anal. Chem.* **2001**, *73*, 5000-5003.

10. Blackburn, G.M.; Gait, M.J. Nucleic acids in chemistry and biology, 2nd ed.; Oxford University Press: New York, 1996.

11. Schildkraut, C.; Lifson, S. Dependence of the melting temperature of DNA on salt concentration. *Biopolymers*. **1965**, *3*, 195-208.

12. Asara, J. Enhancing spectra in desorption/ionization mass spectrometry through the use of chemical additives. Michigan State University, 1999.

13. Takayama, M. Formation of $M^{+\cdot}$ ions and electronic excitation under fast-atom bombardment conditions by using a liquid matrix. *J. Am. Soc. Mass Spectrom.* **1995**, *6*, 114-119.

14. Currie, G.; Yates, J. III. Analysis of oligodeoxynucleotides by negative-ion matrix-assisted laser desorption mass spectrometry. *J. Am. Soc. Mass Spectrom.* **1993**, *4*, 955-963.

15. Wu, Z.; Biemann, K. The MALDI mass spectra of carbosilane-based dendrimers containing up to eight fixed positive or 16 negative charges. *Int. J. Mass Spectrom. Ion Processes*. **1997**, *165-166*, 349-361.

16. Pieles, U.; Zürcher, W.; Schär, M.; Möser, H.E. Matrix-assisted laser-desorption ionization time-of-flight mass-spectrometry – A powerful tool for the mass and sequence-analysis of natural and modified oligonucleotides. *Nucleic Acid Res.* **1993**, *21*, 3191-3196.

17. Asara, J.; Allison, J. Enhanced detection of oligonucleotides in UV MALDI MS using the tetraamine spermine as a matrix additive. *Anal. Chem.* **1999**, *71*, 2866-2870.

18. Asara, J.M.; Hess, J.S.; Lozada, E.; Dunbar, K.R.; Allison, J. Evidence for binding of dirhodium bis-acetate units to adjacent GG and AA sites on single-stranded DNA. *J. Am. Chem. Soc.* **2000**, *122*, 8-13.

19. Distler, A.M.; Allison, J. 5-Methoxysalicylic acid and spermine: a new matrix for the matrix-assisted laser desorption/ionization mass spectrometry analysis of oligonucleotides. *J. Am. Soc. Mass Spectrom.* **2001**, *12*, 456-462.

20. Esposito, D.; Del Vecchio, P.; Barone, G. Interaction with natural polyamines and thermal stability of DNA. A DSC study and a theoretical reconsideration. *J. Am. Chem. Soc.* **1997**, *119*, 2606-2613.

21. Pelta, J.; Livolant, F.; Sikorav, J.L. DNA aggregation induced by polyamines and cobalthexammine. *J. Biol. Chem.* **1996**, *271*, 5656-5662.

22. Karthe, P.; Gautham, N. Structure of d(CACGCG)-d(CGCGTG) in crystals grown in the presence of rutheniumIII hexammine chloride. *Acta Cryst.* **1998**, *D54*, 501-509.

23. Nunn, C.M. Crystal structure of d(AGGBrCATGCCT): implications for cobalt hexammine binding to DNA. *J. Biomol. Struct. Dyn.* **1996**, *14*, 49-55.

24. Malinina, L.V.; Makhaldiani, V.V.; Tereshko, V.A.; Zarytova, V.F.; Ivanova, M.F. Phase diagrams for DNA crystallization systems. *J. Biomol. Struct. Dyn.* **1987**, *5*, 405-433.

25. Ramakrishnan, B.; Sekharudu, C.; Pan, B.; Sundaralingam, M. Near-atomic resolution crystal structure of an A-DNA decamer d(CCCGATCGGG): cobalt hexammine interaction with A-DNA. *Acta Cryst.* **2003**, *D59*, 67-72.

26. Kankia, B.K.; Buckin,V.; Bloomfield, V.A. Hexamminecobalt(III)-induced condensation of calf thymus DNA: circular dichroism and hydration measurements. *Nucleic Acids Res.* **2001**, *29*, 2795-2801.

27. Hettich, R.L. Formation and characterization of iron-oligonucleotide complexes with matrix-assisted laser desorption/ionization Fourier transform ion cyclotron resonance mass spectrometry. *J. Am. Soc. Mass Spectrom.* **1999**, *10*, 941-949.

28. Gao, X.; Patel, D.J. Solution structure of chromomycin·DNA complex. *Biochemistry.* **1989**, *28*, 751-762.

29. Aich, P.; Sen, R.; Dasgupta, D. Role of magnesium ion in the interaction between chromomycin A_3 and DNA: binding of chromomycin A_3-Mg^{2+} complexes with DNA. *Biochemistry.* **1992**, *31*, 2988-2997.

30. Bradbury, E.M.; Moss, T.; Hayashi, H.; Hjelm, R.P.; Suau, P.; Stephens, R.M.; Baldwin, J.P.; Cranerobinson, C.; Nucleosomes, histone interactions, and role of histone-H3 and histone-H4. *Cold Spring Harb. Sym.* 1977, *42*, 277-286.

31. Porschke, D. Nature of protamine-DNA complexes: a special type of ligand binding co-operativity. *J. Mol. Biol.* **1991**, *222*, 423-433.

32. Ausió, J. Histone H1 and evolution of sperm nuclear basic proteins. *J. Biol. Chem.* **1999**, *274*, 31115-31118.

33. Harrison, J.G.; Balasubramanian, S. Synthesis and hybridization analysis of a small library of peptide-oligonucleotide conjugates. *Nucl. Acids Res.* **1998**, *26*, 3136-3145.

34. Robledo-Luiggi, C.; Vera, M.; Cobo, L.; Jaime, E.; Martínez, C.; González, J. Partial intercalation with nucleic acids of peptides containing aromatic and basic amino acids. *Biospectroscopy.* **1999**, *5*, 313-322.

35. Bradley, D.F.; Stellwagen, N.C.; O'Konski, C.T.; Paulson, C.M. Electric birefringence and dichroism of acridine orange and methylene blue complexes with polynucleotides. *Biopolymers.* **1972**, *11*, 645-652.

36. OhUigin, C.; McConnell, D.J.; Kelly, J.M.; van der Putten, W.J.M. Methylene blue photosensitised strand cleavage of DNA: effects of dye binding and oxygen. *Nucleic Acids Res.* **1987**, *15*, 7411-7427.

VI. Solid Phase: Desorption/Ionization

In the last phase of the MALDI experiment, the analyte molecules finally evolve into gas phase ions, reactions (3a-e, 3a'-e'). There may be direct desorption of matrix molecules and ions, and analyte molecules and ions, from the excited crystals, reactions 3a-c. The possibility of desorption of larger clusters has been proposed. Desolvation reactions, similar to those proposed in ESI, could then lead to gas phase analyte ions, reactions 3d,e. If multiply-charged ions are generated from clusters, recombination with electrons would yield the observed species. The formation of gas phase ions through desorbed clusters has recently been considered by Karas [1].

If the analyte duplex is intact to this point in the experiment, what factors may lead to its destruction or stabilization? If singly-charged duplex ions are desorbed either directly from the condensed phase or from a large gas phase cluster, fragmentation may occur due to a number of circumstances. First, the energy content may be sufficient for dissociation to occur. The $(M_1M_2-H)^-$ ion could be unstable in the gas phase because of the energy transferred into the complex during excitation. It could also be unstable because of complex charge distributions such as multiple anionic sites or multiple protonated bases within the ion that carries an overall single charge. When the solvent is removed, repulsive forces could be sufficient to lead to fragmentation. While Karas proposed that multiply charged species may be initially formed in the gas phase in MALDI, and recombination reactions occur, so that singly charged ions are the "lucky survivors", his prime focus was on peptides, which could be formed with +n charges, and could react with desorbed electrons [1]. Since oligonucleotides would most likely be desorbing with excess negative charges, recombination would have to be with available

cations ($Na^{+}_{(g)}$) and desorbed proton donors such as $(T+H)^{+}$. If charge recombination were an important part of the gas phase aspect of MALDI, this would be detrimental to the stabilization of DNA duplexes, since recombination reactions are exothermic. If duplexes remain intact until the step where gas phase ions are formed, approaches may be developed to stabilize the duplexes at this point.

What form does the double-stranded species, M_1M_2, take in the crystals after evaporation of the solvents, and how does this influence the MALDI mass spectra?

There are those who feel that analytes are trapped in the MALDI matrix in neutral form, while others find it obvious, "based on chemical common sense", to expect that the target is a solid solution with species in forms representative of their states in solution [1]. If oligonucleotides are present in the solid matrix containing multiple charges, a condition determined during the target formation step, then the impact of this fact may be seen in the final step. The energy required to desorb and essentially desolvate multiply charged ions simply does not appear to be available in MALDI. Thus, it is important to consider this aspect, since it is an issue that is more important for oligonucleotides than for peptides. The state of the analyte might be controllable by the pH or ionic strength. The existence of oligonucleotides in a charged state would explain why DNA desorption is more difficult than peptides desorption with DNA signals having greater dependence on size of the analyte. However, the strands may also exist in a neutral state. For this case, when the crystal forms from the solution, the ionic form present in the solution must convert to the neutral form. If the oligonucleotide has no charges, it will undergo desorption and ionization like a peptide or other neutral analyte.

There are several solution conditions that will play a role in the charge state of the analyte in the MALDI target. The first of these is pH. In basic and neutral solutions, this variable may be relatively simple to investigate. The pK_a of the phosphate backbone indicates how many phosphate groups should be ionized with a matrix such as ATT. At a neutral pH, there could also be a distribution of positive and negative charges on a single strand. At lower pH's, the phosphates can be protonated. With a neutral phosphate

backbone, the duplex would be more stable than a duplex with negatively charged phosphate backbones. However, at a very low pH, all of the phosphates may be in neutral form with some of the nitrogen bases protonated as well. The protonation of the nitrogen bases eliminates their ability to hydrogen bond to opposing bases, decreasing the stability of the duplex.

Again, for a system where conditions have been found such that MALDI analysis of a duplex yields a spectrum where at least a portion of the duplex remains such as Figure 2.33, it is important to map out the variation of the quantifiers with pH of the solution. As a droplet evaporates, the concentrations change making it difficult to interpret a set of spectra obtained by growing crystals from solutions with simply a range of initial pH values. Adding a strong acid, HCl, or a strong base, NaOH, will not provide much information about the pH throughout the MALDI process. For this reason, buffers will be used to keep the pH constant during most of the evaporation process. It may be difficult to determine, when changes are observed, if the changes are due to the stability of the duplex in the first phase of the experiment or in the final desorption step. While difficult, this is clearly an important question and pH is a relevant variable in this regard.

Using duplex 1 as the analyte and ATT/sp as the matrix, the influence of pH was explored. The ATT/sp starting solution had a pH of around 7.5. This allowed for the detection of double-stranded DNA as shown in Figure 2.26. The starting matrix and analyte solution were then buffered to various pH values: 5.0, 6.0, 7.0, 8.0, and 9.0. For comparison, hydrochloric acid was added to an ATT/sp matrix solution to yield a pH of 2.0.

If analyte molecules can be trapped in the matrix in an ionic form, as the duplex ions desorb, the negative charges on the double-stranded oligonucleotides will lead to repulsive interactions, dissociating the duplex. In order to understand the charge state of the DNA in the MALDI target, the charge state in solution must be understood. ESI-MS was a useful tool to study the charge states of an oligonucleotide in solution. In ESI, a single-stranded oligonucleotide, $d(T_{12})$, in solution, was injected into the mass spectrometer and a negative-ion spectrum was recorded. The pH of the starting solution was around 7.5, similar to that of the ATT/sp matrix starting solution. The spectrum contained two peaks representing two charge states of the oligonucleotide. The -2 and -3 charge states were seen in the ESI-MS experiment. This suggests the oligonucleotide may only contain 2-3 charges when in solution.

If the duplex remains intact until the final step, and the gas phase ions promptly and extensively dissociate, how can the species be stabilized?

The dissociation of the duplex ions may be due to energy content of the desorbed ions. If this is the case, the addition of fucose may help at this phase of the experiment as well. A certain amount of energy is required to desorb molecules and ions from the MALDI target. If the amount of energy deposited into the analyte exceeds the amount of energy needed for desorption, the analyte will be desorbed with an excess of energy. This excess energy may be sufficient to dissociate the complex. The addition of non-absorbing species such as fucose to the matrix may decrease the energy transferred to the analyte and enable the molecules to desorb intact, but not dissociate once in the gas phase.

Matrix additives used to increase the bond dissociation energy of the duplex may also stabilize the duplex in the desorption/ionization process. If molecules known to bind to DNA can increase the dissociation energy of the duplex, the excited gas phase ions may not have enough energy to break the non-covalent bonds holding the two strands together. Additives such as spermine have been found to form a stable complex. Spermine even holds the duplex together throughout the desorption/ionization step evident by the observation of the $(M_1M_2+sp)^+$ peak in the spectrum. While the formation of this complex is not ideal, it provides insights on how to stabilize the duplex ions in the gas phase. The presence of the $(M_1M_2+sp)^+$ peak in the spectrum also shows that the additives discussed in the Solid Phase: Excitation section may also stabilize the duplex in the desorption/ionization step.

The bond dissociation energy of the gas phase duplex may be small due to the charge distribution as discussed previously. In order to change the situation and investigate this aspect, the charges on the phosphate groups need to be eliminated. To do so, the phosphates on the oligonucleotides could be alkylated through a tributylstannyl phosphate intermediate [2-3]. While this synthesis has been used for small oligonucleotides containing only 2 nucleotides, the synthesis was not successful for larger oligonucleotides with 12 nucleotides. While the derivitization experiment was not successful to neutralize the phosphates, conclusions can be drawn from the PNA duplex spectrum shown previously in Chapter 1. In PNA, there are the same nitrogen bases contained in DNA, but the phosphate backbone is replaced with a peptide backbone. This peptide backbone does not carry negative charges. For this reason, comparisons can be drawn from the PNA data and the DNA data. Both DNA and PNA duplexes dissociate in the MALDI experiment. This means the presence of negative charges on the phosphate backbone of DNA does not cause duplex dissociation.

It is possible that all desorbed double-stranded DNA ions have sufficient energy to break the non-covalent bonds holding together the strands even if the bond dissociation energy has been increased. If this is true, excited double-stranded ions, $(M_1M_2-H)^{-*}$, can be cooled by collisions in the gas phase to prevent their dissociation. When $(M_1M_2-H)^{-*}$ collides with a neutral molecule, the excited ion can transfer energy before it dissociates. It has been proposed that many collisions occur for desorbed ions, explaining the fact that matrix and analyte ions form with similar velocity distributions [4]. Thus, collisional processes after desorption may already occur. It has been suggested that fucose

influences MALDI spectra because the fucose molecule thermally degrades into small molecules (CO_2, H_2O), collisionally cooling the desorbed ions.

In order to cool the analyte ions, collisions must take place very early in the process, before the accelerating field is applied and before dissociation occurs. Any approach that may create a higher pressure just above the MALDI target was considered. For example, $NaCO_3$ thermally decomposes to form CO_2 and Na_2O. If a MALDI target is coated with a layer of transparent material such as $NaCO_3$, ions may experience a larger number of collisions prior to acceleration and detection. When this experiment was performed, there was no increase in the values of the DSRR and higher laser powers were needed to detect the single-stranded species. Glycerol was also added to the MALDI sample plate, in close proximity to the solid being irradiated. Glycerol has a very low vapor pressure. The glycerol molecules constantly evaporate during the course of the experiment and allow the analyte ions to collisionally de-excite. Again, the presence of glycerol on the plate did not result in any increase in the DSRR value.

While this method could provide a way for molecules to collisionally de-excite, potential problems could arise due to collision induced dissociation (CID). With CID, the desorbed analyte ions moving at a high velocity would collide with a neutral molecule. This collision would then create excited analyte ions that may then dissociate. While CID is a possibility, this does not appear to be taking place. When examining the data for the fucose experiment, Figure 2.26, there are no ions detected representing fragments of the duplex or the single-stranded oligonucleotides.

References

1. Karas, M.; Glückmann, M.; Schäfer, J. Ionization in matrix-assisted laser desorption/ionization: singly charged molecular ions are the lucky survivors. *J. Mass Spectrom.* **2000**, *35*, 1-12.

2. Ohuchi, S.; Takashi, I.; Tsujiaki, H. o-Alkylation of dialkyl phosphates and o-alkyl phosphonates via the stannyl intermediates. *Nucleosides and Nucleotides.* **1992**, *11*, 749-757.

3. Ayukawa, H.; Ohuchi, S.; Ishikawa, M.; Hata, T. Alkylation of phosphate group of nucleotides via tributylstannyl phosphate derivatives. *Chem. Lett.* **1995**, 81.

4. Juhasz, P.; Vestal, M.L.; Martin, S.A. On the initial velocity of ions generated by matrix-assisted laser desorption ionization and its effect on the calibration of delayed extraction time-of-flight mass spectra. *J. Am. Soc. Mass Spectrom.* **1997**, *8*, 209-217.

VII. Conclusions

Since the non-covalent interactions that hold the complexes together are disrupted during the MALDI experiment, each phase of the MALDI process was examined. The results of these experiments have been published and a reprint of the article is included in Appendix C. The various steps of the experiment were presented and considered as points in the experiment where the duplex is disrupted. While the dissociation of the duplex does not occur due to interactions with the metal plate, organic solvents, or matrix molecules, the separation of the duplex could occur during the liquid phase portion of the experiment. Dissociation during the liquid phase of the experiment explains the random dimerization seen in many of the experiment presented here. It is possible that as the crystal surface grows, the analyte may interact with the surface and dissociate. While additives may stabilize the duplex oligonucleotides in the MALDI experiment, the complex still dissociates. When HPA is used as the matrix, random dimerization is consistently seen. The double-stranded DNA may have a higher affinity for the growing HPA crystals.

Although the analyte is not completely stabilized in the MALDI experiment, information can be learned from the partial dissociation of non-covalent complexes. This is particularly true when analyzing multi-subunit proteins such as cytochrome c oxidase. The mass spectrometric analysis of cytochrome c oxidase will be discussed in Chapter 3.

CHAPTER 3. Mass Spectrometric Analysis of the Protein Subunit, Lipid, and Heme Components of Cytochrome c Oxidase from *R. Sphaeroides* and the Stabilization of Non-covalent Complexes from the Enzyme

I. Introduction

Information provided from the DNA studies can offer insight into the MALDI analysis of other types of non-covalent complexes. As mentioned previously, cellular function is often determined by processes that involve non-covalent interactions, such as enzyme with substrate, receptor with hormone, and antibody with antigen [1]. In addition to transitory interactions, enzymes often exist as non-covalent complexes of several protein subunits. Cytochrome c oxidase, the focus of this work, is such an enzyme, with numerous subunits ranging from 4 to 13 depending on the source of the protein.

Cytochrome c oxidase is a multisubunit membrane protein that acts as the terminal complex of the respiratory chain in both mitochondria and bacteria. The enzyme from *Rhodobacter sphaeroides* consists of four protein subunits. During the catalytic cycle, electrons are transferred from cytochrome c, via a transitory interaction, through two copper centers and two heme groups, to reduce oxygen to water. In addition to the hemes, metals, and protein subunits, six phospholipids have been resolved in the crystal structure of the bacterial enzyme. Based on the electron density, they were determined to be phosphatidylethanolamines [2]. While lipids are not always included in discussions of the enzyme's structure and function, it is clear from the crystal structure that these components play an integral role. Over 30% of all the proteins encoded by the human genome are membrane proteins and many are important drug targets, yet few have been

crystallized. The content and influence of lipids on the properties of these proteins is becoming recognized as an important issue [3-4].

As with all intrinsic membrane proteins, the subunits of cytochrome c oxidase have hydrophobic domains. This enzyme presents a challenge to mass spectrometry not only because of its hydrophobicity, but because it exists as a non-covalent complex of the subunits associated with lipids and hemes. While positive-ion UV MALDI MS analysis of this analyte may be expected to yield one peak representing the protonated complex at approximately 130,000 Da, the complex dissociates in the MALDI experiment with only some of the protein subunits detected. How and why the complex dissociates is not clear. However, if all the components can be detected, MALDI can prove to be a useful analytical tool. Ideally, a MALDI matrix would allow for the optimal detection of all the components, but in this instance it is not the case. Here we demonstrate that the use of different matrices and matrix additives can allow for MALDI detection of all components of the complex, as well as stabilize the intact cytochrome c oxidase and limit the extent of dissociation. The results provide new information on the composition of the enzyme and connectivity of components parts.

References

1. Pramanik, B.N.; Bartner, P.L.; Mirza, U.A.; Liu, Y.H.; Ganguly, A.K. Electrospray ionization mass spectrometry for the study of non-covalent complexes: an emerging technology. *J. Mass Spectrom.* **1998**, *33*, 911-920.

2. Svensson-Ek, M.; Abramson, J.; Larsson, G.; Törnroth, S.; Brzezinki, P.; Iwata, S. The X-ray crystal structures of wild-type and EQ(I-286) mutant cytochrome c oxidases from *Rhodobacter sphaeroides*. *J. Mol. Biol.* **2002**, *321*, 329-339.

3. Camara-Artigas, A.; Brune, D.; Allen, J.P. Interactions between lipids and bacterial reaction centers determined by protein crystallography. *Proc. Natl. Acad. Sci. USA*. **2002**, *99*, 11055-11060.

4. Garavito, R.M.; Ferguson-Miller, S. Detergents as tools in membrane biochemistry. *J. Biol. Chem.* **2001**, *276*, 32403-32406.

II. Structure of Cytochrome c Oxidase

Enzymes such as cytochrome c oxidase often exist as a non-covalent complex of several protein subunits. Cytochrome c oxidase is the terminal complex of the respiratory chain in both mitochondria and bacteria and plays a crucial role in the energy transfer process. This enzyme is the last step in the electron transfer chain to reduce molecular oxygen to water. Cytochrome c oxidase is a protein complex that is integrated into the mitochondrial membrane of eukaryotes and into the cytoplasmic membrane of several species of bacteria, Figure 3.1.

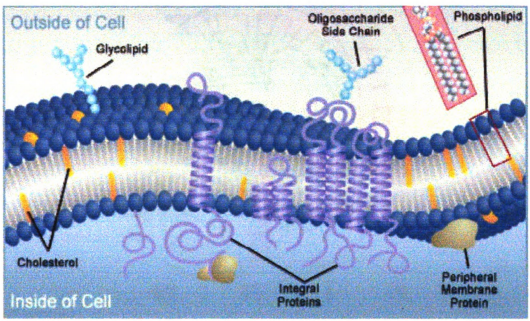

Figure 3.1. Schematic of a cell membrane. This figure was reproduced from reference 1.

Cytochrome c oxidase from *Rhodobacter sphaeroides* consists of four protein subunits. Cytochrome c oxidase belongs to the superfamily of heme-copper oxidases. Both mammalian and *R. sphaeroides* cytochrome c oxidase contain four reactive metal centers including heme a, heme a_3, Cu_A, and Cu_B as well as a non-reactive calcium ion.

Electron transfer in the enzyme is initiated when cytochrome c binds to subunit II on the external side of the membrane. During the catalytic cycle, electrons are transferred from the protein cytochrome c through the cytochrome c oxidase via two copper ions and two heme groups. The interaction of subunit II and the cytochrome c protein is demonstrated in Figure 3.2.

Figure 3.2. Structure of cytochrome c oxidase from *R. sphaeroides.* This figure was reproduced from reference 2.

The cytochrome c oxidase from *R. sphaeroides* can serve as a model for mammalian cytochrome c oxidase and will be used throughout this discussion. The structure of subunit I is the largest and most conserved subunit of the cytochrome c oxidase enzyme. Subunit I contains both hemes, the magnesium, and the calcium. The

magnesium site is located at the interface of subunit I with subunit II. While the magnesium may not have a specific function, it is important in stabilization of the whole protein complex.

Subunit II is composed of two parts. On the nitrogen terminal side there is a hydophobic domain that spans the membrane. There is also a carbon terminal side that is hydrophillic in nature. It is this domain that possesses the ligands that bind to the two copper ions as well as the carboxyl residues that bind to cytochrome c. Subunit II interacts strongly with subunit I and is bound partly by the stabilizing magnesium ion.

Subunit III has many transmembrane helices. Again, the function of this subunit is not fully understood, but it is believed to maintain the functional integrity of the enzyme complex. Little is know about subunit IV as well. It was recently discovered in a high-resolution crystal structure. Subunit IV has no homology with any of the 13 subunits of the bovine cytochrome c oxidase.

In addition to the hemes, metals, and proteins, six phospholipids have been resolved in the crystal structure of the enzyme. Based on the electron density, four of the lipids were determined to be phosphatidylethanolamines [3]. While hemes and lipids are not always included in discussions of the enzyme, these components play an integral role in establishing its structure. Membrane proteins are found in cellular membranes composed of lipids. Lipids such as phosphatidylcholine, phosphatidylethanolamine, phosphatidylglycerol, and cardiolipin determine the biophysical and biochemical properties of the membrane proteins [4]. As shown in Figure 3.3, lipids are highly affiliated with subunit four of the cytochrome c oxidase.

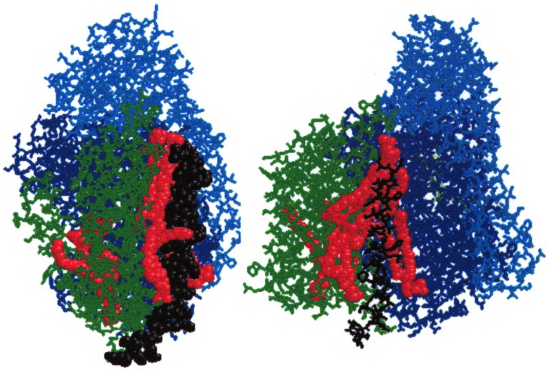

Figure 3.3. The X-ray crystal structure of cytochrome c oxidase. Phospholipids are shown in red, subunit I is shown in dark blue, subunit II is shown in light blue, subunit III is shown in green and subunit IV is shown in black. This figure was reproduced from reference 2.

In the crystal structure of cytochrome c oxidase form *R. sphaeroides*, six phospholipids have been identified. Four of these phospholipids have been identified as phosphatidylethanolamine and the other two lipids have not been identified due to poor resolution. Two of the phospholipids are buried in a v-shaped cleft in subunit III with one interacting with subunit I as well. The rest of the lipid molecules are found at the interface between subunit IV and subunits I/III. These lipids are responsible for separating subunit IV almost completely from the rest of the enzyme.

The lipids believed to be associated with cytochrome c oxidase are rather diverse. Glycerophospholipids are the most commonly found membrane lipids. Glycerol serves as the backbone for these lipids with two acyl groups attached to the glycerol as well as the phosphate group. The phosphate of these lipids is often linked to hydrophilic groups such as choline (phosphatidylcholine), ethanolamine (phosphatidylethanolamine), inositol (phosphatidylinositol), serine (phosphatidylserine), and glycerol (phosphatidylglycerol). The structures of the most common phospholipids found in the bacteria are shown in Figure 3.4.

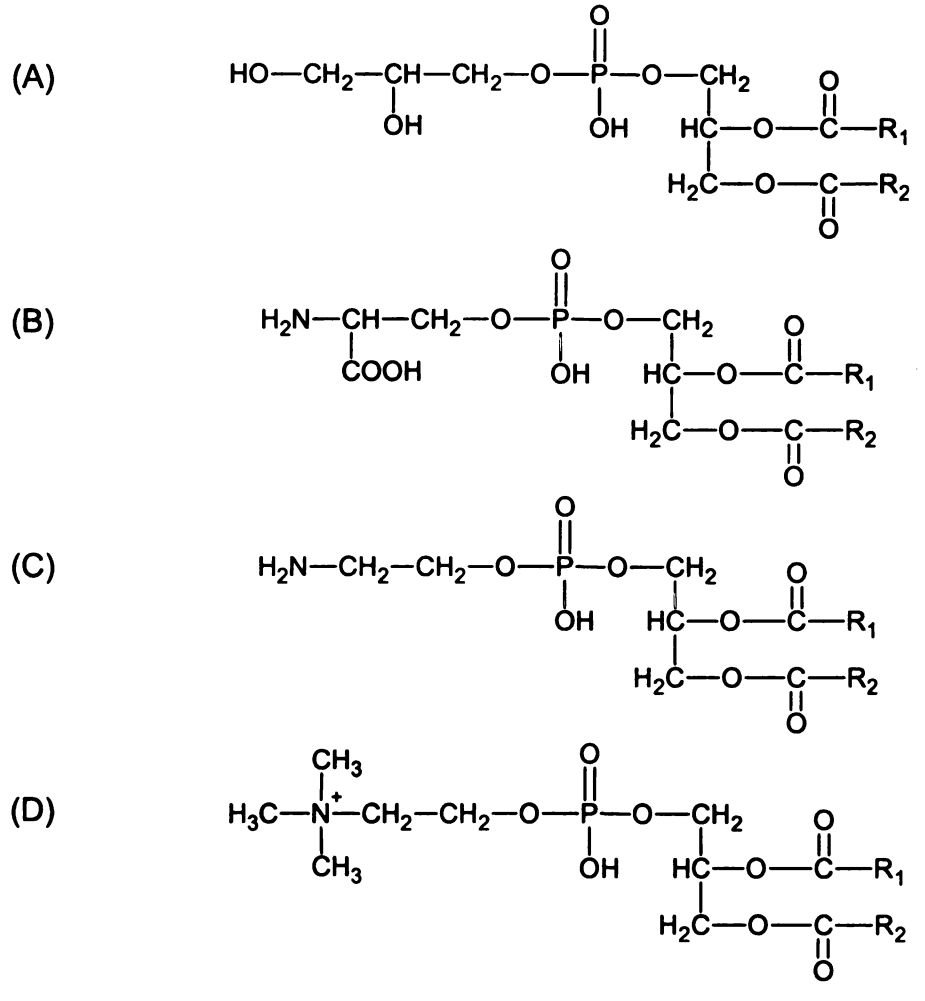

Figure 3.4. Structure of phospholipids found in *R. sphaeroides* bacteria. (A) Phosphatidyl glycerol, (B) Phosphatidyl serine, (C) Phosphatidyl ethanolamine, (D) Phosphatidyl choline. $R_1$and R_2 represent the carbons chains of the fatty acids.

The membranes of *R. sphaeroides* bacteria are also known to contain a variety of glycolipids. A glycolipids contains a saccharide group in place of the phosphate group. The glycerol backbone is still present with two fatty acid groups attached. The glycolipids known to exist in this bacterium include monogalactosyl diacylglycerol and digalactosyl diacylglycerol. It is also possible for the glycolipids to possess functional groups stemming from the saccharide. Sulfolipids such as sulfoquinovosyl diacylglycerol contains a sulfate on the sugar group. The structures of three glycolipids are shown in Figure 3.5.

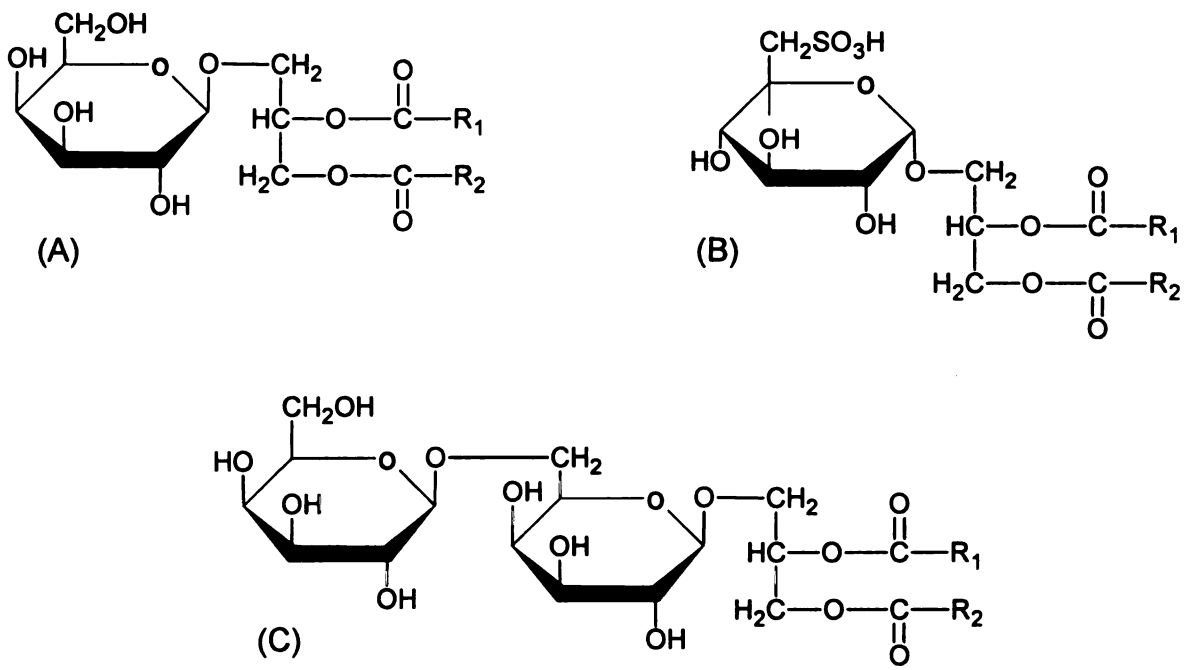

Figure 3.5. Structure of the glycolipids found in *R. sphaeroides* bacteria. (A) Monogalatosyl diacylglycerol, (B) Sulfoquinovosyl diacylglycerol, (C) Digalactosyl diacylglycerol. $R_1$and R_2 represent the carbons chains of the fatty acids.

Another lipid that is of particular interest is cardiolipin. Compared to the structure of the lipids shown previously, cardiolipin is rather unique, Figure 3.6. Cardiolipin is structurally similar to phosphatidyl glycerol. Figure 3.4 (D). However,

cardiolipin has another phosphatidyl glycerol lipid attached to the primary glycerol backbone. This gives a cardiolipin molecule three glycerol backbones and four fatty acid group. The cardiolipin molecule also has a molecular weight of greater than 1000 g/mol, much higher than other lipids in the bacteria.

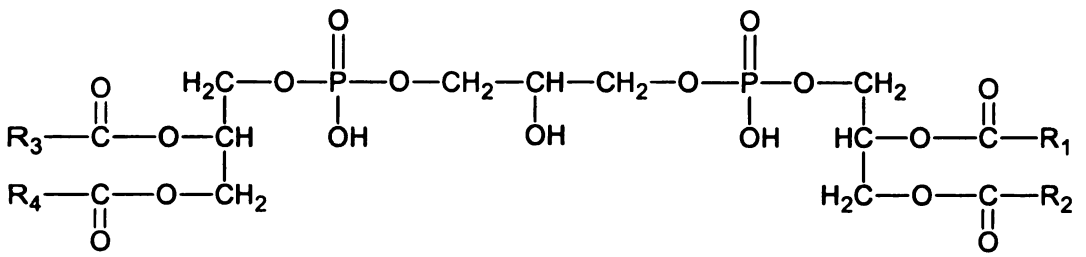

Figure 3.6. Structure of cardiolipin molecule. R_1, R_2, R_3, and R_4 represent the carbons chains of the fatty acids.

As with many membrane proteins, cytochrome c oxidase has hydrophobic subunits. This enzyme presents a challenge to mass spectrometry not only due to its hydrophobicity but because it exists as a non-covalent complex of the four protein subunits, lipids, and hemes. While positive-ion UV MALDI MS analysis of this analyte may be expected to yield one peak representing the protonated complex at 130,000 Da, the complex dissociates completely during the desorption/ionization process with only some of the protein subunits detected. How and why the complex dissociates in the MALDI experiment is not clear. However, if the complex does dissociate and all the components can be detected, MALDI can prove to be a useful analytical tool for protein chemists. While, ideally, a MALDI matrix would allow for the optimal detection of all the components, this is not the case. Here we demonstrate that the use of different matrices and matrix additives can allow for the detection of all components of the complex, stabilize the intact cytochrome c oxidase, and limit the extent of the dissociation to determine information on the connectivity of components.

References

1. Cell Biology Tutorial, University of Arizona, February 4, 2002, http://www.biology.arizona.edu/cell_bio/problem_sets/membranes/overview.html

2. Hilmi, Yasmin. Use of mutagensis, novel detergents, and lipid analysis to optimize condition for achieving high resolution 3-dimensional crystal structure of *Rhodobacter sphaeroides* cytochrome c oxidase. Michigan State University, 2002. East Lansing, MI.

3. Svensson-Ek, M.; Abramson, J.; Larsson, G.; Törnroth, S.; Brzezinki, P.; Iwata, S. The X-ray crystal structures of wild-type and EQ(I-286) mutant cytochrome c oxidases from *Rhodobacter sphaeroides*. *J. Mol. Biol.* **2002**, *321*, 329-339.

4. Camara-Artigas, A.; Brune, D.; Allen, J.P. Interactions between lipids and bacterial reaction centers determined by protein crystallography. *Proc. Natl. Acad. Sci. USA*. **2002**, *99*, 11055-11060.

III. Experimental

The compounds, 2,5-dihydroxybenzoic acid (DHB), 6-aza-2-thiothymine (ATT), sinapinic acid (SA), 2′,4′-dihydroxyacetophenone (DHAP), fucose, and calcium chloride were purchased from Sigma-Aldrich (St. Louis, MO). Sucrose was purchased from the Mallinckrodt Specialty Chemical Company (Paris, KY). The standard lipids used in the experiments were purchased in chloroform from Avanti Polar Lipids, Inc. (Alabaster, AL). The decyl maltoside and dodecyl maltoside used as detergents to solubilize the proteins were purchased from Anatrace, Inc. (Maumee, OH). Dodecyl maltoside is also referred to as lauryl maltoside (LM). All solvents used were HPLC grade.

Rhodobacter sphaeroides was used as a homologous host for overproduction of cytochrome c oxidase protein. When plasmids carrying engineered versions of the genes for cytochrome c oxidase subunits are placed into *R. sphaeroides* strains that are missing these genes [1-2], the bacteria produce large quantities of the engineered cytochrome c oxidase proteins [3]. Addition of six histidines to the end of one of the subunits [4-5] allows simple and rapid purification of the protein by nickel affinity chromatography. The sequences of the four subunits of *Rhodobacter sphaeroides* are shown in Table 3.1. The molecular weights of the subunits are included in the table as well.

Rhodobacter sphaeroides strains 25-1, 157, and 167, which overexpress different versions of cytochrome c oxidase, were grown and cell membranes were prepared as described previously [2,4]. Cytochrome c oxidase protein from strain 25-1 (sample CcO1) was isolated by nickel affinity column chromatography without further purification as described [4].

Table 3.1. Sequence of *R. Sphaeroides* Cytochrome c Oxidase Subunits

Subunit	Sequence	Molecular Weight
Subunit I	MADAAIHGHEHDRRGFFTRWFMSTNHKDIGVLYLF TGGLVGLISVAFTVYMRMELMAPGVQFMCAEHLES GLVKGFFQSLWPSAVENCTPNGHLWNVMITGHGIL MMFFVVIPALFGGFGNYFMPLHIGAPDMAFPRMNN LSYWLYVAGTSLAVASLFAPGGNGQLGSGIGWVLY PPLSTSESGYSTDLAIFAVHLSGASSILGAINMIT TFLNMRAPGMTMHKVPLFAWSIFVTAWLILLALPV LAGAITMLLTDRNFGTTFFQPSGGGDPVLYQHILW FFGHPEVYIIVLPAFGIVSHVIATFAKKPIFGYLP MVYAMVAIGVLGFVVWAHHMYTAGLSLTQQSYFMM ATMVIAVPTGIKIFSWIATMWGGSIELKTPMLWAL GFLFLFTVGGVTGIVLSQASVDRYYHDTYYVVAHF HYVMSLGAVFGIFAGIYFWIGKMSGRQYPEWAGKL HFWMMFVGANLTFFPQHFLGRQGMPRRYIDYPEAF ATWNFVSSLGAFLSFASFLFFLGVIFYTLTRGARV TANNYWNEHADTLEWTLTSPPPEHTFEQLPKREDW ERAPAH	63147 (I) 63016 (I') 64040 (I'+Ht1) I' = I – Met Ht1 = SNH_6
Subunit II	MRHSTTLTGCATGAAGLLAATAAAAQQQSLEIIGR PQPGGTGFQPSASPVATQIHWLDGFILVIIAAITI FVTLLILYAVWRFHEKRNKVPARFTHNSPLEIAWT IVPIVILVAIGAFSLPVLFNQQEIPEADVTKVTGY QWYWGYEYPDEEISFESYMIGSPATGGDNRMSPEV EQQLIEAGYSRDEFLLATDTAMVVPVNKTVVVQVT GADVIHSWTVPAFGVKQDAVPGRLAQLWFRAEREG IFFGQCSELCGISHAYMPITVKVVSEEAYAAWLEQ **ARGGTY**ELSSVLPATPAGVSVE	32931 (II) 29122 (IIA) 29340 (IIB+Ht2) 30661 (IIC) IIA = II – [1-25] – [288-303] IIB = IIA – [282-287] IIC = II – [1-25] Ht2 = H_6
Subunit III	MAHAKNHDYHILPPSIWPFMASVGAFVMLFGAVLW MHGSGPWMGLIGLVVVLYTMFGWWSDVVTESLEGD HTPVVRLGLRWGFILFIMSEVMFFSAWFWSFFKHA LYPMGPESPIIDGIFPPEGIITFDPWHLPLINTLI LLCSGCAATWAHHALVHENNRRDVAWGLALAIALG ALFTVFQAYEYSHAAFGFAGNIYGANFFMATGFHG FHVIVGTIFLLVCLIRVQRGHFTPEKHVGFEAAIW YWHFVDVVWLFLFASIYIWGQ	30172 (III) 30041 (III') III' = III – Met
Subunit IV	MAETNKGTGPMADHSHPAHGHVAGSMDITQQEKTF AGFVRMVTWAAVVIVAALIFLALANA	6390 (IV) 6259 (IV') 5403 (IVA) 5272 (IVA') IV' = IV – Met IVA = IV – [1-10] IVA' = IVA – Met

For further purification of cytochrome c oxidase from *Rhodobacter* strain 157 (sample CcO2), the protein concentration was first determined using the Pierce (Rockford, IL) BCA protein assay kit, modified to include 0.25% deoxycholate in the buffers. The membrane sample was then diluted to a final protein concentration of 10 mg/mL. Lauryl maltoside was then added to the membrane sample to a final concentration of 1%. The solution was stirred in the cold for 15-20 minutes before ultracentrifugation at 200,000 g for 30 minutes. The supernatant was loaded onto a home-packed QIAGEN (Valencia, CA) Ni-NTA superflow column attached to a fast performance liquid chromatography (FPLC) system. After washing the sample with 13 column volumes of buffer A (10 mM Tris, 40 mM KCl, 10 mM imidazole, 0.05% LM, pH=8.0) , the enzyme was eluted with a linear gradient from 0% to 100% buffer B (10mM Tris, 40 mM KCl, 150 mM imidazole, 0.05% LM, pH=8.0) over 15 column volumes. After the first column, green fractions were pooled, concentrated, and washed using a Millipore (Billerica, MA) Amicon Centriplus YM-100 concentrator.

For further purification, the sample was loaded onto a Pharmacia (Peapack, NJ) MonoQ column connected to an FPLC system. After loading the sample and washing with 2 column volumes of buffer A (10 mM Tris, 0.05% LM, pH=8.0), the enzyme was eluted with a linear gradient from 0% to 100% buffer B (10 mM Tris, 0.05% LM and 500 mM KCl, pH=8.0) over 20 column volumes. Often there were two peaks in the chromatogram as well as an elongated tail following the second peak. In this case, only fractions from the second peak were collected. The active fractions were pooled, washed and concentrated using Centriplus YM-100. Approximately 50 mL of 10 mM Tris, 0.24%

decyl maltoside at a pH of 8.0 was used to wash the enzyme to ensure the buffer was completely exchanged.

For further purification of cytochrome c oxidase from *Rhodobacter* strain 167 (sample CcO3), the same purification methods were applied except that in the nickel column purification step, buffer A contained 10mM Tris, 220mM KCl, 1mM imidazole, pH 8.0 and 0.05% dodecyl maltoside, and buffer B contained 10mM Tris, 220mM KCl, 150mM imidazole, pH 8.0 and 0.05% dodecyl maltoside .

Saturated solutions of the MALDI matrices ATT, SA, and DHAP were made using a 1:1 acetonitrile/water solution. The DHB solution was made at a concentration of 25 mM in 1:1 acetonitrile/water solution. Stock solutions of fucose, sucrose, and calcium chloride were made at concentrations of 25 mM in water. When additives such as sucrose were used in the MALDI experiment, a volume of the additive solution was added to an equal volume of the protein solution before being deposited on the MALDI target.

The standard lipid solutions were diluted with chloroform to concentrations of 1 pmol/μL. In order to analyze the standard lipid solutions and the lipid extracts from the enzyme, 1 μL of DHB was spotted on the plate and allowed to dry. A microliter of the lipid solution was then deposited, since the two solvent systems are incompatible.

Linear MALDI mass spectra were recorded on a PerSeptive Biosystems (Framingham, MA) Voyager delayed extraction (DE) time-of-flight linear (TOF) mass spectrometer equipped with a nitrogen laser (337 nm, 3 ns pulse). For the positive ion MALDI spectra reported here, the accelerating voltage was 20 kV, the delay time, selected for optimum resolution, was 450 ns, the grid voltage was 94.0 % of the

accelerating voltage, and the magnitude of the guide wire voltage was 0.30% of the accelerating voltage. Transients from 50 laser shots were averaged for each spectrum. Reflectron and post source decay (PSD) MALDI mass spectra were recorded on a PerSeptive Biosystems (Framingham, MA) Voyager-DE STR Biospectrometry workstation equipped with a reflectron TOF mass spectrometer. For these experiments, the accelerating voltage was 20 kV, the grid voltage was 80% of the accelerating voltage, and the delay time was 100 ns. The mirror ratio for the first PSD stitch spectrum was 1.00 and the mirror decrement ratio was set at 0.90. Ten stitches were acquired for every PSD spectrum. Typically, transients from 50 laser shots were averaged for each stitch.

FTMS spectra were acquired on a Bruker Daltonics (Billerica, MA) Apex III mass spectrometer with a 7 Tesla superconducting shielded magnet. Argon was used as the collision gas for the experiments. Samples were introduced into the electrospray ion source using a syringe pump at a flow rate of 1 μL/min.

Images in this dissertation are presented in color.

References

1. Shapleigh, J.P.; Gennis, R.B. Cloning, sequencing, and deletion from the chromosome of the gene encoding subunit I of the aa_3-type cytochrome c oxidase of *Rhodobacter sphaeroides*. *Mol. Micro.* **1992**, *6*, 635-642.

2. Zhen, Y.; Qian, J.; Follmann, K.; Hayward, T.; Nilsson, T.; Dahn, M; Hilmi, Y.; Hamer, A.G.; Hosler, J.; Ferguson-Miller, S. Overexpression and purification of cytochrome c oxidase from *Rhodobacter sphaeroides*. *Protein Expr. Purif.* **1998**, *13*, 326-336.

3. Hosler, J.P.; Fetter, J.; Tecklenburg, M.M.J.; Espe, M.; Lerma, C.; Ferguson-Miller, S. Cytochrome aa_3 of *Rhodobacter sphaeroides* as a model for mitochondrial cytochrome c oxidase. Purification, kinetics, proton pumping, and spectral analysis. *J. Biol. Chem.* **1992**, *267*, 24264-24272.

4. Hiser, C.; Mills, D.A.; Schall, M.; Ferguson-Miller, S. C-terminal truncation and histidine-tagging of cytochrome c oxidase subunit II reveals the native processing site, shows involvement of the c-terminus in cytochrome c binding, and improves the assay for proton pumping. *Biochemistry* **2001**, *40*, 1606-1615.

5. Mitchell, D.M.; Gennis, R.B. Rapid purification of wildtype and mutant cytochrome c oxidase from Rhodobacter sphaeroides by Ni^{2+}-NTA affinity chromatography. *FEBS Lett.* **1995**, *368*, 148-150.

III. Results and Discussion

Cytochrome c oxidase from *R. sphaeroides* contains four protein subunits. The sequences of these subunits are listed in Table 3.1. These four subunits have different sequences because of differing sites of processing and the addition of Histidine tags. These changes in sequence are also listed in Table 3.1. The cytochrome c oxidase enzyme may contain different versions of the subunits shown in Table 3.1. In this work, three versions of cytochrome c oxidase were used. Sample CcO1 has a histidine-tagged subunit I (I'+Ht1), a subunit II with an artificially-processed C-terminus (IIA), a native subunit III (III'), and two naturally occurring forms of subunit IV (IV' and IVA'). Sample CcO2 is the same as CcO1 but with overexpressed, artificially-shortened version of subunit IV (IVA') and a subunit II with 25 amino acids removed from the N-terminus (IIC). Sample CcO3 has a native subunit I (I'), an artificially-processed and histidine-tagged subunit II (IIB+Ht2), a native subunit III (III'), and an overexpressed, engineered longer version of subunit IV (IV'). These three versions are indicated in Table 3.2.

Table 3.2. Cytochrome c Oxidase Samples Used in this Work

Oxidase sample	Subunit I	Subunit II	Subunit III	Subunit IV
CcO1	I' + Ht1	IIA	III'	IV' and IVA'
CcO2	I' + Ht1	IIC	III'	IVA'
CcO3	I'	IIB + Ht2	III'	IV'

When analyzing large proteins in MALDI MS, sinapinic acid (SA) is commonly used as a matrix. When Ni-column purified CcO1 (from a solution which also contains a solubilizing detergent) is analyzed using MALDI MS with SA, the complex completely dissociates and the individual subunits I, II, and III are detected with varying efficiency,

Figure 3.7. Clearly, singly and doubly charged forms of a component with a molecular weight of around 64,000 g/mol are present and two additional components with similar molecular weights of approximately 30,000 g/mol can be resolved. The expected masses for the subunits are shown in Table 3.1. The lipids that are assumed to be present have molecular weights in the 700-1500 g/mol range, but are not detected due to a high baseline in the low mass region of the spectrum. The smallest of the subunits, subunit IV, has a molecular mass of approximately 5300 Da and is not detected in the MALDI

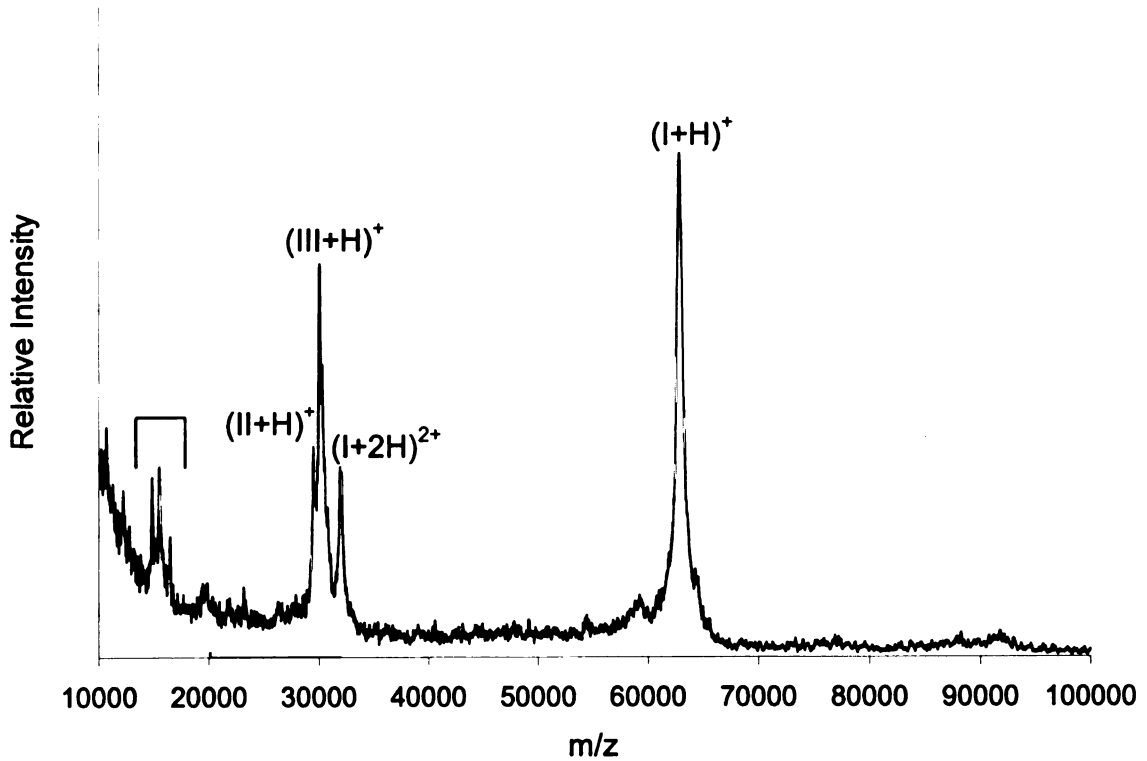

Figure 3.7. Positive-ion linear MALDI-TOF spectrum of cytochrome c oxidase sample CcO1 using SA as the matrix.

experiment. Also, no intact enzyme is detected. Reflectron capabilities were available and reflectron mode was used to increase resolution in the low m/z regions. However, when analyzing the region shown in Figure 3.7 using a reflectron TOF MS, the peaks representing subunits I-III could not be detected.

In Figure 3.7, the large protein subunits are detected. While this is important, the detection of the other components is essential as well. A method is needed to monitor enzyme content during purification, to allow for the detection of all parts of the cytochrome c oxidase complex. Ideally, all of the necessary information could be acquired in one experiment, but this is not always possible. In these experiments, the challenge was divided into three mass ranges: 500-2000 Da (lipid region), 5-10 kDa (subunit IV), and 20-70 kDa (subunit I-III). Enhanced detection of the complete non-covalent complex was also a goal (>100 kDa). Each mass range was considered and the problems were approached in a stepwise manner in order to develop a method for the analysis of the entire enzyme. To enhance the various m/z regions of the spectrum as well as to preserve the intact enzyme, several matrices and additives were evaluated and developed.

Lipid region (500-2,000 Da)

When analyzing membrane enzymes such as cytochrome c oxidase, the protein subunits are often the primary focus [1-2]. However, part of a complete analysis is the characterization of the lipids present. Lipids play a significant role in the structure of membrane proteins, as revealed in several recently published high resolution X-ray crystal structures [3-5]. The lipids may be critical in stabilizing a homogeneous conformation at the molecular level [6], and thus should be formally considered as part of the enzyme.

Many types of lipids have been previously studied using a variety of mass spectrometry techniques [7]. Phospholipids isolated from biological membranes have

been studied using both ESI and MALDI MS [8]. Lipid mixtures have also been analyzed in MALDI MS, although at levels above those commonly used for analytes [9-10]. Also, structural information for phospholipids has been determined using MALDI or ESI coupled to a Fourier transform ion cyclotron resonance mass spectrometer (FT-ICR MS) [11].

When analyzing the components of cytochrome c oxidase with molecular masses under 2000 Da, analysis is complicated not only by the complex mixture of lipids present, but also by the presence of the detergent. Throughout these MS studies, the solubilizing detergent used was lauryl maltoside. This detergent has a molecular weight of 510 g/mol and appears in the spectra as a protonated molecule at 511 Da, a sodium ion adduct, $(M+Na)^+$, at 533 Da, or a potassium ion adduct, $(M+K)^+$, at 549 Da. When the concentration of the detergent is kept below a value of 1 mM, little interference occurs. At higher concentrations, signal suppression results in both MALDI and ESI. Electrospray is particularly sensitive, even to non-ionic detergents such as lauryl maltoside. When ESI was used to desorb/ionize cytochrome c oxidase samples, detergent molecules formed singly-charged dimer and trimer ions yielding peaks with m/z values as high as 1531 Da. A high concentration of detergent often resulted in the suppression of lipid peaks, making the analysis of the cytochrome c oxidase samples by ESI very difficult.

In a MALDI experiment, no peaks representing the lipids were detected using SA as the matrix due to the high baseline at low m/z values. This, in part, could be due to the higher laser powers necessary to detect the large protein subunits. In order to enhance the lipid region of the spectrum, the matrix can be changed and reflectron mode can be used.

When the matrix DHB is used for the samples, the matrix effects are decreased allowing the peaks representing the lipids to be detected, Figure 3.8. The cytochrome c oxidase used in Figure 3.8 was the same Ni-column purified sample used in Figure 3.7. The labels shown in Figure 3.8 indicate the head group of the lipid, the total number of carbons in the fatty acid chains, and the number of sites of unsaturation in the alkyl groups.

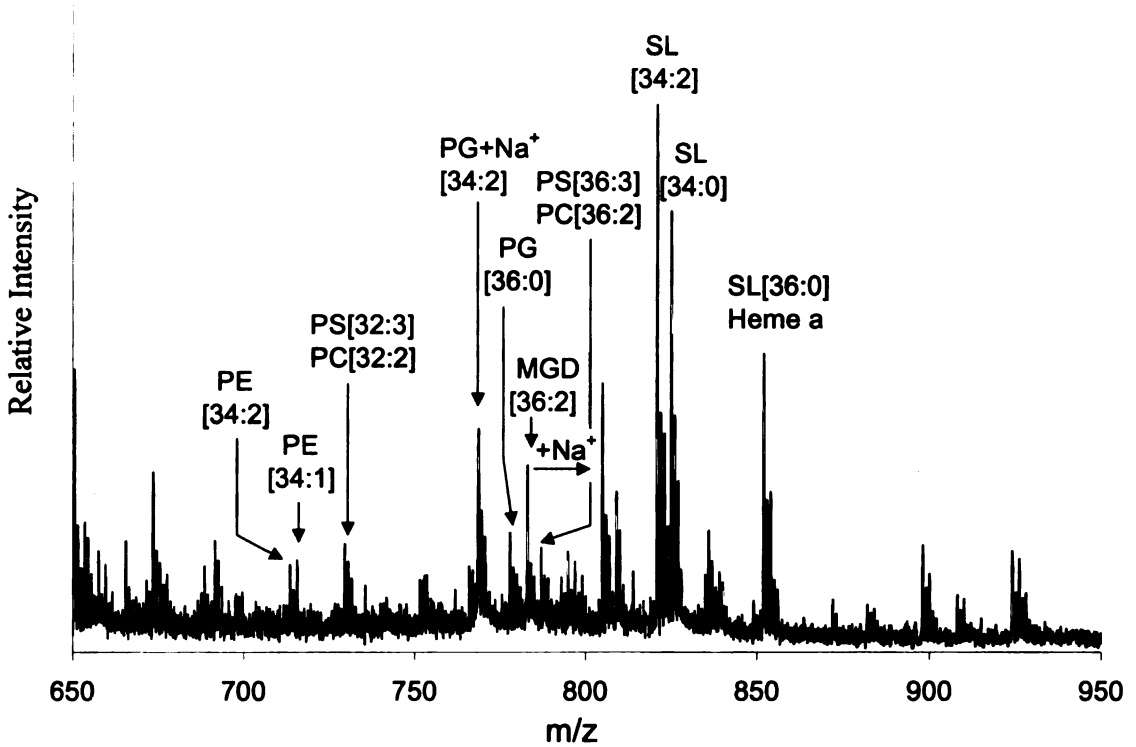

Figure 3.8. Lipid region of the postive-ion reflectron MALDI-TOF spectrum of cytochrome c oxidase sample CcO1 using DHB as the matrix. MGD(monogalactosyldiacylglycerol), PC(phosphatidylcholine), PE(phosphatidylethanolamine), PG(phosphatidylglycerol), PS(phosphatidylserine), SL(sulfolipid).

For example, the peak in Figure 3.8 at m/z 819 Da is labeled SL[34:2]. That is, the lipid is a sulfolipid with two fatty acid groups that contain a total of 34 carbons with 2 sites of unsaturation. There are a variety of fatty acid chain combinations that could give this

very result including SL(18:0, 16:2), SL(18:2, 16:0), and SL(18:1, 16:1). For simplicity, the peak is labeled as the sum of the fatty acid chain carbons. Several peaks have been labeled in Figure 3.8. At 716 Da, there is a peak representing a PE with 34 carbons and two sites of unsaturation. There is also a peak 2 Da higher representing a PE with only one site of unsaturation. In addition to phospholipids, there are also sugar-containing lipids in the spectrum. At 783 Da, there is a peak representing a monogalactosyl diacylglycerol (MGD). Also, 22 mass units higher at 805 Da, there is a peak representing the sodiated MGD[36:2]. At 819 Da and 823 Da, there are peaks due to the presence of sulfolipids. These two peaks represent sulfolipids with the same number of carbons in the fatty acid. They differ only in the number of sites of unsaturation. The sulfolipid yielding a peak at 819 Da has two sites of unsaturation while the sulfolipid that yields a peak at 823 Da has no sites of unsaturation.

While many peaks in Figure 3.8 could be assigned to a specific type of lipid based on m/z values alone, several peaks could not confidently be identified. The peak detected at 851.5 Da could represent heme *a* with a nominal mass of 852 Da or a sulfolipid with saturated fatty acids that contain 36 carbons that would have a nominal mass of 851 Da. Peaks that correlated to phosphatidylcholines and phosphatidylserines were difficult to assign due to the similarity in the mass of the head group. The peak at 730 Da could be from a PS lipid with fatty acid combination [32:3] or the PC lipid [32:2]. At 786 Da, there is also the possibility of PC[36:2] or PS[36:3].

While determining the masses of the lipids and the types of lipids present is important in mass spectrometric analysis, structural information is needed as well. When the lipid components were detected, a peak was observed at m/z 786. After performing

PSD analysis on this peak, a fragment ion was produced at m/z 184. This peak corresponds to the head group of a PC lipid. If the peak at m/z 786 represented a PS lipid, the fragment ion would have an expected mass of 186 Da. In order to further confirm the structure of the peak at 786, a standard solution of phosphatidylcholine (18:1, 18:1) was analyzed. When post-source decay (PSD) is performed on the peak at 786, a fragment ion at m/z 184 was detected. The PSD spectra for the m/z 786 from the standard and the cytochrome c oxidase sample are shown in Figure 3.9.

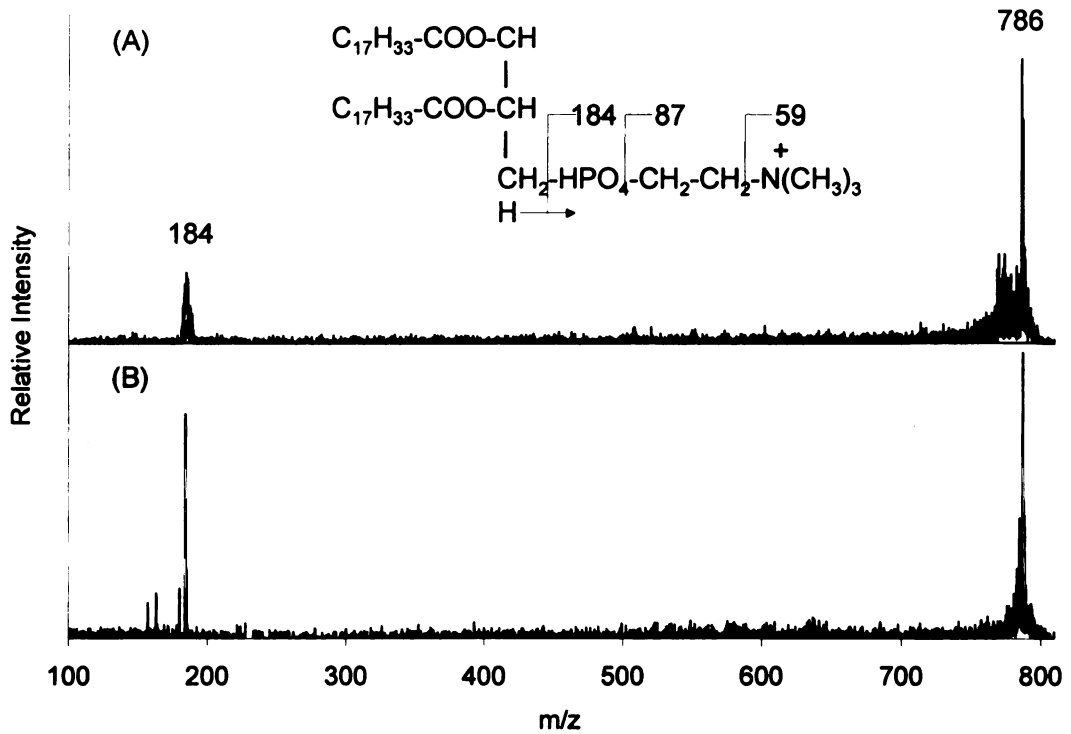

Figure 3.9. Positive-ion PSD MALDI-TOF spectra of the m/z 786 peak of (A) PC (18:1,18:1) standard and (B) cytochrome c oxidase sample CcO1. DHB was used as the matrix.

From the mass of the head group, the mass of the precursor ion, and the information about the types of fatty acids found in *Rhodobacter sphaeroides* [12], the fatty acid composition was assumed to be 18:1, 18:1. Small additional peaks in Figure 3.9 (B) are

likely PSD fragments from precursor ions close to m/z 786 since the MALDI-TOF-PSD experiment does not provide unit resolution for precursor selection.

While the lipids are important for stabilization of the enzyme, the purification processes performed to isolate a membrane protein often strip away many of the lipids. It then becomes important to understand the types of lipids present at various stages of purification. When the protein is first solublized from a membrane preparation in these experiments, there are 70 phosphate-containing lipids per average protein molecule and only 16-23 and 8-11 phospholipids/oxidase molecule after Ni^{2+}-NTA purification and subsequent MonoQ column purification respectively [13]. These results suggest that 10-15 lipids may be specifically affiliated with the oxidase. An analytical method that allows for the detection of the lipid and protein components provides important information from the purification standpoint and is a key for standardizing procedures for crystallography [6]. Further information to assist in understanding the crystal growth process can also be determined by dissolving and analyzing the crystals grown for X-ray analysis. Since a variety of lipids can be analyzed in the MALDI experiment, X-ray crystallographers have a rapid means to analyze their enzymes after the various phases of purification. Often lipids are analyzed using thin-layer chromatography (TLC). This provides information about the classes of lipids present, but does not provide any specific information about the fatty acids chains. The MALDI experiment yields more molecular information including the masses of the lipids present.

When analyzing cytochrome c oxidase solutions after various purification steps, the lipid content can be determined from the MALDI mass spectra. The mass spectra of cytochrome c oxidase solutions from the various levels of purification contain fewer lipid

peaks than the solutions directly isolated from the membrane without any purification procedures, Figure 3.10. In Figure 3.10, the cytochrome c oxidase solution was analyzed after (A) initial isolation, (B) Ni-column purification, and (C) both MonoQ and Ni-

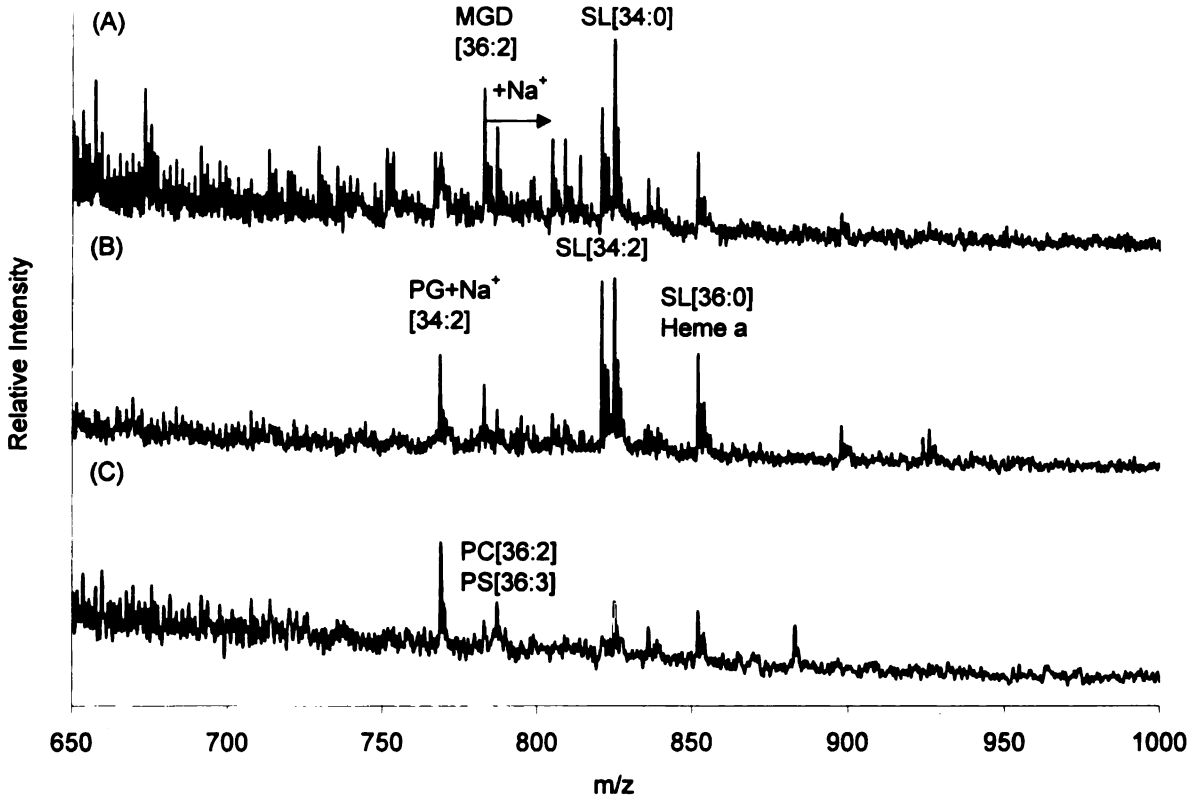

Figure 3.10. Lipid region of positive-ion reflectron MALDI-TOF spectra for different stages of cytochrome c oxidase (A) unpurified, (B) Ni-column purified, and (C) Mono-Q purified.

column purification. Many conclusions can be drawn from this experiment.

The MGD[36:2] decreases in relative intensity with every step of purification. While the relative peak height of the peaks representing SL[34:2] and SL[34:0] changes in the first two phases of isolation and purification, the relative peak intensity of the SL decreases after the MonoQ purification, Figure 3.10 (C). The PG[34:2] seems to remain associated with the enzyme through both purification processes. The peak at 852 Da, SL[36:0] or

heme a, also remains in solution throughout the purification steps. When MALDI analysis was performed on redissolved crystals from X-ray analysis, the resulting spectrum indicated that lipids are further lost in the crystal growth process as well.

Heme

The lipids are not the only cofactors present in cytochrome c oxidase. Non-covalently bound hemes are essential in the transport of electrons and protons. In the bacterium *R. sphaeroides*, the type of heme present in cytochrome c oxidase is heme *a*. This type of heme contains four different side groups: vinyl, methyl, carboxylic acid, and farnesyl.

Lipid extracts from the various stages of purification of CcO1 oxidase were analyzed using TLC. Bands from the TLC plates were excised and extracted with chloroform to retrieve the lipids [13]. These extracts were again analyzed using MALDI MS. It was found that extracts from several of the bands yielded a peak at an m/z value of 852 Da. This peak is also seen in the partial spectrum of the isolated enzyme, Figure 3.8. The PSD spectrum of the peak at 852 Da is shown in Figure 3.11. This is the m/z region of the experiment where the lipids are found, but the PSD spectrum is not characteristic of a lipid. The fragment ions are consistent with those expected for heme *a*. The structure of heme *a* is also shown in Figure 4 with the m/z values of the heme fragments. As shown in Figure 3.8, the peak at 852 was assigned as a sulfolipid or a heme group. With the information determined from the PSD spectrum, this peak can now be assigned as representing heme *a*.

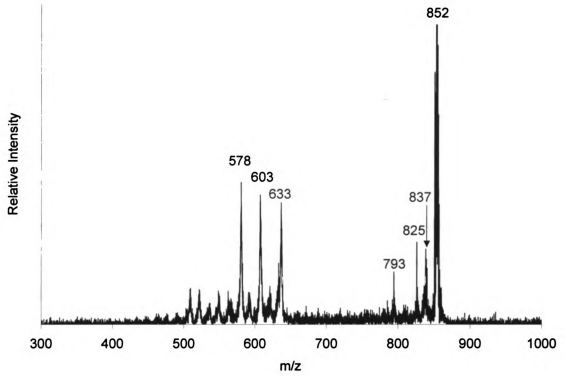

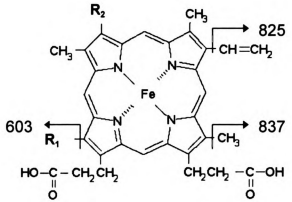

Figure 3.11. PSD MALDI-TOF spectrum of the 852 peak of cytochrome c oxidase sample CcO1. DHB was used as the matrix. The structure of heme *a* is shown as well. R_1 represents a formyl group and R_2 represents a farnesyl group.

Subunit IV (5-10 kDa region)

Important information can be determined about the molecular weight of subunit IV, which was not detected in the initial analysis, Figure 3.7. The full-length form of subunit IV has a predicted molecular weight of 6390.38 g/mol while a shorter form of the protein has a predicted molecular weight of 5403.28 g/mol. The sequence of the longer form of subunit IV is shown in Table 3.1. The underlined portion of the sequence may be removed by processing, or translation may start at the methionine following the underlined portion, to produce the shorter form. In this discussion, the shorter version of subunit IV will be referred to as IVA and the longer version will be referred to as IV.

In Figure 3.7, subunits I-III are detected at high laser powers with a high background when SA is used as the matrix. At lower laser power, subunit IV is detected with poor resolution and the lipids are not detected. When the matrix is changed to DHB, sensitivity and resolution increase for both the lipids and subunit IV. With the enhanced detection of subunit IV, much can be learned about the enzyme. When different versions of cytochrome c oxidase are analyzed, mass spectral analysis can easily identify which version of subunit IV is present, Figure 3.12. The CcO3 sample, Figure 3.12(A), from a strain of *R. sphaeroides* engineered to produce the longer form of the subunit, contains the expected subunit IV (6300kDa). The CcO1 sample analyzed in Figure 3.12(B) contains subunit IVA and a small amount of subunit IV, which suggests that the shorter form predominates in the wild-type bacteria which do not overexpress an engineered form. The CcO2 sample from a strain engineered to produce the shorter version of the subunit, shows the expected peak representing subunit IVA(5300 kDa), Figure 3.12(C). From Figure5, the mass of subunit IVA was found to be 5273 Da and subunit IV was

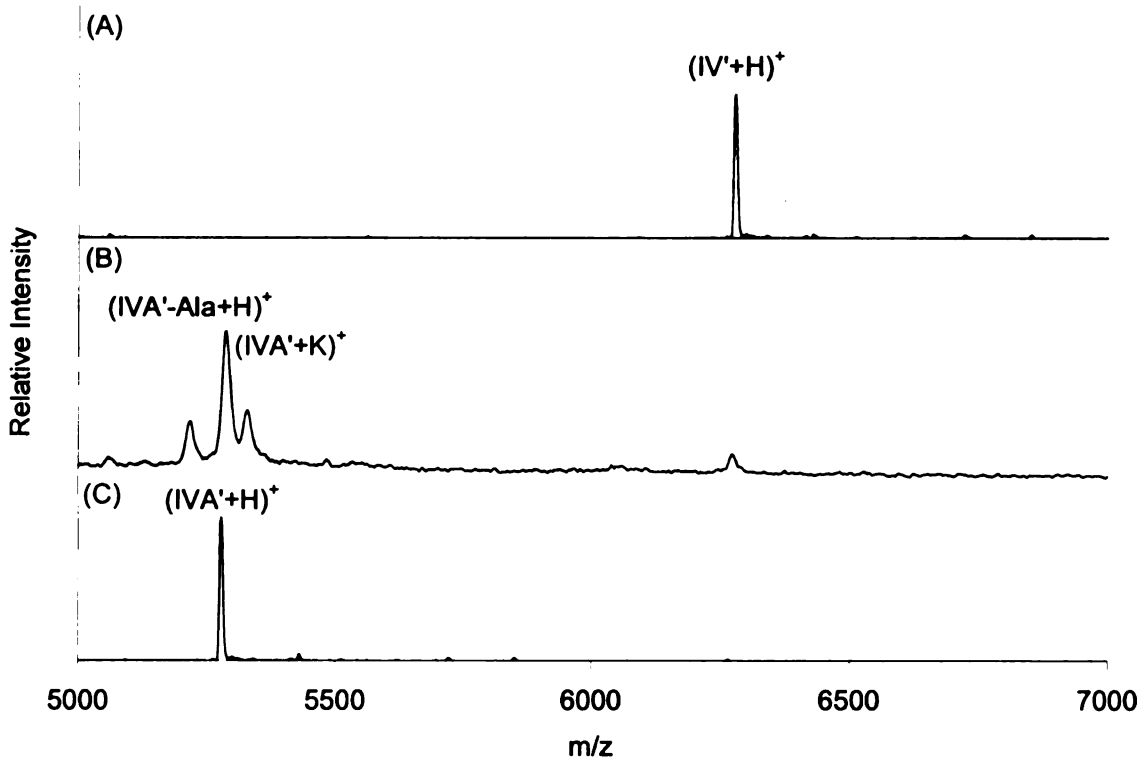

Figure 3.12. A portion of the positive-ion linear MALDI-TOF spectra of cytochrome c oxidase sample CcO3 (A), sample CcO1 (B), and sample CcO2 (C), showing subunits IV' and IVA'. DHB was used as the matrix for each experiment.

found to be 6260 Da. While the sequence in Table 1 shows an N-terminal methionine on both subunit IV and IVA, the m/z values from Figure 5 are 131 Da lower than expected. This is consistent with the loss of the N-terminal methionine for each version of subunit IV. The peaks in the spectrum actually represent subunit IV' and IVA' , using the nomenclature shown in Table 3.1. Several experiments were performed and the average molecular weight information from these experiments is shown in Table 3.3. N-terminal amino acid sequencing of both forms of the subunit has also indicated removal of the starting methionines [14]. Unexpectedly, in Figure 3.12(B) an additional peak 71 Da lower than the peak representing IVA' is seen. This represents the subunit IVA' with the additional loss of an alanine at the N terminus.

The molecular weight information determined from the MALDI TOF experiment was confirmed for both subunit IV' and IVA' using ESI-FTICR MS. A sample of CcO1 cytochrome c oxidase was dissolved in an acetonitrile/formic acid solution at a concentration of approximately 1 micromolar. This solution was then infused into the electrospray source at a rate of one microliter/minute. While no peaks representing the larger subunits were detected, peaks from subunit IVA' were detected in the electrospray FTICR MS experiment. In order to demonstrate the varying resolution from the MALDI TOF experiment to the ESI FTICR MS experiment, spectra from each experiment are shown in Figure 3.13. The spectrum in Figure 3.13(A) is from the MALDI TOF experiment shown in Figure 3.13(C). The Figure shown in 3.13(B) is the deconvoluted ESI-FTMS data and the spectrum shown in Figure 3.13(C) represents the theoretical isotope distribution for subunit IVA' at a resolution of 30000. The most intense peak in the theoretical spectrum is 5271.8493 Da. The most intense peak in the experimental FTMS experiment was 5271.8390, corresponding to an error of 2 ppm. Although the data are not shown, a peak was detected for subunit IV'. The most intense peak in its deconvoluted spectrum was 6258.3228 Da while the theoretical mass of the most intense peak was 6258.2984 Da. This corresponds to an error of less than 4 ppm. The information from the FTMS spectra confirms the sequences of subunits IV' and IVA' given in Table 3.1.

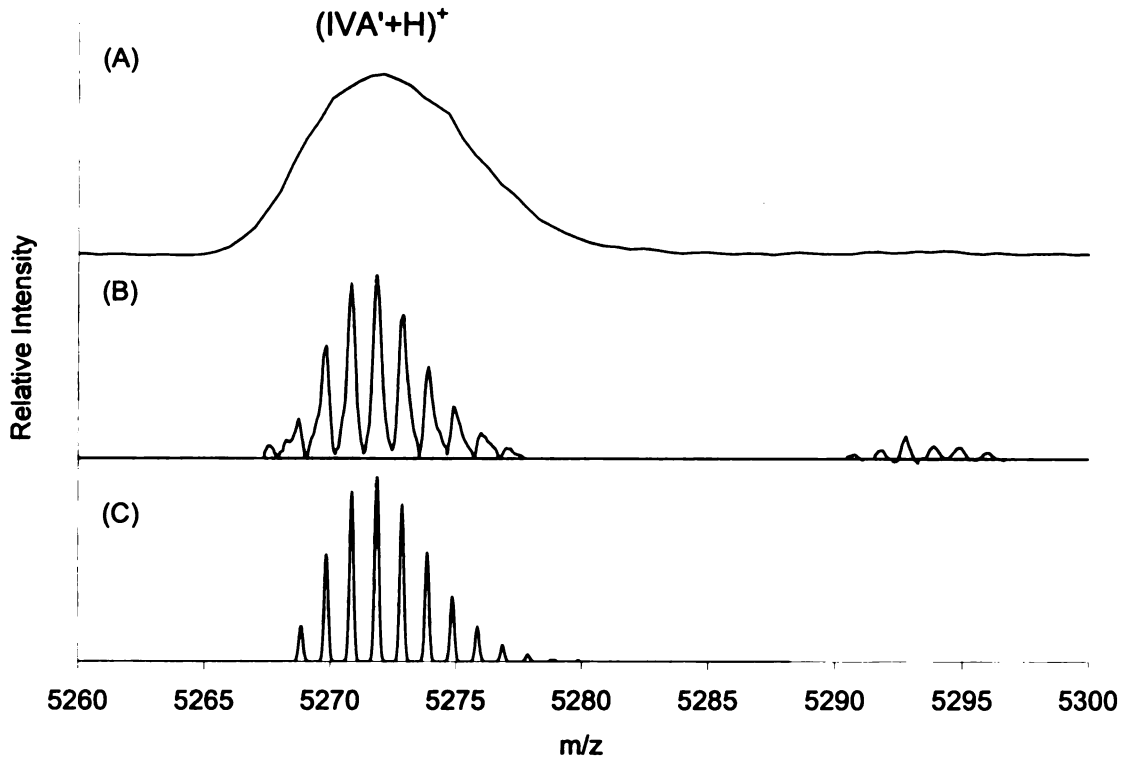

Figure 3.13. (A) Positive-ion MALDI-TOF spectrum of subunit IVA' using DHB as the matrix. (B) Deconvoluted ESI-FTICR spectrum of subunit IVA'. (C) Theoretical isotope distribution for subunit IVA'.

Subunits I-III (20-70 kDa Region)

As shown in Figure 3.7, the larger subunits of cytochrome c oxidase are detected with varying efficiency. This is due to, in part, the nature of the enzyme. Proteins such as cytochrome c oxidase found in cell membranes are hydrophobic and are much more difficult to handle. Hydrophobic proteins often have a tendency to precipitate or aggregate in aqueous solution. These proteins are often solubilized and stabilized with a detergent, if solution experiments on the active form are being performed. However, such additives lead to complications during mass spectrometric analysis. Sensitivity decreases in both MALDI MS [15] and ESI MS experiments [16] when detergents are

present. While the removal of detergents may improve the sensitivity, this may lead to problems when analyzing enzymes that require detergents to maintain their higher order structure in solution.

While the mass spectrometric analysis of membrane proteins proves to be difficult, success has been reported with a variety of techniques. Previously, 2-(4-hydroxyphenylazo)benzoic acid (HABA) has been used as a matrix in MALDI experiments to detect subunit I-III of cytochrome c oxidase from *R. sphaeroides* [17]. In the resulting spectrum, the peaks representing subunit II and III are of lower intensity than the peaks representing the singly- or doubly-charged subunit I. Sinapinic acid was used to analyze the bovine version of the enzyme as well, although a spectrum containing the peaks representing the largest subunits was not reported [18]. Also, partial success has been reported using electrospray [19-22].

There has been greater success when analyzing other types of hydrophobic peptides and proteins [23-25]. Previously, MALDI MS has been used to analyze hydrophobic peptides with the peptide being solubilized in aqueous formic acid prior to the addition of sinapinic acid as the matrix [26]. Other approaches have included the use of chloroform/methanol as the solvent for both the matrix and the peptide [24]. Analysis of hydrophobic peptides and proteins is still difficult, possibly due to the low ionization efficiencies in both MALDI-MS and ESI-MS [25].

While SA as a matrix allows for the detection of subunits I, II, and III, Figure 3.7, the matrix, 2',4'-dihydroxyacetophenone (DHAP) allows for the enhanced detection of subunits II and III, Figure 3.14. DHAP is a useful matrix in this application, since it

suppresses the formation of the doubly charged subunit I as well, simplifying the m/z 20-30 kDa region of the spectrum.

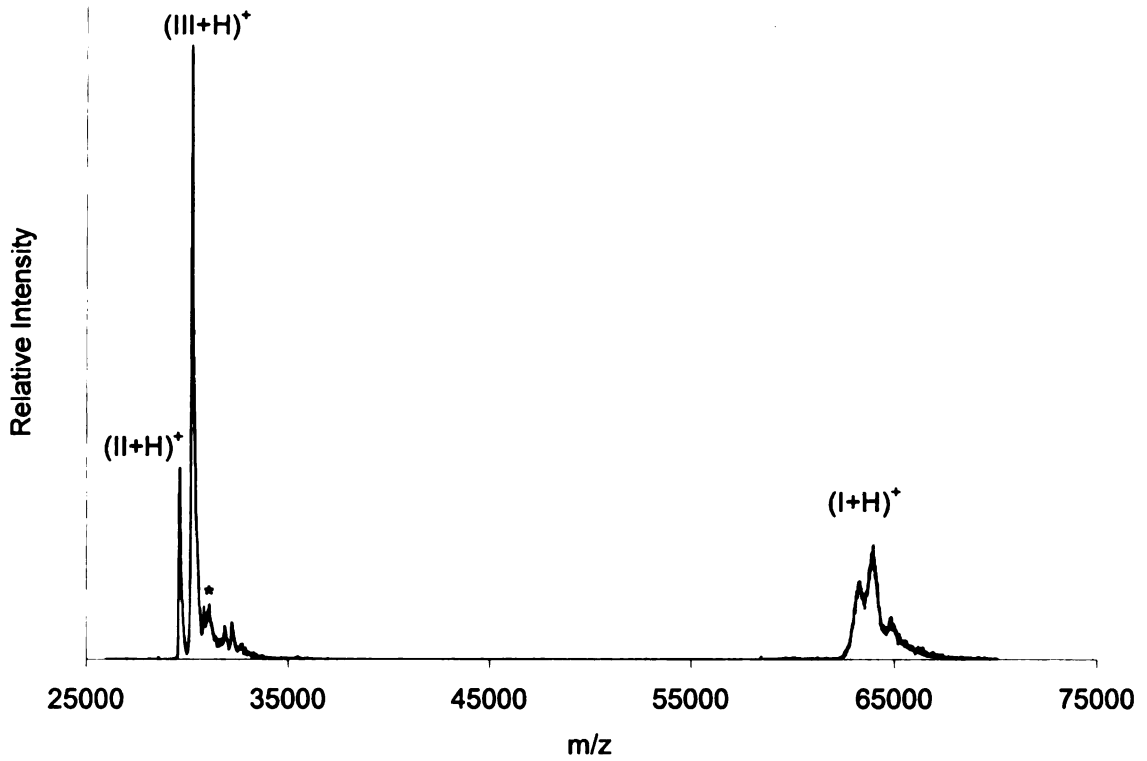

Figure 3.14. A portion of the positive ion linear MALDI-TOF spectrum of cytochrome c oxidase sample CcO3. DHAP was used as the matrix.

When analyzing high molecular weight compounds using MALDI-TOF MS, often there are small shifts in the m/z value of a given peak from spectrum to spectrum. Since molecular weight information was desired for all of the subunits of CcO1 and CcO3 cytochrome c oxidases purified by various methods, the m/z values from several different MALDI experiments were averaged. The results of these measurements are listed in Table 3.3. While the standard deviations shown in Table 3.3 are large, the deviations are still within the mass difference of only 1-2 amino acids. This insures that there cannot be substantial errors in the accepted sequences.

Table 3.3. Measured and Expected Masses of Cytochrome c Oxidase Subunits

Subunit	Sample	Measured Mass (Da)	Standard Deviation	Expected Mass (Da)	Subunit Assignment
Subunit I	CcO1	63939.64	111.21	64039.62	I'+Ht
Subunit I	CcO3	62864.27	89.35	63015.59	I'
Subunit II	CcO1	29167.65	15.39	29122.33	IIA
Subunit II	CcO3	29359.14	62.05	29339.53	IIB+Ht
Subunit III	CcO1	30021.57	26.31	30041.14	III'
Subunit III	CcO3	30140.85	105.07	30041.14	III'
Subunit IV	CcO1	5272.53	0.92	5272.09	IVA'
Subunit IV	CcO1	6259.73	1.52	6259.19	IV'
Subunit IV	CcO3	6260.05	1.87	6259.19	IV'

While the masses of subunits I-III cannot accurately be determined using MALDI-TOF MS, the average molecular weight values shown in Table 3.3 can provide information about the processing of the cytochrome c oxidase in the bacteria. For example, the full-length amino acid sequence for subunit I corresponds to a molecular weight of 63146.79 g/mol or, with the N-terminal methionine removed, 63015.59 g/mol. As prepared for study in specific experiments, subunit I can be engineered to have a His-tag (Ht1), 64170.82 g/mol, and may also have the N-terminal methionine removed, 64039.62 g/mol (I'+Ht1). The C-terminal His-tag used for subunit I contains 2 amino acids in addition to six histidines: SNHHHHHH. When examining the results shown in Table 2, the CcO1 protein contained the engineered His-tagged protein while the CcO3 sample contained the naturally processed protein without the presence of a His-tag.

For the analysis of subunit II, similar results were found. In the CcO1 sample, subunit II did not contain a His-tag and the portions of the sequence underlined in Table 1 were removed as expected. This was confirmed by the mass spectrometric data that contained a peak at 29167 Da, close to the expected value of 29122 Da. Also, in the CcO3 sample, subunit II was the part of the enzyme engineered with a C-terminal His-tag

consisting of only six histidines. For this protein, the portion of the sequence shown in bold in Table 3.1 was cleaved from the protein, in addition to the underlined portion. The mass of this protein, IIB+Ht2, was expected to be 29339 Da and this is close to what is seen in the mass spectrum.

When examining the results from the CcO1 samples, it can be determined that subunit III was processed with the loss of the N-terminal methionine. The expected mass for the N-terminally truncated subunit III (III') is 30041 g/mol. This is in agreement with the data shown in Table 1. Due to the large standard deviation for the results from the CcO3 form, no conclusions can be drawn from this data regarding the processing of the protein, although processing is expected to be identical to that of the CcO1 sample.

Non-covalent complexes

When cytochrome c oxidase is purified, lipids are partially removed in the process. The removal of lipids from the enzyme is known to weaken the complex. In addition to lipid removal, organic solvents, matrix, and low pH can also weaken the complex so that dissociation occurs and only the individual subunits are detected in the MALDI experiment. If dissociation could be eliminated, the complete, intact enzyme could be detected. An additional possibility, limited dissociation, could also be useful. If fragments of the complete complex remained bound as non-covalent subcomplexes, the aspects of connectivity could be realized. For example, when changing the MALDI matrix from SA to DHAP, the region of the spectrum around the peak for subunit I changes, as shown in Figure 3.14. There are peaks detected at 63.7 kDa and 64.5 kDa as well. It is possible these peaks could represent the addition of a heme or lipid to subunit

I. Due to the deviations in these mass measurements, it is impossible to assign these peaks to subunit I plus a specific lipid or heme. As an example, the peak at 63.7 kDa could represent the addition of a lipid (≈700 Da) to subunit I'. The peak at 64.5 kDa could have a number of assignments. First, the addition of two lipids (≈700 Da) is likely. The peak could also represent the addition of 1 cardiolipin molecule (≈1500 Da) to the subunit I'. The peak could represent the heme (858 Da) and a lipid (≈700 Da) bound to subunit I' as well. In the region of the spectrum around 30 kDa, there are peaks representing subunit IIA (29.5 kDa) and subunit III' (30 kDa). There are also four peaks from 30.5-33 kDa. As an example, the peak denoted with an asterisk is at 31 kDa. This peak could represent the addition of a cardiolipin (≈1500 Da) to subunit IIA.

In order to decrease the extent of enzyme dissociation, stabilizing compounds can be added to the cytochrome c oxidase solution. The presence of compounds such as sugars has been found to stabilize proteins in solution. While the exact mechanism of the stabilization effect remains unknown, it has been found that both sucrose and glucose strengthen the pairwise interaction between hydrophobic groups in model systems and stabilize the proteins to heat denaturation through the effect on the structure of water [27]. Sucrose has been found to decrease the denaturation of a protein when exposed to a denaturing agent such as guanidine hydrochloride [28]. Since the organic solvents and matrix molecules used in MALDI may denature the protein in solution, the presence of a stabilizing compound such as sucrose could maintain the non-covalent forces between the subunits of the enzyme.

When sucrose is added to the CcO1 cytochrome c oxidase sample and a MALDI analysis is performed using sinapinic acid as the matrix, several peaks are detected that represent complexes of the cytochrome c oxidase subunits, Figure 3.15. There is a broad

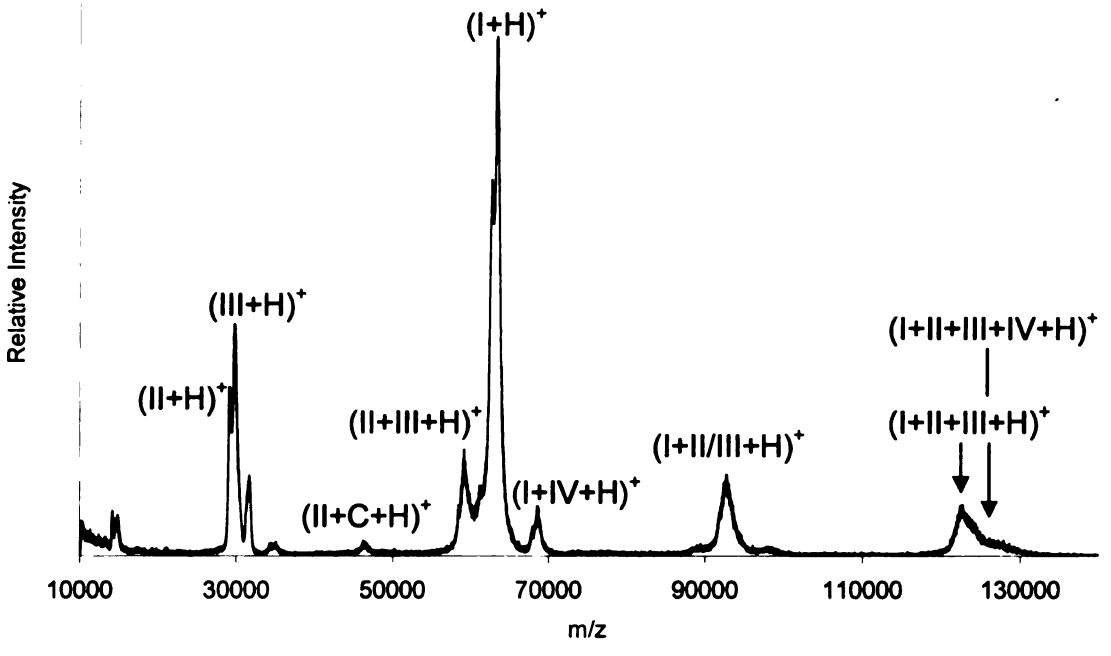

Figure 3.15. Positive-ion linear MALDI-TOF spectrum of cytochrome c oxidase sample CcO1. The cytochrome c oxidase was the nickel column purified sample from Table 2. In the labels, I represents subunit I'+Ht, II represents subunit IIA, III represents subunit III', C represent cytochrome c. SA was used as the matrix with sucrose as a matrix additive.

peak from 34-35.5 kDa representing subunit IVA' bound to subunit IIA (34.4 kDa) or III' (35.3 kDa) as well as a peak at 69 kDa representing subunit IVA' bound to subunit I' (expected 68287). These data are consistent, structurally, with the location of subunit IVA' between subunits I' and III' in the crystal structure [5]. Subunit IV does not appear to be in contact with subunit IIA [5], so the 34-35.5 kDa peak most likely represents an association of subunits III' and IVA'. At 59 kDa, there is a peak due to the binding of subunit IIA to subunit III'. The complex of [I', IIA, IVA'] or [I, III', and IVA'] is detected

at approximately 93 kDa. At 125 kDa, there is a broad peak representing the intact complex with and without subunit IVA'. In these experiments, subunit IVA' may be present at a lower concentration than subunits I-III due to lower expression (lack of engineered overexpression in sample CcO1). Subunit IVA' may also dissociate more easily from the complex, since subunit IVA' is usually surrounded by lipids [5] and may be more easily stripped from the complex during purification as lipids are removed. Therefore it may be expected that some of the intact enzyme will consist of only subunit I, II, and III as shown at the high m/z end of the spectrum in Figure 3.15.

Several peaks in the spectrum represent complexes of subunit IV and other subunits. Why are these partial dissociations of the enzyme not random? Subunit IV contacts subunits I and III through lipids in the crystal structure [5], so it is not surprising that combinations of subunit IV with subunits I and III can be detected. Subunit IV does not appear to be in contact with subunit II, so association of these two subunits would not be expected.

There is also a peak at approximately 46.5 kDa. This m/z value for this peak does not match any combinations of the oxidase subunits. The peak is very broad, but similar in mass to subunit II bound to cytochrome *cy* (17,681 g/mol), the hydrophobically anchored cytochrome c believed to be the normal electron transfer partner of the *R. sphaeroides* cytochrome c oxidase [29]. The complex of cytochrome *c* bound to subunit IIA would have an expected mass of 46,803 g/mol. This is approximately what is seen in the spectrum. It is also interesting to note that cytochrome *cy* is only found bound to subunit II. During the electron transfer process, cytochrome *c* binds to subunit II on the external side of the membrane.

Can the complexes detected be representative of complete dissociation of the enzyme followed by random recombination during MALDI matrix crystal growth? There are several reasons why we believe this is not the case. A peptide, M, can be detected as a dimer, $(2M+H)^+$, in the MALDI experiment, but only at high concentrations of the peptide. The initial concentrations used in these experiments were less than 10 μM. Also, the observed peaks are not representative of random recombination. For example, if cytochrome *c* were concentrated enough, one would expect to see subunits I and III, as well as subunit II, bound to the cytochrome *c* protein. However, this is not the case.

Through the use of sucrose, peaks representing the partial dissociation of cytochrome c oxidase can also provide information on the subunit-lipid interactions in the intact protein. While the X-ray crystal structure reveals that subunit IV is affiliated with subunits I and III, the crystal structure shows lipids bound to subunit IV as well. When sucrose was used as a matrix additive with sinapinic acid, the subunit IV region of the spectrum changed, Figure 3.16. The sample analyzed in Figure 3.16 is the same CcO1 sample analyzed in Figure 3.12(B). In addition to the peaks representing the two versions of subunit IV, additional peaks are seen. In Figure 3.16, a PC is detected bound to subunit IVA'.

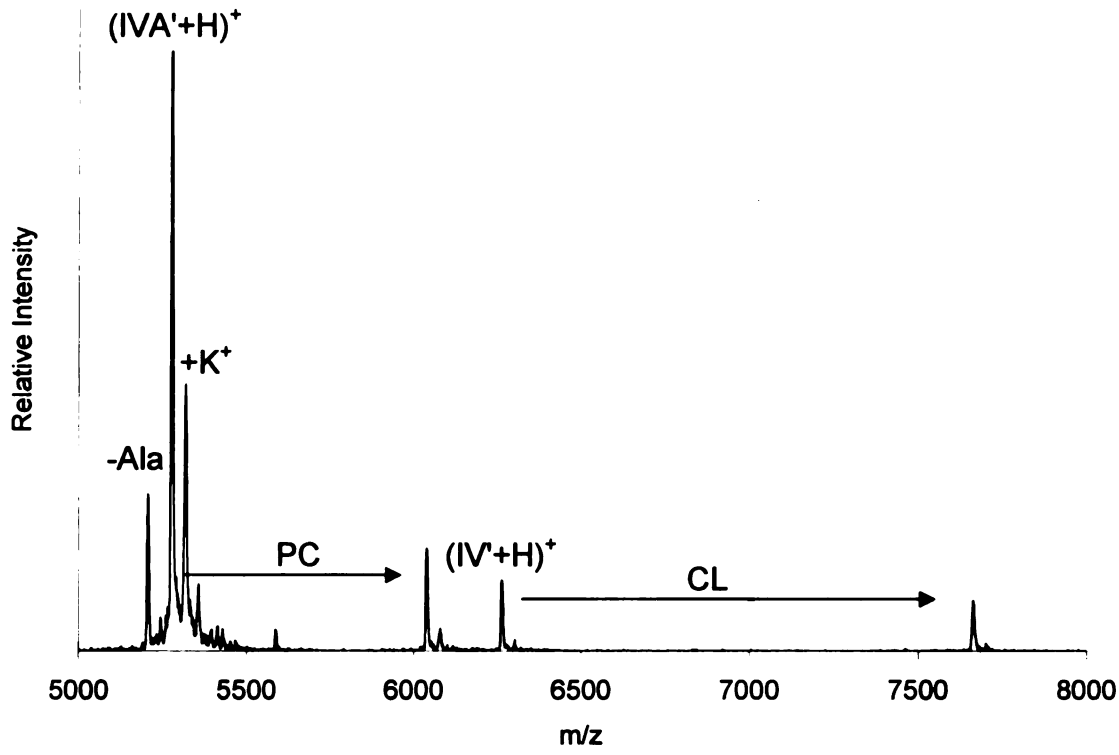

Figure 3.16. Positive-ion linear MALDI-TOF spectrum of cytochrome c oxidase. SA/sucrose was used as the matrix.

When a highly purified solution of CcO3 is analyzed prior to crystal growth, several lipids are detected including PG, MGD, SL, and PC. Crystals are then grown for x-ray crystallographic analysis. After the x-ray analysis, the crystal was dissolved in water and the solution was analyzed using MALDI MS. The PG, MGD, and SL did not remain bound to the enzyme during the crystal growth process. The PC was present in both spectra suggesting that PC most likely remains bound to subunit IVA'. This is consistent with the results shown in Figure 3.16.

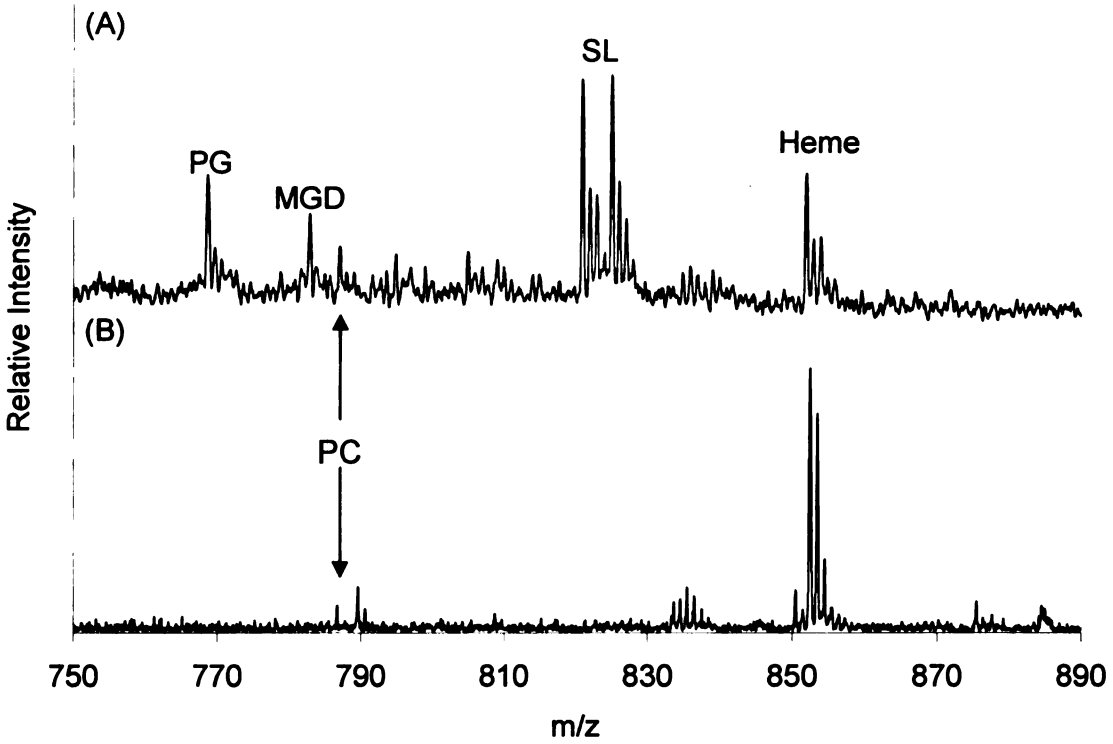

Figure 3.17. Positive-ion reflectron MALDI-TOF spectra of cytochrome c oxidase after (A) before and (B) after crystal growth process. DHB was used as the matrix.

References

1. Musatov, A.; Robinson, N.C. Subunit analysis of bovine cytochrome bc_1 by reverse phase HPLC and determination of the molecular masses by electrospray ionization mass spectrometry. *Biochemistry* **1994**, *33*, 10561-10567.

2. Liu, Y-C.; Sowdal, L.; Robinson, N.C. Separation and quantitation of cytochrome c oxidase subunits by reversed-phase high performance liquid chromatography. *Arch. Bioch. Biop.* **1995**, *324*, 135-142.

3. Tsukihara, T.; Aoyama, H.; Yamashita, E.; Tomizaki, T.; Yamaguchi, H.; Shinzawa-ltoh, K.; Nakashima, R.; Yaono, R.; Yoshikawa, S. The whole structure of the 13-subunit oxidized Cytochrome c Oxidase at 2.5 A. *Science* **1996**, *272*, 1136-1144.

4. Luecke, H.; Schobert, B.; Richter, H.T.; Cartailler, J.P.; Lanyi, J.K. Structure of bacteriorhodopsin at 1.55 A resolution. *Mol. Biol.* **1999**, *291*, 899-911.

5. Svensson-Ek, M.; Abramson, J.; Larsson, G.; Törnroth, S.; Brzezinki, P.; Iwata, S. The X-ray crystal structures of wild-type and EQ(I-286) mutant cytochrome c oxidases from *Rhodobacter sphaeroides*. *J. Mol. Biol.* **2002**, *321*, 329-339.

6. Garavito, R.M.; Ferguson-Miller, S. Detergents as tools in membrane biochemistry. *J. Biol. Chem.* **2001**, *276*, 32403-32406.

7. Jensen, N.J.; Gross, M.L. A comparison of mass spectrometry methods for structural determination and analysis of phospholipids. *Mass Spectrom. Rev.* **1988**, *7*, 41-69.

8. Kim, B.H.; Chang, Y.S.; Lee, B.D.; Ryu, S.H.; Shin, D.H. Mass spectrometric analysis of change in phospholipids in biological membrane by external environmental effects. *Microchem. J.* **1999**, *63*, 3-8.

9. Schiller, J.; Süb, R.; Petković, M.; Hilbert, N.; Müller, M.; Zschörnig, O.; Arnhold, J.; Arnold, K. CsCl as an auxiliary reagent for the analysis of phosphatidylcholine mixtures by matrix-assisted laser desorption and ionization time-of-flight mass spectrometry (MALDI-TOF MS). *Chem. Phys. Lipids.* **2001**, *113*, 123-131.

10. Petković, M.; Schiller, J.; Müller, M.; Benard, S.; Reichl, S.; Arnhold, K.; Arnold, J. Detection of individual phospholipids in lipid mixtures by matrix-assisted laser desorption/ionization time-of-flight mass spectrometry: phosphatidylcholine prevents the detection of further species. *Anal. Biochem.* **2001**, *289*, 202-216.

11. Marto, J.A.; White, F.M.; Seldomridge, S.; Marshall, A.G. Structural chacterization of phospholipids by matrix-assisted laser desorption/ionization

fourier transform ion cyclotron resonance mass spectrometry. *Anal. Chem.* **1995**, *67*, 3979-3984.

12. Imhoff, J. Polar lipids and fatty acids in the genus *Rhodobacter*. *System. Appl. Microbiol.* **1991**, *14*, 228-234.

13. Hilmi, Y. Use of mutagenesis, novel detergents, and lipid analysis to optimize conditions for achieving high resolution 3-dimentional crystal structure of *Rhodobacter sphaeroides* cytochrome c oxidase. Ph.D Thesis. Michigan State University. 2002.

14. Hiser, C.; Ferguson-Miller, S.M. 2003. Personal communication.

15. Jeannot, M.A.; Zheng, J.; Li, L. Observation of gel-induced protein modifications in sodium dodecylsulfate polyacrylamide gel electrophoresis and its implications for accurate molecular weight determination of gel-separated proteins by matrix-assisted laser desorption ionization time-of-flight mass spectrometry. *J. Am. Soc. Mass Spectrom.* **1999**, *10*, 512-520.

16. Loo, J.A. Studying noncovalent protein complexes by electrospray ionization mass spectrometry. *Mass Spectrom. Rev.* **1997**, *16*, 1-23.

17. Ghaim, J.B.; Tsatsos, P.H.; Katsonouri, A.; Mitchell, D.M.; Salcedo-Hernandez, R.; Gennis, R.B. Matrix-assisted laser desorption ionization mass spectrometry of membrane proteins: demonstration of a simple method to determine subunit molecular weights of hydrophobic subunits. *Biochim. Biophys. Acta.* **1997**, *1330*, 113-120.

18. Marx, M.K.; Mayer-Posner, F.; Soulimane, T.; Buse, G. Matrix-assisted laser desoprtion/ionization mass spectrometry analysis and thiol-group determination of isoforms of bovine cytochrome c oxidase, a hydrophobic multisubunit membrance protein. *Anal. Biochem.* **1998**, *256*, 192-199.

19. Whitelegge, J.P.; Gundersen, C.B.; Faull, K.F. Electrospray-ionization mass spectrometry of intact intrinsic membrane proteins. *Prot. Sci.* **1998**, *7*, 1423-1430.

20. Barnidge, D.R.; Dratz, E.A.; Jesaitis, A.J.; Sunner, J. Extraction method for analysis of detergent-solubilized bacteriorhodopsin and hydrophobic peptides by electrospray ionization mass spectrometry. *Anal.Biochem.* **1999**, *269*, 1-9.

21. Hess, S.; Cassels, F.J.; Pannell, L.K. Identification and characterization of hydrophobic *Escherichia coli* viruelence proteins by liquid chromatography-electrospray ionization mass spectrometry. *Anal. Biochem.* **2002**, 123-130.

22. Whitelegge, J.P.; Coutre, J.L.; Lee, J.C.; Engel, C.K.; Prive, G.G.; Faull, K.F.; Kaback, H.R. Toward the bilayer proteome, electrospray ionization-mass spectrometry of large, intact transmembrane proteins. *Proc. Natl. Acad. Sci. USA.* **96**, 10695-10698.

23. Schindler, P.A.; Van Dorsselaer, A.; Falick, A.M. Analysis of hydrophobic proteins and peptides by electrospray ionization mass spectrometry. *Anal. Biochem.* **1993**, *213*, 256-263.

24. Green-Church, K.B.; Limbach, P.A. Matrix-assisted laser desorption/ionization mass spectrometry of hydrophobic peptides. *Anal. Chem.* **1998**, *70*, 5322-5325.

25. Breaux, G.A.; Green-Church, K.B.; France, A.; Limbach, P.A. Surfactant-aided, matrix-assisted laser desorption/ionization mass spectrometry of hydrophobic and hydrophilic peptides. *Anal. Chem.* **2000**, *72*, 1169-1174.

26. Schey, K.L. Hydrophobic proteins and peptides analyzed by matrix-assisted laser desorption/ionization. *Methods Mol. Biol.* **1996**, *61*, 227-230.

27. Back, J.F.: Oakenfull, D.; Smith, M.B. Increased thermal stability of proteins in the presence of sugars and polyols. *Biochemistry*, **1979**, *18*, 5191-5196.

28. Taylor, L.S.; York, P.; Williams, A.C.; Edwards, H.G.M.; Mehta, V.; Jackson, G.S.; Badcoe, I.G.; Clarke, A.R. Sucrose reduces the efficiency of protein denaturation by chaotropic agent. *Biochim. Biophys. Acta.* **1995**, *1253*, 39-46.

29. Myllykallio, H.; Zannoni, D.; Daldal, F. The membrane-attached electron carrier cytochrome c_y from *Rhodobacter sphaeroides* is functional in respiratory but not in photosynthetic electron transfer. *Proc. Natl. Acad. Sci. USA* **1999**, *96*, 4348-4353.

V. Conclusions

When analyzing the cytochrome c oxidase complex, there are many components to consider including the protein subunits, hemes, and lipids. Typically, analysis requires the extraction of the components from the intact complex. We have shown here a method for analyzing the protein subunits, hemes, and lipids in one MALDI experiment. When using DHB as a matrix, the protein subunits, hemes, and lipids were detected. There are advantages to performing the analysis on a solution of the intact enzyme. We have analyzed lipid extracts of the enzyme and found the chloroform-solubilized extracts to be difficult to handle. The lipid extracts were also unstable in the chloroform and are easily oxidized. When analyzed in the aqueous enzyme solution, the lipids were more stable, easy to handle, and produced better signals in the MALDI experiment. This makes MALDI an attractive method for lipid component analysis in membrane proteins because the need for extraction of the lipids is eliminated. All the components of the complex can be detected and characterized in the MALDI experiment with the selection of the correct matrix and matrix additives.

In cytochrome c oxidase from *R. sphaeroides*, all the subunits are connected to each other and all are likely associated with lipids, but these connections are not all equal in area and strength. The unique connectivity information from the partial dissociation of the enzyme in mass spectrometry adds a new dimension to our understanding of the lipid/protein complex. Information from the partial dissociation may be even more valuble for enzymes containing more subunits, such as the 13-subunit cytochrome c oxidase from bovine heart.

APPENDIX A

5-Methoxysalicylic Acid and Spermine: A New Matrix for the Matrix-Assisted Laser Desorption/Ionization Mass Spectrometry Analysis of Oligonucleotides

Anne M. Distler and John Allison*
Department of Chemistry, Michigan State University, East Lansing, Michigan, USA

5-Methoxysalicylic acid (MSA) is demonstrated to be a useful matrix for matrix-assisted laser desorption/ionization time-of-flight (TOF) mass spectrometry of oligonucleotides, when desorption/ionization without fragmentation is desired. When MSA is combined with the additive spermine, the need for desalting is reduced. The MSA/spermine matrix yields linear TOF mass spectra with improved resolution, less fragmentation, and less intense alkali ion adduct peaks than those spectra obtained using 3-hydroxypicolinic acid and 6-aza-2-thiothymine with spermine or diammonium hydrogen citrate as additives. Instrumental conditions are discussed to improve the spectral resolution, specifically the use of longer delay times in the delayed-extraction ion source. (J Am Soc Mass Spectrom 2001, 12, 456–462) © 2001 American Society for Mass Spectrometry

Matrix-assisted laser desorption/ionization mass spectrometry (MALDI MS), developed by Karas et al. [1], has been extensively used to analyze biological compounds at the subpicomole level. To date, most of the published MALDI MS work has involved the analysis of peptides and proteins. MALDI MS has also been used for the analysis of oligonucleotides [2, 3]. The development of MALDI matrices optimized for the analysis of oligonucleotides has lagged behind that for peptides [4], but is currently receiving considerable attention. This report discusses the performance of 5-methoxysalicylic acid, with spermine as a matrix additive, for the detection of oligonucleotides in MALDI with the suppression of prompt fragmentation in the linear time-of-flight (TOF) MS experiment.

Oligonucleotides and DNA behave very differently than peptides and proteins in the MALDI experiment. Differences of note include the sensitivity, extent of prompt fragmentation, the need for cleanup prior to analysis, and resolution.

Certainly, for all classes of biomolecules studied by MALDI, as sample handling methods and TOF instruments have been developed, typical sample sizes used for analysis have decreased. Peptide analysis at the subpicomole level was rapidly achieved, although it has taken longer to realize similar MALDI detection limits for oligonucleotides. There have been significant advances from earlier reports of MALDI analyses of oligonucleotides, in which 10–100 pmol of material were required, to recent reports that show clear detectability at the femtomole level [5, 6].

When a pure peptide is analyzed by MALDI-TOF MS, it usually yields a single mass spectrometric peak representing the intact molecule (in protonated or deprotonated form). Matrices and sample conditions have been reported to increase the extent of prompt fragmentation of peptides in MALDI [7], but experimentalists have little predictable control over the process, generally. In contrast, oligonucleotides frequently fragment promptly and extensively in linear TOF MS [8].

The analysis of pure samples certainly makes mass spectral interpretation easier for all biomolecules. Depending on whether compounds are isolated from biological sources, from electrophoresis experiments (gels or membranes), or are synthesized, peptides and oligonucleotides may be presented for mass spectrometry analysis in the presence of compounds such as salts, buffers, and glycerol, frequently in higher relative amounts than the analytes. In all cases, high amounts of salts can sufficiently change the MALDI target material to lower analyte signals. Glycerol is usually a problem as a component when the first step of the MALDI experiment is to grow crystals. In terms of the spectra that result, salts have a very different impact when analyzing peptides compared to oligonucleotides. If NaCl is present, two peaks may appear representing a single peptide in positive ion mode, most frequently representing the $[M + H]^+$ and $[M + Na]^+$ ions, separated by 22 Da. As the salt contribution increases,

Address reprint requests to Dr. John Allison, Department of Chemistry, Michigan State University, East Lansing, MI 48824-1322. E-mail: allison@cem.msu.edu

1044-0305/01/$20.00
PII S1044-0305(00)00212-4

Received September 7, 2000
Revised November 30, 2000
Accepted November 30, 2000

sodium adducts become more intense. The presence of salts has a much more dramatic influence on the MALDI spectra of oligonucleotides. With an ionic phosphodiester backbone, oligonucleotides can contain a large number of anionic sites that must combine with an assortment of cationic species such as H^+, Na^+, and K^+ to desorb in a singly charged form. Combinations of cations to provide a charge balance can lead to a substantial number of peaks representing the intact molecule. Whenever ions for a single species are generated with a range of *m/z* values, detection limits are lowered. Also, it becomes much more difficult to detect multiple components of similar mass. Certainly, a simple situation is to generate one mass spectral peak per component, not several.

In the analysis of oligonucleotides with MALDI TOF MS, the resolution achieved is often less than what would be realized for peptides of similar size. Adduct formation and nucleotide base loss have frequently been cited as causes of the reduced resolution [9]. For larger oligonucleotides, this is clearly the case. However, even for smaller sequences with resolved sodium and potassium adducts, resolution for an oligonucleotide is less than that obtained for a peptide of similar mass on the same instrument. The use of an ion reflector does not dramatically improve the resolution of oligonucleotides in MALDI MS [10]. One of the few instances in which relatively small oligonucleotides were analyzed by MALDI and spectra containing isotopic resolution were obtained was recently published, using a MALDI TOF instrument with an extended flight tube [11]. We show that, for the TOF instrument used in this work utilizing gridded ion optical components and delayed extraction (DE), "nontraditional" ion source settings can improve the resolution.

Although peptides and oligonucleotides have many differences in terms of their MALDI MS analysis, they also have some notable similarities in terms of the development of the analytical utility of mass spectrometry for their analysis. Early in the history of MALDI, demonstrations of the ability to generate signals from large, intact, ionized proteins maintained excitement for this new method, allowing it to be further developed. Whereas positive results had been reported for proteins with molecular weights (MW) of several hundred thousand, the mass spectral peaks were very broad, and it was difficult to extract what would be considered in mass spectrometry an accurate mass. The early results showed that, in most cases, MW's determined were more useful than those derived from gel electrophoresis. Today, the real strength of MALDI in protein analysis does not lie in its ability to generate ions of intact proteins, but in the subpicomolar sensitivity obtainable for smaller peptides. The analysis of enzymatic and chemical digestion products is the application that is making the real contributions to protein analysis. Scientists have certainly worked to demonstrate that large oligonucleotides can be characterized by MALDI as well. Whereas a few reports have been published demonstrating the detection of 50-mers, the MALDI response is much more sharply a function of MW than is observed for peptides, making the detection of large oligonucleotides far from routine. Because a potential application was the use of mass spectrometry to replace gel electrophoresis when sequencing DNA using the Sanger method, the requirement of the mass spectrometry method was different than when sequencing peptides. Peaks with good resolution must be detectable not only at low *m/z* values, but over a very wide mass range, because the approach for DNA analysis is a ladder sequencing method. Although mass spectrometry may not in the near future replace gels for DNA sequencing, other powerful applications are emerging, notably the analysis of single nucleotide polymorphisms (SNPs) [12, 13]. In this area, mixtures of small oligonucleotides, usually with molecular weights less than 6000 Da, are generated which are indicative of errors in genetic code. This is an application to which MALDI MS is well suited. Certainly, the need continues to develop methods for improved analysis of oligonucleotides of all sizes. The SNP application is clearly driving method development for analyses of oligonucleotides of sizes for which the challenges are not the creation of new instruments, but improved matrix chemistry. The goals continue to be lower detection limits, the ability to perform analyses with less or no cleanup (recognizing the contaminants most commonly encountered, and that purification steps always lead to sample loss), and to identify experimental conditions in which fragmentation is decreased or eliminated. Certainly, in the analysis of mixtures, if one could rely on generating only one peak per component, as is common for peptides, then the analysis of mixtures of oligonucleotides would be much easier.

Many matrices have been developed for peptide analysis [14, 15] by MALDI such as nicotinic acid, ferulic acid, sinapinic acid, and 2,5-dihydroxybenzoic acid. Because, generally, these are not as useful for oligonucleotide analysis, alternate matrices have been identified [16, 17]. Several matrices were found to be compatible for the analysis of oligonucleotides using UV lasers, including 3-hydroxypicolinic acid (HPA) [18] and 6-aza-2-thiothymine (ATT) [19]. Since the development of these matrices, HPA has become the standard matrix for the analysis of larger nucleic acids while ATT is used for sequences containing less than 25 bases [2]. In addition to UV-MALDI, work has been done using infrared lasers [20, 21]. Successful matrices for IR-MALDI include succinic acid and urea [22]. Because matrix selection alone does not overcome some of the problems associated with the MALDI MS analysis of oligonucleotides, a number of matrix additives have been developed. The utility of ammonium salts has been demonstrated to reduce the formation of alkali ion adducts. Ammonium acetate was the first to be used in the MALDI experiment [8]. Since then, other ammonium salts have appeared in the literature with the most successful being diammonium hydrogen citrate [23, 24].

Thus, if an oligonucleotide exists in solution in polyanionic form as P^{n-}, it forms a singly charged anion by adding combinations of H^+, Na^+, and K^+ ions. If NH_4^+ ions are present, these compete effectively with alkali ions in complexing with negatively charged phosphates. During the desorption/ionization process, ammonia is lost, leaving protons behind. In this paper, the fully protonated form of an oligonucleotide, $[P^{n-} + nH^+]$, the "free acid form," will be referred to as M. If no alkali ions are involved and all of the phosphates are neutralized by protons, negative ion MALDI yields deprotonated molecules, designated as $[M - H]^-$. In our lab, the role of polyamines as matrix additives has been explored and spermine was found to improve MALDI spectra for single-stranded oligonucleotides, eliminating both the need for ammonium citrate as well as desalting [5, 25].

We demonstrate here that 5-methoxysalicylic acid (MSA) is useful in the MALDI analysis of oligonucleotides. In our experiences, it is unique in generating intact oligonucleotide ions with very little fragmentation. MSA is not a new matrix in the field of MALDI. It has been suggested that a mixture of MSA, 2,5-dihydroxybenzoic acid, and fucose is a useful matrix for the analysis of peptides [26], whereas MSA with 9-anthracenecarboxylic acid has been demonstrated as a matrix for the analysis of polymers [27]. MSA has also been used in a multicomponent matrix when quantitation was being attempted [28]. We show here that MSA is also an effective matrix for the analysis of oligonucleotides. The MALDI spectra obtained using MSA are compared here to those obtained using the traditional HPA and ATT matrices. Best results were obtained using spermine as an additive, rather than diammonium hydrogen citrate.

Experimental

The 12-mer oligodeoxyribonucleotide d(CGCGAATTCGCG) was purchased from the Michigan State University Macromolecular Structure, Sequencing, and Synthesis Facility (East Lansing, MI). The stock solution used had a concentration of 46.6 pm/μL and was used without desalting. The matrices 6-aza-2-thiothymine and 5-methoxysalicylic acid were purchased from Aldrich (Milwaukee, WI). Spermine and 3-hydroxypicolinic acid were purchased from Fluka (Milwaukee, WI). All matrices were used without further purification. When spermine was used as a matrix additive, it was prepared at a concentration of 25 mM in water. When diammonium hydrogen citrate (J.T. Baker, Phillipsburg, NJ) was used, it was prepared at a concentration of 50 mM in water. Saturated matrix solutions were made using a 1:1 acetonitrile/additive solution. Samples were prepared by mixing 1 μL of analyte solution with 1 μL of the matrix solution on a gold sample plate and allowing the mixture to air dry.

MALDI mass spectra were recorded using an Applied Biosystems (Framingham, MA) Voyager delayed extraction linear time-of-flight mass spectrometer equipped with a nitrogen laser (337 nm, 3 ns pulse). For the negative ion MALDI spectra reported here, the accelerating voltage was −15 kV, the delay time was 700 ns, the grid voltage was 94.5% of the accelerating voltage, and magnitude of the guide wire voltage was 0.20% of the accelerating voltage. Typically, 50 laser shots were averaged for each spectrum.

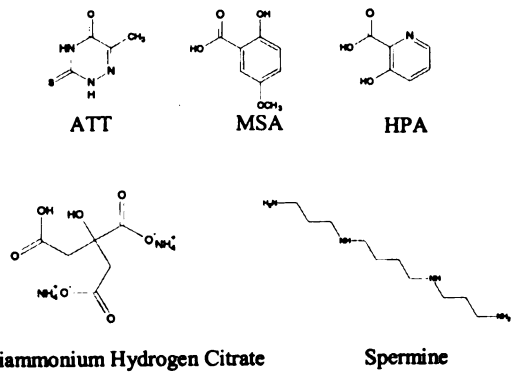

Figure 1. Structures of the matrices and additives used in this study.

UV/visible spectra of aqueous solutions of the matrices were recorded using an ATI Unicam (Cambridge, UK) UV2 spectrophotometer. All spectra were acquired with a scan speed of 120 nm/min, a data interval of 0.5 nm, and a 2.0 nm bandwidth. Spectra were acquired for three matrices, each at a concentration of 2.0×10^{-5} M. Quartz cuvettes were used with water in the reference cuvette.

Results and Discussion

To demonstrate the advantages of MSA as a MALDI matrix for oligonucleotide analysis, we selected the Dickerson dodecamer, d(CGCGAATTCGCG), referred to here as DD, as an example of a typical oligonucleotide. We have obtained similar results for a variety of other oligonucleotides, including d(ACCCACCCACCC), d(AAAAACCAAAAA), d(TTTTTGGTTTTT), and d(CCGGAATTGGCC). DD was chosen as an example, because it has been used extensively in the literature, and contains all four bases. Furthermore, while all of these oligonucleotides fragment in typically used matrices such as ATT, DD fragments most extensively. The nomenclature suggested by McLuckey [29] is used to identify fragment ions.

Data are shown for the analysis of DD using the three matrices HPA, ATT, and MSA. Their structures are shown in Figure 1. Using the traditional additive, diammonium hydrogen citrate (DHC), these three matrices yield the spectra shown in Figure 2. The ATT/DHC mixture yields the complex spectrum shown in Figure 2a. The resolution for the peak representing the deprotonated molecule at m/z 3645 is low, and extensive

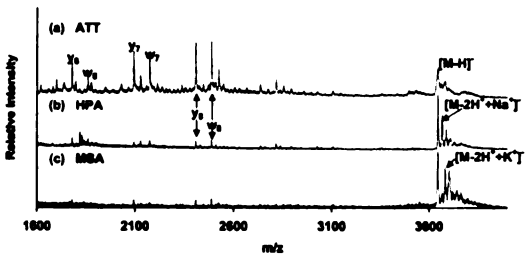

Figure 2. MALDI-MS negative-ion mass spectra of DD with DHC as an additive using (*a*) ATT, (*b*) HPA, and (*c*) MSA.

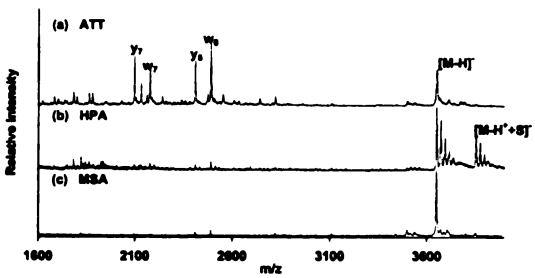

Figure 3. MALDI-MS negative-ion mass spectra of DD with spermine (S) as an additive using (*a*) ATT, (*b*) HPA, and (*c*) MSA.

fragmentation occurs. The y_8 and w_8 peaks, which are more intense than that for the deprotonated molecule, are formed following phosphodiester bond cleavage between the G and A nucleosides. In contrast, the HPA/DHC matrix produces a much different MALDI spectrum, Figure 2b. The deprotonated molecule is the dominant peak in the spectrum, with only small fragment ion peaks present. In comparing Figure 2a, b, the fragment ions do not change when the matrix is changed, but HPA produces fewer fragment ions. The resolution for the deprotonated molecule peak is clearly higher than in the ATT/DHC spectrum. At *m/z* values above *m/z* 3645, a series of sodium ion adducts are observed, in which an H^+ is replaced by a sodium ion in the mono-anion. The low mass shoulder on the *m/z* 3689 peak ($[M - 3H^+ + 2Na^+]^-$) is a potassium adduct, $[M - 2H^+ + K^+]^-$.

The spectrum obtained using MSA/DHC as the matrix, shown in Figure 2c, closely resembles that obtained using HPA/DHC. There are fewer detectable fragment ions in Figure 2c and the peaks are less intense, compared to those in Figure 2a, b. Again, the change in matrix does not yield a substantial change in the fragmentation pattern, but changes the extent of fragmentation. The deprotonated molecule peak is again the most intense in the spectrum. It is interesting to note that the potassium adduct has greater intensity than the monosodium adduct. In Figure 2c, alkali ion adducts contribute to the unresolved high *m/z* "tail." Although the addition of ammonium citrate reduces cation adduction, there is still a need for desalting. The ammonium citrate clearly works more efficiently when used with HPA or MSA, and does provide spectra that are superior to those obtained using the matrices alone. Clearly, the choice of matrix (as well as the choice of additive [30]) has a substantial impact on the extent of fragmentation, with MSA allowing for desorption of intact oligonucleotides with minimal formation of fragment ions. A reduction of fragmentation accompanied by formation of an intense peak representing the doubly charged molecular ion has also been seen using 3-HPA, at an excitation wavelength of 355 nm [31].

In our experience, spermine is found to be consistently superior to ammonium citrate as a matrix additive. As shown in Figure 3, the choice of matrix affects the performance of spermine as an additive. The negative ion MALDI spectrum obtained using ATT/spermine as the matrix. Figure 3a, yields a fragmentation pattern similar to that seen using DHC as an additive, Figure 2a. Regardless of the additive, fragment ions are more abundant than the deprotonated molecule. With spermine as the additive, the resolution of the $[M - H]^-$ peak increases, and only small sodium and potassium adduct peaks are present. In addition to the alkali ion adducts, there are two small higher-*m/z* peaks that represent a matrix and a spermine adduct. This is not the case in the HPA/spermine spectrum shown in Figure 3b. Although the fragmentation is minimal, the spermine adduct becomes a dominant peak in the spectrum. Spermine is ineffective in eliminating the formation of alkali ion adducts in HPA for this experiment. The five sodium adducts in the *m/z* range 3667–3755 increased in intensity from those observed when HPA/DHC is the matrix. Adduct ions are also formed in which both spermine and alkali ions are attached.

When combined with spermine, MSA is an ideal matrix for the desorption/ionization of intact oligonucleotides, as shown in Figure 3c. The spectrum obtained using the MSA/spermine matrix contains very small w_8–w_{10} and y_8 fragment ions. The peak representing the intact analyte is fully resolved with the sodium and potassium adducts greatly reduced. The spermine adduct is of low intensity compared to the intact, deprotonated molecule. Also, there is no peak representing the doubly deprotonated molecule as seen previously in other spectra of oligonucleotides containing negligible fragmentation [31]. Thus, if the goal is to obtain spectra in which one oligonucleotide yields a single peak, MSA will limit fragmentation and spermine will limit the formation of adducts, and this combination of MSA and spermine retains the favorable properties of each matrix component. The performance of spermine has been discussed previously and it is not our intention to reintroduce it here. We do note that the oligonucleotide samples were used as supplied from the Michigan State University Macromolecular Structure, Sequencing, and Synthesis Facility. As synthesized, using standard methods [32], these samples had a high, but poorly defined salt content, and contained other contaminants

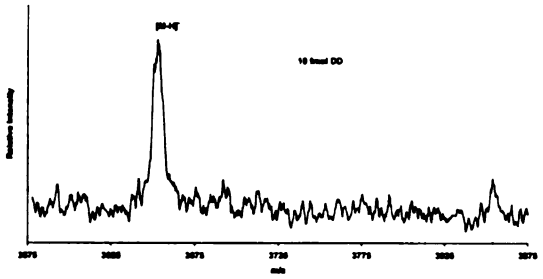

Figure 4. MALDI-MS negative-ion mass spectrum of 10 fmol of DD, using MSA/spermine as the matrix.

such as a buffer. For oligonucleotides made in this way, desalting is unnecessary if spermine is used.

The spectra in Figures 2 and 3 were obtained using 47 pmol of oligonucleotide as the analyte. With this amount, the spectra are strong and the differences can be clearly documented. The MSA/spermine combination allows for spectra to be obtained with sample amounts below 1 pmol. Figure 4 shows a portion of the spectrum obtained using the MSA/spermine combination with a total of 10 fmol of DD in the target. A signal-to-noise ratio of 12:1 is achieved (prior to smoothing).

The results presented here clearly show that matrix selection can have a dramatic influence on the extent of fragmentation of oligonucleotides. For the three matrices studied, MSA and HPA are both organic acids, and ATT is considered as a neutral matrix. If ATT were drawn in the enol form, all three would have aromatic hydroxy groups that could be the source of protons for analyte ionization in the positive ion MALDI experiment. Rather than considering structural features such as specific functional groups, there may be a correlation between matrix performance and molar absorptivities. The UV/visible spectra of equimolar aqueous solutions of the three matrices used in this work are shown in Figure 5. As suggested by their spectra, MSA has the greatest molar absorptivity at 337 nm with a value of 2240 M^{-1} cm^{-1}. ATT and HPA have molar absorptivities at 337 nm of 1135 and 911 M^{-1} cm^{-1}, respectively. Although the UV experiment was conducted in solution, we expect a similar result for the solid matrices. This is reflected in the fact that, when MSA is used as a matrix, significantly lower laser powers are required to generate intense signals. If a matrix is an efficient "light harvester," with a high molar absorptivity, absorbing crystals may quickly achieve higher temperatures than would crystals of molecules with lower extinction coefficients. Because the matrix molecules absorb the energy, time is required for energy to flow from matrix molecules into analyte molecules [33]. At higher temperatures, desorption rates increase, decreasing the time in which energy can flow into the analyte. The result would be less prompt fragmentation. This is one possible explanation for the reduced fragmentation observed when MSA is used. With the data provided here, our intention is not to develop predictive capabilities for fragmentation of oligonucleotide ions as a function of matrix choice, but rather to establish that fragmentation is greatly reduced by use of the MSA/spermine matrix combination.

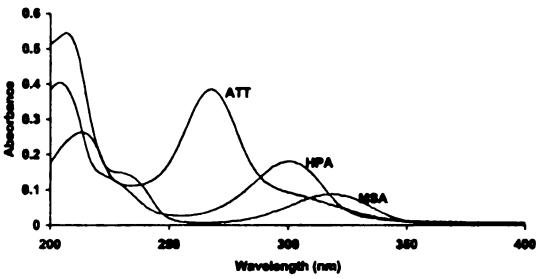

Figure 5. UV-visible spectra of the matrices. For each, the concentration (aqueous) was 2.0×10^{-5} M.

Whenever new matrices are proposed, the question of sample spot homogeneity should be addressed. Formation of MSA crystals is visibly different than for ATT and HPA. The MSA solution, applied to a MALDI plate, tends to spread more than other matrices, yielding a thinner, more uniform bed of crystals. Spectra such as those shown can be obtained at most points across the target, unlike the other matrices for which the crystal growth is more extensive around the outer edges of the target.

All of the spectra shown were obtained with what we consider to be "nontraditional" tuning of the MALDI DE-TOF instrument used for this work. The PE Biosystems TOF mass spectrometer uses a "gridded" ion source and a linear TOF mass analyzer; changes in voltages suggested here may not have the same effect on spectra obtained using instruments that do not employ grids. If analyzing a peptide with a molecular weight in the 3000–4000 range, an accelerating voltage of 20 kV, a grid voltage of 94%–95% the accelerating voltage, a guide wire voltage of approximately 0.05%, and a delay time of 100 ns are the typical conditions selected for optimal resolution. Using these conditions, the resolution obtained for an oligonucleotide is much less than that for a peptide of similar mass. The reduction in resolution for oligonucleotides could result from a number of causes including ion fragmentation in the ion source during acceleration, and slow desorption/ionization-kinetics following laser irradiation. Fragmentation which occurs on a time scale longer than the ion generation and shorter than the acceleration time will be manifested in a linear TOF experiment as tails on the fragment ion peaks towards higher *m/z* values [34]. However, the spectra shown here have negligible tailing on the fragments peaks and more prominent tailing on the peak correlating to the intact ion. Processes other than fragmentation during acceleration must occur which lead to the decreased resolution in an oligonucleotide spectrum. The slow desorption/ionization ki-

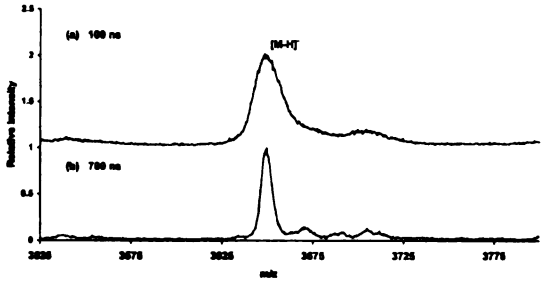

Figure 6. MALDI-MS negative-ion mass spectra of DD with MSA/spermine as the matrix with (*a*) 100 ns delay and (*b*) 700 ns delay.

netics for an oligonucleotide may be another cause of decreased resolution. Oligonucleotides are more polar than peptides or proteins and, thus, require more energy to generate intact, gas phase ions [10]. Increasing the delay time is one way to compensate for the processes that may lead to low resolution. Improvements in resolution as a function of tuning are not unique to the one instrument on which these experiments were performed. Improvements were also observed on a PerSeptive Biosystems Voyager STR DE instrument. A portion of the DD spectrum obtained using MSA/spermine and the standard tuning is shown in Figure 6a; the same region of the spectrum, obtained using a much longer delay time, is shown in Figure 6b. For longer delay times, slightly higher guide wire voltages are recommended. This combination results in much improved resolution. The optimized conditions, a guide wire voltage of 0.200% and a delay time of 700 ns, provide improved resolution for all peaks in the spectrum in both positive and negative ion modes. This result is not matrix specific. Although we make this observation, and routinely use long delay times when obtaining MALDI spectra of oligonucleotides, there is no one process that could clearly be linked to the delay time-resolution correlation. Low resolution for oligonucleotides under standard ion source conditions does not appear to be due to decomposition of the intact anions during acceleration, because spectra obtained using long delay times do not contain fragment ion peaks that are absent or less intense when short delay times are used. Desorption kinetics, linked to the unique variety of charge states of the oligonucleotides that may be trapped in the matrix, may be very different than those for peptides that are trapped in predominantly neutral form.

If the combination of a new matrix and modified tuning leads to the advantage of increased resolution, one may expect the improvement to be further realized by using a reflectron. Again, oligonucleotides behave very differently than do peptides in MALDI MS [10]. Resolution is much lower for oligonucleotides and the use of a reflectron does not significantly improve the resolution [10]. When analyzing DD with each of the three matrices on a Voyager STR in reflectron mode, there is no change in resolution. The $[M - H]^-$ peak is smaller and the spectra are worse than if a linear TOF MS is used. The intensity of the $[M - H]^-$ peak may decrease in reflectron mode because we have delayed all fragmentation from prompt (in source) to occurring in the flight tube. If this is the case, a post-source decay experiment should yield an intense spectrum. This is not observed. It is possible an electron may be ejected from the $[M - H]^-$ species leaving [M − H] in the flight tube. Whatever the mechanism, best results are achieved for oligonucleotides in negative mode in a linear MALDI experiment.

Conclusion

Although HPA/DHC and ATT/DHC are matrix/additive combinations commonly used for oligonucleotide analyses, MSA proves to be a superior matrix for detection of the intact analyte in the 12–20 base pair range when spermine is used as an additive. The MSA/spermine matrix provides alkali ion adducts of low abundance, little fragmentation, and better resolution when compared to ATT and HPA with either DHC or spermine. Spermine, when used with MSA, reduces the need for desalting of oligonucleotide samples.

Although analyses of double-stranded oligonucleotides have been reported with several matrices [21, 22], such noncovalently bound complexes are still difficult to routinely detect intact. In most cases, if a double-stranded oligonucleotide is analyzed using MALDI MS, peaks representing only the single strands are observed in the spectrum. Although MSA/spermine is very effective as a matrix for single strands, it does not allow for double strands to be detected as intact ions. The search continues for a matrix that will routinely allow such noncovalent interactions to remain intact.

References

1. Karas, M.; Bachmann, D.; Bahr, U.; Hillenkamp, F. *Int. J. Mass Spectrom. Ion Processes* **1987**, *78*, 53–68.
2. Nordhoff, E.; Kirpekar, F.; Roepstorff, P. *Mass Spectrom. Rev.* **1996**, *15*, 67–138.
3. Limbach, P. A. *Mass Spectom. Rev.* **1996**, *15*, 297–336.
4. Zhang, L.-K.; Gross, M. L. *J. Am. Soc. Mass Spectrom.* **2000**, *11*, 854–865.
5. Asara, J.; Allison, J. *Anal. Chem.* **1999**, *71*, 2866–2870.
6. Roskey, M. T.; Juhasz, P.; Smirnov, I. P.; Takach, E. J.; Martin, S. A.; Haff, L. A. *Proc. Natl. Acad. Sci. USA* **1996**, *93*, 4724–4729.
7. Lavine, G.; Allison, J. *J. Mass Spectrom.* **1999**, *34*, 741–748.
8. Currie, G.; Yates, J. III. *J. Am. Soc. Mass Spectrom.* **1993**, *4*, 955–963.
9. Nordhoff, E.; Cramer, R.; Karas, M.; Hillenkamp, F.; Kirpekar, F.; Kristiansen, K.; Roepstorff, P. *Nucleic Acids Res.* **1993**, *21*, 3347–3357.
10. Juhasz, P.; Roskey, M. T.; Smirnov, I. P.; Haff, L. A.; Vestal, M. L.; Martin, S. A. *Anal. Chem.* **1996**, *68*, 941–946.
11. Koomen, J. M.; Russell, D. H. *J. Mass Spectrom.* **2000**, *35*, 1025–1034.
12. Griffin, T. J.; Smith, L. M. *Anal. Chem.* **2000**, *72*, 3298–3302.

13. Fei, Z.; Smith, L. M. *Rapid Commun. Mass Spectrom.* **2000,** *14,* 950–959.
14. Börnsen, K. O.; Schär, M.; Widmer, H. M. *Chimica* **1990,** *44,* 412–416.
15. Hillenkamp, F.; Karas, M.; Ingendoh, A.; Stahl, B. In *Biological Mass Spectrometry;* Burlingame, A.; McCloskey, J. A., Eds.; Elsevier Scientific: Amsterdam, 1990; p 49.
16. Parr, G. R. Fitzgerald, M. C.; Smith, L. M. *Rapid Commun. Mass Spectrom.* **1992,** *6,* 369–372.
17. Spengler, B.; Pan, Y.; Cotter, R. J.; Kan, L. S. *Rapid Commun. Mass Spectrom.* **1990,** *4,* 99–102.
18. Wu, K. J.; Steding, A.; Becker, C. H. *Rapid Commun. Mass Spectrom.* **1993,** *7,* 142–146.
19. Lecchi, P.; Le, H. M. T.; Pannell, L. K. *Nucleic Acids Res.* **1995,** *23,* 1276–1277.
20. Kirpekar, F.; Berkenkamp, S.; Hillenkamp, F. *Anal. Chem.* **1999,** *71,* 2334–2339.
21. Berkenkamp, S.; Kirpekar, F.; Hillenkamp, F. *Science* **1998,** *281,* 260–262.
22. Nordhoff, E.; Ingendoh, A.; Cramer, R.; Overberg, A.; Stahl, B.; Karas, M.; Hillenkamp, F.; Crain, P. F. *Rapid Commun. Mass Spectrom.* **1992,** *6,* 771–776.
23. Li, Y. C. I.; Cheng, S. W.; Chan, T. W. D. *Rapid Commun. Mass Spectrom.* **1998,** *12,* 993–998.
24. Pieles, U.; Zürcher, W.; Schär, M.; Möser, H. E. *Nucleic Acid Res.* **1993,** *21,* 3191–3196.
25. Asara, J. M.; Hess, J. S.; Lozada, E.; Dunbar, K. R.; Allison, J. *J. Am. Chem. Soc.* **2000,** *122,* 8–13.
26. Gusev, A. I.; Wilkinson, W. R.; Proctor, A.; Hercules, D. M. *Anal. Chem.* **1995,** *67,* 1034–1041.
27. Tang, X.; Dreifuss, P.; Vertes, A. *Rapid Commun. Mass Spectrom.* **1995,** *9,* 1141–1147.
28. Gusev, A. I.; Wilkinson, W. R.; Protor, A.; Hercules, D. M. *Fresenius J. Anal. Chem.* **1996,** *354,* 455–463.
29. McLuckey, S. A.; Van Berkel, J.; Glish, G. L. *J. Am. Soc. Mass Spectrom.* **1992,** *3,* 60–70.
30. Zhu, Y. F.; Chung, C. N.; Taranenko, N. I.; Allman, S. L; Martin, S. A.; Haff, L.; Chen, C. H. *Rapid. Commun. Mass Spectrom.* **1996,** *10,* 383–688.
31. Zhu, L.; Parr, G.; Fitzgerald, M. C.; Nelson, C. M.; Smith, L. M. *J. Am. Chem. Soc.* **1995,** *117,* 6048–6056.
32. Applied Biosystems. *Models 392 and 394 DNA/RNA Synthesizers User's Manual, Part 902351, Document Revision B.* Norwalk, CT, March 1994.
33. Vertes, A.; Gijbels, R.; Levine, R. D. *Rapid Commun. Mass Spectrom.* **1990,** *4,* 228–233.
34. Nordhoff, E.; Karas, M.; Cramer, R.; Hahner, S.; Hillenkamp, F.; Kirpekar, F.; Lezius, A.; Muth, J.; Meier, C.; Engels, J. W. *J. Mass Spectrom.* **1993,** *30,* 99–112.

APPENDIX B

Anal. Chem. **2001**, *73*, 5000–5003

Improved MALDI-MS Analysis of Oligonucleotides through the Use of Fucose as a Matrix Additive

Anne M. Distler and John Allison*

Department of Chemistry, Michigan State University, East Lansing, Michigan 48824-1322

With the development of matrix additives, the MALDI-MS analysis of oligonucleotides has improved greatly. When the monosaccharide fucose is combined with the matrix, the homogeneity of the MALDI target, signal strength, and signal duration are increased. The sensitivity of the MALDI experiment increases, allowing for improved detection of components in a complex mixture of oligonucleotides, such as that encountered in sequencing experiments. The addition of fucose to the matrix also causes a reduction in the extent of fragmentation of oligonucleotides.

Matrix-assisted laser desorption/ionization mass spectrometry (MALDI-MS), developed by Karas et al.,[1] allows for the characterization of many types of molecules with great speed and efficiency. MALDI-MS has emerged as an important technique for the analysis of biomolecules, such as peptides and oligonucleotides. Despite the success of the technique, MALDI-time-of-flight (TOF) MS, has several disadvantages, including variable resolution and discrimination against components of mixtures. In addition, simple target preparation methods typically result in poor sample–target homogeneity.

Matrix additives have been developed in response to limitations of the MALDI experiment in its simplest form. Matrix additives, such as nitrocellulose, improve spectra from peptide and protein samples contaminated with salts and synthetic polymers.[2] Spermine as an additive effectively desalts oligonucleotide samples, eliminating the need for purification prior to analysis.[3] Carbohydrates as matrix additives have also been successfully used for MALDI analyses. Sucrose and glucose were first used as matrixes in infrared (IR) laser desorption, multiphoton-ionization (MUPI)-MS with a reflectron TOF mass spectrometer.[4] D-Glucose, D-ribose, and D-fructose were first used in combination with the matrix 2,5-dihydroxybenzoic acid (DHB) in order to increase resolution in ultraviolet (UV) MALDI analyses of peptides, performed using Fourier transform mass spectrometry (FTMS).[5] The use of carbohydrates as matrix additives was then extended to MALDI-TOFMS in the analysis of mixtures from peptide digestions, with fucose being most effective.[6] When equal amounts of fucose and matrix were combined, several improvements in the experiments resulted, including simultaneous desorption and ionization of an increased number of components in a peptide mixture (compared to that seen with matrix alone), reduction in sodium adduct formation, improved sample spot homogeneity and reproducibility, and higher resolution.[6]

Attempts have been made to explain the role of fucose as a matrix additive in the MALDI experiment. It has been suggested that a multicomponent matrix produces a more homogeneous collection of crystals by minimizing the "variation of the analyte-to-matrix molar ratio and analyte concentration".[7] It has also been suggested that fucose may rapidly decompose to yield $CO_{2(g)}$ and $H_2O_{(g)}$, which can collisionally cool gas-phase ions during desorption.[5] Other effects of fucose have been linked to its ability to cool the matrix, since it is a nonabsorbing component of the matrix mixture.[5] This is an interesting idea. If MALDI target crystals that contain both absorbing and nonabsorbing molecules can be grown, then perhaps less energy will be deposited per unit volume, resulting in lower temperatures being achieved upon laser excitation. In considering a possible additive that does not absorb at 337 nm, a sugar may be a reasonable option. Monosaccharides are soluble in the solvents commonly used in MALDI. Although not aromatic, they contain some of the structural features that many matrixes have and have a size similar to that of typical matrix molecules. However, one would not likely turn to fucose as the first choice. When analyzing peptides by MALDI-FTMS, Billeci et al. evaluated the effect of incorporating glucose, fructose, β-lactose, maltose, and sucrose at various concentrations, and found fucose to be the most useful.[6] For oligonucleotide analysis by MALDI-TOFMS, we evaluated fructose, glucose, sucrose, galactose, and maltose as matrix additives. Fucose remains uniquely effective for this application, as well.

When analyzing oligonucleotides using MALDI-MS, additives have proven to be important. MALDI analysis of oligonucleotides has been a greater challenge than peptide analysis. First, new matrixes were needed in order to successfully detect intact oligonucleotide ions. The search for better matrixes still continues.[8] The development of additives was an important step.

* Phone: 517-355-9715, ext 492. Fax: 517-353-1793. E-mail: allison@cem.msu.edu.

(1) Karas, M.; Bachmann, D.; Bahr, U.; Hillenkamp, F. *Int. J. Mass Spectrom. Ion Processes.* **1987**, *78*, 53–68.
(2) Kussman, M.; Nordhoff, E.; Rahbek-Nielsen, H.; Haebel, S.; Rossel-Larsen, M.; Jakobsen, L.; Gobom, J.; Mirgorodskaya, E.; Kroll-Kristensen, A.; Palm, L.; Roepstorff, P. *J. Mass Spectrom.* **1997**, *32*, 593–601.
(3) Asara, J.; Allison, J. *Anal. Chem.* **1999**, *71*, 2866–2870.
(4) Beavis, R. C.; Lindner, J.; Grotemeyer, J.; Schlag, E. W. *Chem. Phys. Lett.* **1988**, *146*, 310–314.
(5) Köster, C.; Castoro, J. A.; Wilkins, C. L. *J. Am. Chem. Soc.* **1992**, *114*, 7572–7574.
(6) Billeci, T. M.; Stults, J. T. *Anal. Chem.* **1993**, *65*, 1709–1716.
(7) Gusev, A. I.; Wilkinson, W. R.; Proctor, A.; Hercules, D. M. *Anal. Chem.* **1995**, *67*, 1034–1041.
(8) Distler, A. M.; Allison, J. *J. Am. Soc. Mass Spectrom.* **2001**, *12*, 456–462.

10.1021/ac015550+ CCC: $20.00
Published on Web 09/19/2001

Additives such as ammonium citrate[9,10] and spermine[3] serve a specific purpose, the reduction of alkali-ion adducts. Fucose as an additive offers a different contribution to oligonucleotide analysis. If a sample has a high sodium chloride concentration *and* forms heterogeneous crystals, can two additives be used, and are their influences additive? There is a possibility that if the crystal composition reflects solution composition, the matrix can be diluted to the point that a MALDI experiment is no longer taking place if too many additives are used simultaneously. In our experience, the use of multiple additives has had no adverse effects on the MALDI experiment. When spermine, fucose, and matrix are combined, the advantages of both spermine and fucose are realized.

Although fucose has been used to aid in the analysis of peptides and proteins, no work has been reported on the effects of fucose in oligonucleotide analysis. Here, we present several benefits of using fucose in the MALDI analysis of oligonucleotides. These benefits include a reduction in fragmentation, increased detection of components in a complex mixture, improved sample spot homogeneity, and increased signal duration.

EXPERIMENTAL SECTION

The oligonucleotides used in this work were purchased from the Michigan State University Macromolecular Structure, Sequencing, and Synthesis Facility (East Lansing, MI). The stock solutions had concentrations of 50 pmol/μL and were used without purification. The 6-aza-2-thiothymine (ATT), 5-methoxysalicylic acid (MSA, an oligonucleotide matrix developed at Michigan State University[8]), and L-fucose were purchased from Aldrich Inc (Milwaukee, WI). Spermine (sp) and 3-hydroxypicolinic acid (HPA) were purchased from Fluka (Milwaukee, WI). All matrixes were used without further purification. The aqueous fucose solution was made at a concentration of 50 mM. When spermine was used as a matrix additive, it was prepared at a concentration of 25 mM in water. Saturated matrix solutions were made using a 1:1 acetonitrile:spermine solution or 1:1 acetonitrile:water. Samples were prepared by mixing 1 μL of the analyte solution with 1 μL of the fucose solution and 1 μL of the co-matrix solution on a gold sample plate. The mixture was then allowed to air-dry.

A Sequazyme oligonucleotide sequencing kit containing the enzymes and buffers necessary for the digestion of oligonucleotides for subsequent analysis by MALDI-MS was purchased from PE Biosystems (Framingham, MA). HPA, snake venom phosphodiesterase (SVP), bovine spleen phosphodiesterase (BSP), and the standard oligonucleotide d(AGGCATGCAAGCTTGAGTATTCTAT) were diluted according to the instructions provided in the kit. Several dilutions of the SVP and BSP were made in order to provide a range of sequence coverage. The procedure for exonuclease digestions has been described previously.[11] Briefly, ammonium citrate buffer (pH = 9.4) was used for SVP digestions, and BSP reaction buffer was used for BSP digestions. A 1-μL portion of the oligonucleotide solution was diluted to 3 μL in a microtube. The manufacturer of the sequencing kit suggests that

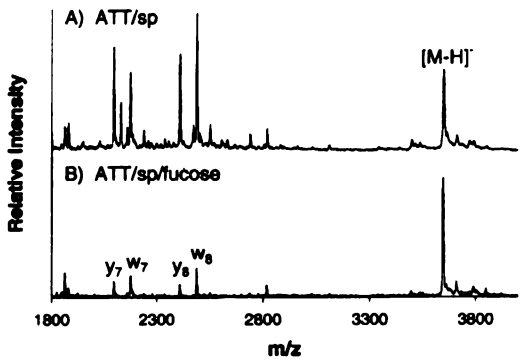

Figure 1. MALDI-MS negative ion mass spectra of d(CGCGAATTCGCG) using (A) ATT/spermine (sp) as a matrix and (B) ATT/sp/fucose as a matrix.

100–400 picomoles of material are needed for sequence analysis using an exonuclease. To the microtube, 1 μL of the diluted enzyme was added, along with 1 μL of the appropriate buffer. The solutions were incubated at 37 °C for 20 min before analysis by MALDI-MS.

Linear MALDI mass spectra were recorded on a PerSeptive Biosystems (Framingham, MA) Voyager delayed-extraction time-of-flight linear (TOF) mass spectrometer equipped with a nitrogen laser (337 nm, 3-ns pulse). Typically, 50 laser shots were averaged for each spectrum. For the negative ion MALDI spectra reported here, the accelerating voltage was −15 kV, the delay time was 700 ns,[8] the grid voltage was 94.5% of the accelerating voltage, and the magnitude of the guide wire voltage was 0.20% of the accelerating voltage. We have previously reported that longer delay times improve resolution for oligonucleotides.[8] No changes in the extent of fragmentation are observed when longer delays are used.

RESULTS AND DISCUSSION

The behavior of oligonucleotides in the MALDI experiment differs greatly from that of peptides. Although a pure sample of a peptide usually yields a single peak representing the intact molecule, oligonucleotides frequently undergo prompt fragmentation in linear TOF mass spectrometers.[12] Although fragmentation can be very useful in structure determination, it is often a complication, especially when dealing with mixtures. The literature shows[13,14] that the Dickerson dodecamer, d(CGCGAATTCGCG), has been extensively studied. When employing ATT, a matrix typically used for MALDI analysis of oligonucleotides, the Dickerson dodecamer fragments extensively, as shown in Figure 1 A. The peaks representing fragment ions are of greater intensity than the peak representing the intact, molecular ion. The most intense peak corresponds to the w_8 fragment at m/z 2489. When fucose is used in combination with ATT, the extent of fragmentation is reduced (Figure 1B). The molecular ion peak is now the most intense peak in the spectrum. Decreased fragmentation suggests

(9) Li, Y. C. I.; Cheng, S. W.; Chan, T. W. D. *Rapid Commun. Mass Spectrom.* **1998**, *12*, 993–998.
(10) Pieles, U.; Zürcher, W.; Schär, M.; Möser, H. E. *Nucleic Acids Res.* **1993**, *21*, 3191–3196.
(11) Smirnov, I. P.; Roskey, M. T.; Juhasz, P.; Takach, E. J.; Martin, S. A.; Haff, L. A. *Anal. Biochem.* **1996**, *238*, 19–25.
(12) Currie, G.; Yates III, J. *J. Am. Soc. Mass Spectrom.* **1993**, *4*, 955–963.
(13) Drew, H. R.; Wing, R. M.; Takano, T.; Broka, C.; Tanaka, S.; Itakura, K.; Dickerson, R. E. *Proc. Natl. Acad. Sci. U.S.A.* **1981**, *78*, 2179–2183.
(14) Chiu, T. K.; Kaczor-Grzeskowiak, M.; Dickerson, R. E. *J. Mol. Biol.* **1999**, *292*, 589–608.

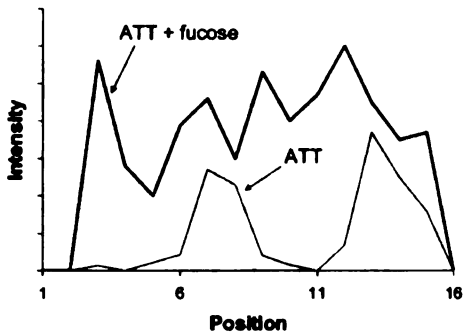

Figure 2. Intensity of the $[M - H]^-$ peak for $d(T)_{12}$ plotted against position across the sample spot. The thinner line represents the sample spot created using the matrix ATT without additives, and the line in bold represents the sample spot with ATT as the matrix and fucose as an additive. The ratio of the areas under the two curves is 3.6.

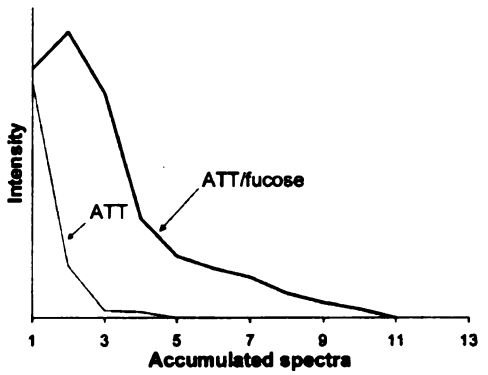

Figure 3. Intensity of the $[M - H]^-$ peak of $d(T)_{12}$ plotted against the number of accumulated 50-shot spectra from a single location. The unbolded line represents analysis of the target created using the matrix ATT without additives, and the line in bold denotes the target made with ATT as the matrix and fucose as an additive. The area under the curve created using ATT/fucose is 3.5 times that for the curve generated using ATT alone.

that either less energy is deposited into the analyte in the desorption/ionization process, or it is subsequently collisionally cooled. In addition to a reduction in the extent of fragmentation, there is an increase in resolution for the $[M - H]^-$ peak from 400 (fwhm) without fucose to 600 (fwhm) with fucose. We do note that the oligonucleotide samples were used as supplied from the Michigan State University Macromolecular Structure, Sequencing, and Synthesis Facility. As synthesized, these samples had a high, but poorly defined, salt content and contained other contaminants. When analyzed using ATT alone, the molecular ion peak for the oligonucleotide has a high mass tail that extends to an m/z value of 3800 as a result of alkali ion adduction. As shown in Figure 1AB, the addition of spermine to the matrix eliminates the need for purification of the oligonucleotide solution. The performance of spermine has been discussed previously.[3,8]

In addition to spectral changes, fucose affects the MALDI target homogeneity. Often, target crystals created using the dried droplet method[15] are inhomogeneous, with only certain portions of the target yielding strong signals. The homogeneity of the MALDI target is of growing importance as the extent of automation in MALDI analysis increases. Elaborate methods are being developed for increasing spot uniformity, including the use of electrospray techniques to produce a uniform distribution of crystals.[16] The addition of fucose to the matrix solution provides a simple alternative. To demonstrate this, two MALDI targets were made by the dried droplet method, with one using ATT as the matrix and the other using ATT/fucose. Spectra were taken from 16 equally spaced sites across the span of each well. At each location, spectra from 50 laser shots were averaged and recorded. All experiments were performed at the same laser power. The oligonucleotide $d(T)_{12}$ was used in this experiment, because only a peak representing the intact molecular ion is detected. The intensities of the $[M - H]^-$ peak in each spectrum for both the target made with ATT and that with ATT/fucose were plotted against the position in the well, shown in Figure 2. At half of the locations in the ATT target, either no signal or weak signals could be detected. The data shown for ATT in Figure 2 is not unexpected, indicative of the "doughnut"-shaped ring of crystals that typically forms. This was not the case in the ATT/fucose target. At every location across the well, strong signals were achieved. The strongest signal from the ATT target was of comparable intensity to the weakest signal from the ATT/fucose target. Similar results were achieved in experiments performed with HPA and HPA/fucose targets. With a homogeneous sample spot, automation could more easily be used in analysis, because a spectrum can more likely be obtained from any default starting position. The amount of time necessary for analysis would also be greatly decreased.

In addition to an improvement in crystal uniformity, signal duration is increased with the addition of fucose to the sample spot. Again, the oligonucleotide $d(T)_{12}$ was used to document this aspect. A location was selected in the target that gave ample signal. The intensity of the molecular ion peak was then recorded from the spectrum corresponding to the sum of 50 laser shots. Spectra were taken repeatedly, with each set of 50 transients resulting in a spectrum from the same sample location on the MALDI target until the signal-to-noise ratio was <2. These results are shown in Figure 3. The sample spot with ATT alone allowed for 4 spectra to be acquired without changing location, but 10 acceptable spectra (500 shots) were acquired from the sample spot with ATT/fucose. An increase in signal duration in the ATT/fucose target can explain one of the aspects of the results seen in Figure 2. With a prolonged signal, the peaks in the ATT/fucose spectra will be more intense than those spectra resulting from the ATT target.

The increase in both sample spot homogeneity and signal duration, as well as the reduction in the extent of fragmentation, results in an increase in sensitivity. Increased sensitivity is important when analyzing mixtures, such as those from exonuclease digestions. Sequencing using exonucleases is an important application for the MALDI mass spectrometric analysis of oligonucleotides. When using the exonuclease sequencing method, enzymes of various concentrations are used in order to maximize sequence coverage for a range of oligonucleotide sizes. Each digestion reaction yields a set of several oligonucleotides of

(15) Karas, M.; Hillenkamp, F. *Anal. Chem.* **1988**, *60*, 2301–2303.
(16) Hensel, R. R.; King, R. C.; Owens, K. G. *Rapid Commun. Mass Spectrom.* **1997**, *11*, 1785–1793.

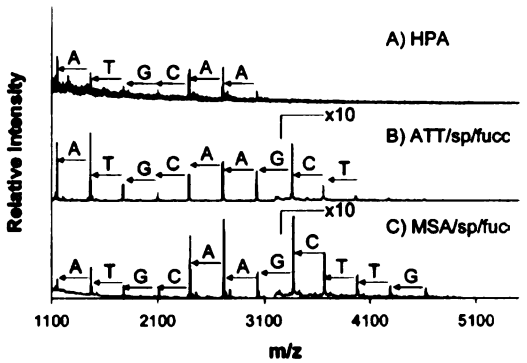

Figure 4. MALDI-MS negative ion mass spectra of the digestion products of d(AGGCATGCAAGCTTGAGTATTCTAT) using the matrixes (A) HPA, (B) ATT/sp/fucose, and (C) MSA/sp/fucose as in the original document and shown in Fig. 5.

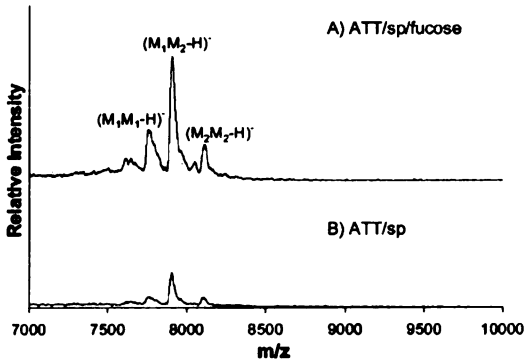

Figure 5. MALDI-MS negative ion mass spectra of the double-stranded oligonucleotide, d(CGCGAATTCGCG) bound to its complement, d(TTCGCGAATTCGCG). In (A), when ATT/sp/fucose matrix is used, the intensity of the duplex ions increased 3-fold in comparison to (B) the spectrum taken using only ATT/sp as the matrix.

varying length. MALDI analyses were performed on the same digestion products with various combinations of matrixes and matrix additives. When HPA, MSA/spermine, and ATT/spermine were used as matrixes without fucose, 7 digestion products were detected. The spectrum obtained using HPA is shown in Figure 4 A. When fucose is added to the ATT/spermine sample, 10 digestion products are easily detected (Figure 4B). When the same digestion mixture is analyzed using MSA/spermine/fucose, 12 digestion products are clearly seen (Figure 4C). With the increase in number of digestion products detected, more sequence information is provided from each reaction, and fewer enzyme dilutions are necessary to achieve complete sequence coverage. Also note that although the sequencing kit recommended that 100–400 pmol be used in the analysis, only 50 pmol was used here. This explains the low signal-to-noise ratio in Figure 4A. Fucose offers increased sensitivity, hence, an increased signal-to-noise ratio.

With the addition of fucose, several spectral changes are seen when analyzing double-stranded oligonucleotides as well. As shown in Figure 5, the detection of the duplex differs when fucose is included in the matrix crystal. In Figure 5A, the double-stranded oligonucleotide is detected using ATT/spermine/fucose as a matrix, but in Figure 5B, the analyte is detected using only ATT/spermine. In Figure 5A, the addition of fucose to ATT/spermine during sample preparation increases the intensity of the duplex 3-fold relative to the intensity of the peaks representing the single strand for the same laser power.

The addition of fucose to the sample can increase resolution, as well. This was realized when analyzing a double-stranded oligonucleotide composed of single strands that differ in molecular weight by 9 Da. When analyzing the duplex d(AAAAACCAAAAA) annealed to d(TTTTTGGTTTTT), only one peak representing one of the single-stranded species is detected when the matrix ATT/spermine is used (spectrum not shown). When the duplex is analyzed, again using ATT as the matrix with both fucose and spermine as additives, the resolution improves from 400 (fwhm) to 700 (fwhm) to allow for the clear detection of both the TG-containing strand as well as the AC-containing strand. The peaks representing the single-stranded species are also of equal intensity when fucose is used. This experiment demonstrates an improvement in resolution, as well as a more uniform response for all components, with the addition of fucose to the MALDI target.

CONCLUSIONS

As the MS analysis of single nucleotide polymorphisms (SNPs) develops, the improvement of sample-spot homogeneity in MALDI-MS will be essential. Because of the large number of samples required, SNP detection is becoming a highly automated process, from the creation of the sample spot to analysis of the spot by MALDI-MS.[17] With this automation, there is a need for an increased probability of successfully acquiring a spectrum from all positions on a sample spot. With an increase in the crystal bed homogeneity through the uses of fucose, analysis time will be decreased. In addition, the increase in sensitivity improves the probability of successful analyses.

When analyzing molecules using MALDI-MS, the ability to detect the analyte is reflected in the signal-to-noise ratio of the experiment. We find that signals are consistently higher in the analysis of oligonucleotides when fucose is used as a matrix additive. To document this, two MALDI targets were created which contained the same amount of an oligonucleotide. The first target was made using ATT; the second, with ATT/fucose. For each, 10 random locations in the target were selected. From each location, 10 spectra that were the sum of 10 transients were generated, and these 10 spectra combined to give a single spectrum. When fucose is added, the noise is unchanged, but the signal for the oligonucleotide is an order of magnitude larger. From our experiences and the data shown in Figures 2 and 3, at least an order of magnitude increase in signal is expected.

Received for review June 29, 2001. Accepted August 20, 2001.

AC015550+

(17) Li, J.; Butler, J. M.; Tan, Y.; Lin, H.; Royer, S.; Ohler, L.; Shaler, T. A.; Hunter, J. M.; Pollart, D. J.; Monforte, J. A.; Becker, C. H. *Electrophoresis* **1999**, *20*, 1258–1265.

APPENDIX C

Additives for the Stabilization of Double-Stranded DNA in UV-MALDI MS

Anne M. Distler and John Allison
Department of Chemistry, Michigan University, East Lansing, Michigan, USA

Molecular complexes such as double-stranded oligonucleotides contain non-covalent bonds that are difficult to maintain in the MALDI experiment. Quantifiers are introduced in order to evaluate, summarize, and compare spectra from experiments in which additives are used to stabilize duplex oligonucleotides. Compounds known to complex with and stabilize duplex molecules can be useful as additives in MALDI. Spermine and methylene blue, present at concentrations similar to the matrix, are detected, bound to the duplex. When peptides are used as additives, the duplex is stabilized when the peptide is present at an amount less than that of the duplex. (J Am Soc Mass Spectrom 2002, 13, 1129–1137) © 2002 American Society for Mass Spectrometry

Ultraviolet matrix-assisted laser desorption/ionization mass spectrometry (UV MALDI MS) [1] has become an important technique for the analysis of biomolecules such as peptides and oligonucleotides. While analysis of oligonucleotides initially lagged behind peptide analysis, the development of new matrices and matrix additives has made significant improvements in oligonucleotide characterization by MALDI MS [2–7]. The first additives used with oligonucleotides were ammonium salts such as ammonium hydrogen citrate [8] and ammonium fluoride [9, 10]. It is assumed that the additive alters the charge state or environment in which the analyte exists in the target crystals. In addition to the elimination of multiple alkali-ion adduction, the ammonium salt seems to play a significant role in enhancing both the desorption and the ionization of intact oligonucleotides [9]. Recently, other additives have been developed for the MALDI analysis of oligonucleotides, notably the tetraamine spermine [2, 3], related amines [11], and fucose [4, 5].

Through the use of additives, UV MALDI MS has been used successfully to study many types of covalent molecules. However, molecular complexes containing non-covalent bonds are more difficult to analyze in the UV MALDI experiment. Using a technique such as UV MALDI MS, a double-stranded oligonucleotide can be desorbed and ionized as a singly charged, gas phase ion, although only a few examples have been reported [12–14]. While oligonucleotides used in this study are 12–14 bases in length, these duplexes can serve as models for DNA/drug binding studies. Duplexes of low molecular weight are particularly useful because the resolution in a MALDI-time-of-flight (TOF) MS experiment is sufficient to detect small, organic molecules bound to the duplex. Also, they represent an analytical challenge of mass spectrometry, representative of non-covalent complexes, for which techniques could be developed to stabilize them.

When a double-stranded oligonucleotide, M_1M_2, is analyzed in negative-ion MALDI-TOF MS from a simple matrix/analyte target, only ions representing the two single strands, $(M_1 - H)^-$ and $(M_2 - H)^-$, are usually detected [15]. Since M_1M_2 is not detected as $(M_1M_2 - H)^-$ or $(M_1M_2 + H)^+$ in UV MALDI MS, the duplex must dissociate at some point before acceleration and detection of the ions. There are many steps in the MALDI experiment where the double-stranded species could denature including the initial formation of the MALDI target and the desorption/ionization (D/I) process. The presence of stabilizing additives in the experiment may maintain the non-covalent complex throughout all phases of the experiment.

There are several compounds known to complex with and stabilize double-stranded DNA at the cellular level. In cells, DNA is negatively-charged due to the ionization of the phosphate groups in the phosphodiester backbone. The phosphate groups can be affiliated with counter-ions such as sodium ions, magnesium ions, and polyamines such as spermine [16, 17]. The polyamines are positively charged at physiological pH and bind to DNA, shielding the negative charges and decreasing the repulsion between the strands. Spermine allows double-stranded DNA to condense into a more compact structure in cells [18]. When oligonucleotides are crystallized for X-ray crystallographic analysis, spermine is frequently added to facilitate crystal growth [18, 19]. Spermine may also stabilize the duplex in the MALDI experiment.

While not naturally found in cells, several small,

Address reprint requests to Dr. J. Allison, Chemistry Department, Michigan State University, East Lansing, MI 48824, USA. E-mail: allison@cem.msu.edu

1044-0305/02/$20.00
PII S1044-0305(02)00430-0

Received April 5, 2002
Revised May 15, 2002
Accepted May 20, 2002

organic compounds are known to bind to the major and minor grooves of double-stranded oligonucleotides or intercalate between the bases. The presence of such species may stabilize the duplex through the MALDI crystal growth and desorption/ionization processes. One example is ethidium bromide. Ethidium (Et) is a positively-charged species that is known to intercalate between the bases of duplexes. Ethidium bromide has been found to stabilize the double-stranded duplex poly(dT) bound to poly(dA), increasing the melting temperature by 14 °C [20, 21].

While certain small molecules are known to stabilize double-stranded DNA, larger molecules such as proteins and peptides may also have a stabilizing effect on duplexes. Interactions between DNA and proteins play important roles in many biochemical processes. Chromosomes contain DNA and an equal mass of histone and non-histone proteins [22]. Histones, molecular weights between 13,000 and 30,000 g/mol, are highly conserved across species and contain many basic residues. These positively-charged amino acid side chains interact with and stabilize the DNA through salt bridges.

Similar to histones, protamines are arginine-rich proteins found in sperm cells. Cationic protamines bind to DNA with their α-helices in the major groove of the DNA, where they enable the tight packing of the duplexes [23]. While the main driving forces for protamine-DNA binding are the ionic interactions, there is a distinct cooperativity that cannot be explained on the basis of electrostatic interactions alone [24]. Protamines perform functions similar to histones, but are generally smaller, with molecular weights between 4000 and 10,000 g/mol [25]. Non-covalent complexes between proteins and oligonucleotides have been studied in UV MALDI previously [26]. However, the effect of the presence of peptides on the spectra of double-stranded oligonucleotides has not been examined.

There is no new matrix or additive that allows for the complete conservation of the intact duplex in UV MALDI MS. For this reason, insights must be extracted from the smaller spectral changes that can be measured when the experimental variables are changed. We introduce here three simple quantifiers that allow for UV MALDI spectra of double-stranded oligonucleotides to be evaluated, summarized, and compared. Using these quantifiers, we demonstrate that the presence of stabilizing additives has a measurable effect on the duplex region of the resulting UV MALDI mass spectra. The quantifiers allow one to maintain a numerical focus on the goals in these measurements, possibly leading to the development of a blended matrix (with multiple additives), in which components each serve to chemically address different aspects of this system.

Experimental

The double-stranded oligonucleotides used in this work were purchased from the Michigan State University Macromolecular Structure, Sequencing, and Synthesis Facility (East Lansing, MI) and are shown in Table 1, with their molecular weights and melting temperatures (T_m). They are all stable in solution at room temperature with melting temperatures ranging from 28 to 42 °C. The presence of the duplex in the initial solutions was confirmed by UV analysis at 259 nm.

Table 1. Oligonucleotides used in this work

Name	Sequence	Average molecular weight	T_m*
Duplex 1	5'-CCGGAATTGGCC-3'	3646	
	3'-GGCCTTAACCGGTT-5'	4254	40 °C
Duplex 2	5'-ACCCACCCACCC-3'	3480	
	3'-TGGGTGGGTGGG-5'	3813	42 °C
Duplex 3	5'-AAAAACCAAAAA-3'	3648	
	3'-TTTTTGGTTTTT-5'	3638	28 °C

*T_m is the melting temperature at which the duplex dissociates.

The peptides, dynorphin A, fibrinogen binding inhibitor peptide (FBI peptide), β-melanocyte stimulating hormone (β-MSH), katacalcin, kemptide, trilysine, N-ε-acetyl-lysine, leucine enkephalin, Boc-MNF-amide, hexaalanine, trialanine methyl ester, and triserine were all purchased from Sigma (St. Louis, MO) and used without further purification. Peptides were dissolved in MilliQ water at concentrations of 1.0 pmol/μL.

The stock duplex solutions had concentrations of 25 pmol/μL. The compounds, 6-aza-2-thiothymine (ATT), chromomycin, daunomycin, ethidium bromide, methylene blue, distamycin, and Hoechst 33258 were purchased from Aldrich Inc. (Milwaukee, WI). Spermine (sp) and 3-hydroxypicolinic acid (HPA) were purchased from Fluka (Milwaukee, WI). When spermine was used as a matrix additive, it was prepared at a concentration of 25 mM in water. The stock solutions of ethidium bromide and methylene blue were 1 mM in water. Saturated matrix solutions were made using a 1:1 acetonitrile/spermine solution or 1:1 acetonitrile/water. For experiments performed with ethidium bromide and methylene blue, the oligonucleotide solution was mixed with an equal volume of the additive solution prior to spotting on the sample plate. For those experiments using peptides as additives, a microliter of a peptide stock solution was combined with a microliter of the stock double-stranded oligonucleotide solution. When incubated, the peptide/oligonucleotide solution was heated to 37 °C for 15 min. A microliter of the resulting solution was spotted onto the MALDI target with a microliter of the matrix solution.

Linear MALDI mass spectra were recorded on a PerSeptive Biosystems (Framingham, MA) Voyager delayed-extraction time-of-flight (TOF) linear mass spectrometer equipped with a nitrogen laser (337 nm, 3 ns pulse). For the negative ion MALDI spectra reported here, the accelerating voltage was −15 kV, the delay time, selected for optimum resolution, was 700 ns [3], the grid voltage was 94.5% of the accelerating voltage,

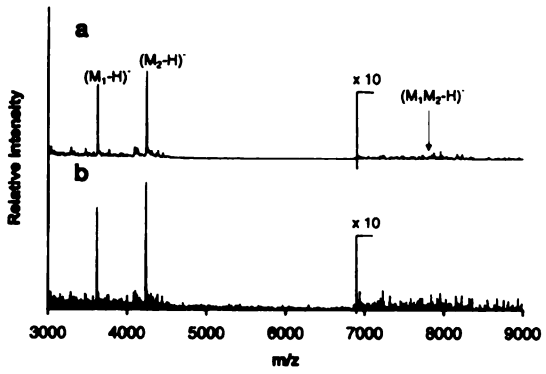

Figure 1. The negative-ion UV MALDI mass spectra of duplex 1 using (a) ATT and (b) HPA as matrices. Duplex 1 consists of two strands with molecular weights of 3646 g/mol and 4254 g/mol. The strand with the lower molecular weight is referred to as M_1 while the strand with the larger molecular weight is referred to as M_2. No duplex ions are detected (position indicated by arrow) giving a DSRR of 0.

and the magnitude of the guide wire voltage was 0.20% of the accelerating voltage. Typically, transients from 50 laser shots were averaged for each spectrum.

Melting temperature studies and UV analyses were performed using an ATI Unicam (Cambridge, UK) UV2 spectrophotometer. Oligonucleotides have strong UV absorption maxima at 259 nm. This absorption arises almost entirely from the complex electronic transitions in the purine and pyrimidine components [23]. In double-stranded oligonucleotides, the base-base stacking results in a decrease in molar absorptivity compared to that for the two single-stranded components. This is known as the hyperchromic effect. For melting studies, UV spectra were taken using the oligonucleotide solutions at room temperature. The analyte solutions were then heated to 90 °C in a sand bath for 10 min in order to denature the double-stranded oligonucleotides. If the duplex existed at room temperature, the absorbance should increase by 10% due to the unstacking of the aromatic bases upon denaturation. To insure renaturation of the duplex, the absorbance can again be recorded after the solution returns to room temperature. All spectra were acquired from 200 to 400 nm with a scan speed of 120 nm/min, a data interval of 0.5 nm, and a 2.0 nm bandwidth. Quartz cuvettes with a 1 cm path length were used, with water in the reference cuvette.

Results and Discussion

When analyzing duplex 1 using ATT and HPA as matrices, only peaks representing the two single strands are detected, Figure 1a and b respectively. While these matrices have previously shown promise for the detection of non-covalent complexes in UV MALDI MS [12, 13], the duplex is not preserved in these experiments. This may be related to size differences between the two experiments. Similar results are achieved with duplex 2; no intact duplex peaks are detected even though these duplexes have melting points which indicate that they are stable at room temperature. When analyzing duplex 3, a small peak representing the duplex with a loss of a guanine is seen. No peak is detected representing the intact $(M_1M_2 - H)^-$ species. All the experiments were completed with the same level of double-stranded oligonucleotide. We have examined the correlation between the amount of duplex deposited on the target and the double-stranded region of the spectrum and have found no influence, when working in a normal range for MALDI samples (1–100 pmol of analyte).

Due to the negatively charged phosphate backbone, negative-ion mode is often used to study oligonucleotides in MALDI MS and will be used in this discussion. When analyzing the annealed double-stranded species, M_1M_2, in negative-ion mode, ions representing the single strands, $(M_1 - H)^-$ and $(M_2 - H)^-$, dominate the spectrum. Negative-ion spectra exhibit better resolution and a higher signal-to-noise ratio. In order to measure the success of an experiment, several criteria will be used when an additive allows for the detection of duplex ions. The strand with the lower molecular weight will be denoted as M_1 while the larger complementary strand will be denoted as M_2. The ratio of the intensity (I) of the $(M_1 - H)^-$ peak to the intensity of the $(M_2 - H)^-$ peak is of interest. In previous experiments, our laboratory has analyzed double-stranded oligonucleotides in the UV-MALDI experiment where only ions from one of the strands are formed. This result is unexpected since the complementary strands are present in equal amounts and are of comparable molecular weights. This effect appears to depend on both the sequence of the oligonucleotides and the matrix used in the experiment. The ratio of the intensity of the $(M_1 - H)^-$ peak to the intensity of the $(M_2 - H)^-$ peak is referred to as the single strand distribution (SSD), eq 1.

$$SSD = \frac{I(M_1)}{I(M_2)} \quad (1)$$

Note that the nomenclature used in eq 1 is not, technically, correct. We chose to write $I(M_1)$ rather than $I(M_1 - H)^-$, for example, to allow the quantifier to be used in either negative or positive ion experiments.

To the extent that the single strand ions may evolve from the duplex, we would like to monitor how the SSD value correlates with other variables in the experiment, and to determine if the SSD correlates with single strand composition. If, for example, the single strand ions are fragments of the singly charged gas phase duplex, then one may expect that the decision of which strand retains the charge would be determined by the base composition of the individual strands. On the other hand, if duplex dissociation occurs early in the experiment, one may anticipate an SSD of 1.0. For the spectra shown in Figure 1a and b, the SSD values are

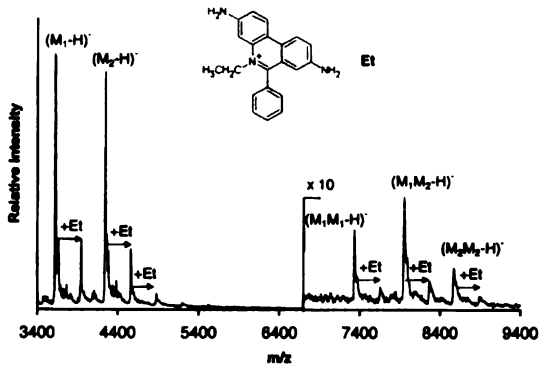

Figure 2. The negative-ion MALDI mass spectrum of duplex 1. HPA was used as the matrix with ethidium (Et) bromide as an additive. Ethidium adducts of both the single and double-stranded oligonucleotides are observed. The SSD is 1.0, DSRR is 0.05, and the WCSF is 0.5. The additive duplex ratio is 40:1.

both 0.9. That is, D/I of the larger strand is slightly favored.

The goal of this project is to optimize the ratio of the intensity of the double strand peak to the intensities of the single strand peaks. This double strand retention ratio (DSRR) is defined in eq 2.

$$\text{DSRR} = \frac{I(M_1M_2)}{I(M_1) + I(M_1M_2) + I(M_2)} \quad (2)$$

While the SSD values were 0.9 in Figure 1a and b, the DSRR was zero for both experiments. The most intense analyte-related peaks in the spectrum represent the $(M_1 - H)^-$ and $(M_2 - H)^-$ ions. The duplex must have dissociated before the acceleration and detection of the ions. The presence of stabilizing additives in the target may hold the complex together. Several experiments were performed using stabilizing additives in order to study their effect on the SSD and DSRR values for each spectrum.

As mentioned previously, ethidium bromide has been found to stabilize duplexes in solution. When used in the MALDI experiment, equal volumes of duplex 1 and ethidium bromide solutions were combined. One microliter of the oligonucleotide:ethidium solution was spotted on the MALDI target with one microliter of the HPA matrix solution. The molar amounts of components of the target are matrix:additive:oligo, 2000:40:1. This is typical since effective additives for MALDI MS are usually present at molar amounts greater than the analyte. The resulting spectrum is shown in Figure 2, with the structure of the ethidium ion. The ethidium cation binds to both the single and double-stranded species of duplex 1. That is, in addition to analyte ions, $(A - H)^-$, there are also $(A - 2H + Et)^-$ ions observed. With the appearance of the dimer peaks, the DSRR increases from 0 (in Figure 1b) to 0.05.

While the DSRR increases with the addition of ethidium bromide, the goal of this work is to retain the maximum extent of Watson-Crick base pairing when detecting a double-stranded species. If the M_1M_2 duplex completely dissociates during crystal formation, some fraction of M_1 and M_2 may recombine in a non-Watson-Crick pairing. The single-stranded species, M_1 and M_2, can, and clearly do, form three different dimers: M_1M_1, M_1M_2, and M_2M_2. In order to quantify the amount of Watson-Crick pairing involved, we will calculate a Watson-Crick selectivity factor (WCSF), eq 3.

$$\text{WCSF} = \frac{I(M_1M_2)}{I(M_1M_1) + I(M_1M_2) + I(M_2M_2)} \quad (3)$$

If the experiment begins with pure duplex and complete dissociation occurs, during crystal growth, then there will be equimolar amounts of M_1 and M_2 available in the solution on the sample plate. If random dimer formation occurs, a WCSF value of 0.5 would be expected. This suggests that the distribution of duplex peaks was dictated by random condensation events. Even in peptide analysis, non-specific dimerization has been observed [27]. As the value of the WCSF approaches 1, Watson-Crick base pairing is preserved and, presumably, the non-covalent forces were maintained throughout the MALDI experiment. When changing the variables in the MALDI experiment, the value of the WCSF provides information about the nature of the species detected and gives direction to subsequent experiments.

In Figure 2, while there are peaks representing the $(M_1M_2 - H)^-$ species, there are also peaks representing the $(M_1M_1 - H)^-$ and $(M_2M_2 - H)^-$ species. While the DSRR increased from 0 to 0.05, the WCSF is 0.5, suggesting random dimerization. If random dimerization occurs, the duplex may completely dissociate and the single strands are likely dimerizing with no sequence specificity as the crystals are growing. Thus, while ethidium addition does result in "dimer ions", we conclude that this additive does not stabilize the initial duplex throughout the UV-MALDI experiment.

Other compounds known to bind to double-stranded DNA [23] were evaluated as matrix additives as well including chromomycin, distamycin, berenil, daunomycin, and methylene blue. Of these compounds, distamycin and berenil were found to bind to the single-stranded oligonucleotides in the UV-MALDI experiment. There were, however, no duplex or dimer peaks detected, giving a DSRR of zero for both additives. The SSD was 0.7 for the berenil experiment and 1.0 for the distamycin experiment. Chromomycin and daunomycin had no apparent effects on the experiment.

Methylene blue was also found to bind to the single-stranded oligonucleotide. The experimental procedure used for the ethidium bromide experiments was followed using methylene blue as the additive. The solution was then spotted with ATT as the matrix. The resulting spectrum is shown in Figure 3, with the

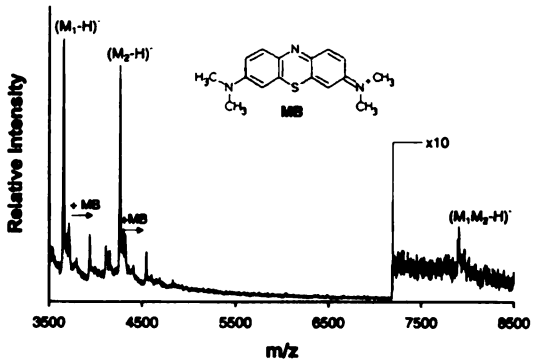

Figure 3. The negative-ion MALDI mass spectrum of duplex 1 with methylene blue as an additive. ATT was used as the matrix. The SSD is 0.9, the DSRR is 0.03, and the WCSF is 1.0. The additive duplex ratio is 40:1.

structure of the methylene blue cation. While methylene blue (MB) is observed bound to the single-stranded species, its presence appears to stabilize the duplex as well, Figure 3. In this experiment, the DSRR value was 0.03, the SSD was 0.9, and the WCSF was 1.0. With a WCSF of 1.0, it appears that a portion of the duplex was maintained throughout the entire UV-MALDI experiment, due to the presence of this additive, although the duplex represents only a small percentage of the initial complex.

In addition to intercalating and groove-binding molecules, spermine was also found to be an effective additive. When spermine is used with ATT, there are significant changes in the double-stranded region of the spectrum. Figure 4a shows the spectrum of duplex 3 when ATT and spermine are used as a matrix and Figure 4b shows a spectrum of the same duplex with ATT as the matrix. Without spermine, a peak representing a duplex fragment, due to the loss of a guanine, is

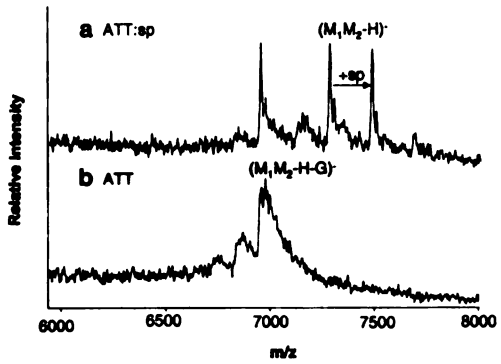

Figure 4. Portions of the negative-ion MALDI mass spectra of duplex 2 using (a) ATT/sp and (b) ATT as the matrix. Note the intact duplex ion is formed when spermine is present while only a duplex ion fragment is formed with ATT alone. In the ATT/sp experiment, the DSRR is 0.10 and the WCSF is 1.0. The SSD is 1.0 for both experiments. The additive:duplex ratio is 500:1.

seen. When spermine is present, two additional peaks are seen. The intact, deprotonated duplex, $(M_1M_2 - H)^-$ is detected as well as its spermine (sp) adduct, $(M_1M_2 - H + sp)^-$. Compared to Figure 1a, the DSRR increases from zero to 0.1. The SSD values are 1.0 for both experiments. The WCSF value for this spectrum is 1, with only high mass peaks relating to the M_1M_2 species being detected.

While spermine may contribute to duplex stability in the crystal growth event, the detection of $(M_1M_2 - H + sp)^-$ suggests that a spermine complex was formed and remained intact through the D/I event. The effect is duplex-dependent. Spermine stabilizes duplex 3, but when ATT:sp is used in the analysis of duplex 1 or 2, ions representing the intact duplex are not exclusively detected; peaks representing $(M_1M_1 - H)^-$ and $(M_2M_2 - H)^-$ are detected as well.

In Figure 4a, while most of the duplex dissociated, some duplex ions were detected in the MALDI analysis. The addition of spermine to the matrix has, at some point in the experiment, allowed for the detection of what appears to be authentic double-stranded DNA ions with Watson-Crick base-pairing preserved. The improvement in resolution when spermine is added may suggest that spermine-duplex adducts are trapped in the crystals. This may lower the average number of negative charges on trapped oligonucleotides, simplifying desorption kinetics.

While spermine stabilizes the duplex during the MALDI experiment, it also acts to effectively displace alkali ions, decreasing the abundance of sodium and potassium adducts [2]. Spermine may serve an important role in the eventual development of a mixed matrix for duplex analysis. Addition of spermine is preferable to sample purification. In analyzing other biopolymers by MS, it is certainly common to purify by, for example, ion exchange if a sample has a high salt content. However, when the analyte is a DNA duplex, this may not be a logical procedure to use. Ions such as Na^+ and K^+ stabilize duplexes; melting points are lowered when salts are removed [28]. Thus, desalting may well decrease the success of a duplex analysis by UV-MALDI MS. Spermine allows for some salt to be present, and displaces alkali ions as the target is formed.

In the evaluation of spermine as an additive, Figure 4, the double-stranded oligonucleotide is detected in both experiments. In Figure 4b, the presence of salts interferes with the analysis. The duplex oligonucleotide may form many alkali ion adducts leading to decreased resolution and signal-to-noise ratio. The presence of spermine in Figure 4a leads to an improvement in the resolution. The presence of spermine in the matrix solution may also improve the results of experiments using other additives such as methylene blue. If the experiment in Figure 3 is repeated with a matrix solution containing spermine, the resolution in the duplex region is improved, the DSRR value increases, and a methylene blue adduct is detected in the duplex region, Figure 5. The DSRR increases significantly from 0.03 in

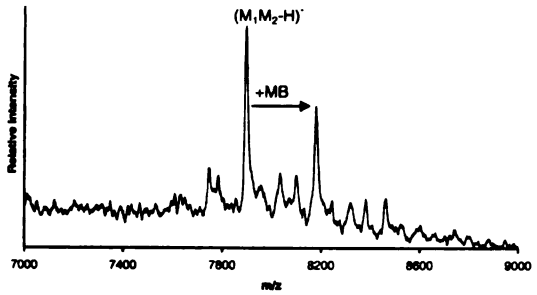

Figure 5. A portion of the negative-ion MALDI mass spectrum of duplex 1 with methylene blue (MB) as an additive. ATT:sp was used as the matrix. The DSRR is 0.05 and the WCSF is 1.0. The spermine:MB:duplex ratio is 500:40:1.

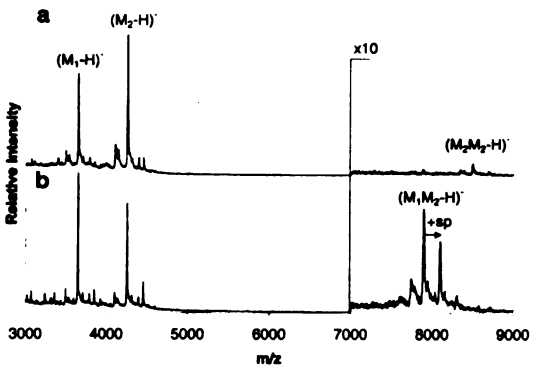

Figure 6. Negative-ion MALDI mass spectra of duplex 1 with (a) no peptide present and (b) with β-MSH present. ATT:sp was used as the matrix for both experiments. 25 pmol of duplex and 1 pmol of β-MSH were deposited onto the MALDI target. For (a), the SSD is 0.7, the DSRR is 0.006, and the WCSF is 0.3. For (b), the SSD is 1.1, the DSRR is 0.06, and the WCSF is 1.0. The peptide:duplex ratio is 1:25.

Figure 3 to 0.07 in Figure 5. The WCSF is 1.0 and the SSD is 0.9.

There have been many cases in UV-MALDI MS where a complex is observed, possibly as an analyte with a matrix molecule or analyte with an additive. It may be significant that, when the additive MB appears to allow intact duplex detection, there is direct evidence in the spectrum for existence of the M_1M_2·MB complex. This suggests that MB forms a strong complex with the duplex that is more stable than the duplex alone, and that it is involved in duplex preservation in the target preparation step.

If some small molecules that are known to interact with DNA can stabilize the duplex in the MALDI experiment, larger molecules such as proteins and peptides may also have a stabilizing effect. In an experiment designed in our laboratory to explore the differences in resolution and sensitivity between a peptide and an oligonucleotide in UV-MALDI-MS, a solution was prepared that contained equal amounts of a peptide and oligonucleotide of similar molecular weights. In the resulting spectra, peaks were detected for the peptide, $(P + H)^+$, the oligonucleotide, $(O + H)^+$, and a peptide-oligonucleotide complex, $(P + O + H)^+$. Similar results have been reported previously [29]. In order to examine the influence of peptides on double-stranded oligonucleotides, several peptides were combined with duplex oligonucleotides and analyzed by UV MALDI-MS. The peptides were used at a level of 1 pmol or less. An additive that is most effective at a level similar to that of the analyte, rather than that of the matrix, will be referred to as a microadditive (with the hope that there will not be a future need to separately define nanoadditives, picoadditives, etc).

Duplex 1 was used for the experiments designed to evaluate peptides as microadditives with ATT:spermine as the matrix, Figure 6a. The SSD is 0.7 and the DSRR is 0.006. While the intact duplex, $(M_1M_2 - H)^-$ is detected in this experiment, the peak representing the $(M_2M_2 - H)^-$ species is surprisingly intense, giving the spectrum a WCSF of 0.3.

When only 1 pmol of β-MSH was added to the target (which contained 25 pmol of duplex) used to obtain Figure 6a, the spectrum shown in Figure 6b is obtained. The SSD changes dramatically to 1.1, the DSRR is 0.06, and the WCSF is 1.0. There are no peaks representing either $(M_1M_1 - H)^-$ or $(M_2M_2 - H)^-$. In this experiment, β-MSH stabilized, to some extent, double-stranded DNA ions in UV MALDI MS, *when present at a level of one picomole on the MALDI target*. Other peptides evaluated are listed in Table 2. All peptides were used as additives by adding 1 pmol of peptide to 25 pmol of duplex 1 and analyzed using ATT:sp as the matrix. The DSRR and SSD values are listed in the table. All WCSF values are 1.

The peptides evaluated as microadditives can be grouped based both on their size and amino acid content. It is possible that the most successful experiments would have involved peptides that have a size similar to that of the oligonucleotide. From spermine experiments performed previously [2, 3], we have learned that additives capable of multiple interactions with the oligonucleotides are important. For this reason, the number of basic residues in the peptide may be important, with multiple basic residues increasing the number of electrostatic interactions possible. Previously it was determined that peptides containing basic residues increase the melting temperature of duplex oligonucleotides in solution [30]. Protonated backbone nitrogens may aid in stabilization as well.

When examining the data in Table 2, attempts were made to correlate the experimental results with the structural features of the peptides. The two peptides used with the most notable success were dynorphin A and β-MSH. Both of these larger peptides contain basic residues with three arginines and two lysines out of the 17 amino acids in dynorphin A and six basic residues out of the 22 amino acids residues in β-MSH including three lysines, two arginines, and one histidine. Dynor-

Table 2. Peptide additives and their influence on UV MALDI spectra of duplex 1

Peptide	Peptide sequence	SSD	WCSF	DSRR	% Arg	% Lys	MW
Dynorphin A	YGGFLRRIRPKLKWDNQ	1.1	1.0	0.1	17.65	11.76	2147.50
β-MSH	AEKKDEGPYRMEHFRWGSPPKD	1.1	1.0	0.1	9.09	13.64	2660.90
Katacalcin	DMSSDLERDHRPHVSMPQNAN	1.1	1.0	0.0	9.52	0.00	2436.60
Kemptide	LRRASVA	0.9	1.0	0.0	28.57	0.00	771.90
FBI peptide	HHLGGAKQAGDV	1.0	1.0	0.0	0.00	8.33	1189.30
Trilysine	KKK	1.0	1.0	0.0	0.00	100.00	402.50
N-ε-acetyl-Lys	K	1.0	1.0	0.0	0.00	100.00	188.23
Leucine enkephalin	YGGFL	1.0	1.0	0.0	0.00	0.00	555.60
Boc-MNF amide	BMNF	0.8	1.0	0.0	0.00	0.00	510.60
Hexaalanine	AAAAAA	1.0	1.0	0.0	0.00	0.00	444.50
Trialanine methyl ester	AAA	0.9	1.0	0.0	0.00	0.00	305.30
Triserine	SSS	1.1	1.0	0.0	0.00	0.00	279.20

phin A and β-MSH presumably interact with the double-stranded oligonucleotides at multiple sites. The backbone nitrogens may be important in the stabilization of the duplex. A positively-charged backbone in a peptide may behave similarly to spermine in solution. The side chains of the peptide may also play an important role. The amino acids, tyrosine, phenylalanine, and tryptophan, contain aromatic side chains. These side chains may partially intercalate between the nitrogen-containing bases of the oligonucleotide, stabilizing the duplex. Increases in the melting temperature of duplex DNA have been reported when in the presence of peptides containing phenylalanine residues [31]. Basic side chains may also play an important role as discussed previously.

Since peptides containing only alanine residues were not as successful as additives, it appears that the backbone nitrogens are not effective in stabilizing the duplex. Small peptides containing basic residues such as Lys-Lys-Lys were found to increase the DSRR value although these smaller peptides were less effective than Dynorphin A and β-MSH. Similarly, peptides containing aromatic side chains were also capable of increasing the DSRR values for the experiments.

Since the best results are seen with the peptides Dynorphin A and β-MSH, which contain both aromatic and basic amino acids, it is not perhaps the size of the peptide that is of primary importance, but the spacing between basic amino acids. When basic amino acids in a larger peptide are separated by other residues, the separation between those basic residues may be similar to the spatial separation between the phosphates of the oligonucleotide. This may lead to greater stabilization of the duplex. Clearly, more work is required to find the optimal peptide, but these experiments establish structural aspects of the additives that are important and show that peptides can, at relatively low levels, stabilize to some extent duplexes in the UV MALDI experiment.

In order to maximize the interaction between the peptides and the double-stranded oligonucleotides, several conditions were varied in the experiments. At first the peptide and oligonucleotide were combined on the MALDI plate before the addition of the matrix. To insure thorough mixing, peptide and oligonucleotide solutions were also premixed before deposition on the target. There was no difference between spectra acquired using on target mixing or premixed solutions. A solution of the peptide and oligonucleotide was also pre-mixed and incubated at both room temperature and at 37 °C prior to MALDI analysis. When incubated at either temperature, samples again yielded spectra similar to the unincubated samples.

For the data shown in Table 2, one picomole of each peptide was used in the formation of the MALDI target. While 1 pmol was optimal for most peptides, improvements were seen with as little as 50 fmol of peptides present in the target. FBI peptide, katacalcin, and β-MSH all yielded duplex spectra with improved DSRR values with less than 1 pmol of peptide present in the target. While addition of these peptides to the MALDI target improved the DSRR, the β-MSH peptide gave the best results. Figure 7 shows the negative-ion MALDI mass spectrum of a target containing 100 fmol of β-MSH and 25 pmol of double-stranded oligonucleotide, using ATT:sp as the matrix. The SSD was 0.94, the DSRR was 0.09 and the WCSF was 1.00. The presence of

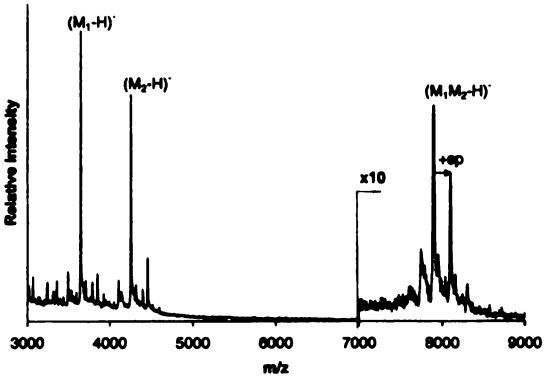

Figure 7. Negative-ion MALDI mass spectrum of duplex 1 with 100 fmol of β-MSH and ATT:sp as the matrix. The SSD is 0.94, the DSRR is 0.09, and the WCSF is 1.00. The peptide:duplex ratio is 1:250.

the peptide still influences the resulting mass spectrum even when the relative concentration of the oligonucleotide:peptide is 250:1.

All of the experiments reported here were performed on a single "batch" of a given duplex. We have purchased synthetic, annealed duplexes from both an on-campus facility and from commercial suppliers. In the case of the Michigan State University Facility, oligonucleotides are usually synthesized as primers and we are one of a few groups on campus that request synthesized strands and their annealed duplexes. We have found that some sources occasionally provide a duplex that is more stable than the same duplex in another batch. Salts and buffers that are commonly provided in such samples, while not specified, could alter resulting MALDI spectra. All of the spectra presented here have been duplicated on multiple dates from the same sample, and from other batches of the same sample, to confirm that no result was influenced by an impurity or contaminant in a single batch. From multiple experiments on identical samples, we believe that the quantities reported here are reflections of the relative influence of the additives discussed. Spectra were obtained from several locations across the target. Those shown represent an average for the target. In identical experiments, the WCSF and SSD quantifiers are reproducible to 10%. For example, in Figure 7, the WCSF value was 1.0 ± 0.1 and the SSD has a value of 0.94 ± 0.90. This was not the case for the DSRR values. For the experiments shown here, the DSRR values reported ranged from 0 to 0.1. The experiments that yielded DSRR values of zero did so consistently. When duplex peaks were detected in an experiment, the DSRR values were reproducible to 25%. For the additives shown, typically 5–10% of the duplex molecules were stabilized in the experiment, and can be viewed as having similar stabilizing capabilities.

Conclusion

Methylene blue, spermine, and β-MSH as additives allow for the detection of small intact DNA duplexes. Each of these compounds must be capable of stabilizing double-stranded DNA in at least the crystal growth process, and possibly in the desorption/ionization process as well. While these additives all increase the DSRR values, they may participate in a different way throughout the MALDI process. For example, spermine aids in the crystallization of the duplex, and complexes with the oligonucleotide during crystal growth. During the desorption/ionization of the oligonucleotide, the spermine may dissociate from the duplex, resulting in the detection of the intact duplex, $(M_1M_2 - H)^-$. The spermine may also stabilize the duplex through the desorption/ionization process with the $(M_1M_2 + sp - H)^-$ species being detected. In order for the spermine to bind to the DNA and stabilize it, the spermine must be present at a concentration equal to, or greater than, the oligonucleotide concentration. In contrast, peptides are capable of stabilizing the duplex oligonucleotides even when present at concentrations less than that of the oligonucleotide. The peptides may stabilize the duplex through another mechanism. If the peptide can stabilize the duplex whether it is present at a level of 1 pmol or 50 fmol (always present at a level less than the 25 pmol of duplex used for each experiment presented here), each peptide may be capable of interacting with more than one duplex throughout the experiment. Since the peptide is needed in only a catalytic amount, it may be acting as a chaperone for the double-stranded oligonucleotides. The peptide may bind and stabilize the duplex during the crystal growth step. After depositing the duplex on the growing crystal surface, the peptide may dissociate from the duplex, allowing it to interact with another duplex still in solution.

Alternatively, the equilibrium constant for a duplex-spermine complex may be much smaller than that for a duplex-peptide complex. Thus, to achieve the same effect, a greater concentration of spermine is needed, although the mechanism is the same. Even speculating on this possibility is difficult because it is not known how many additive molecules interact with a single duplex. In order to fully understand this process, the stoichiometry of the critical step must be known.

Since peptide-duplex complexes are not detected in these MALDI experiments, a chaperone mechanism is more likely. While it may be different from the mechanism for spermine, the peptide-oligonucleotide interaction, in some ways, parallels the behavior of spermine. When crystals of oligonucleotides are required for X-ray crystallographic studies, spermine is frequently added to facilitate crystal growth. However, spermine is usually not found in the crystals that are formed. Multiply protonated, positively-charged spermines presumably interact with the oligonucleotides, but the spermine molecules are efficiently eliminated as the crystals grow. In a similar way, peptides such as β-MSH may bind with duplexes only until they become incorporated into the matrix crystal, and become released at that time.

Why do DNA duplexes dissociate in the UV MALDI experiment? Results presented here suggest that extensive, if not complete, dissociation occurs in the first step during growth of the crystal target. We have investigated the possibility that the duplexes dissociate in the initial solution due to the organic solvents and excess matrix molecules, but these do not appear to be sufficient for inducing dissociation. One possibility is the crystals themselves. When a duplex lands on a growing crystal in the initial solution, multiple possibilities follow. It may desorb from the surface in duplex form, it may incorporate into the crystal in duplex form, or it may dissociate, leaving one strand bound to the surface. If the matrix crystals are responsible for dissociation of non-covalent complexes that are analyte in a MALDI experiment, methods for more rapid crystal growth could result in more efficient trapping of such complexes for subsequent analysis.

References

1. Karas, M.; Bachmann, D.; Bahr, U.; Hillenkamp, F. Matrix-Assisted Ultraviolet-Laser Desorption of Non-Volatile Compounds. *Int. J. Mass Spectrom.* **1987,** *78,* 53–68.
2. Asara, J. M.; Allison, J. Enhanced Detection of Oligonucleotides in UV MALDI MS Using Tetraamine Spermine as a Matrix Additive. *Anal. Chem.* **1999,** *71,* 2866–2870.
3. Distler, A. M.; Allison, J. 5-Methoxysalicylic Acid and Spermine: A New Matrix for the Matrix-Assisted Laser Desorption/Ionization Mass Spectrometry Analysis of Oligonucleotides. *J. Am. Soc. Mass Spectrom.* **2001,** *12,* 456–462.
4. Distler, A. M.; Allison, J. Improved MALDI-MS Analysis of Oligonucleotides through the Use of Fucose as a Matrix Additive. *Anal. Chem.* **2001,** *73,* 5000–5003.
5. Shahgholi, M.; Garcia, B. A.; Chiu, N. H. L.; Heaney, P. J.; Tang, K. Sugar Additives for MALDI Matrices Improve Signal Allowing the Smallest Nucleotide Change (A:T) in a DNA Sequence to be Resolved. *Nucleic Acids Res.* **2001,** *29,* e91/1–e91/10.
6. Koomen, J. M.; Russell, W. K.; Hettick, J. M.; Russell, D. H. Improvement of Resolution, Mass Accuracy, and Reproducibility in Reflected Mode DE-MALDI-TOF Analysis of DNA Using Fast Evaporation-Overlayer Sample Preparations. *Anal. Chem.* **2000,** *72,* 3860–3866.
7. Zhang, L. K.; Gross, M. L. Matrix-Assisted Laser Desorption/Ioniation Mass Spectrometry Methods for Oligodeoxynucleotides: Improvements in Matrix, Detection Limits, Quantification, and Sequencing. *J. Am. Soc. Mass Spectrom.* **2000,** *11,* 854–865.
8. Pieles, U.; Zürcher, W.; Schär, M.; Möser, H. E. Matrix-Assisted Laser Desorption Ionization Time-of-Flight Mass Spectrometry: A Powerful Tool for the Mass and Sequence Analysis of Natural and Modified Oligonucleotides. *Nucl. Acids Res.* **1993,** *21,* 3191–3196.
9. Yi, Y. C. L.; Cheng, S.; Chan, T. W. D. Evaluation of Ammonium Salts as Co-matrices for Matrix-Assisted Laser Desorption/Ionization Mass Spectrometry of Oligonucleotides. *Rapid. Commun. Mass Spectrom.* **1998,** *12,* 993–998.
10. Cheng, S. W.; Chan, T. W. D. Use of Ammonium Halides as Co-matrices for Matrix-Assisted Laser Desorption/Ionization Studies of Oligonucleotides. *Rapid Commun. Mass Spectrom.* **1996,** *10,* 907–910.
11. Vandell, V. E.; Limbach, P. A. Polyamine Co-matrices for Matrix-Assisted Laser Desorption/Ionization Mass Spectrometry of Oligonucleotides. *Rapid Commun. Mass Spectrom.* **1999,** *13,* 2014–2021.
12. Lecchi, P.; Panell, L. K. The Detection of Intact Double-Stranded DNA by MALDI. *J. Am. Soc. Mass Spectrom.* **1995,** *6,* 972–975.
13. Kirpekar, F.; Berkenkamp, S.; Hillenkamp, F. Detection of Double-Stranded DNA by IR- and UV-MALDI Mass Spectrometry. *Anal. Chem.* **1999,** *71,* 2334–2339.
14. Little, D. P.; Jacob, A.; Becker, T.; Braun, A.; Darnhofer-Demar, B.; Jurinke, C.; van den Boom, D.; Koster, H. Direct Detection of Synthetic and Biologically Generated Double-Stranded DNA by MALDI-TOF MS. *Int. J. Mass Spectrom. Ion Processes* **1997,** *169/170,* 323–330.
15. Tang, K.; Taranenko, N. I.; Allman, S. L.; Chen, C. H.; Chang, L. Y.; Jacobson, K. B. Picolinic-Acid as a Matrix for Laser Mass-Spectrometry of Nucleic-Acids and Proteins. *Rapid Commun. Mass Spectrom.* **1994,** *8,* 673–677.
16. Shui, X.; McFail-Isom, L.; Hu, G. G.; William, L. D. The B-DNA Dodecamer at High Resolution Reveals a Spine of Water on Sodium. *Biochemistry* **1998,** *37,* 8341–8355.
17. Halle, B.; Denisov, V. P. Water and Monovalent Ions in the Minor Groove of B-DNA Oligonucleotides as Seen by NMR. *Biopolymers* **1998,** *48,* 210–233.
18. Tippin, D. B.; Sundaralingam, M. Nine Polymorphic Crystal Structures of d(CCGGGCCGG), d(CCGGGCCm(5)CGG), d(Cm(5(CGGGCCm(5)CGG), and d(CCGGGCC(Br)(5)CGG) in Three Different Conformations: Effects of Spermine Binding and Methylation on the Bending and Condensation of A-DNA. *J. Mol. Biol.* **1997,** *267,* 1171–1185.
19. Egli, M.; Williams, L. D.; Gao, Q.; Rich, A. Structure of the Pure-Spermine Form of Z-DNA (Magnesium Free) at 1-A Resolution. *Biochemistry* **1991,** *30,* 11388–11402.
20. Tishchenko, E. I.; Karapetyan, A. T.; Borisova, O. F. Different Complexes of Ethidium Bromide and Their Role in Stabilizing the $(dA)_n{\cdot}(dT)_n$ Structure. *Mol. Biol.* **1996,** *30,* 826–829.
21. Vardevanyan, P. O.; Antonyan, A. P.; Manukyan, G. A.; Karapetyan, A. T.; Shchyolkina, A. K.; Borisova, O. F. Ethidium Bromide Binding to Native and Denatured Poly(dA)Poly(dT). *Mol. Biol.* **2000,** *34,* 272–276.
22. Bradbury, E. M. Nucleosome and Chromatin Structures and Functions. *J. Cell. Biochem.* **1998,** *30/31,* 177–184.
23. Blackburn, G. M.; Gait, M. J. *Nucleic Acids in Chemistry and Biology; 2nd ed.* Oxford University Press: New York, 1996.
24. Porschke, D. Nature of Protamine-DNA Complexes: A Special Type of Ligand Binding Cooperativity. *J. Mol. Biol.* **1991,** *222,* 423–433.
25. Ausió, J. Histone H1 and Evolution of Sperm Nuclear Basic Proteins. *J. Biol. Chem.* **1999,** *274,* 31115–31118.
26. Tang, X.; Callahan, J. H.; Zhou, P.; Vertes, A. Noncovalent Portein-Oligonucleotide Interactions Monitored by Matrix-Assisted Laser Desorption/Ionization Mass Spectrometry. *Anal. Chem.* **1995,** *67,* 4542–4548.
27. Karas, M.; Hillenkamp, F. Laser Desorption Ionization of Proteins with Molecular Masses Exceeding 10,000 Daltons. *Anal. Chem.* **1988,** *60,* 2299–2301.
28. Schildkraut, C.; Lifson, S. Dependence of the Melting Temperature of DNA on Salt Concentration. *Biopolymers* **1965,** *3,* 195–208.
29. Lin, S.; Cotter, R. J.; Woods, A. S. Detection of Non-Covalent Interaction of Single and Double Stranded DNA with Peptides by MALDI-TOF. *Proteins* **1998,** *S2,* 12–21.
30. Harrison, J. G.; Balasubramanian, S. Synthesis and Hybridization Analysis of a Small Library of Peptide–Oligonucleotide Complexes. *Nucleic Acids Res.* **1998,** *26,* 3136–3145.
31. Robledo-Luiggi, C.; Vera, M.; Cobo, L.; Jaime, E.; Martinez, C.; Gonzalez, J. Partial Intercalation with Nucleic Acids of Peptides Containing Aromatic and Basic Amino Acids. *Biospectroscopy* **1999,** *5,* 313–322.